Numerical analysis of some saddle point formulation with X-FEM type approximation on cracked or fictitious domains

Saber Amdouni

N°d'ordre xxxx-ISAL-XXXX

Thèse de Doctorat

Spécialité

Mathématiques Appliquées

Présentée par

Saber AMDOUNI
Ingénieur Génie Mécanique ENIT

Pour obtenir le grade de

Docteur de l'Institut National des Sciences Appliquées de Lyon et l'École Nationale d'Ingénieurs de Tunis

Sujet de thèse:

Numerical analysis of some saddle point formulation with X-FEM type approximation on cracked or fictitious domains

Soutenue le 31 Janvier 2013 devant le jury composé de:

Faker BEN BELGACEM	Universitè de Technologie de Compiègne	Rapporteur
Patrice HAURET	MICHELIN, Centre de Technologies de Ladoux	Examinateur
Bertrand MAURY	Universitè Paris sud, Orsay	Examinateur
Saloua MANI-AOUDI	Faculté des sciences de Tunis	Examinateur
Maher MOAKHER	École Nationale d'ingénieurs de Tunis	Co-directeur
Nicolas MOËS	Ecole Centrale de Nantes	Rapporteurs
Jérôme POUSIN	Institut National des Sciences Appliquées de Lyon	Examinateur
Yves RENARD	Institut National des Sciences Appliquées de Lyon	Co-directeur

Acknowledgments

Contents

Chapter 1

Introduction

The title of this thesis is "Numerical analysis of some saddle point formulation with X-FEM type approximation on cracked or fictitious domains". It concerns the mathematical and numerical analysis of convergence and stability of mixed or hybrid formulation of constrained optimization problem with Lagrange multiplier method in the framework of the eXtended Finite Element Method (X-FEM). We begin by introducing the incompressible and compressible elastostatic problems. Then we present the unilateral contact condition in the elastostatic cracked domains. After that we give some general aspects of the eXtended Finite Element Method (X-FEM). Finally we present the outline of this thesis.

Contents

1.1 Incompressible and compressible elasticity problem

1.1.1 Basic concept for the linear elasticity

Let us consider the deformation of an elastic body occupying, in the initial configuration, a domain $\Omega \in \mathbb{R}^2$ where plane strain assumption are assumed. Let $\mathbf{u}$ be the displacement field that satisfies the assumption of small perturbations : small displacements and transformations, respectively

$$\mathbf{u} = (u_1, u_2) \quad \text{with} \mid \mathbf{u} \mid \ll L \quad \text{and} \quad \mid \frac{\partial u_i}{\partial x_j} \mid \ll 1 \qquad \text{in } \Omega \quad \text{with } i, j \in \{1, 2\}$$

with L is a characteristic length of the solid.
The linearized strain tensor is defined by

$$\varepsilon_{ij} = \frac{1}{2}\left(\frac{\partial u_i}{\partial x_j} + \frac{\partial u_j}{\partial x_i}\right) \qquad \text{in } \Omega \quad \text{with } i,j \in \{1,2\}.$$

The stress tensor $\boldsymbol{\sigma}$ is given by the anisotropic material behavior law

$$\boldsymbol{\sigma}(\mathbf{u}) = \mathbb{C} : \boldsymbol{\varepsilon}(\mathbf{u}), \qquad \text{in } \Omega,$$

with $\mathbb{C}$ a fourth order elastic tensor characterizing the material rigidity.
In the case of an isotropic material (i.e., which behaves in the same way in all directions) the law of material behavior is reduced to the Hooke's law

$$\boldsymbol{\sigma}(\mathbf{u}) = \lambda \ \mathrm{tr}\,\boldsymbol{\varepsilon}(\mathbf{u})\, I + 2\mu\, \boldsymbol{\varepsilon}(\mathbf{u}), \tag{1.1}$$

with λ and μ are the Lamé coefficients, which are positives and defined by

$$\mu = \frac{E}{2(1+\nu)} \quad \text{and} \quad \lambda = \frac{E\nu}{(1+\nu)(1-2\nu)},$$

E is the Young modulus and ν the Poisson's ratio.

1.1.2 Compressible strong and weak formulations

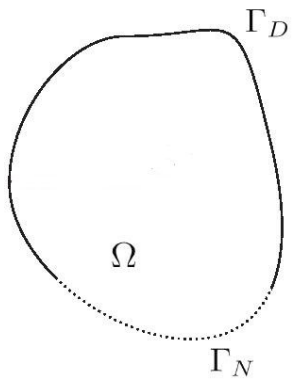

Figure 1.1: Domain

In this section, the equations of the general problem of a cracked solid are recalled. Let $\Omega \subset \mathbb{R}^2$ be the cracked domain, Γ_c denotes the crack and Γ the boundary of Ω. We assume that $\Gamma \setminus \Gamma_c$ is partitioned in two parts: Γ_N where a Neumann surface force $\mathbf{t}$ is applied and Γ_D where a Dirichlet condition $\mathbf{u} = \mathbf{0}$ is imposed (see figure 1.1). We assume that we have a traction free-condition on Γ_c. Let $\mathbf{f}$ be the body force applied on Ω. The equilibrium equation,

constitutive law and boundary conditions are given by

$$-\operatorname{div}\boldsymbol{\sigma}(\mathbf{u}) = \mathbf{f}, \qquad \text{in} \quad \Omega, \tag{1.2}$$

$$\boldsymbol{\sigma}(\mathbf{u}) = \mathbb{C} : \boldsymbol{\varepsilon}(\mathbf{u}), \qquad \text{in} \quad \Omega, \tag{1.3}$$

$$\mathbf{u} = \mathbf{0}, \qquad \text{on} \quad \Gamma_D, \tag{1.4}$$

$$\boldsymbol{\sigma}(\mathbf{u}) \cdot \mathbf{n} = \mathbf{t}, \qquad \text{on} \quad \Gamma_N, \tag{1.5}$$

$$\boldsymbol{\sigma}(\mathbf{u}) \cdot \mathbf{n} = \mathbf{0}, \qquad \text{on} \quad \Gamma_c. \tag{1.6}$$

with $\mathbf{n}$ is the outside normal to the domain Ω.
Let us define the space $\mathbf{H}^1(\Omega) = H^1(\Omega, \mathbb{R}^2) = [H^1(\Omega)]^2$ where $H^1(\Omega)$ denotes the classical Sobolev space. Let V be the space of admissible displacements given by

$$V = \left\{ \mathbf{u} \in \mathbf{H}^1(\Omega) \quad ; \quad \mathbf{u} = \mathbf{0} \quad \text{on} \quad \Gamma_D \right\}.$$

Taking the inner product of the equilibrium equation (1.2) with $\mathbf{v} \in V$, and integrating over Ω leads to

$$-\int_\Omega \operatorname{div}\boldsymbol{\sigma}(\mathbf{u}) \cdot \mathbf{v}\, d\Omega = \int_\Omega \mathbf{f} \cdot \mathbf{v}\, d\Omega.$$

Using Green's formula for elasticity, we obtain

$$\int_\Omega \boldsymbol{\sigma}(\mathbf{u}) : \boldsymbol{\varepsilon}(\mathbf{v})\, d\Omega = \int_\Omega \mathbf{f} \cdot \mathbf{v}\, d\Omega + \int_{\partial\Omega} \boldsymbol{\sigma}(\mathbf{u})\, \mathbf{n} \cdot \mathbf{v}\, d\Omega.$$

Taking into account the boundary conditions, the previous equation reads

$$\int_\Omega \boldsymbol{\sigma}(\mathbf{u}) : \boldsymbol{\varepsilon}(\mathbf{v})\, d\Omega = \int_\Omega \mathbf{f} \cdot \mathbf{v}\, d\Omega + \int_{\partial\Omega} \mathbf{t} \cdot \mathbf{v}\, d\Omega \qquad \forall \mathbf{v} \in \mathbf{V}.$$

By using equation (1.3), the weak formulation can be written

$$\text{Find } \mathbf{u} \in V \text{ such that} \qquad a(\mathbf{u}, \mathbf{v}) = L(\mathbf{v}) \qquad \forall \mathbf{v} \in \mathbf{V},$$

with

$$a(\mathbf{u}, \mathbf{v}) = \int_\Omega \boldsymbol{\varepsilon}(\mathbf{v}) : \mathbb{C} : \boldsymbol{\varepsilon}(\mathbf{u})\, d\Omega,$$

$$L(\mathbf{v}) = \int_\Omega \mathbf{v}^T\, \mathbf{f}\, d\Omega + \int_{\partial\Omega} \mathbf{v}^T\, \mathbf{t}\, d\Omega.$$

Given $\mathbf{f} \in \mathbf{L}^2(\Omega)$ and $\mathbf{t} \in \mathbf{L}^2(\Gamma_N)$, thanks to Korn's inequality which implies the coercivity of $a(\mathbf{u}, \mathbf{v})$, the existence and uniqueness of the solution to the weak formulation are garanteed by Lax-Milgram's Lemma [1]

1.1.3 Incompressible formulation

For incompressible elasticity problems, the classical formulation is unsatisfactory. Indeed, the discretized problem leads to locking solution. To solve this problem, Hermann proposed a particular form of the principle of Hellinger-Reisner [2]. He reformulated this principle by decoupling the volume and deviatoric contributions of stress and strain. If we assume that the deviatoric

part is calculated from the displacement and the hydrostatic pressure is an independent variable, we find the mixed formulation in $\mathbf{u}$ and p.

The problem of linear elasticity is given by the system:

$$\begin{aligned} -\operatorname{div}\boldsymbol{\sigma} &= \mathbf{f}, && \text{in} \quad \Omega, \\ \boldsymbol{\sigma} &= \mathbb{C} : \boldsymbol{\varepsilon}, && \text{in} \quad \Omega, \\ \mathbf{u} &= \mathbf{0}, && \text{on} \quad \Gamma_D, \\ \boldsymbol{\sigma}\cdot\mathbf{n} &= \mathbf{t}, && \text{on} \quad \Gamma_N, \\ \boldsymbol{\sigma}\cdot\mathbf{n} &= \mathbf{0}, && \text{on} \quad \Gamma_c. \end{aligned}$$

Let p be the hydrostatic pressure defined in two dimensions by:

$$p = -\frac{\operatorname{tr}(\boldsymbol{\sigma})}{2}.$$

Now we decompose the stress tensor $\boldsymbol{\sigma}$ in two parts: the spherical part and the deviatoric part $\boldsymbol{\sigma}^d$ given by:

$$\boldsymbol{\sigma}^d(\mathbf{u}) = \boldsymbol{\sigma}(\mathbf{u}) + p\,\mathbf{I} = 2\mu\boldsymbol{\varepsilon}^d(\mathbf{u}),$$

where

$$\boldsymbol{\varepsilon}^d(\mathbf{u}) = \boldsymbol{\varepsilon}(\mathbf{u}) - \frac{\operatorname{div}(\mathbf{u})}{2}\,\mathbf{I}.$$

For a linear isotropic materials we have:

$$\boldsymbol{\sigma} = \lambda(\operatorname{div}\mathbf{u})\mathbf{I} + 2\mu\boldsymbol{\varepsilon}(\mathbf{u}),$$

where λ and μ are the two Lamé coefficients which are assumed to be positive.
Let k be a bulk modulus given by: $k = \dfrac{E}{3(1-2\nu)}$ Then

$$\begin{aligned} \operatorname{tr}(\boldsymbol{\sigma}) &= \operatorname{tr}(\lambda(\operatorname{div}\mathbf{u})\mathbf{I} + 2\mu\boldsymbol{\varepsilon}(\mathbf{u})) = \lambda(\operatorname{div}\mathbf{u})\operatorname{tr}(\mathbf{I}) + 2\mu\operatorname{tr}(\boldsymbol{\varepsilon}(\mathbf{u})) \\ &= (3\lambda + 2\mu)(\operatorname{div}\mathbf{u}) = 3k(\operatorname{div}\mathbf{u}). \end{aligned}$$

Therefore

$$p = -k\operatorname{div}\mathbf{u}. \tag{1.7}$$

When the material is incompressible ($\nu = 0.5$), the bulk modulus tends to infinity. This means that the displacement field must be divergence free when the behavior tends to be incompressible and

$$\boldsymbol{\sigma}(\mathbf{u}) = \boldsymbol{\sigma}^d(\mathbf{u}) + p\,\mathbf{I}$$

Then the strong mixed formulation is written as follows

$$-\operatorname{div}[\boldsymbol{\sigma}^d - p\,\mathbf{I}] = \mathbf{f} \qquad \text{in} \qquad \Omega, \tag{1.8}$$

$$\operatorname{div}\mathbf{u} + \frac{1}{k}p = 0 \qquad \text{in} \qquad \Omega. \tag{1.9}$$

When k goes to infinity, the problem (1.8) and (1.9) becomes the incompressible problem

$$-\operatorname{div}[\boldsymbol{\sigma}^d - p\,\mathbf{I}] = \mathbf{f} \quad \text{in} \quad \Omega \tag{1.10}$$

$$\operatorname{div}\mathbf{u} = 0 \quad \text{in} \quad \Omega \tag{1.11}$$

Let $V = \left\{\mathbf{v} \in \mathbf{H}^1(\Omega) \quad \text{with } \mathbf{u} = 0 \text{ on } \Gamma_D\right\}$ and $Q = \mathbf{L}^2(\Omega)$.
Multiplying the first equation (resp. the second equation) of the strong formulation by a test function $\mathbf{v} \in V$ (resp. $q \in Q$). On applying Green's formula for elasticity, we find the weak mixed formulation

$$\begin{cases} \text{Find } (\mathbf{u}, p) \in (V, Q) \text{ such that:} \\ \int_\Omega \boldsymbol{\sigma}^d(\mathbf{u}) : \boldsymbol{\varepsilon}(\mathbf{v})\, d\Omega - \int_\Omega p \operatorname{div}\mathbf{v}\, d\Omega = \int_\Omega \mathbf{f}\cdot\mathbf{v}\, d\Omega + \int_{\Gamma_N} \mathbf{t}\cdot\mathbf{v}\, d\Gamma, & \forall \mathbf{v} \in V, \\ \int_\Omega q \operatorname{div}\mathbf{u}\, d\Omega = 0, & \forall q \in Q. \end{cases}$$

Subsequently, the weak mixed formulation of the isotropic incompressible linear elastic problem is written as:

$$\begin{cases} \text{Find } (\mathbf{u}, p) \in (V, Q) \text{ such that:} \\ a(\mathbf{u}, \mathbf{v}) - b(\mathbf{v}, p) = L(\mathbf{v}), & \forall \mathbf{v} \in V, \\ b(\mathbf{u}, q) = 0, & \forall q \in Q, \end{cases} \tag{1.12}$$

with:
$a(\mathbf{u}, \mathbf{v}) = \int_\Omega \boldsymbol{\sigma}^d(\mathbf{u}) : \boldsymbol{\varepsilon}(\mathbf{v})\, d\Omega$,
$b(\mathbf{v}, p) = \int_\Omega p \operatorname{div}\mathbf{v}\, d\Omega$,
$L(\mathbf{v}) = \int_\Omega \mathbf{f}\cdot\mathbf{v}\, d\Omega + \int_{\Gamma_N} \mathbf{t}\cdot\mathbf{v}\, d\Gamma$.

Proposition 1 ([1]). *Let $a : V \otimes V \longrightarrow \mathbb{R}$ and $b : V \otimes Q \longrightarrow \mathbb{R}$ be two continuous bilinear forms that satisfy:*

- *The bilinear form $a(\cdot,\cdot)$ is coercive on $\ker B$,i.e.,*

$$\exists \alpha > 0 \quad ; \quad a(\mathbf{v}, \mathbf{v}) \geq \alpha \parallel \mathbf{v} \parallel^2_{1,\Omega} \ \forall \mathbf{v} \in \ker B.$$

- *There exists a constant $\beta > 0$ such that the following inf-sup condition holds:*

$$\inf_{q \in Q} \sup_{\mathbf{v} \in V} \frac{b(\mathbf{v}, q)}{\parallel q \parallel_{0,\Omega} \parallel \mathbf{v} \parallel_{1,\Omega}} \geq \beta.$$

Then there exists a unique solution $(\mathbf{u}, p)$ of the weak formulation (1.12).

Remark: The coercivity condition follows from the Korn's inequality. To show the inf sup condition it suffices to show that $\operatorname{Im} B$ is closed.

1.1.3.1 Discrete problem

Discretization of the elasticity problem follows the usual steps. We approximate $(\mathbf{u}, p)$ by $(\mathbf{u}_h, p_h) \in V_h \otimes Q_h$. The subspaces V_h and Q_h are finite dimensional that will be defined later. The discretized problem is then:

$$\left\{ \begin{array}{ll} \text{Find } (\mathbf{u}_h, p_h) \in (V_h, Q_h) \text{ such that} & \\ a(\mathbf{u}_h, v_h) - b(\mathbf{v}_h, p_h) = L(\mathbf{v}_h), & \forall \mathbf{v}_h \in V_h, \\ b(\mathbf{u}_h, q_h) = 0, & \forall q_h \in Q_h. \end{array} \right. \tag{1.13}$$

Proposition 2 (Existence and uniqueness of the discrete problem [1]). *Under the following conditions:*

- *The bilinear form $a(\cdot,\cdot)$ is coercive on $\ker B_h$ i.e.;*

$$\exists \alpha > 0 \quad ; \quad a(\mathbf{v}_h, \mathbf{v}_h) \geq \alpha \parallel \mathbf{v}_h \parallel^2_{1,\Omega} \ \forall \mathbf{v}_h \in \ker B_h.$$

- *There exists a constant $\beta_h > 0$ such that the following inf-sup condition holds:*

$$\inf_{q \in Q_h} \sup_{\mathbf{v} \in V_h} \frac{b(\mathbf{v}_h, q_h)}{\parallel q_h \parallel_{0,\Omega} \parallel \mathbf{v}_h \parallel_{1,\Omega}} \geq \beta_h$$

There exists a unique solution (u_h, p_h) of the discrete weak formulation (1.13).

Remark: The constant β_h appears in the error bound so that we can loose the convergence of the discrete solution to the continuous solution. To avoid this problem we must show that:

$$\inf_{q \in Q_h} \sup_{\mathbf{v} \in V_h} \frac{b(\mathbf{v}_h, q_h)}{\parallel q_h \parallel_{0,\Omega} \parallel \mathbf{v}_h \parallel_{1,\Omega}} \geq \beta_0 > 0,$$

with β_0 independent of h. This condition it is the Ladyzhenskaya-Brezzi-Babuska condition (LBB) sometimes called ins-sup condition [1].

1.1.3.2 Stability of the mixed formulation

Proposition 3 ([1]). *Under the assumptions of existence and uniqueness of solutions $(\mathbf{u}, p)$ and $(\mathbf{u}_h, p_h)$ of continuous and discrete problems (1.12) and (1.13) and if the LBB condition is satisfied then:*

$$\parallel \mathbf{u} - \mathbf{u}_h \parallel_{1,\Omega} + \parallel p - p_h \parallel_{0,\Omega} \leq c \left[\inf_{\mathbf{v}_h \in V_h} \parallel \mathbf{u} - \mathbf{v}_h \parallel_{1,\Omega} + \inf_{q_h \in Q_h} \parallel p - q_h \parallel_{0,\Omega} \right].$$

The constant c appearing in the preceding proposition depends, among other things, on $\frac{1}{\alpha}$ and $\frac{1}{\beta_0}$ hence the importance that the latter constant does not depend on h. Therefore, despite the inf-sup condition is satisfied, we do not have always converge towards the exact solution. The preceding proposition is valid only if the LBB condition is verified. However, the verification of

this condition for a couple (V_h, Q_h) is very difficult to prove in practical situations. Therefore, the numerical evaluation of the inf-sup has been widely studied (see Chapelle and Bathe [3]). The numerical evaluation gives an indication of the verification of the LBB condition for a given finite element discretization. The numerical inf-sup test is based on the following proposition.

Proposition 4 ([3]). *Let $[B]$, $[M]_{uu}$ and $[M]_{pp}$ be the matrices associated with the bilinear form $b(\cdot,\cdot)$, the $\mathbf{H}^1$-inner product in V_h and the $\mathbf{L}^2$-inner product in Q_h and Let μ_{min} the smallest nonzero eigenvalue of the eigenvalue problem :*

$$[B]^T [M]_{uu}^{-1} [B] \mathbf{V} = \mu^2 [M]_{pp} \mathbf{V}.$$

Then the value of β_0 in the LBB condition is simply μ_{min}.

The numerical test proposed in [3] is to check the stability of the mixed formulation by calculating β_h with increasingly refined meshes. Indeed, if $\log(\beta_h)$ continuously decreases as h tends to 0, Chapelle and Bathe [3] predicted that the finite element violates the LBB condition. Otherwise, if β_h stabilizes when the number of elements increases, then the numerical inf-sup test is verified.

1.2 Contact condition

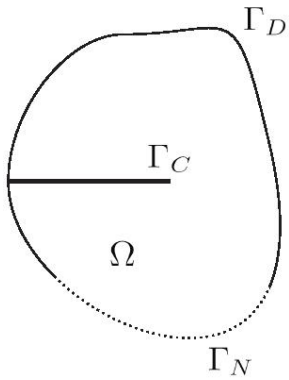

Figure 1.2: Cracked domain

The contact phenomenon was introduced by Léonard de Vinci in the fifteenth century. However, the mathematical study of the contact phenomenon is quite recent. In 1882, Hertz [4] solved the contact problem of two elastic bodies with curved surfaces. In 1933 Signorini formulate the general problem of the equilibrium of a linearly elastic body in contact with a rigid frictionless foundation. The unilateral contact condition was formulated by Signorini in 1959 [5]. The first rigorous analysis of a class of Signorini problems was done in the work of Fichira [6] where the Signorini problem was solved by using variational inequality. In this work, we are mainly interested in the elastostatic unilateral contact problem in cracked domain: frictionless or frictional unilateral contact.

1.2.1 Frictionless unilateral contact condition in cracked domain

The frictionless unilateral contact condition is expressed by the following complementarity relation:

$$[\![u_n]\!] \leq 0, \quad \sigma_n(\mathbf{u}) \leq 0, \quad \sigma_n(\mathbf{u})[\![u_n]\!] = 0, \quad \sigma_t(\mathbf{u}) = \mathbf{0}, \tag{1.14}$$

where $[\![u_n]\!]$ is the jump of the normal displacement across the crack Γ_C (see Fig 1.2).
The inequality $[\![u_n]\!] \leq 0$ shows that there is no penetration between the crack lips. The rest of this condition shows that if there is no contact (i.e., $[\![u_n]\!] < 0$), then there is no reaction between the crack lips of the crack, i.e. $\sigma_n(\mathbf{u}) = 0$; if there is contact (i.e., $[\![u_n]\!] = 0$), then there is a normal compression force ($\sigma_n(\mathbf{u}) < 0$) between the crack lips. The absence of the tangential forces of friction is expressed by $\sigma_t(\mathbf{u}) = 0$.

1.2.2 Frictional unilateral contact condition in cracked domain

The simplest friction law is the Tresca friction. It allows to write the unilateral contact problem as a constrained optimization problem. It reads as follows:

$$\begin{cases} |\sigma_t(\mathbf{u})| \leq s, & \text{a.e. on } \Gamma_C, \\ \text{if} \quad [\![\mathbf{u}_t]\!] = 0, & \text{then} \quad |\sigma_t(\mathbf{u})| < s, \\ \text{if } [\![\mathbf{u}_t]\!] \neq 0 & \text{then} \quad \sigma_t(\mathbf{u}) = -s\frac{[\![u_t]\!]}{|[\![u_t]\!]|}, \end{cases} \tag{1.15}$$

where $s \in L^2(\Gamma_C)$, $s \geq 0$ denotes the given slip threshold supposed independent of the normal stress. This condition expresses two physical situation: slip when $[\![\mathbf{u}_t]\!] \neq 0$ and stick when $[\![\mathbf{u}_t]\!] = 0$.
Often, especially in engineering literature, the slip threshold s is chosen as:

$$s = \mathcal{F}|\sigma_n(\mathbf{u})|$$

where $\mathcal{F}$ is the coefficient of friction. This choice leads to the classical version of Coulomb's law:

$$\begin{cases} |\sigma_t(\mathbf{u})| \leq -\mathcal{F}\sigma_n(\mathbf{u}), & \text{a.e.} \quad \text{on } \Gamma_C, \\ \text{if} \quad [\![\mathbf{u}_t]\!] = 0, & \text{then} \quad |\sigma_t(\mathbf{u})| < -\mathcal{F}\sigma_n(\mathbf{u}), \\ \text{if } [\![\mathbf{u}_t]\!] \neq 0 & \text{then} \quad \sigma_t(\mathbf{u}) = \mathcal{F}\sigma_n(\mathbf{u})\frac{[\![u_t]\!]}{|[\![u_t]\!]|}. \end{cases} \tag{1.16}$$

1.3 X-FEM: General aspects

1.3.1 Example introducing the concept of enrichment

To introduce the concept of discontinuous enrichment, we present an academic example [7]. Let Ω be the cracked domain. This domain is meshed by the classical finite-element method as indicated in Fig. 1.3.

A classical finite-element approximation associated with the duplicated mesh nodes is:

$$\mathbf{u}_h(\mathbf{x}) = \sum_{i=1}^{10} \mathbf{u}_i N_i(\mathbf{x})$$

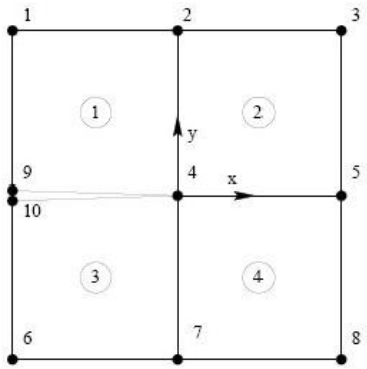

Figure 1.3: Finite element mesh near a crack tip, the circled numbers are element numbers

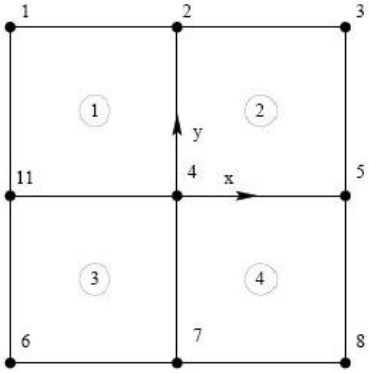

Figure 1.4: Regular mesh without a crack

with $\mathbf{u}_i$ is the displacement at node i and N_i is the scalar shape function associated with this node.
Set $\mathbf{a} = \dfrac{\mathbf{u}_9 + \mathbf{u}_{10}}{2}$, and $\mathbf{b} = \dfrac{\mathbf{u}_9 - \mathbf{u}_{10}}{2}$ then : $\mathbf{u}_9 = \mathbf{a} + \mathbf{b}$ and $\mathbf{u}_{10} = \mathbf{a} - \mathbf{b}$ and we can express $\mathbf{u}_h$ in terms of $\mathbf{a}$ and $\mathbf{b}$ by:

$$\mathbf{u}_h(\mathbf{x}) = \sum_{i=1}^{8} \mathbf{u}_i N_i(\mathbf{x}) + \mathbf{a}\,(N_9(\mathbf{x}) + N_{10}(\mathbf{x})) + \mathbf{b}\,(N_9(\mathbf{x}) + N_{10}(\mathbf{x}))H \tag{1.17}$$

where H is the jump function defined by:

$$H\begin{pmatrix} x \\ y \end{pmatrix} = \begin{cases} 1 & \text{if} \quad y > 0 \\ -1 & \text{if} \quad y < 0 \end{cases}$$

In the enriched finite-element method the nodes 9 and 10 shown in Fig. 1.3 are replaced by the single node 11 as shown in Fig. 1.4. By setting $N_{11} = (N_9 + N_{10})$, the finite element approximation (1.17) has the following form:

$$\mathbf{u}_h(\mathbf{x}) = \sum_{i=1}^{8} \mathbf{u}_i N_i(\mathbf{x}) + \mathbf{a}\, N_{11}(\mathbf{x}) + \mathbf{b}\, N_{11}(\mathbf{x})H(\mathbf{x}),$$

where the two terms on the left represent the classical finite-element approximation, and the third term represents the enrichment at the discontinuity. Hence, the notion of enrichment of the classical discretization space is introduced to enable the decoupling between the mesh and the domain discontinuities. We note that the X-FEM mesh (see Fig. 1.4) is performed without the geometrical discontinuity of the crack.

1.3.2 Classical X-FEM enrichment

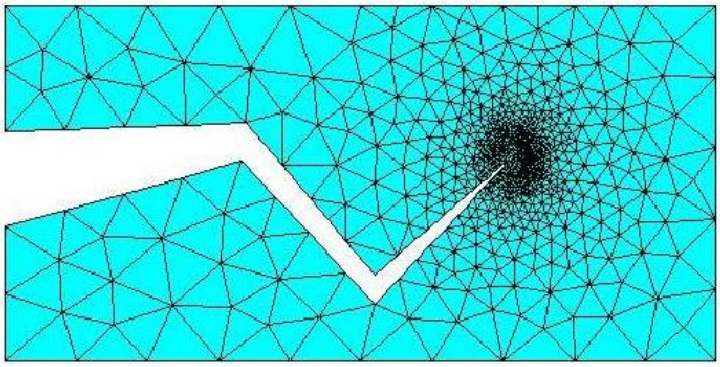

Figure 1.5: Cracked domain with FEM mesh

In the presence of a crack, there are two types of discontinuities: a strong discontinuity that results from a geometrical discontinuity of the studied domain and is reflected by a discontinuity in the displacement field; and a weak discontinuity at the crack tip which is manifested by the presence of a singularity in the stress field at the crack tip (see Fig. 1.5).
To represent these two types of discontinuities, the space of classical finite element discretization is enriched by two types of enhancements:

- Heaviside enrichment.
- Westergaard enrichment.

This enrichment procedure was introduced for the first time in 1999 by Möes et al. [7, 8].

1.3.2.1 Heaviside enrichment

To represent the jump of displacement across the crack Γ_c, Moës et al. used the Heaviside-like function:

$$H(\mathbf{x}) = \begin{cases} 1 & \text{if} \quad (\mathbf{x} - \mathbf{x}^*) \cdot \mathbf{n} > 0 \\ -1 & \text{elsewhere} \end{cases}$$

where $\mathbf{x}^*$ denotes the crack tip position vector and $\mathbf{n}$ is the outward unit normal to the crack. Indeed, all the nodes for which the support of their shape functions are completely cut by the crack (nodes represented by a circle in Fig. 1.6) are enriched by the Heaviside-like function.

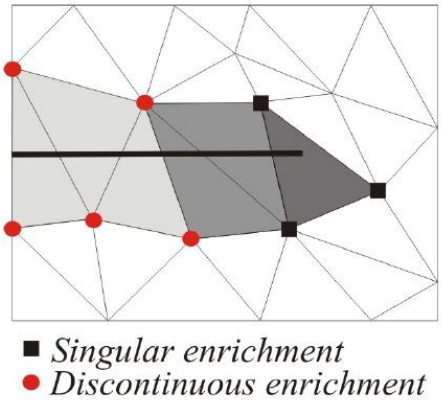

Figure 1.6: X-FEM enrichment

1.3.2.2 Enrichment with singular functions

To represent the singularity at the crack tip, the approximation of the displacement field is enriched with Westergaard functions based on asymptotic expansion of the displacement field of linear fracture mechanics [9] . For an isotropic homogeneous material, these functions have the following form [9]:

$$\begin{cases} u_x = \dfrac{1}{2\mu}\sqrt{\dfrac{r}{2\pi}}\left[K_I\cos(\frac{\theta}{2})\left(\delta-\cos(\theta)\right)+K_{II}\sin(\frac{\theta}{2})\left(\delta+2+\cos\theta\right)\right], \\ u_y = \dfrac{1}{2\mu}\sqrt{\dfrac{r}{2\pi}}\left[K_I\sin(\frac{\theta}{2})\left(\delta-\cos(\theta)\right)+K_{II}\cos(\frac{\theta}{2})\left(\delta-2+\cos\theta\right)\right]. \end{cases}$$

with:
K_I and K_{II} are the stress intensity factors,
r and θ are the polar coordinates with respect to the crack tip,

$$\delta = \begin{cases} 3-4\nu & \text{for plane strain,} \\ \dfrac{3-\nu}{1+\nu} & \text{for plane stress.} \end{cases}$$

These functions can be generated by the basis given by the four elementary functions:

$$F = \left\{\sqrt{r}\sin\frac{\theta}{2}, \sqrt{r}\cos\frac{\theta}{2}, \sqrt{r}\sin\frac{\theta}{2}\sin\theta, \sqrt{r}\cos\frac{\theta}{2}\sin\theta\right\}.$$

We note that only the first function of this basis is discontinuous across the crack. The other functions of the basis are added to improve accuracy.
For this type of enrichment, the set of nodes whose support of the shape function is partially cut by the crack (nodes represented by a square in the Fig. 1.6), are enriched by the Westergard functions.

1.3.2.3 Space discretization

The strategy for enrichment in classical X-FEM has two main steps:

- The nodes for which the support of their shape function is completely cut by the crack are enriched by the Heaviside-like function.

- The nodes for which the support of their shape function contains the crack tip are enriched with the singular functions of Westergaard.

Thereafter, the space discretization of X-FEM is the direct sum of a classical finite element method V_h and the enrichment space associated to X-FEM such as:

$$V_h = \left\{ \mathbf{w}_h \,;\, \mathbf{w}_h(\mathbf{x}) = \sum_{i \in I} \mathbf{u}_i \varphi_i(\mathbf{x}) \qquad \text{with} \quad \mathbf{u}_i \in \mathbb{R}^2 \right\},$$

$$E_h = \left\{ \mathbf{e}_h \,;\, \mathbf{e}_h(\mathbf{x}) = \sum_{i \in I_H} \mathbf{a}_i \, H(\mathbf{x}) \varphi_i(\mathbf{x}) + \sum_{i \in I_F} \sum_{\alpha=1}^{4} \mathbf{b}_i^{\alpha} \, F_\alpha(r,\theta) N_i(\mathbf{x}) \text{ with } \quad \mathbf{a}_i, \mathbf{b}_i^{\alpha} \in \mathbb{R}^2 \right\},$$

where I_H and I_F are the sets of node indices enriched by the function H and the functions F_α, respectively. $N_i(\mathbf{x})$ and $\varphi_i(\mathbf{x})$) are the scalar shape functions associated with the classical finite-element method of order 1 and order k, respectively.
Consequently, the X-FEM enriched space can be written as:

$$\mathcal{V}_h = E_h \oplus V_h.$$

Hence the displacement field is written as follows:

$$\mathbf{u}_h(\mathbf{x}) = \sum_{i \in I} \mathbf{u}_i \varphi_i(\mathbf{x}) \; + \sum_{i \in I_H} \mathbf{a}_i \, H(\mathbf{x}) \varphi_i(\mathbf{x}) \; + \sum_{i \in I_F} \sum_{\alpha=1}^{4} \mathbf{b}_i^{\alpha} \, F_\alpha(r,\theta) N_i(\mathbf{x}).$$

1.3.3 Fixed enrichment area and convergence rate

The classical X-FEM, while reducing the error level, does not improve the convergence rate compared to a classical finite element method (see [9] and [10]). This can be explained by the fact that the topological enrichment only affects one layer of elements in the crack tip. So, when h goes to 0, the size of the zone of influence of the enrichment also tends to 0. To remedy this problem a geometrical enrichment is introduced. The idea is to enrich by the singular functions all the degrees of freedom contained in a whole fixed area around the crack tip (see Fig. 1.7). This variant of X-FEM reduces the errors with respect to the classical X-FEM and improves the convergence rate. In fact, one gains an optimal convergence (of order h for the H^1-norm with a P_1 finite element). However the conditioning of the associated linear system becomes higher when the number of degrees of freedom increases (see [11]). The X-FEM with fixed enrichment area is an expensive strategy since a large number of degrees of freedom is enriched by the singular functions.

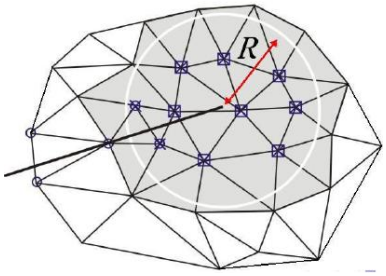

Figure 1.7: Geometrical enrichment

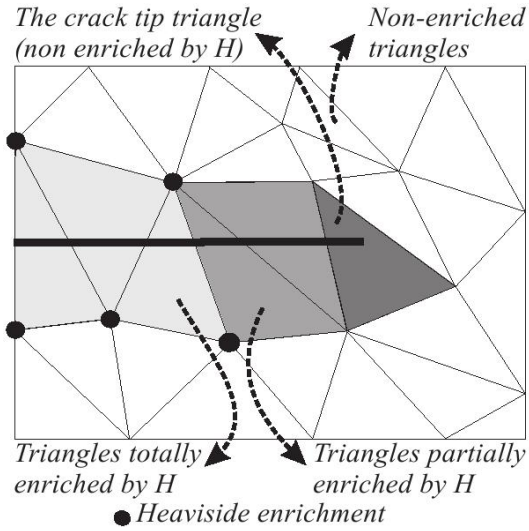

Figure 1.8: Enrichment strategy

1.3.4 X-FEM with a cut-off function

This enrichment was first introduced in 2006 by Chahine et al. (see [12]). This method gives optimal convergence results without increasing significantly the computational cost and without degrading the condition number of the linear system. This is done by using a cut-off function to localize the singular enrichment area. This means that with this function we enrich the entire area of crack tip, see Fig. 1.8.

1.3.4.1 X-FEM cut-off enriched space

As for the classical X-FEM, the X-FEM cut-off enriched space can be written as:

$$\tilde{\mathcal{V}}_h = \tilde{E}_h \oplus V_h.$$

with

$$\tilde{E}_h = \left\{ \mathbf{e}_h \,;\, \mathbf{e}_h(\mathbf{x}) = \sum_{i \in I_H} \mathbf{a}_i \, H(\mathbf{x}) \varphi_i(\mathbf{x}) \, + \sum_{\alpha=1}^{4} \mathbf{c}_\alpha \, F_\alpha(r,\theta) \chi(r) \quad \text{with} \;\; \boldsymbol{a}_i, \mathbf{c}_\alpha \in \mathbb{R}^2 \right\},$$

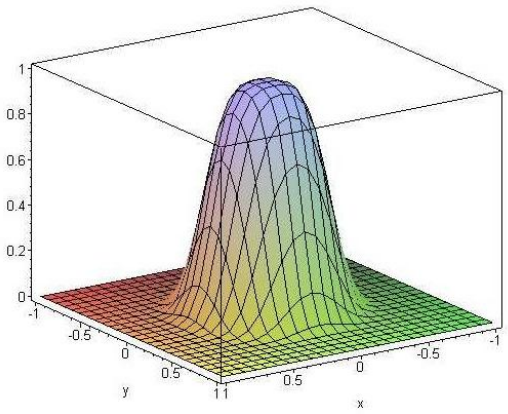

Figure 1.9: Cut-off function example

and χ is a cut-off function (see Fig. 1.9). The cut-off function is identical to a polynomial of order 5 between r_0 and R_1 such that:

$$\begin{cases} \chi(r) = 1 & \text{if } \mathrm{r} < \mathrm{r}_0 \\ \chi(r) = 0 & \text{if } \mathrm{r} > \mathrm{r}_1 \end{cases} \tag{1.18}$$

Then, the displacement field takes the following form:

$$\mathbf{u}_h(\boldsymbol{x}) = \sum_{i \in I} \mathbf{u}_i \varphi_i(\mathbf{x}) + \sum_{i \in I_H} \mathbf{a}_i \, H(\mathbf{x}) \varphi_i(\mathbf{x}) + \sum_{\alpha=1}^{4} \mathbf{c}_\alpha \, F_\alpha(r, \theta) \chi(r).$$

1.3.4.2 Convergence of X-FEM cut-off

Chahine et al. [12] have proved analytically that for shape functions of order 1, the rate of convergence is of order h. They also proved this result numerically for shape functions of order 1 and 2. In addition, this enrichment strategy keeps the optimal convergence without increasing the computational cost and without degraded the conditioning of the associated linear system.

1.4 Outline of the thesis

We consider saddle-point systems of equations resulting from the approximate numerical solution of PDEs (incompressible elastostatic problem, unilateral contact problem and elliptic boundary value problem) with Lagrange multiplier in the framework of the eXtended Finite Element Method X-FEM. Independently of the physical problem to be solved, the approximation spaces of the primal variable and the Lagrange multiplier can not be chosen independently from each other. Indeed, compatibility conditions (the onerous Inf-sup (or LBB) condition) must be satisfied to have convenient approximation. This condition ensures that discrete solutions converge to the exact solution as the mesh size h goes to zero. The purpose of this thesis is to find a way to prove or to overcome the onerous Inf-sup condition for such problem coming from the resolution

of constrained optimization problem with Lagrange multiplier. Except the first chapter, each chapter of this thesis corresponds to a published or submitted paper.

This thesis is organized as follows. In Chapter 2, we present a mathematical and numerical analysis of convergence and stability of the mixed formulation for incompressible elasticity in cracked domains. The goal is to extend the analysis of the X-FEM cut-off, done in the case of compressible elasticity, to the incompressible one. A mathematical proof of the inf-sup condition of the discrete mixed formulation with X-FEM is established for some enriched fields. We also give a mathematical result of quasi-optimal error estimate. Finally, we validate these results with numerical tests. In Chapter 3, we present a priori error estimates on the approximation of contact conditions in the framework of the eXtended Finite-Element Method (X-FEM) for two dimensional elastic bodies. This method allows to perform finite-element computations on cracked domains by using meshes of the uncracked domain. We consider a stabilized Lagrange multiplier method whose particularity is that no discrete inf-sup condition is needed in the convergence analysis. The contact condition is prescribed on the crack with a discrete multiplier which is the trace on the crack of a finite-element method on the uncracked domain, avoiding the definition of a specific mesh of the crack. Additionally, we present numerical experiments which confirm the efficiency of the proposed method. In chapter 4 a new consistent method based on local projections for the stabilization of a Dirichlet condition is presented in the framework of finite-element method with a fictitious domain approach. The presentation is made on the Poisson problem but the theoretical and numerical results can be extended straightforwardly to any elliptic boundary value problem. A numerical comparison is performed with the Barbosa-Hughes stabilization technique. The advantage of the new stabilization technique is to affect only the equation on multipliers and thus to be equation independent. In chapter 5, we propose a local projection stabilized Lagrange multiplier method to approximate the two-dimensional linear elastostatics unilateral contact problem with Tresca friction in the framework of the eXtended Finite Element Method (X-FEM). This last method allows to perform finite-element computations on cracked domains by using meshes of the uncracked domain. We study the existence, uniqueness and a priori error estimate of several hybrid discrete formulations.

Chapter 2

Numerical convergence and stability of mixed formulation with X-FEM cut-off

This chapter has been published in The European Journal of Computational Mechanics [13].

Contents

2.1 Introduction

The presence of a crack in a structure reveals two types of discontinuities: a strong discontinuity that requires an adapted mesh to the shape of the crack, hence the domain is meshed at each time step; and a weak discontinuity that requires refinement at the crack tip. These two operations lead to a huge computational cost. In order to overcome these difficulties we use the eXtended Finite Element Method (X-FEM). This method allows to model cracks, material inclusions and holes on nonconforming meshes. It was introduced by Moës et al. [7]. It consists in enriching the basis of the classical finite element method by a step function along the crack line and by some non-smooth functions representing the asymptotic displacement around the crack tip. To obtain an optimal accuracy, Chahine et al. introduced a new enrichment strategy [12]: the so called X-FEM cut-off. This enrichment strategy uses a cut-off function to locate the crack tip surface. In their work, Chahine et al. have shown that the X-FEM cut-off has an optimal convergence rate of order h and that the conditioning of the stiffness matrix does not deteriorate. In this work, we extend the numerical results given by Chahine et al. [12] to an incompressible isotropic linear plane elasticity problem in fracture mechanics. In particular, this formulation must satisfy the so-called inf-sup or "Ladyzhenskaya-Brezzi-Babuška condition" (LBB) condition.

2.2 Model problem and discretization

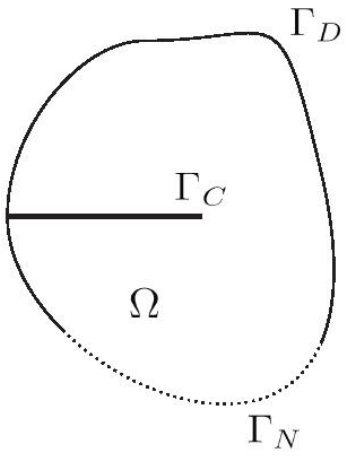

Figure 2.1: Cracked domain

Let Ω be a two-dimensional cracked domain, Γ_c denotes the crack and Γ the boundary of Ω. We assume that $\Gamma \setminus \Gamma_c$ is partitioned into two parts: Γ_N where a Neumann surface force $\mathbf{t}$ is applied and Γ_D where a Dirichlet condition $\mathbf{u} = \mathbf{0}$ is prescribed (see Fig. 2.2). We assume that we have a traction-free condition on Γ_c. Let $\mathbf{f}$ be the body force applied on Ω. The equilibrium equation, constitutive law and boundary conditions are given by

$$-\operatorname{div} \sigma(\mathbf{u}) = \mathbf{f}, \qquad \text{in} \quad \Omega, \tag{2.1}$$

$$\sigma(\mathbf{u}) = \lambda \operatorname{tr} \varepsilon(\mathbf{u})\, I + 2\mu\, \varepsilon(\mathbf{u}), \qquad \text{in} \quad \Omega, \tag{2.2}$$

$$\mathbf{u} = \mathbf{0}, \qquad \text{on} \quad \Gamma_D, \tag{2.3}$$

$$\sigma(\mathbf{u}) \cdot \mathbf{n} = \mathbf{t}, \qquad \text{on} \quad \Gamma_N, \tag{2.4}$$

$$\sigma(\mathbf{u}) \cdot \mathbf{n} = \mathbf{0}, \qquad \text{on} \quad \Gamma_c. \tag{2.5}$$

with $\varepsilon(\mathbf{u}) = \dfrac{1}{2}(\nabla \mathbf{u} + \nabla \mathbf{u}^T)$ and $\mathbf{n}$ is the outside normal to the domain Ω.
Let $V = \left\{ \mathbf{v} \in \mathbf{H}^1(\Omega) \quad \text{with } \mathbf{u} = 0 \text{ on } \Gamma_D \right\}$, $Q = \mathbf{L}^2(\Omega)$, σ^d the deviatoric part of σ and p the hydrostatic pressure. By a classical way we find the weak mixed formulation [1]

$$\begin{cases} \text{Find } (\mathbf{u}, p) \in (V, Q) \text{ such that:} \\ a(\mathbf{u}, \mathbf{v}) - b(\mathbf{v}, p) = L(\mathbf{v}), \qquad \forall \mathbf{v} \in \mathbf{V}, \\ b(\mathbf{u}, q) = 0, \qquad \forall q \in Q, \end{cases} \tag{2.6}$$

with $a(\mathbf{u}, \mathbf{v}) = \int_\Omega \sigma^d(\mathbf{u}) : \varepsilon(\mathbf{v})\, d\Omega$, $b(\mathbf{v}, p) = \int_\Omega p \operatorname{div} \mathbf{v}\, d\Omega$, $L(\mathbf{v}) = \int_\Omega \mathbf{f} \cdot \mathbf{v}\, d\Omega + \int_{\Gamma_N} \mathbf{t} \cdot \mathbf{v}\, d\Gamma$.
Discretization of the elasticity problem follows the usual steps. Let τ_h an affine mesh of the non cracked domain $\overline{\Omega}$. We approximate $(\mathbf{u}, p)$ by $(\mathbf{u}_h, p_h) \in V_h \times Q_h$. The subspaces V_h and Q_h are finite dimensional spaces that will be defined later. The discretized problem is then:

$$\begin{cases} \text{Find } (\mathbf{u}_h, p_h) \in (V_h, Q_h) \text{ such that} \\ a(\mathbf{u}_h, v_h) - b(\mathbf{v}_h, p_h) = L(\mathbf{v}_h), & \forall \mathbf{v}_h \in V_h, \\ b(\mathbf{u}_h, q_h) = 0, & \forall q_h \in Q_h. \end{cases} \tag{2.7}$$

The existence of a stable finite element approximate solution $(\mathbf{u}_h, p_h)$ depends on choosing a pair of spaces V_h and Q_h such that the following LBB condition holds:

$$\inf_{q_h \in Q_h} \sup_{\mathbf{v}_h \in V_h} \frac{b(\mathbf{v}_h, q_h)}{\| q_h \|_{0,\Omega} \| \mathbf{v}_h \|_{1,\Omega}} \geq \beta_0,$$

where $\beta_0 > 0$ is independent of h [1]. The satisfaction of this condition for a couple (V_h, Q_h) is very difficult to prove in practical situations. Therefore, the numerical evaluation of the inf-sup has been widely used [3]. It gives an indication of the verification of the LBB condition for a given finite element discretization.

2.3 X-FEM cut off approximation spaces

The idea of X-FEM is to use a classical finite element space enriched by some additional functions. These functions result from the product of global enrichment functions and some classical finite element functions. we consider the variant of X-FEM which uses a cut-off function to define the singular enrichment surface. The classical enrichment strategy for this problem is to use the asymptotic expansion of the displacement and pressure fields at the crack tip area. Indeed, the displacement is enriched by the Westergaard functions:

$$F^u = \left\{ F_j^u(x), 1 \leq j \leq 4 \right\} = \left\{ \sqrt{r} \sin \frac{\theta}{2}, \sqrt{r} \cos \frac{\theta}{2}, \sqrt{r} \sin \frac{\theta}{2} \sin \theta, \sqrt{r} \cos \frac{\theta}{2} \sin \theta \right\},$$

where (r, θ) are polar coordinates around the crack's tip. These functions allow to generate the asymptotic non-smooth function at the crack's tip [11]. For the pressure, the asymptotic expansion at the crack tip is given by $p(r,\theta) = \frac{2K_I}{3\sqrt{2\pi r}} \cos \frac{\theta}{2} + \frac{2K_{II}}{3\sqrt{2\pi r}} \sin \frac{\theta}{2}$ where K_I and K_{II} are the stress intensity factors. This expression is used to obtain the basis of enrichment of the pressure in the area of the crack's tip [14]:

$$F^p = \left\{ F_j^p(x), 1 \leq j \leq 2 \right\} = \left\{ \frac{1}{\sqrt{r}} \cos \frac{\theta}{2}; \frac{1}{\sqrt{r}} \sin \frac{\theta}{2} \right\}.$$

The displacement and pressure are also enriched with a Heaviside-like function at the nodes for which the support of the corresponding shape functions is totally cut by the crack. Using this enrichment strategy, the discretization spaces V_h and Q_h take the following forms:

$$V_h = \left\{ \mathbf{v}_h = \sum_{i \in I} \alpha_k \boldsymbol{\psi}_{u,k} + \sum_{i \in I_H} \beta_k H \boldsymbol{\psi}_{u,k} + \sum_{j=1}^{4} \gamma_j F_j^u \chi; \quad \alpha_k, \beta_k, \gamma_j \in \mathbb{R} \right\},$$

$$Q_h = \left\{ p_h = \sum_{i \in I} p_i \, \varphi_{p,i} + \sum_{i \in I_H} b_i^p H \varphi_{p,i} + \sum_{j=1}^{2} c_j^p F_j^p \chi; \quad p_i, b_i^p, c_j^p \in \mathbb{R} \right\},$$

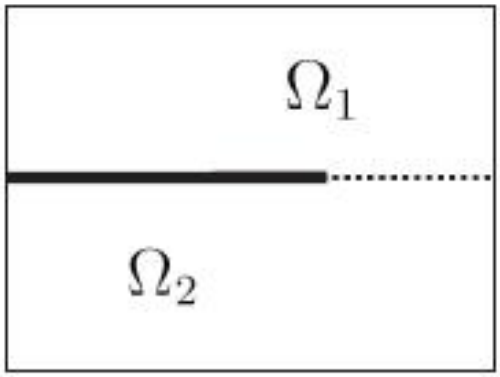

Figure 2.2: Domain decomposition

with I the set of node indices of τ_h, I_H the set of node indices of τ_h for which the supports of the shape functions are totally cut by the crack, $\varphi_{u,i}$ (resp. $\varphi_{p,i}$) being the scalar shape functions for displacement (resp. for pressure), $\boldsymbol{\psi}_{u,k}$ being the vector shape functions defined by $\boldsymbol{\psi}_{u,k} = \begin{cases} \begin{pmatrix} \varphi_{u,i} \\ 0 \end{pmatrix} & \text{if } i = \dfrac{k+1}{2}, \\ \\ \begin{pmatrix} 0 \\ \varphi_{u,i} \end{pmatrix} & \text{if } i = \dfrac{k}{2}, \end{cases}$, $H(\cdot)$ is the Heaviside-like function used to represent the discontinuity across the straight crack and defined by $H(\mathbf{x}) = \begin{cases} +1 & \text{if } (\mathbf{x}-\mathbf{x}^*)\cdot\mathbf{n}^+ \geq 0, \\ -1 & \text{otherwise,} \end{cases}$ and χ being a $\mathscr{C}^1$-piecewise function which is polynomial of degree 3 in the annular region $r_0 \leq r \leq r_1$, and satisfies $\chi(r) = 1$ if $r < r_0$ and $\chi(r) = 0$ if $r > r_1$. In our case we take $\chi(r) = \dfrac{2r^3 - 3(r_0+r_1)r^2 + 6r_1r_0r + (r_0 - 3r_1)r_0^2}{(r_0-r_1)^3}$ if $r_0 \leq r \leq r_1$ with $r_0 = 0.01$ and $r_1 = 0.49$.

2.4 Proof of inf-sup condition and error analysis

In this section we prove that the LBB condition holds for the P_2/P_0 element without the singular enrichment of the pressure. In order to simplify the presentation we assume that the crack cuts the mesh far enough from the vertices. We use a general technique introduced by Brezzi and Fortin [1].

2.4.1 Construction of a H_1-stable interpolation operator

The proof of the LBB condition requires the definition of an interpolation operator adapted to the proposed method. Since the displacement field is discontinuous across the crack on Ω, we divide Ω into Ω_1 and Ω_2 according to the crack (Γ_c) and a straight extension ($\tilde{\Gamma}_c$) of it (Fig. 2.2). Let $\mathbf{u}^k$ be the restriction of $\mathbf{u}$ to Ω_k, $k \in \{1,2\}$. As $\mathbf{u} \in \mathbf{H}^1(\Omega)$ then there exists an extension

$\tilde{\mathbf{u}}^k$ in $\mathbf{H}^1(\overline{\Omega})$ of $\mathbf{u}^k$ to $\overline{\Omega}$ such that:

$$\| \tilde{\mathbf{u}}^k \|_{1,\Omega} \leq C_k \| \mathbf{u}^k \|_{1,\Omega_k}, \tag{2.8}$$

where C_k is independent of $\mathbf{u}$ [15].

Definition 1. *Given a displacement field $\mathbf{u} \in \mathbf{H}^1(\Omega)$ and two extensions $\tilde{\mathbf{u}}^1$ and $\tilde{\mathbf{u}}^2$ of $\mathbf{u}^1$ and $\mathbf{u}^2$ in $\mathbf{H}^1(\overline{\Omega})$, respectively, we define $\Pi_1\mathbf{u}$ as the element of V_h such that:*

$$\Pi_1\mathbf{u} = \sum_{j\in I\setminus I_H} \boldsymbol{\alpha}_j\varphi_j + \sum_{j\in I_H} \left[\boldsymbol{\beta}_j\varphi_j H_1 + \boldsymbol{\gamma}_i\varphi_j H_2\right], \tag{2.9}$$

with

$$H_1(\mathbf{x}) = \begin{cases} 1 & \text{if} \quad \mathbf{x} \in \Omega_1, \\ 0 & \text{if} \quad \mathbf{x} \in \Omega_2, \end{cases} \qquad H_2(\mathbf{x}) = 1 - H_1(\mathbf{x}),$$

$$\boldsymbol{\alpha}_i = \frac{1}{|\,\Delta_i\,|}\int_{\Delta_i} \tilde{\mathbf{u}}^k \mathrm{d}x \ \text{ if } \mathbf{x}_\mathrm{i} \in \Omega_\mathrm{k}, \quad \boldsymbol{\beta}_\mathrm{i} = \frac{1}{|\,\Delta_\mathrm{i}\,|}\int_{\Delta_\mathrm{i}} \tilde{\mathbf{u}}^1 \mathrm{dx},$$

$$\boldsymbol{\gamma}_i = \frac{1}{|\,\Delta_i\,|}\int_{\Delta_i} \tilde{\mathbf{u}}^2 \mathrm{d}x, \ S_j := \bigcup\{S \in \tau_h : \mathrm{supp}(\varphi_j) \cap S \neq \emptyset\},$$

where Δ_j is the maximal ball centered at x_j such that $\Delta_j \subset S_j$ and $\{\mathbf{x}_j\}_{j=1}^J$ are the interior nodes of mesh τ_h.

This definition is inspired by the work of Chen and Nochetto [16].

Lemma 1. *The interpolation operator defined by [2.9] satisfies $\forall \mathbf{u} \in \mathbf{H}_0^1(\Omega)$*

$$\| \Pi_1\mathbf{u} \|_{1,\Omega} \leqslant C \| \mathbf{u} \|_{1,\Omega}, \tag{2.10}$$

$$\| \mathbf{u} - \Pi_1\mathbf{u} \|_{r,\Omega} \leqslant Ch^{1-r} \ \| \mathbf{u} \|_{1,\Omega}, \quad r = \{0,1\}. \tag{2.11}$$

Proof: In the proof we take $i \in \{1,2\}$, $k = 3-i$ and $\tilde{s}$ the union of all elements surrounding the elment s of τ_h.

In order to prove this Lemma, we calculate the above estimates locally on every different type of triangles: non-enriched triangles, triangles cut by the straight extension of the crack, triangles partially enriched by the discontinuous functions, triangles containing the crack tip and triangles totally enriched by the discontinuous functions. Before, let us establish the following intermediary result:

Lemma 2. *Let δ be a cracked square of size h centered at the crack tip (see Fig. 2.3) and $f \in H^1(\delta)$ with $f(\boldsymbol{x}) = 0$, $\forall x \in \tilde{\Gamma}_c \bigcap \delta$ (where $\tilde{\Gamma}_c$ is the extension of the crack Γ_c). Then, there exists $c > 0$, independent of h such that:*

$$\| f \|_{0,\delta} \leq ch \| \nabla f \|_{0,\delta} \,. \tag{2.12}$$

Proof: Dividing the square into two parts δ^+ (above the crack) and δ^- (below the crack). Let $\hat{f^+} = f \circ T_k$ defined on the reference rectangle $\hat{\delta^+}$ (assumed of size 1) obtained by an affine

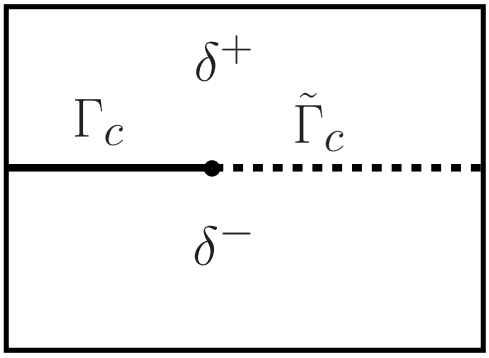

Figure 2.3: Centered domain on the crack tip

transformation T_K of the rectangle δ^+. Then, by construction, $\hat{f^+}(\boldsymbol{x}) = 0\ \forall \boldsymbol{x} \in \{x_1 \geq 0\} \times \{x_2 = 0\}$ which implies the following Poincaré inequality:

$$\| \hat{f^+} \|_{0,\hat{\delta^+}} \leq c \| \nabla \hat{f^+} \|_{0,\hat{\delta^+}} . \tag{2.13}$$

Using inequality [2.13] and the fact that the mesh is affine we obtain:

$$\begin{aligned} \| f \|_{0,\delta^+} &\leq c \mid \det(J_K) \mid^{1/2} \| \hat{f^+} \|_{0,\hat{\delta^+}} \leq c \mid \det(J_K) \mid^{1/2} \| \nabla \hat{f^+} \|_{0,\hat{\delta^+}} \\ &\leq c \mid \det(J_K) \mid^{-1/2} \| J_K \|_2 \mid \det(J_K) \mid^{1/2} \mid f \mid_{1,\delta^+} \leq c\, h \mid f \mid_{1,\delta^+} \end{aligned}$$

where $| \cdot |_{1,\delta^+}$ the $\mathbf{H}^1$ semi-norm on δ^+. Thus

$$\| f \|_{0,\delta^+} \leq c\, h \mid f \mid_{1,\delta^+}, \tag{2.14}$$

Similarly we prove the same result for δ^- which finish the proof of Lemma 2.

Non-enriched triangles:

Let s be a non-enriched triangle in Ω_i. In this case we have $\Pi_1 \mathbf{u} = \Pi_1 \tilde{\mathbf{u}}^i$ on Ω_i. Because $\tilde{\mathbf{u}}^i$ is continuous over Ω this operator is equivalent to the classical operator of Chen and Nochetto [16]. Then we have

$$\| \Pi_1 \mathbf{u} \|_{1,s} = \| \Pi_1 \tilde{\mathbf{u}}^i \|_{1,s} \leqslant c \| \tilde{\mathbf{u}}^i \|_{1,\tilde{s}} \tag{2.15}$$

and

$$\| \mathbf{u} - \Pi_1 \mathbf{u} \|_{r,s} = \| \mathbf{u}^i - \Pi_1 \tilde{\mathbf{u}}^i \|_{r,s} = \| \tilde{\mathbf{u}}^i - \Pi_1 \tilde{\mathbf{u}}^i \|_{r,s} \leqslant c h^{1-r} \| \tilde{\mathbf{u}}^i \|_{1,\tilde{s}}, \tag{2.16}$$

Triangles cut by the straight extension of the crack or containing the crack tip:

Let s be a triangle cut by the straight extension of the crack or containing the crack tip (see Fig. 2.4(c)). Then $\Pi_1 \mathbf{u} = \boldsymbol{\alpha}_1 \varphi_1 + \boldsymbol{\alpha}_2 \varphi_2 + \boldsymbol{\alpha}_3 \varphi_3$ on s, with: $\boldsymbol{\alpha}_1 = \frac{1}{\mid \Delta_1 \mid} \int_{\Delta_1} \tilde{\mathbf{u}}^1 \, \mathrm{d}x$, $\boldsymbol{\alpha}_2 = \frac{1}{\mid \Delta_2 \mid} \int_{\Delta_2} \tilde{\mathbf{u}}^2 \, \mathrm{d}x$ and $\boldsymbol{\alpha}_3 = \frac{1}{\mid \Delta_3 \mid} \int_{\Delta_3} \tilde{\mathbf{u}}^2 \, \mathrm{d}x$.
We remark that:

$$\Pi_1 \mathbf{u} = \tilde{\boldsymbol{\alpha}}_1 \varphi_1 + \boldsymbol{\alpha}_2 \varphi_2 + \boldsymbol{\alpha}_3 \varphi_3 + (\boldsymbol{\alpha}_1 - \tilde{\boldsymbol{\alpha}}_1) \varphi_1 = \Pi_1 \tilde{\mathbf{u}}^2 + (\boldsymbol{\alpha}_1 - \tilde{\boldsymbol{\alpha}}_1) \varphi_1,$$

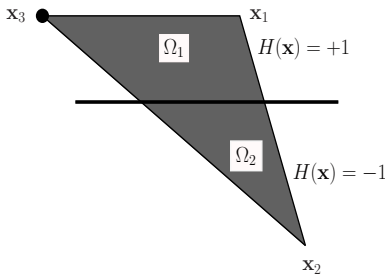

(a) A triangle partially enriched by the discontinuous functions

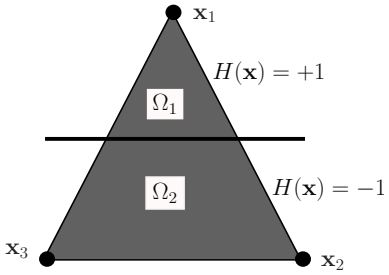

(b) A triangle totally enriched by the discontinuous functions

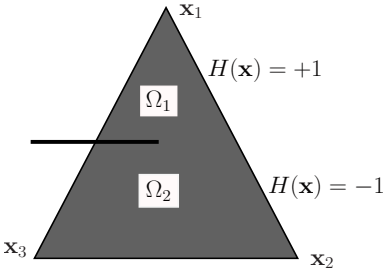

(c) A triangle containing the crack tip

Figure 2.4: The different types of enriched triangles. The enrichment with the Heaviside-like function are marked with a bullet.

with $\tilde{\boldsymbol{\alpha}}_1 = \dfrac{1}{|\,\Delta_1\,|}\int_{\Delta_1} \tilde{\mathbf{u}}^2\,\mathrm{d}x$. By the triangle inequality, we may write

$$\begin{aligned} \|\,\Pi_1\mathbf{u}\,\|_{1,s} &\leqslant \|\,\Pi_1\tilde{\mathbf{u}}^2\,\|_{1,s} + |\,\boldsymbol{\alpha}_1 - \tilde{\boldsymbol{\alpha}}_1\,|\,\|\,\varphi_1\,\|_{1,s},\\ \|\,\mathbf{u} - \Pi_1\mathbf{u}\,\|_{r,s} &\leqslant \|\,\mathbf{u} - \Pi_1\tilde{\mathbf{u}}^2\,\|_{r,s} + |\,\boldsymbol{\alpha}_1 - \tilde{\boldsymbol{\alpha}}_1\,|\,\|\,\varphi_1\,\|_{r,s}\\ &\leqslant \|\,\mathbf{u} - \tilde{\mathbf{u}}^2\,\|_{r,s} + \|\,\tilde{\mathbf{u}}^2 - \Pi_1\tilde{\mathbf{u}}^2\,\|_{r,s} + |\,\boldsymbol{\alpha}_1 - \tilde{\boldsymbol{\alpha}}_1\,|\,\|\,\varphi_1\,\|_{r,s}, \end{aligned}$$

where

$$\begin{aligned} \|\,\varphi_1\,\|_{r,s} &\leqslant ch^{1-r} && \text{because } \varphi_1 \text{ is the piecewise } P_1 \text{ basis function,}\\ \|\,\Pi_1\tilde{\mathbf{u}}^2\,\|_{r,s} &\leqslant ch^{1-r}\,\|\,\tilde{\mathbf{u}}^2\,\|_{1,\tilde{s}} && \text{because } \tilde{\mathbf{u}}^k \text{ is continuous over } \Omega\ ,\\ \|\,\mathbf{u} - \tilde{\mathbf{u}}^2\,\|_{0,s} &\leqslant c\,h\,\|\,\mathbf{u} - \tilde{\mathbf{u}}^2\,\|_{1,\delta}, \end{aligned}$$

and if we use Cauchy-Schwartz inequality and Lemma 2 we obtain

$$|\,\boldsymbol{\alpha}_1 - \tilde{\boldsymbol{\alpha}}_1\,| \leqslant \frac{\sqrt{|\,\Delta_1\,|}}{|\,\Delta_1\,|}\ \|\,\tilde{\mathbf{u}}^1 - \tilde{\mathbf{u}}^2\,\|_{0,\Delta_1} \leqslant c\frac{h}{\sqrt{|\,\Delta_1\,|}}\,\|\,\nabla(\tilde{\mathbf{u}}^1 - \tilde{\mathbf{u}}^2)\,\|_{0,\delta}\ .$$

Therefore

$$\|\,\Pi_1\mathbf{u}\,\|_{1,s} \leqslant c\big(\,\|\,\tilde{\mathbf{u}}^2\,\|_{1,\tilde{s}} + \|\,\tilde{\mathbf{u}}^1 - \tilde{\mathbf{u}}^2\,\|_{1,\delta}\,\big) \tag{2.17}$$

$$\|\,\mathbf{u} - \Pi_1\mathbf{u}\,\|_{r,s} \leqslant ch^{1-r}\,\big(\,\|\,\mathbf{u} - \tilde{\mathbf{u}}^2\,\|_{1,s} + \|\,\tilde{\mathbf{u}}^2\,\|_{1,\tilde{s}} + \|\,\tilde{\mathbf{u}}^1 - \tilde{\mathbf{u}}^2\,\|_{1,\delta}\,\big), \tag{2.18}$$

Triangles partially enriched by the discontinuous functions:
Let s be a triangle partially enriched by the discontinuous functions (see Fig. 2.4(a)). In this

case we have $\Pi_1\mathbf{u} = \Pi_1\tilde{\mathbf{u}}_1 + (\boldsymbol{\alpha}_2 - \tilde{\boldsymbol{\alpha}}_2)\varphi_2$ on $s \cap \Omega_1$ and $\Pi_1\mathbf{u} = \Pi_1\tilde{\mathbf{u}}_2 + (\boldsymbol{\alpha}_1 - \tilde{\boldsymbol{\alpha}}_1)\varphi_1$ on $s \cap \Omega_2$ with $\tilde{\boldsymbol{\alpha}}_1 = \dfrac{1}{\mid \Delta_1 \mid}\int_{\Delta_1} \tilde{\mathbf{u}}^2 \, \mathrm{d}x$ and $\tilde{\boldsymbol{\alpha}}_2 = \dfrac{1}{\mid \Delta_2 \mid}\int_{\Delta_2} \tilde{\mathbf{u}}^1 \, \mathrm{d}x$.
In the same manner we prove that

$$\| \Pi_1\mathbf{u} \|_{1,s\cap\Omega_i} \leqslant c \left(\| \tilde{\mathbf{u}}_i \|_{1,\tilde{s}} + \| \tilde{\mathbf{u}}^k - \tilde{\mathbf{u}}^i \|_{1,\delta} \right), \tag{2.19}$$

$$\| \mathbf{u} - \Pi_1\mathbf{u} \|_{r,s\cap\Omega_i} \leqslant c h^{1-r} \left(\| \tilde{\mathbf{u}}^i \|_{1,\tilde{s}} + \| \tilde{\mathbf{u}}^k - \tilde{\mathbf{u}}^i \|_{1,\delta} \right). \tag{2.20}$$

Triangles totally enriched by the discontinuous functions
Let s be the triangle totally enriched by the discontinuous functions (see Fig. 2.4(b)). In this case we have: $\Pi_1\mathbf{u} = \Pi_1\tilde{\mathbf{u}}^i$ on $s \cap \Omega_i$. Then we have

$$\| \Pi_1\mathbf{u} \|_{1,s\cap\Omega_i} \leqslant \| \Pi_1\tilde{\mathbf{u}}^i \|_{1,s}, \tag{2.21}$$

$$\| \mathbf{u} - \Pi_1\mathbf{u} \|_{r,s\cap\Omega_i} \leqslant \| \tilde{\mathbf{u}}^i - \Pi\tilde{\mathbf{u}}^i \|_{1,s} \leqslant c\, h^{1-r} \ \| \tilde{\mathbf{u}}^i \|_{r,\tilde{s}} \tag{2.22}$$

Inequalities [2.15], [2.17], [2.19], [2.21] imply the first inequality of Lemma 1. Inequalities [2.16], [2.18], [2.20], [2.22], imply the second and third inequalities of Lemma 1.

2.4.2 Construction of a local interpolation operator

In this subsection we prove the discrete inf-sup condition for the P_2/P_0 element with the additional assumption, that the crack cuts the mesh far enough from the nodes.

Definition 2. *Let $\mathbf{u} \in \mathbf{H}^1(\Omega)$. We define $\Pi_2\mathbf{u}$ as the element of V_h such that*

$$\Pi_2\mathbf{u} = \sum_{k\in\tau_h/\tau_H} \sum_{i=1}^{3} \boldsymbol{\alpha}_i\varphi_i + \sum_{k\in\tau_H} \sum_{i=1}^{3} \left(\boldsymbol{\beta}_i\varphi_i H_1 + \boldsymbol{\gamma}_i\varphi_i H_2\right), \tag{2.23}$$

where τ_H is the set of triangle totally cut by the crack, φ_i is the classical finite element shape function of order 2 associated to node i being the center of the edge e_i of the element K and with

$$\boldsymbol{\alpha}_i = \frac{\int_{e_i} \mathbf{u}}{\int_{e_i} \varphi_i}, \quad \boldsymbol{\beta}_i = \frac{\int_{e_i\cap\Omega_1} \mathbf{u}}{\int_{e_i\cap\Omega_1} \varphi_i}, \quad \boldsymbol{\gamma}_i = \frac{\int_{e_i\cap\Omega_2} \mathbf{u}}{\int_{e_i\cap\Omega_2} \varphi_i}.$$

Lemma 3. *Suppose that the crack cuts the mesh far enough from the nodes then the interpolation operator defined by [2.23] satisfies $\forall \mathbf{u} \in V_h$*

$$\int_{s\setminus\Gamma_c} \operatorname{div}(\mathbf{u} - \Pi_2\mathbf{u}) = 0 \qquad \forall s \in \tau_h,$$

$$\| \Pi_2\mathbf{u} \|_{1,s\cap\Omega_i} \leq c \left(h^{-1} \| \tilde{\mathbf{u}}^i \|_{0,s} + \mid \tilde{\mathbf{u}}^i \mid_{1,s}\right) \qquad \forall s \in \tau_h.$$

Therefore, the discrete inf-sup condition for the P_2/P_0 element holds.

Proof: The first equation is obvious. Now let s be a triangle totaly cut by the crack. Then by using triangle inequality, the hypothesis "crack far enough from nodes" and Cauchy-Schwarz

inequality we have:

$$| \Pi_2 \mathbf{u} |_{1,\widehat{s\cap\Omega_i}} \leq c \ | \widehat{\Pi_2 \mathbf{u}} |_{1,\widehat{s\cap\Omega_i}} \leq c \sum_{j=1}^{3} | \int_{\widehat{e_j\cap\Omega_i}} \hat{\mathbf{u}} | \ \frac{| \hat{\varphi}_j |_{1,\widehat{s\cap\Omega_i}}}{| \int_{\widehat{e_j\cap\Omega_i}} \hat{\varphi}_j |}$$
$$\leq c \sum_{j=1}^{3} \int_{\widehat{e_j\cap\Omega_i}} | \hat{\mathbf{u}} | \leq c \sum_{j=1}^{3} \int_{\hat{e}_j} | \hat{\tilde{\mathbf{u}}}^i | \leq c \ \| \hat{\tilde{\mathbf{u}}}^i \|_{1,\hat{s}}$$

and by a scaling argument we have:

$$\| \Pi_2 \mathbf{u} \|_{1,s\cap\Omega_i} \leq c \, (h^{-1} \| \tilde{\mathbf{u}}^i \|_{0,s} + | \tilde{\mathbf{u}}^i |_{1,s}). \tag{2.24}$$

Now for non-enriched triangle we use the same argument to prove:

$$\| \Pi_2 \mathbf{u} \|_{1,s} \leq c \, (h^{-1} \| \mathbf{u} \|_{0,s} + | \mathbf{u} |_{1,s}), \tag{2.25}$$

which finishes the proof of Lemma 3.

2.4.3 Error analysis

We suppose in this section that the non-cracked domain $\bar{\Omega}$ has a regular boundary, and that $\mathbf{f}$, $\mathbf{t}$ are smooth enough, for the solution $(\mathbf{u}, p)$ of the mixed elasticity problem to be written as a sum of a singular part $(\mathbf{u}_s, p_s)$ and a regular part $(\mathbf{u} - \mathbf{u}_s \, , \, p - p_s)$ in Ω satisfying $\mathbf{u} - \mathbf{u}_s \in \mathbf{H}^2$ and $p - p_s \in \mathbf{H}^1$.

Proposition 5. *Under the assumption of existence and uniqueness of solutions* $(\mathbf{u}, p)$ *and* $(\mathbf{u}_h, p_h)$ *of the continuous [2.6] and discrete [2.7] mixed elasticity problems, and if the LBB condition is satisfied, then:*

$$\| \mathbf{u} - \mathbf{u}_h \|_{1,\Omega} + \| p - p_h \|_{0,\Omega} \leq c \, h \, \left[\, \| \mathbf{u} - \chi \mathbf{u}_s \|_{2,\Omega} + \| p - \chi p_s \|_{1,\Omega} \, \right],$$

where χ *is the cut-off function.*

Proof. By using the equivalent Céa lemma (see [1]) we have $\forall \mathbf{v}_h \in V^h$ and $q_h \in Q^h$:

$$\| \mathbf{u} - \mathbf{u}_h \|_{1,\Omega} + \| p - p_h \|_{0,\Omega} \leq c \, \left[\, \| \mathbf{u} - \mathbf{v}_h \|_{1,\Omega} + \| p - q_h \|_{0,\Omega} \, \right]. \tag{2.26}$$

Now let $\Pi_h \mathbf{u}$ be the classical interpolation operator introduced by [17] then we have:

$$\| \mathbf{u} - \Pi_h \mathbf{u} \|_{1,\Omega} \leq c \, h \ \| \mathbf{u} - \chi \mathbf{u}_s \|_{2,\Omega} \, . \tag{2.27}$$

Let $\Pi_h p = \Pi_1 p + \sum_{i=1}^{2} c_i F_{ip} \, \chi = \Pi_1 p + \chi \, p_s$, where Π_1 is the interpolation operator defined in Section 2.4.1. Then:

$$\| p - \Pi_h p \|_{0,\Omega} = \| p_r - \Pi_1 p_r \|_{0,\Omega} \leq c \, h \ \| p_r \|_{1,\Omega} \, . \tag{2.28}$$

Finally, the result of Proposition 5 can be obtained by choosing $\mathbf{v}_h = \Pi_h \mathbf{u}$ and $q_h = \Pi_h p$ in [2.26] and by using equations [2.27] and [2.28].

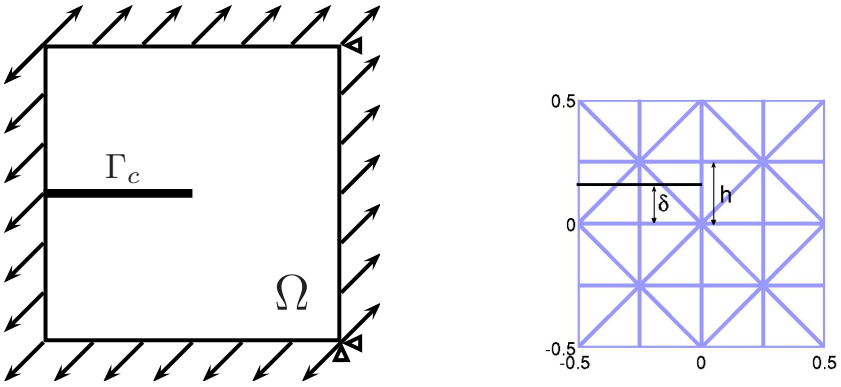

(a) Cracked specimen (b) Position of the crack.

Figure 2.5: Cracked specimen and position of the crack

2.5 Numerical study

The numerical tests are made on a non-cracked domain defined by $\bar{\Omega} =]-0.5, 0.5[\times]-0.5, 0.5[$, and the considered crack is the line segment $\Gamma_c =]-0.5; 0[\times\{0\}$ (see Fig. 2.5(a)). To remove rigid body motions, we eliminate three degrees of freedom (see Fig. 2.5(a)). In this numerical test, we impose only a boundary condition of Neumann type (see Fig. 2.5(a)), in order to avoid possibility of singular stress for mixed Dirichlet-Neumann condition at transition points. The finite element method is defined on a structured triangulation of $\bar{\Omega}$. The von Mises stress for this test is presented in Fig. 2.6(b). As expected the von Mises stress is concentrated at the crack tip. The notation P_i (resp. P_i^+) means that we use an extended finite-element method of order i (resp. with an additional cubic buble function) and P_j disc means that we use a discontinuous extended finite-element method. The reference solution is obtained with a structured $P_2/P1$ method and $h = 1/160$.

2.5.1 Numerical inf-sup test

In this section we numerically study the inf-sup condition and its dependence on the position of the crack. First, the inf-sup condition is evaluated using gradually refined structured triangulation meshes. The evolution of the numerical inf-sup value is plotted in Fig. 2.6(a) with respect to the element size. From this figure we can conclude that the numerical inf-sup value is stable

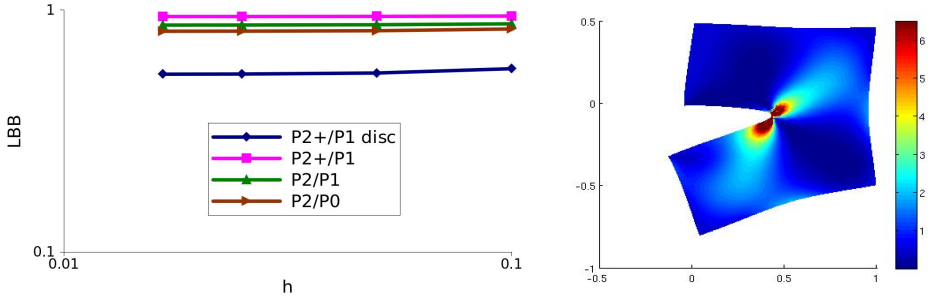

(a) Evaluation of the inf-sup condition (b) von Mises stress

Figure 2.6: Evolution of the inf-sup condition for mixed problem and von Mises stress ($\delta = 0$)

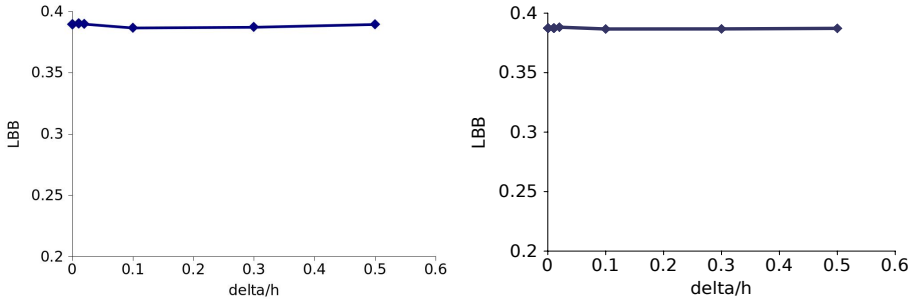

(a) $h = 1/10$ (b) $h = 1/100$

Figure 2.7: Evolution of the inf-sup condition as a function of the position of the crack

for all studied formulations. Let δ be the crack position as shown in Fig. 2.5(b). To test the influence of the position of the crack on the inf-sup condition, we check the LBB condition by decreasing δ. The tests are made, on a P_1^+/P_1 formulation, with $h = 1/100$ (see Fig. 2.7(a)) and $h = 1/10$ (see Fig. 2.7(b)). The results presented in Figs. 2.7(a) and 2.7(b) show that the inf-sup condition remains bounded regardless of the position of the crack. Hence, one can conclude that the formulation is stable independently of the position of the crack.

2.5.2 Convergence rate and the computational cost

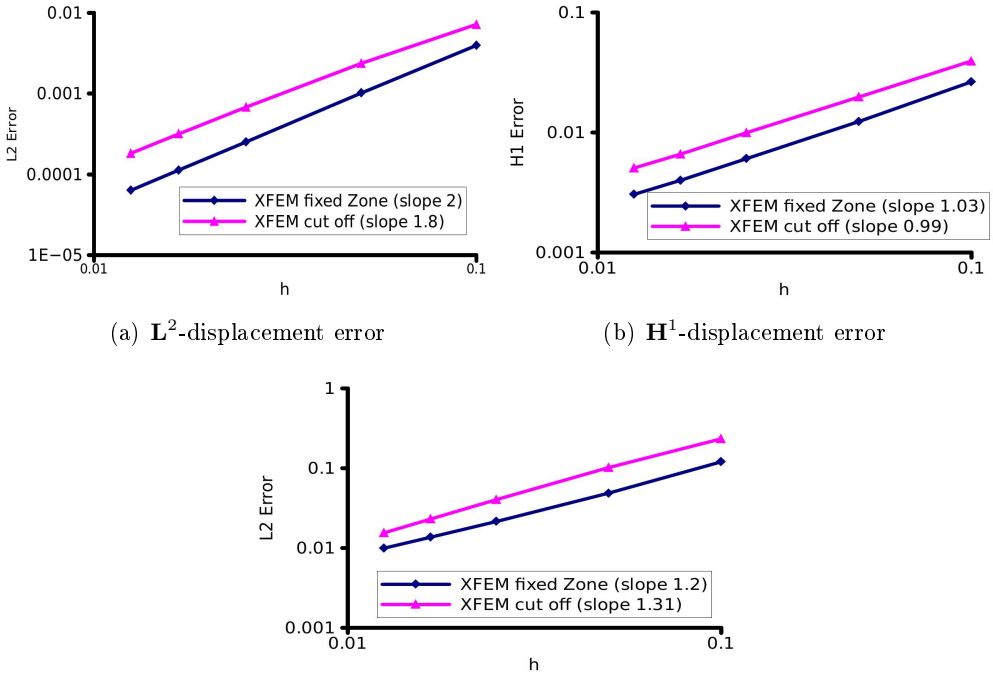

(a) $\mathbf{L}^2$-displacement error (b) $\mathbf{H}^1$-displacement error

(c) L^2-pressure error

Figure 2.8: Errors for the mixed problem with enriched P_1^+/P_1 elements.

Figures 2.8(a), 2.8(b) and 2.8(c) show a comparison between the convergence rates of the X-FEM fixed area and X-FEM cut off for the $\mathbf{L}^2$-norm and $\mathbf{H}^1$-norm ($P1^+/P_1$ element are used). These errors were obtained by running the test problem for some values of the parameter n_s, where n_s

Number of cells in each direction	Number of degrees of freedom	
	X-FEM fixed enrichment area	X-FEM Cut Off
40	13456	11516
60	30046	25666
80	53376	45416

Table 2.1: Number of degrees of freedom for enriched $P_2/P1$ element

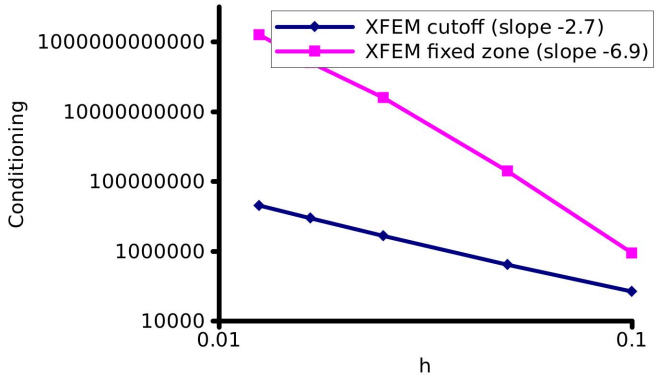

Figure 2.9: Conditioning number of the stiffness matrix for enriched $P_2/P1$ element

is the number of subdivision (number of cells) in each direction $h = \frac{1}{n_s}$. Figure 2.8(b) confirms that the convergence rate for the energy norm is of order h for both variants of the X-FEM: with fixed area and cut-off. Figure 2.8(a) shows that the convergence rates for the $\mathbf{L}^2$-norm in displacement is of order h^2 for both variants. Figure 2.8(c) shows that the convergence rates for the $\mathbf{L}^2$-norm in pressure is h for both variants. Compared to the X-FEM method with a fixed enrichment area, the convergence rate for X-FEM cut-off is very close but the error values are a bit larger. In order to test the computational cost of X-FEM cut-off, Table (2.1) shows a comparison between the number of degrees of freedom for different refinements of the classical method X-FEM with fixed enrichment area and the cut-off method. This latter enrichment leads to a significant decrease in the number of degrees of freedom. The condition number of the linear system associated to the cut-off enrichment is much better than the one associated with the X-FEM with a fixed enrichment area (see Fig. 2.9). We can conclude that, similarly to the X-FEM with fixed enrichment area, the X-FEM cut-off leads to an optimal convergence rate and also reduces the approximation errors but without significant additional costs.

The numerical tests of the higher order X-FEM method (P_2^+/P_1 disc, P_2^+/P_1, P_2/P_1 and P_2/P_0) do not give an optimal order of convergence (see Figs. 2.10(a), 2.10(b), 2.10(c) and 2.10(d)). This means that the enrichment function does not capture the behavior of the solution at the crack's tip. This result was expected as the asymptotic displacement at the crack tip belongs to $\mathbf{H}^{3/2-\eta}(\Omega)$ for all $\eta > 0$. Then, for the X-FEM cut-off, the convergence rate remains limited to $h^{3/2}$ with high order polynomials. To have an optimal convergence rate, one must make an asymptotic expansion of order 2 to find the correct expression of the enrichment basis

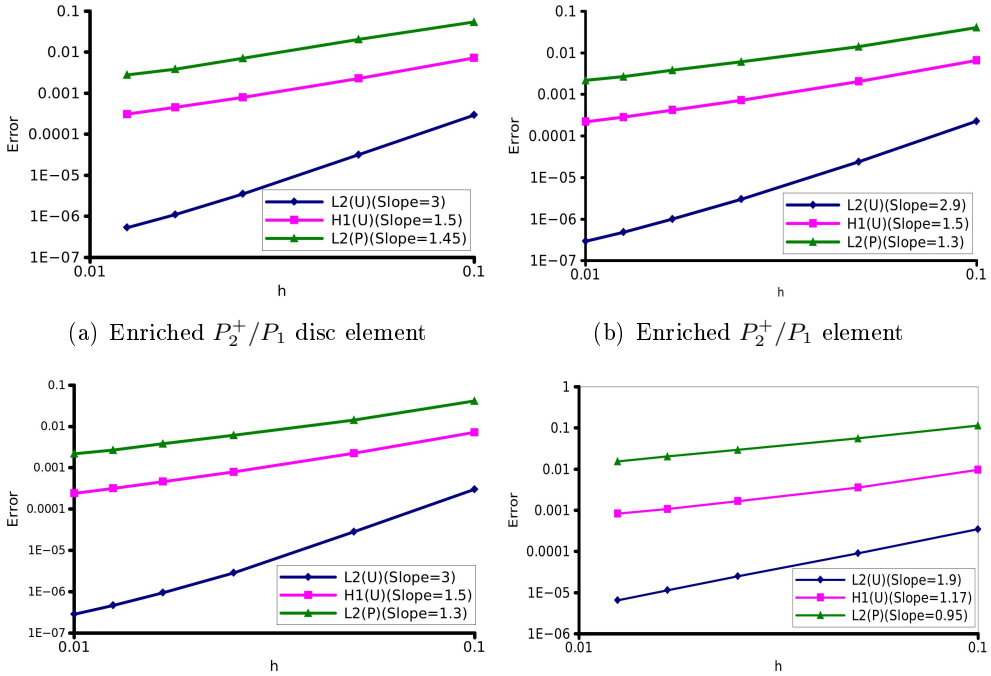

(a) Enriched P_2^+/P_1 disc element

(b) Enriched P_2^+/P_1 element

(c) Enriched P_2/P_1 element

(d) Enriched P_2/P_0 element

Figure 2.10: Convergence rate for the high-order elements (logarithmic scales) for the displacement and pressure.

2.6 Conclusion

From this study we can conclude that the X-FEM cut-off mixed formulation is stable, regardless of the position of the crack. Similarly to the X-FEM with fixed enrichment area, the X-FEM cut-off gives an optimal convergence rate but without significant additional costs. For shape functions of higher order, the convergence rate is limited to $h^{3/2}$. This result was expected as the main singularity belongs to $\mathbf{H}^{5/2-\eta}(\Omega)$ for all $\eta > 0$.

Chapter 3

A stabilized Lagrange multiplier method for the enriched finite-element approximation of contact problems of cracked elastic bodies

This chapter has been published in ESAIM:Mathematical Modelling and Numerical Analysis [18]

Contents

3.1 Introduction

With the aim of gaining flexibility in the finite-element method, Moës, Dolbow and Belytschko [7] introduced in 1999 the XFEM (eXtended Finite-Element Method) which allows to perform finite-element computations on cracked domains by using meshes of the non-cracked domain. The main feature of this method is the ability to take into account the discontinuity across the crack and the asymptotic displacement at the crack tip by addition of special functions into the finite-element space. These special functions include both non-smooth functions representing the singularities at the reentrant corners (as in the singular enrichment method introduced in [19]) and also step functions (of Heaviside type) along the crack.

In the original method, the asymptotic displacement is incorporated into the finite-element space multiplied by the shape function of a background Lagrange finite-element method. In this paper, we deal with a variant, introduced in [12], where the asymptotic displacement is

multiplied by a cut-off function. After numerous numerical works developed in various contexts of mechanics, the first a priori error estimate results for XFEM (in linear elasticity) were recently obtained in [12] and [17]: in the convergence analysis, a difficulty consists in evaluating the local error in the elements cut by the crack by using appropriate extension operators and specific estimates. In the latter references, the authors obtained an optimal error estimate of order h (h being the discretization parameter) for an affine finite-element method under H^2 regularity of the regular part of the solution (keeping in mind that the solution is expected to be at most in $H^{\frac{3}{2}-\varepsilon}$ for all $\varepsilon > 0$).

Let us remark that some convergence analysis results have been performed on a posteriori error estimation for XFEM. A simple derivative recovery technique and its associated a posteriori error estimator have been proposed in [20, 21, 22, 23]. These recovery based a posteriori error estimations outperform the super-convergent patch recovery technique (SPR) introduced by Zienkiewicz and Zhu. In [24], an error estimator of residual type for the elasticity system in two space dimensions is proposed.

Concerning a priori error estimates for the contact problem of linearly elastic bodies approximated by a standard affine finite-element method, a rate of convergence of order $h^{3/4}$ can be obtained for most methods (see [25, 26, 27] for instance). An optimal order of h (resp. $h\sqrt[4]{|\log(h)|}$ and $h\sqrt{|\log(h)|}$) has been obtained in [28] (resp. [25] and [29]) for the direct approximation of the variational inequality and with the additional assumption that the number of transition between contact and non contact is finite on the contact boundary. However, for stabilized Lagrange multiplier methods and with the only assumption that the solution is in $H^2(\Omega)$, the best a priori error estimates proven is of order $h^{3/4}$ (see [30]). This limitation may be only due to technical reasons since it has never been found on the numerical experiments. It affects the a priori error estimates we present in this paper.

Only a few works have been devoted to contact and XFEM, and they mainly use two methods to formulate contact problems: penalty method and Lagrange multiplier method. In penalty method, the penetration between two contacting boundaries is introduced and the normal contact force is related to the penetration by a penalty parameter [31]. Khoei et al. [32, 33] give the formulation with the penalization for plasticity problems. Contrary to penalization techniques, in the method of Lagrangian multipliers, the stability is improved without compromising the consistency of the method. Dolbow et al. [34] propose a formulation of the problem of a crack with frictional contact in 2D with an augmented Lagrangian method. Géniaut et al. [35, 36] choose an XFEM approach with frictional contact in the three dimensional case. They use a hybrid and continuous formulation close to the augmented Lagrangian method introduced by Ben Dhia [37]. Pierres et al. in [38] introduced a method with a three-fields description of the contact problem, the interface being seen as an autonomous entity with its own discretization.

In all the works cited above, a uniform discrete inf-sup condition is theoretically required between the finite-element space for the displacement and the one for the multiplier in order to obtain a good approximation of the solution. However, a uniform inf-sup condition seems to be very difficult to establish on the crack since it does not coincide with element edges and since it is even impossible to establish with some pairs of finite element spaces when the crack coincides with element edges. Consequently, we consider a stabilization method which avoids the need of such an inf-sup condition. This method, which provides stability of the multiplier

by adding supplementary terms in the weak formulation, has been originally introduced and analyzed by Barbosa and Hughes in [39, 40]. The great advantage is that the finite-element spaces on the primal and dual variables can be chosen independently. Note that, in [41], the connection was made between this method and the former one of Nitsche [41]. The studies in [39, 40] were generalized to a variational inequality framework in [42] (Signorini-type problems among others). This method has also been extended to interface problems on non-matching meshes in [43, 44] and more recently for bilateral (linear) contact problems in [45] and for contact problems in elastostatics [30].

None of the previous works treats the error estimates for contact problems approximated by the XFEM method. The rapid uptake of the XFEM method by industry requires adequate error estimation tools to be available to the analysts. Our purpose in this paper is to extend the work done in [30] to the enriched finite-element approximation of contact problems of cracked elastic bodies.
The paper is organized as follows. In Section 2, we introduce the formulation of the contact problem on a crack of an elastic structure. In Section 3, we present the elasticity problem approximated by both the enrichment strategy introduced in [12] and the stabilized Lagrange multiplier method of Barbosa-Hughes. A subsection is devoted to a priori error estimates following three different discrete contact conditions (the study is restricted to piecewise affine and constant finite element methods) . Finally, in Section 4, we present some numerical experiments on a very simple situation. We compare the stabilized and the non-stabilized cases for different finite-element approximations. Optimal rates of convergence are observed for the stabilized case. The influence of the stabilization parameter is also investigated.

3.2 Formulation of the continuous problem

We introduce some useful notations and several functional spaces. In what follows, bold letters like $\mathbf{u}, \mathbf{v}$, indicate vector-valued quantities, while the capital ones (e.g., $\mathbf{V}, \mathbf{K}, \ldots$) represent functional sets involving vector fields. As usual, we denote by $(L^2(.))^d$ and by $(H^s(.))^d$, $s \geq 0, d = 1, 2$ the Lebesgue and Sobolev spaces in d-dimensional space (see [15]). The usual norm of $(H^s(D))^d$ is denoted by $\|\cdot\|_{s,D}$ and we keep the same notation when $d = 1$ or $d = 2$. For shortness, the $(L^2(D))^d$-norm will be denoted by $\|\cdot\|_D$ when $d = 1$ or $d = 2$. In the sequel the symbol $|\cdot|$ will denote either the Euclidean norm in $\mathbb{R}^2$, or the length of a line segment, or the area of a planar domain.

We consider a cracked elastic body occupying a domain Ω in $\mathbb{R}^2$. The boundary $\partial\Omega$ of Ω, which is assumed to be polygonal for simplicity, is composed of three non-overlapping parts Γ_D, Γ_N and Γ_C with $\text{meas}(\Gamma_D) > 0$ and $\text{meas}(\Gamma_C) > 0$. A Dirichlet and a Neumann conditions are prescribed on Γ_D and Γ_N, respectively. The boundary part Γ_C represents also the crack location which, for the sake of simplicity, is assumed to be a straight line segment. In order to deal with the contact between the two sides of the crack as a contact between two elastic bodies, we denote by Γ_{C+} and Γ_{C-} each of the two sides of the crack (see Fig. 3.1). Of course, in the initial configuration, both Γ_{C+} and Γ_{C-} coincide. Let $\mathbf{n} = \mathbf{n}^+ = -\mathbf{n}^-$ denote the normal unit

outward vector on Γ_{C+}.

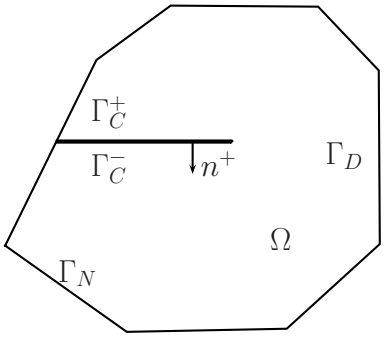

Figure 3.1: *A cracked domain.*

We assume that the body is subjected to volume forces $\mathbf{f} = (f_1, f_2) \in (L^2(\Omega))^2$ and to surface loads $\mathbf{g} = (g_1, g_2) \in (L^2(\Gamma_N))^2$. Then, under planar small strain assumptions, the problem of homogeneous isotropic linear elasticity consists in finding the displacement field $\mathbf{u} : \Omega \to \mathbb{R}^2$ satisfying

$$\mathbf{div}\,\boldsymbol{\sigma}(\mathbf{u}) + \mathbf{f} = \mathbf{0} \quad \text{in } \Omega, \tag{3.1}$$

$$\boldsymbol{\sigma}(\mathbf{u}) = \lambda_{_L}\ \mathrm{tr}\,\boldsymbol{\varepsilon}(\mathbf{u})\, I + 2\mu_{_L}\ \boldsymbol{\varepsilon}(\mathbf{u}), \quad \text{in } \Omega, \tag{3.2}$$

$$\mathbf{u} = \mathbf{0} \quad \text{on } \Gamma_D, \tag{3.3}$$

$$\boldsymbol{\sigma}(\mathbf{u})\mathbf{n} = \mathbf{g} \quad \text{on } \Gamma_N, \tag{3.4}$$

where $\boldsymbol{\sigma} = (\sigma_{ij})$, $1 \le i, j \le 2$, stands for the stress tensor field, $\boldsymbol{\varepsilon}(\mathbf{v}) = (\boldsymbol{\nabla}\mathbf{v} + \boldsymbol{\nabla}\mathbf{v}^{^T})/2$ represents the linearized strain tensor field, $\lambda_{_L} \ge 0$, $\mu_{_L} > 0$ are the Lamé coefficients, and I denotes the identity tensor. For a displacement field $\mathbf{v}$ and a density of surface forces $\boldsymbol{\sigma}(\mathbf{v})\mathbf{n}$ defined on $\partial\Omega$, we adopt the following notations:

$$\mathbf{v}^+ = v_n^+\mathbf{n}^+ + v_t^+\mathbf{t}, \quad \mathbf{v}^- = v_n^-\mathbf{n}^- + v_t^-\mathbf{t} \quad \text{and} \quad \boldsymbol{\sigma}(\mathbf{v})\mathbf{n} = \sigma_n(\mathbf{v})\mathbf{n} + \sigma_t(\mathbf{v})\mathbf{t},$$

where $\mathbf{t}$ is a unit tangent vector on Γ_C, $\mathbf{v}^+$ (resp. $\mathbf{v}^-$) is the trace of displacement on Γ_C on the Γ_C^+ side (resp. on the Γ_C^- side). The conditions describing the frictionless unilateral contact on Γ_C are:

$$[\![u_n]\!] = u_n^+ + u_n^- \le 0, \qquad \sigma_n(\mathbf{u}) \le 0, \qquad \sigma_n(\mathbf{u}) \cdot [\![u_n]\!] = 0, \qquad \sigma_t(\mathbf{u}) = \mathbf{0}, \tag{3.5}$$

where $[\![u_n]\!]$ is the jump of the normal displacement across the crack Γ_C.

We present now some classical weak formulation of Problem (3.1)−(3.5). We introduce the following Hilbert spaces:

$$\mathbf{V} = \left\{\mathbf{v} \in \left(H^1(\Omega)\right)^2 : \quad \mathbf{v} = \mathbf{0} \text{ on } \Gamma_D\right\}, \qquad W = \left\{v_{n|_{\Gamma_C}} : \mathbf{v} \in \mathbf{V}\right\},$$

and their topological dual spaces $\mathbf{V}'$, W', endowed with their usual norms. We also introduce the following convex cone of multipliers on Γ_C:

$$M^- = \Big\{\mu \in W' : \ \langle \mu, \psi \rangle_{W',W} \geq 0 \quad \text{for all } \psi \in W, \psi \leq 0 \ \text{ a.e. on } \Gamma_C\Big\},$$

where the notation $\langle \cdot, \cdot \rangle_{W',W}$ stands for the duality pairing between W' and W. Finally, for $\mathbf{u}$ and $\mathbf{v}$ in $\mathbf{V}$ and μ in W' we define the following forms

$$\begin{aligned} a(\mathbf{u},\mathbf{v}) &= \int_\Omega \boldsymbol{\sigma}(\mathbf{u}) : \boldsymbol{\varepsilon}(\mathbf{v})\, d\Omega, \qquad\qquad b(\mu,\mathbf{v}) = \big\langle \mu, [\![v_n]\!] \big\rangle_{W',W} \\ L(\mathbf{v}) &= \int_\Omega \mathbf{f}\cdot\mathbf{v}\, d\Omega + \int_{\Gamma_N} \mathbf{g}\cdot\mathbf{v}\, d\Gamma. \end{aligned}$$

The mixed formulation of the unilateral contact problem (3.1)−(3.5) consists then in finding $\mathbf{u} \in \mathbf{V}$ and $\lambda \in M^-$ such that

$$\begin{cases} a(\mathbf{u},\mathbf{v}) - b(\lambda,\mathbf{v}) = L(\mathbf{v}), & \forall\, \mathbf{v} \in \mathbf{V}, \\ b(\mu - \lambda, \mathbf{u}) \geq 0, & \forall\, \mu \in M^-. \end{cases} \tag{3.6}$$

An equivalent formulation of (3.6) consists in finding $(\mathbf{u},\lambda) \in \mathbf{V} \times M^-$ satisfying

$$\mathscr{L}(\mathbf{u},\mu) \leq \mathscr{L}(\mathbf{u},\lambda) \leq \mathscr{L}(\mathbf{v},\lambda), \qquad \forall \mathbf{v} \in \mathbf{V},\ \forall \mu \in M^-,$$

where $\mathscr{L}(\cdot,\cdot)$ is the classical Lagrangian of the system defined as

$$\mathscr{L}(\mathbf{v},\mu) = \frac{1}{2} a(\mathbf{v},\mathbf{v}) - L(\mathbf{v}) - b(\mu,\mathbf{v}).$$

Another classical weak formulation of problem (3.1)−(3.5) is given by the following variational inequality: find $\mathbf{u} \in \mathbf{K}$ such that

$$a(\mathbf{u}, \mathbf{v}-\mathbf{u}) \geq L(\mathbf{v}-\mathbf{u}), \qquad \forall \mathbf{v} \in \mathbf{K}, \tag{3.7}$$

where $\mathbf{K}$ denotes the closed convex cone of admissible displacement fields satisfying the non-interpenetration condition

$$\mathbf{K} = \big\{\mathbf{v} \in \mathbf{V} : \quad [\![v_n]\!] \leq 0 \text{ on } \Gamma_C\big\}.$$

The existence and uniqueness of $(\mathbf{u},\lambda)$ solution to (3.6) has been established in [46]. Moreover, the first argument $\mathbf{u}$ solution to (3.6) is also the unique solution of problem (3.7) and one has $\lambda = \sigma_n(\mathbf{u})$ is in W'.

3.3 Discretization with the stabilized Lagrange multiplier method

3.3.1 The discrete problem

We will denote by $\mathbf{V}^h \subset \mathbf{V}$ a family of enriched finite-dimensional vector spaces indexed by h coming from a family $\mathcal{T}^h$ of triangulations of the uncracked domain $\overline{\Omega}$ (here $h = \max_{T\in\mathcal{T}^h} h_T$

where h_T is the diameter of the triangle T). The family of triangulations is assumed to be regular, i.e., there exists $\beta > 0$ such that $\forall T \in \mathcal{T}^h$, $h_T/\rho_T \leq \beta$ where ρ_T denotes the radius of the inscribed circle in T (see [47]). We consider the variant, called the cut-off XFEM, introduced in [12] in which the whole area around the crack tip is enriched by using a cut-off function denoted by $\chi(\cdot)$. In this variant, the enriched finite-element space $\mathbf{V}^h$ is defined as

$$\mathbf{V}^h = \left\{ \mathbf{v}^h \in (\mathscr{C}(\bar{\Omega}))^2 \ : \ \mathbf{v}^h = \sum_{i\in\mathcal{N}_h} \mathbf{a}_i\varphi_i + \sum_{i\in\mathcal{N}_h^H} \mathbf{b}_i H\varphi_i + \chi \sum_{j=1}^{4} \mathbf{c}_j F_j, \quad \mathbf{a}_i, \mathbf{b}_i, \mathbf{c}_j \in \mathbb{R}^2 \right\} \subset \mathbf{V}.$$

Here $(\mathscr{C}(\bar{\Omega}))^2$ is the space of continuous vector fields over $\bar{\Omega}$, $H(\cdot)$ is the Heaviside-like function used to represent the discontinuity across the straight crack and defined by

$$H(\mathbf{x}) = \begin{cases} +1 & \text{if } (\mathbf{x}-\mathbf{x}^*)\cdot\mathbf{n}^+ \geq 0, \\ -1 & \text{otherwise,} \end{cases}$$

where $\mathbf{x}^*$ denotes the position of the crack tip. The notation φ_i represents the scalar-valued shape functions associated with the classical degree one finite-element method at the node of index i, $\mathcal{N}_h$ denotes the set of all node indices, and $\mathcal{N}_h^H$ denotes the set of nodes indices enriched by the function $H(\cdot)$, i.e., nodes indices for which the support of the corresponding shape function is completely cut by the crack (see Fig. 3.2). The cut-off function is a $\mathscr{C}^1$ piecewise third order polynomial on $[r_0, r_1]$ such that:

$$\begin{cases} \chi(r) = 1 & \text{if } r < r_0, \\ \chi(r) \in (0,1) & \text{if } r_0 < r < r_1, \\ \chi(r) = 0 & \text{if } r > r_1. \end{cases}$$

The functions $\{F_j(\mathbf{x})\}_{1\leq j\leq 4}$ are defined in polar coordinates located at the crack tip by

$$\{F_j(\mathbf{x}),\ 1 \leq j \leq 4\} = \left\{ \sqrt{r}\sin\frac{\theta}{2}, \sqrt{r}\cos\frac{\theta}{2}, \sqrt{r}\sin\frac{\theta}{2}\sin\theta, \sqrt{r}\cos\frac{\theta}{2}\sin\theta \right\}. \tag{3.8}$$

These functions allows to generate the asymptotic non-smooth displacement at the crack tip (see [48] and Lemma A.1).

An important point of the approximation is whether the contact pressure σ_n is regular or not at the crack tip. If it were singular, it should be taken into account by the discretization of the multiplier. Nevertheless, it seems that this is not the case in homogeneous isotropic linear elasticity. This results has not been proved yet, and seems to be a difficult issue. However, if we consider the formulation (3.6) and if we assume that there is a finite number of transition points between contact and non contact zones near the crack tip, then we are able to prove (see Lemma A.1 in Appendix A) that the contact stress σ_n is in $H^{1/2}(\Gamma_C)$.

Now, concerning the discretization of the multiplier, let $\mathbf{x}_0, ..., \mathbf{x}_N$ be given distinct points lying in $\overline{\Gamma_C}$ (note that we can choose these nodes to coincide with the intersection between $\mathcal{T}^h$ and $\overline{\Gamma_C}$). These nodes form a one-dimensional family of meshes of Γ_C denoted by T^H. We set $H = \max_{0\leq i\leq N-1} |\mathbf{x}_{i+1} - \mathbf{x}_i|$. The mesh T^H allows us to define a finite-dimensional space W^H approximating W' and a nonempty closed convex set $M^{H-} \subset W^H$ approximating M^-:

$$M^{H-} = \left\{ \mu^H \in W^H : \mu^H \text{ satisfy a "nonpositivity condition" on } \Gamma_C \right\}.$$

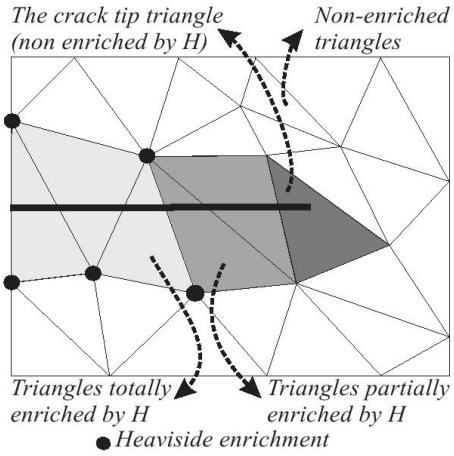

Figure 3.2: *A cracked domain.*

Following [30], we consider two possible elementary choices of W^H:

$$W_0^H = \left\{ \mu^H \in L^2(\Gamma_C) : \mu^H{}_{|(\mathbf{x}_i,\mathbf{x}_{i+1})} \in P_0(\mathbf{x}_i,\mathbf{x}_{i+1}), \forall\, 0 \le i \le N-1 \right\},$$

$$W_1^H = \left\{ \mu^H \in \mathscr{C}(\Gamma_C) : \mu^H{}_{|(\mathbf{x}_i,\mathbf{x}_{i+1})} \in P_1(\mathbf{x}_i,\mathbf{x}_{i+1}), \forall\, 0 \le i \le N-1 \right\},$$

where $P_k(E)$ denotes the space of polynomials of degree less or equal to k on E. This allows to provide the following three elementary definitions of M^{H-}:

$$M_0^{H-} = \left\{ \mu^H \in W_0^H : \mu^H \le 0 \text{ on } \Gamma_C \right\}, \tag{3.9}$$

$$M_1^{H-} = \left\{ \mu^H \in W_1^H : \mu^H \le 0 \text{ on } \Gamma_C \right\}, \tag{3.10}$$

$$M_{1,*}^{H-} = \left\{ \mu^H \in W_1^H : \int_{\Gamma_C} \mu^H \psi^H d\Gamma \ge 0, \forall\, \psi^H \in M_1^{H-} \right\}. \tag{3.11}$$

Now we divide the domain Ω into Ω_1 and Ω_2 according to the crack and a straight extension of the crack (see Fig. 3.3) such that the value of $H(\cdot)$ is $(-1)^k$ on Ω_k, $k = 1, 2$. Now, let R_h be an operator from $\mathbf{V}^h$ onto $L^2(\Gamma_C)$ which approaches the normal component of the stress vector on Γ_C defined for all $T \in \mathcal{T}^h$ with $T \cap \Gamma_C \neq \emptyset$ as

$$R_h(\mathbf{v}^h)_{|T\cap\Gamma_C} = \begin{cases} \sigma_n(\mathbf{v}_1^h), & \text{if } \mid T \cap \Omega_1 \mid \ge \dfrac{\mid T \mid}{2}, \\ \sigma_n(\mathbf{v}_2^h), & \text{if } \mid T \cap \Omega_2 \mid > \dfrac{\mid T \mid}{2}, \end{cases}$$

where $\mathbf{v}_1^h = \mathbf{v}^h{}_{|\Omega_1}$ and $\mathbf{v}_2^h = \mathbf{v}^h{}_{|\Omega_2}$.

This allow us to define the following stabilized discrete approximation of Problem (3.6): find $\mathbf{u}^h \in \mathbf{V}^h$ and $\lambda^H \in M^{H-}$ such that

$$\begin{cases} a(\mathbf{u}^h, \mathbf{v}^h) - b(\lambda^H, \mathbf{v}^h) + \displaystyle\int_{\Gamma_C} \gamma(\lambda^H - R_h(\mathbf{u}^h)) R_h(\mathbf{v}^h) d\Gamma = L(\mathbf{v}^h), & \forall\, \mathbf{v}^h \in \mathbf{V}^h, \\ b(\mu^H - \lambda^H, \mathbf{u}^h) + \displaystyle\int_{\Gamma_C} \gamma(\mu^H - \lambda^H)(\lambda^H - R_h(\mathbf{u}^h)) d\Gamma \geq 0, & \forall\, \mu^H \in M^{H-}, \end{cases} \tag{3.12}$$

where γ is defined to be constant on each element T as $\gamma = \gamma_0 h_T$ where $\gamma_0 > 0$ is a given constant independent of h and H. Problem (3.12) represents the optimality conditions for the Lagrangian

$$\mathcal{L}_\gamma(\mathbf{v}^h, \mu^H) = \frac{1}{2} a(\mathbf{v}^h, \mathbf{v}^h) - L(\mathbf{v}^h) - b(\mu^H, \mathbf{v}^h) - \frac{1}{2} \int_{\Gamma_C} \gamma(\mu^H - R_h(\mathbf{v}^h))^2 d\Gamma.$$

We note that, without loss of generality, we can assume that Γ_C is a straight line segment parallel to the $x-$axis. Let $T \in \mathcal{T}^h$ and $E = T \cap \Gamma_C$. Then, for any $\mathbf{v}^h \in \mathbf{V}^h$ and since $\sigma_n(\mathbf{v}_i^h)$ is a constant over each element, we have

$$\begin{aligned} \|R_h(\mathbf{v}^h)\|_{0,E} &= \|\sigma_n(\mathbf{v}_i^h)\|_{0,E}, \qquad \text{with } i \text{ such that } |T \cap \Omega_i| \geq \frac{|T|}{2}, \\ &= \|\sigma_{yy}(\mathbf{v}_i^h)\|_{0,E}, \\ &= \frac{|E|^{1/2}}{|T \cap \Omega_i|^{1/2}} \|\sigma_{yy}(\mathbf{v}_i^h)\|_{0,T\cap\Omega_i}, \\ &\lesssim h_T^{-\frac{1}{2}} \|\sigma_{yy}(\mathbf{v}_i^h)\|_{0,T\cap\Omega_i}, \\ &= \left(\frac{\gamma}{\gamma_0}\right)^{-\frac{1}{2}} \|\sigma_{yy}(\mathbf{v}_i^h)\|_{0,T\cap\Omega_i}. \end{aligned}$$

Here and throughout the paper, we use the notation $a \lesssim b$ to signify that there exists a constant $C > 0$, independent of the mesh parameters (h, H), the solution and the position of the crack-tip, such that $a \leq Cb$.

By summation over all the edges $E \subset \Gamma_C$ we get

$$\|\gamma^{\frac{1}{2}} R_h(\mathbf{v}^h)\|_{0,\Gamma_C}^2 \lesssim \gamma_0 \|\sigma_{yy}(\mathbf{v}^h)\|_{0,\Omega}^2 \lesssim \gamma_0 \|\mathbf{v}^h\|_{1,\Omega}^2. \tag{3.13}$$

Hence, when γ_0 is small enough, it follows from Korn's inequality and (3.13), that there exists $C > 0$ such that for any $\mathbf{v}^h \in \mathbf{V}^h$

$$a(\mathbf{v}^h, \mathbf{v}^h) - \int_{\Gamma_C} \gamma (R_h(\mathbf{v}^h))^2 d\Gamma \geq C \|\mathbf{v}^h\|_{1,\Omega}^2.$$

The existence of a unique solution to Problem (3.12) when γ_0 is small enough follows from the fact that $\mathbf{V}^h$ and M^{H-} are two nonempty closed convex sets, $\mathcal{L}_\gamma(\cdot,\cdot)$ is continuous on $\mathbf{V}^h \times W^H$, $\mathcal{L}_\gamma(\mathbf{v}^h, .)$ (resp. $\mathcal{L}_\gamma(\cdot, \mu^H)$) is concave (resp. strictly convex) for any $\mathbf{v}^h \in \mathbf{V}^h$ (resp. for any $\mu^H \in M^{H-}$) and $\lim_{\mathbf{v}^h \in \mathbf{V}^h, \|\mathbf{v}^h\|_{\mathbf{V}^h} \to \infty} \mathcal{L}_\gamma(\mathbf{v}^h, 0) = +\infty$ (resp. $\lim_{\mu^H \in M^{H-}, \|\mu^H\|_{W^H} \to \infty} \mathcal{L}_\gamma(0, \mu^H) = -\infty$), see [46, pp. 338–339].

3.3.2 Convergence analysis

First, let us define for any $\mathbf{v} \in \mathbf{V}$ and any $\mu \in L^2(\Gamma_C)$ the following norms:

$$\|\mathbf{v}\| = a(\mathbf{v},\mathbf{v})^{1/2},$$

$$|||(\mathbf{v},\mu)||| = \left(\|\mathbf{v}\|^2 + \|\gamma^{1/2}\mu\|^2_{0,\Gamma_C}\right)^{1/2}.$$

In order to study the convergence error, we recall the definition of the XFEM interpolation operator Π^h introduced in [17].

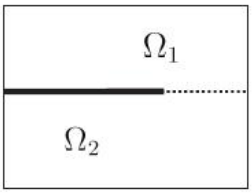

Figure 3.3: *Decomposition of* Ω *into* Ω_1 *and* Ω_2.

We assume that the displacement has the regularity $(H^2(\Omega))^2$ except in the vicinity of the crack-tip where the singular part of the displacement is a linear combination of the functions $\{F_j(\mathbf{x})\}_{1\leq j\leq 4}$ given by (3.8) (see [49] for a justification). Let us denote by $\mathbf{u}_s$ the singular part of $\mathbf{u}$, $\mathbf{u}_r = \mathbf{u} - \chi\mathbf{u}_s$ the regular part of $\mathbf{u}$, and $\mathbf{u}_r^k$ the restriction of $\mathbf{u}_r$ to Ω_k, $k \in \{1,2\}$. Then, for $k \in \{1,2\}$, there exists an extension $\widetilde{\mathbf{u}}_r^k \in (H^2(\overline{\Omega}))^2$ of $\mathbf{u}_r^k$ to $\overline{\Omega}$ such that (see [15])

$$\|\widetilde{\mathbf{u}}_r^1\|_{2,\overline{\Omega}} \lesssim \|\mathbf{u}_r^1\|_{2,\Omega_1},$$
$$\|\widetilde{\mathbf{u}}_r^2\|_{2,\overline{\Omega}} \lesssim \|\mathbf{u}_r^2\|_{2,\Omega_2}.$$

Definition 1 ([17]). *Given a displacement field* $\mathbf{u}$ *satisfying* $\mathbf{u}-\mathbf{u}_s \in H^2(\Omega)$, *and two extensions* $\widetilde{\mathbf{u}}_r^1$ *and* $\widetilde{\mathbf{u}}_r^2$ *in* $H^2(\overline{\Omega})$ *of* $\mathbf{u}_r^1$ *and* $\mathbf{u}_r^2$, *respectively, we define* $\Pi^h\mathbf{u}$ *as the element of* $\mathbf{V}^h$ *such that*

$$\Pi^h\mathbf{u} \;=\; \sum_{i\in\mathcal{N}_h} \mathbf{a}_i\varphi_i \;+\; \sum_{i\in\mathcal{N}_h^H} \mathbf{b}_i H\varphi_i \;+\; \chi\mathbf{u}_s,$$

where $\mathbf{a}_i$, $\mathbf{b}_i$ *are given as follows for* $\mathbf{y}_i$ *the finite-element node associated to* φ_i*:*

if $i \in \{\mathcal{N}_h \setminus \mathcal{N}_h^H\}$ *then* $\mathbf{a}_i = \mathbf{u}_r(\mathbf{y}_i)$,
if $i \in \mathcal{N}_h^H$ *and* $\mathbf{y}_i \in \overline{\Omega}_k$ *for* $k \in \{1,2\}$ *then for* $l = 3-k$:

$$\begin{cases} \mathbf{a}_i = \dfrac{1}{2}\left(\mathbf{u}_r^k(\mathbf{y}_i) + \widetilde{\mathbf{u}}_r^l(\mathbf{y}_i)\right), \\ \mathbf{b}_i = \dfrac{(-1)^k}{2}\left(\mathbf{u}_r^k(\mathbf{y}_i) - \widetilde{\mathbf{u}}_r^l(\mathbf{y}_i)\right). \end{cases}$$

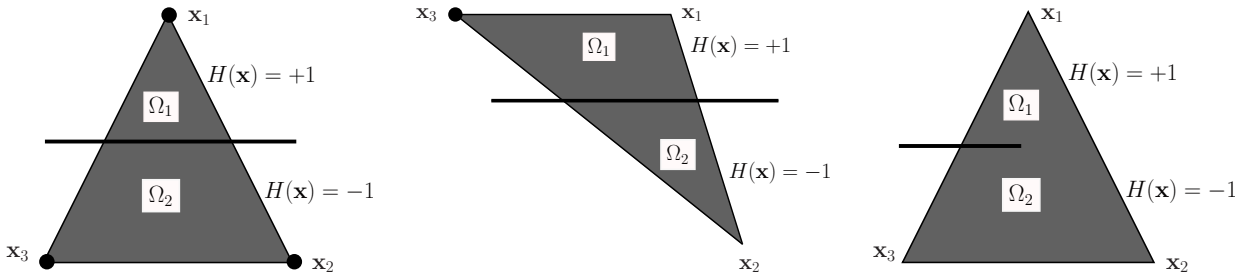

(a) A totally enriched triangle (b) A partially enriched triangle (c) The triangle containing the crack tip

Figure 3.4: The different types of enriched triangles. The enrichment with the heaviside function are marked with a bullet.

From this definition, we can distinguish three different kinds of triangle enriched with the Heaviside-like function H. This is illustrated in Fig. 3.2 and in Fig. 3.4. A totally enriched triangle is a triangle whose finite-element shape functions have their supports completely cut by the crack. A partially enriched triangle is a triangle having one or two shape functions whose supports are completely cut by the crack. Finally, the triangle containing the crack tip is a special triangle which is in fact not enriched by the Heaviside-like function. In [17], the following lemma is proved:

Lemma 3.3.1. *The function* $\Pi^h\mathbf{u}$ *satisfies*

(i) $\Pi^h\mathbf{u} = I^h\mathbf{u}_r + \chi\mathbf{u}_s$ *over a triangle non-enriched by* H,

(ii) $\Pi^h\mathbf{u}|_{T\cap\Omega_k} = I^h\widetilde{\mathbf{u}}_r^k + \chi\mathbf{u}_s$ *over a triangle* T *totally enriched by* H,

where I^h *denotes the classical Lagrange interpolation operator for the associated finite-element method.*

It is also proved in [17] that this XFEM interpolation operator satisfies the following interpolation error estimate:

$$\|\mathbf{u} - \Pi^h\mathbf{u}\| \lesssim h\|\mathbf{u} - \chi\mathbf{u}_s\|_{2,\Omega}, \tag{3.14}$$

For a triangle T cut by the crack, we denote by $E_T^i\mathbf{u}_r$ the polynomial extension of $\Pi^h\mathbf{u}_r|_{T\cap\Omega_i}$ on T (*i.e.* the polynomial $\Pi^h\mathbf{u}_r|_{T\cap\Omega_i}$ extended to T). We will need the following result which gives an interpolation error estimate on the enriched triangles:

Lemma 3.3.2. *Let* T *an element such that* $T\cap\Gamma_C \neq 0$, *then for* $i \in \{1,2\}$ *the following estimates hold:*

$$\begin{aligned}
\|\widetilde{\mathbf{u}}_r^i - E_T^i\mathbf{u}_r\|_{0,T} &\lesssim h_T^2\Big(\|\widetilde{\mathbf{u}}_r^i\|_{2,T} + |\,\widetilde{\mathbf{u}}_r^1 - \widetilde{\mathbf{u}}_r^2\,|_{2,B(\mathbf{x}^*,h_T)}\Big),\\
\|\widetilde{\mathbf{u}}_r^i - E_T^i\mathbf{u}_r\|_{1,T} &\lesssim h_T\Big(\|\widetilde{\mathbf{u}}_r^i\|_{2,T} + |\,\widetilde{\mathbf{u}}_r^1 - \widetilde{\mathbf{u}}_r^2\,|_{2,B(\mathbf{x}^*,h_T)}\Big),
\end{aligned}$$

where h_T *is the size of triangle* T *and* $B(\mathbf{x}^*, h_T)$ *is the ball centered at the crack tip* $\mathbf{x}^*$ *and with radius* h_T.

The proof of this lemma can be found in Appendix B. Let us now give an abstract error estimate for the discrete contact problem (3.12).

Proposition 3.3.3. *Assume that the solution $(\mathbf{u},\lambda)$ to Problem (3.6) is such that $\lambda \in L^2(\Gamma_C)$. Let γ_0 be small enough. Then, the solution $(\mathbf{u}^h,\lambda^H)$ to Problem (3.12) satisfies the following estimate*

$$\begin{aligned}\left|\!\left|\!\left|\left(\mathbf{u}-\mathbf{u}^h,\lambda-\lambda^H\right)\right|\!\right|\!\right|^2 \lesssim & \left[\inf_{\mathbf{v}^h\in\mathbf{V}^h}\left(\left|\!\left|\!\left|\left(\mathbf{u}-\mathbf{v}^h,\sigma_n(\mathbf{u})-R_h(\mathbf{v}^h)\right)\right|\!\right|\!\right|^2+\|\gamma^{-1/2}([\![u_n]\!]-[\![v_n^h]\!])\|^2_{0,\Gamma_C}\right)\right.\\ &+\inf_{\mu\in M^-}\int_{\Gamma_C}(\mu-\lambda^H)[\![u_n]\!]d\Gamma\\ &\left.+\inf_{\mu^H\in M^{H-}}\int_{\Gamma_C}(\mu^H-\lambda)([\![u_n^h]\!]+\gamma(\lambda^H-R_h(\mathbf{u}^h)))d\Gamma\right].\end{aligned}$$

Proof. (This proof is a straightforward adaptation of the proof in [30]) We have

$$\|\gamma^{1/2}(\lambda-\lambda^H)\|^2_{0,\Gamma_C}=\int_{\Gamma_C}\gamma\lambda^2d\Gamma-2\int_{\Gamma_C}\gamma\lambda\lambda^Hd\Gamma+\int_{\Gamma_C}\gamma(\lambda^H)^2d\Gamma.$$

From (3.6) and (3.12) we obtain

$$\int_{\Gamma_C}\gamma\lambda^2d\Gamma\le\int_{\Gamma_C}\gamma\lambda\mu d\Gamma+\int_{\Gamma_C}(\mu-\lambda)[\![u_n]\!]d\Gamma-\int_{\Gamma_C}\gamma(\mu-\lambda)\sigma_n(\mathbf{u})d\Gamma,\ \forall\ \mu\in M^-,$$

$$\int_{\Gamma_C}\gamma(\lambda^H)^2d\Gamma\le\int_{\Gamma_C}\gamma\lambda^H\mu^Hd\Gamma+\int_{\Gamma_C}(\mu^H-\lambda^H)[\![u_n^h]\!]d\Gamma-\int_{\Gamma_C}\gamma(\mu^H-\lambda^H)R_h(\mathbf{u}^h)d\Gamma,\ \forall\ \mu^H\in M^{H-},$$

which gives

$$\begin{aligned}\|\gamma^{1/2}(\lambda-\lambda^H)\|^2_{0,\Gamma_C} \le & \int_{\Gamma_C}\gamma(\mu-\lambda^H)\lambda d\Gamma+\int_{\Gamma_C}\gamma(\mu^H-\lambda)\lambda^Hd\Gamma+\int_{\Gamma_C}(\mu-\lambda)[\![u_n]\!]d\Gamma\\ &-\int_{\Gamma_C}\gamma(\mu-\lambda)\sigma_n(\mathbf{u})d\Gamma+\int_{\Gamma_C}(\mu^H-\lambda^H)[\![u_n^h]\!]d\Gamma-\int_{\Gamma_C}\gamma(\mu^H-\lambda^H)R_h(\mathbf{u}^h)d\Gamma\\ = & \int_{\Gamma_C}(\mu-\lambda^H)[\![u_n]\!]d\Gamma+\int_{\Gamma_C}(\mu^H-\lambda)([\![u_n^h]\!]+\gamma(\lambda^H-R_h(\mathbf{u}^h)))d\Gamma\\ &-\int_{\Gamma_C}\gamma(\lambda^H-\lambda)(\sigma_n(\mathbf{u})-R_h(\mathbf{u}^h))d\Gamma\\ &+\int_{\Gamma_C}(\lambda^H-\lambda)([\![u_n]\!]-[\![u_n^h]\!])d\Gamma,\quad\forall\mu\in M^-,\forall\mu^H\in M^{H-}.\end{aligned}\tag{3.15}$$

According to (3.12) for any $\mathbf{v}^h\in\mathbf{V}^h$ we have

$$\begin{aligned}\|\mathbf{u}-\mathbf{u}^h\|^2 &= a(\mathbf{u}-\mathbf{u}^h,\mathbf{u}-\mathbf{u}^h)\\ &= a(\mathbf{u}-\mathbf{u}^h,\mathbf{u}-\mathbf{v}^h)+a(\mathbf{u}-\mathbf{u}^h,\mathbf{v}^h-\mathbf{u}^h)\\ &= a(\mathbf{u}-\mathbf{u}^h,\mathbf{u}-\mathbf{v}^h)+\int_{\Gamma_C}(\lambda-\lambda^H)([\![v_n^h]\!]-[\![u_n^h]\!])d\Gamma\\ &\quad+\int_{\Gamma_C}\gamma(\lambda^H-R_h(\mathbf{u}^h))R_h(\mathbf{v}^h-\mathbf{u}^h)d\Gamma.\end{aligned}\tag{3.16}$$

From the addition of (3.15) and (3.16), we deduce

$$\begin{aligned}\left|\left|\left|\left(\mathbf{u}-\mathbf{u}^h,\lambda-\lambda^H\right)\right|\right|\right|^2 \leq\ & a(\mathbf{u}-\mathbf{u}^h,\mathbf{u}-\mathbf{v}^h)+\int_{\Gamma_C}(\lambda-\lambda^H)([\![v_n^h]\!]-[\![u_n]\!])d\Gamma+\int_{\Gamma_C}(\mu-\lambda^H)[\![u_n]\!]d\Gamma\\ &+\int_{\Gamma_C}(\mu^H-\lambda)([\![u_n^h]\!]+\gamma(\lambda^H-R_h(\mathbf{u}^h)))d\Gamma\\ &+\int_{\Gamma_C}\gamma(\lambda-\lambda^H)(\sigma_n(\mathbf{u})-R_h(\mathbf{v}^h))d\Gamma+\int_{\Gamma_C}\gamma(\lambda-R_h(\mathbf{u}^h))R_h(\mathbf{v}^h-\mathbf{u}^h)d\Gamma,\end{aligned}\tag{3.17}$$

for all $\mathbf{v}^h\in\mathbf{V}^h$, $\mu\in M^-$ and $\mu^H\in M^{H-}$. The last term in the previous inequality is estimated by using (3.13) and recalling that $\lambda=\sigma_n(\mathbf{u})$ as follows

$$\begin{aligned}&\int_{\Gamma_C}\gamma(\lambda-R_h(\mathbf{u}^h))R_h(\mathbf{v}^h-\mathbf{u}^h)d\Gamma\\ \leq\ & \|\gamma^{1/2}(\sigma_n(\mathbf{u})-R_h(\mathbf{u}^h))\|_{0,\Gamma_C}\gamma_0^{1/2}\|h^{1/2}(R_h(\mathbf{v}^h-\mathbf{u}^h))\|_{0,\Gamma_C}\\ \lesssim\ & \gamma_0^{1/2}\|\mathbf{v}^h-\mathbf{u}^h\|\left(\|\gamma^{1/2}(\sigma_n(\mathbf{u})-R_h(\mathbf{v}^h))\|_{0,\Gamma_C}+\gamma_0^{1/2}\|h^{1/2}(R_h(\mathbf{v}^h-\mathbf{u}^h))\|_{0,\Gamma_C}\right)\\ \lesssim\ & \left(\gamma_0\|\mathbf{v}^h-\mathbf{u}^h\|^2+\|\gamma^{1/2}(\sigma_n(\mathbf{u})-R_h(\mathbf{v}^h))\|_{0,\Gamma_C}^2\right)\\ \lesssim\ & \left(\gamma_0\|\mathbf{u}-\mathbf{u}^h\|^2+\gamma_0\|\mathbf{u}-\mathbf{v}^h\|^2+\|\gamma^{1/2}(\sigma_n(\mathbf{u})-R_h(\mathbf{v}^h))\|_{0,\Gamma_C}^2\right).\end{aligned}\tag{3.18}$$

By combining (3.17) and (3.18), and using Young's inequality we come to the conclusion that if γ_0 is sufficiently small then

$$\begin{aligned}&\left|\left|\left|\left(\mathbf{u}-\mathbf{u}^h,\lambda-\lambda^H\right)\right|\right|\right|^2\\ \lesssim\ & \left[\inf_{\mathbf{v}^h\in\mathbf{V}^h}\left(\|\mathbf{u}-\mathbf{v}^h\|^2+\|\gamma^{1/2}(\sigma_n(\mathbf{u})-R_h(\mathbf{v}^h))\|_{0,\Gamma_C}^2+\|\gamma^{-1/2}([\![u_n]\!]-[\![v_n^h]\!])\|_{0,\Gamma_C}^2\right)\right.\\ &\left.+\inf_{\mu\in M^-}\int_{\Gamma_C}(\mu-\lambda^H)[\![u_n]\!]d\Gamma+\inf_{\mu^H\in M^{H-}}\int_{\Gamma_C}(\mu^H-\lambda)([\![u_n^h]\!]+\gamma(\lambda^H-R_h(\mathbf{u}^h)))d\Gamma\right],\end{aligned}$$

and hence the result follows. □

In order to estimate the first infimum of the latter proposition, we first recall the following Lemma of scaled trace inequality: the following scaled trace inequality (see [50]) for $T\in\mathcal{T}^h$ and $E=T\cap\Gamma_C$:

Lemma 3.3.4 ([50]). *For any $T\in\mathcal{T}^h$ and $\hat{T}$ the reference element let τ_T the affine and invertible mapping in $\mathbb{R}^2$ such that $T=\tau_T(\hat{T})$. Suppose that we have:*

- *Γ_C is a lipschitz continuous crack,*
- *$\|\nabla\tau_T\|_{\infty,T}\lesssim h_T$ and $\|\nabla\tau_{\hat{T}}^{-1}\|_{\infty,T}\lesssim h_T^{-1}$,*

then the following scaled trace inequality holds:

$$\|v\|_{0,\Gamma_C\cap T}\lesssim\left(h_T^{-1/2}\|v\|_{0,T}+h_T^{1/2}\|\nabla v\|_{0,T}\right),\quad\forall v\in H^1(T).\tag{3.19}$$

These two hypotheses of Lemma 3.3.4 are satisfied for regular families of meshes provided that Γ_C is Lipschitz-continuous.
We can deduce the following estimate :

$$\begin{aligned}
\|\gamma^{-1/2}([\![u_n]\!]-[\![(\Pi^h\mathbf{u})\cdot\mathbf{n}]\!])\|_{0,E} &\leq \|\gamma^{-1/2}([\![\mathbf{u}]\!]-[\![\Pi^h\mathbf{u}]\!])\|_{0,E},\\
&\leq \|\gamma^{-1/2}(\mathbf{u}_1-\Pi^h\mathbf{u}_{|\Omega_1})\|_{0,E}+\|\gamma^{-1/2}(\mathbf{u}_2-\Pi^h\mathbf{u}_{|\Omega_2})\|_{0,E},\\
&\leq \|\gamma^{-1/2}(\widetilde{\mathbf{u}}_r^1-\Pi^h\mathbf{u}_{|\Omega_1})\|_{0,E}+\|\gamma^{-1/2}(\widetilde{\mathbf{u}}_r^2-\Pi^h\mathbf{u}_{|\Omega_2})\|_{0,E},\\
&\lesssim h_T^{-1/2}h_T^{-1/2}\|\widetilde{\mathbf{u}}_r^1-E_T^1\mathbf{u}_r\|_{0,T}+h_T^{-1/2}h_T^{1/2}\|\nabla\widetilde{\mathbf{u}}_r^1-\nabla E_T^1\mathbf{u}_r\|_{0,T},\\
&\quad +h_T^{-1/2}h_T^{-1/2}\|\widetilde{\mathbf{u}}_r^2-E_T^2\mathbf{u}_r\|_{0,T}+h_T^{-1/2}h_T^{1/2}\|\nabla\widetilde{\mathbf{u}}_r^2-\nabla E_T^2\mathbf{u}_r\|_{0,T},
\end{aligned}$$

and by using Lemma 3.3.2 (see Appendix B) we have:

$$\|\gamma^{-1/2}([\![u_n]\!]-[\![(\Pi^h\mathbf{u})\cdot\mathbf{n}]\!])\|_{0,E} \lesssim h_T\big(\|\widetilde{\mathbf{u}}_r^1\|_{2,T}+\|\widetilde{\mathbf{u}}_r^2\|_{2,T}+|\ \widetilde{\mathbf{u}}_r^1-\widetilde{\mathbf{u}}_r^2\ |_{2,B(0,h_K)}\big).$$

By summation over all the edges we obtain

$$\|\gamma^{-1/2}([\![u_n]\!]-[\![(\Pi^h\mathbf{u})\cdot\mathbf{n}]\!])\|_{0,\Gamma_C}\lesssim h\|\mathbf{u}-\chi\mathbf{u}_s\|_{2,\Omega}. \tag{3.20}$$

It remains then to estimate $\|\gamma^{1/2}(\sigma_n(\mathbf{u})-R_h(\Pi^h\mathbf{u}))\|_{0,\Gamma_C}$. Still for $T\in\mathcal{T}^h$ and $E=T\cap\Gamma_C$, assuming, without loss of generality, that Γ_C is parallel to the $x-$axis and by using the trace inequality (3.19) we have

$$\begin{aligned}
\|\sigma_n(\mathbf{u})-R_h(\Pi^h\mathbf{u})\|_{0,E} &= \|\sigma_n(\mathbf{u}_r)-\sigma_n(\Pi^h\mathbf{u}_r|_{T\cap\Omega_i})\|_{0,E}, \qquad \text{with } i \text{ such that } |T\cap\Omega_i|\geq\frac{|T|}{2},\\
&= \|\sigma_n(\widetilde{\mathbf{u}}_r^i-\Pi^h\mathbf{u}_r|_{T\cap\Omega_i})\|_{0,E},\\
&\lesssim \left(h_T^{-\frac{1}{2}}\|\sigma_{yy}(\widetilde{\mathbf{u}}_r^i-E_T^i\mathbf{u}_r)\|_{0,T}+h_T^{\frac{1}{2}}\|\nabla\sigma_{yy}(\widetilde{\mathbf{u}}_r^i-E_T^i\mathbf{u}_r)\|_{0,T}\right),\\
&= \left(h_T^{-\frac{1}{2}}\|\sigma_{yy}(\widetilde{\mathbf{u}}_r^i-E_T^i\mathbf{u}_r)\|_{0,T}+h_T^{\frac{1}{2}}\|\nabla\sigma_{yy}(\widetilde{\mathbf{u}}_r^i)\|_{0,T}\right),\\
&\lesssim \left(h_T^{-\frac{1}{2}}\|\widetilde{\mathbf{u}}_r^i-E_T^i\mathbf{u}_r\|_{1,T}+h_T^{\frac{1}{2}}\|\widetilde{\mathbf{u}}_r^i\|_{2,T}\right).
\end{aligned}$$

Then, by summation over all the edges and using again Lemma 3.3.2 the following estimate holds

$$\|\gamma^{1/2}(\sigma_n(\mathbf{u})-R_h(\Pi^h\mathbf{u}))\|_{0,\Gamma_C}\lesssim h\|\mathbf{u}-\chi\mathbf{u}_s\|_{2,\Omega}. \tag{3.21}$$

Putting together the previous bounds (3.14), (3.20) and (3.21) we deduce that

$$\begin{aligned}
\inf_{\mathbf{v}^h\in\mathbf{V}^h} &\left(\left|\left|\left|\Big(\mathbf{u}-\mathbf{v}^h,\sigma_n(\mathbf{u})-R_h(\mathbf{v}^h)\Big)\right|\right|\right|^2+\|\gamma^{-1/2}([\![u_n]\!]-[\![v_n^h]\!])\|_{0,\Gamma_C}^2\right)\\
&\lesssim h^2\|\mathbf{u}-\chi\mathbf{u}_s\|_{2,\Omega}^2.
\end{aligned} \tag{3.22}$$

Finally, we have to estimate the error terms in Proposition 3.3.3 coming from the contact approximation:

$$\inf_{\mu^H\in M^{H-}}\int_{\Gamma_C}(\mu^H-\lambda)([\![u_n^h]\!]+\gamma(\lambda^H-R_h(\mathbf{u}^h)))d\Gamma \tag{3.23}$$

and

$$\inf_{\mu\in M^-}\int_{\Gamma_C}(\mu-\lambda^H)[\![u_n]\!]d\Gamma. \tag{3.24}$$

In order to estimate these terms, we need to distinguish the different contact conditions (i.e., we must specify the definition of M^{H-}). We consider hereafter three different standard discrete contact conditions.

3.3.2.1 First contact condition: $M^{H-}=M_0^{H-}$

We first consider the case of nonpositive discontinuous piecewise constant multipliers where M^{H-} is defined by (3.9). The error estimate is given next.

Theorem 3.3.5. *Let $(\mathbf{u},\lambda)$ be the solution to Problem (3.6). Assume that $\mathbf{u}_r\in(H^2(\Omega))^2$. Let γ_0 be small enough and let $(\mathbf{u}^h,\lambda^H)$ be the solution to the discrete problem (3.12) where $M^{H-}=M_0^{H-}$. Then, for any $\eta>0$ we have*

$$\left|\!\left|\!\left|\Big(\mathbf{u}-\mathbf{u}^h,\lambda-\lambda^H\Big)\right|\!\right|\!\right|\lesssim\big(h\|\mathbf{u}-\chi\mathbf{u}_s\|_{2,\Omega}+h^{1/2}H^{1/2}\|\lambda\|_{1/2,\Gamma_C}+H^{3/4-\eta/2}(\|\mathbf{u}\|_{3/2-\eta,\Omega}+\|\lambda\|_{1/2,\Gamma_C})\big).$$

Proof. Choosing $\mu=0$ in (3.24) yields

$$\inf_{\mu\in M^-}\int_{\Gamma_C}(\mu-\lambda^H)[\![u_n]\!]d\Gamma\le-\int_{\Gamma_C}\lambda^H[\![u_n]\!]d\Gamma\le 0.$$

In (3.23) we choose $\mu^H=\pi_0^H\lambda$ where π_0^H denotes the $L^2(\Gamma_C)$-projection onto W_0^H. We recall that the operator π_0^H is defined for any $v\in L^2(\Gamma_C)$ by

$$\pi_0^Hv\in W_0^H,\quad\int_{\Gamma_C}(v-\pi_0^Hv)\mu\,d\Gamma=0,\quad\forall\mu\in W_0^H,$$

and satisfies the following error estimates for any $0\le r\le 1$ (see [25])

$$H^{-1/2}\|v-\pi_0^Hv\|_{-1/2,\Gamma_C}+\|v-\pi_0^Hv\|_{0,\Gamma_C}\lesssim H^r\|v\|_{r,\Gamma_C}. \tag{3.25}$$

Clearly, $\pi_0^H\lambda\in M_0^{H-}$ and

$$\begin{aligned}\inf_{\mu^H\in M_0^{H-}}\int_{\Gamma_C}(\mu^H-\lambda)([\![u_n^h]\!]+\gamma(\lambda^H-R_h(\mathbf{u}^h)))d\Gamma\ &\le\ \int_{\Gamma_C}(\pi_0^H\lambda-\lambda)[\![u_n^h]\!]d\Gamma\\ &\quad+\int_{\Gamma_C}\gamma(\pi_0^H\lambda-\lambda)(\lambda^H-R_h(\mathbf{u}^h))d\Gamma.\end{aligned} \tag{3.26}$$

The first integral term in (3.26) is estimated using (3.25) as follows

$$\begin{aligned}\int_{\Gamma_C}(\pi_0^H\lambda-\lambda)[\![u_n^h]\!]d\Gamma&=\int_{\Gamma_C}(\pi_0^H\lambda-\lambda)([\![u_n^h]\!]-[\![u_n]\!])d\Gamma+\int_{\Gamma_C}(\pi_0^H\lambda-\lambda)[\![u_n]\!]d\Gamma\\&=\int_{\Gamma_C}(\pi_0^H\lambda-\lambda)([\![u_n^h]\!]-[\![u_n]\!])d\Gamma+\int_{\Gamma_C}(\pi_0^H\lambda-\lambda)([\![u_n]\!]-\pi_0^H[\![u_n]\!])d\Gamma\\&\le\|\pi_0^H\lambda-\lambda\|_{-1/2,\Gamma_C}\|[\![u_n^h]\!]-[\![u_n]\!]\|_{1/2,\Gamma_C}+\|\pi_0^H\lambda-\lambda\|_{0,\Gamma_C}\|[\![u_n]\!]-\pi_0^H[\![u_n]\!]\|_{0,\Gamma_C}\\&\lesssim H\|\lambda\|_{1/2,\Gamma_C}\|\mathbf{u}-\mathbf{u}^h\|+H^{3/2-\eta}\|\lambda\|_{1/2,\Gamma_C}\|[\![u_n]\!]\|_{1-\eta,\Gamma_C}\end{aligned}$$

Therefore, for any $\alpha > 0$ we have

$$\begin{aligned}&\int_{\Gamma_C} (\pi_0^H \lambda - \lambda)[\![u_n^h]\!] d\Gamma \\ &\lesssim \alpha \|\mathbf{u} - \mathbf{u}^h\|^2 + \alpha^{-1} H^2 \|\lambda\|_{1/2,\Gamma_C}^2 + \alpha^{-1} H^{3/2-\eta} \|\lambda\|_{1/2,\Gamma_C}^2 + \alpha H^{3/2-\eta} \|\mathbf{u}\|_{3/2-\eta,\Omega}^2. \end{aligned} \tag{3.27}$$

For the second integral term in (3.26), by using the estimates (3.25), (3.13), (3.21), we have

$$\begin{aligned}\int_{\Gamma_C} \gamma(\pi_0^H \lambda - \lambda)(\lambda^H - R_h(\mathbf{u}^h)) d\Gamma &= \int_{\Gamma_C} \gamma(\pi_0^H \lambda - \lambda)(\lambda^H - \lambda) d\Gamma \\ &\quad + \int_{\Gamma_C} \gamma(\pi_0^H \lambda - \lambda)(\sigma_n(\mathbf{u}) - R_h(\Pi^h \mathbf{u})) d\Gamma \\ &\quad + \int_{\Gamma_C} \gamma(\pi_0^H \lambda - \lambda)(R_h(\Pi^h \mathbf{u}) - R_h(\mathbf{u}^h)) d\Gamma \\ &\lesssim \gamma_0^{1/2} h^{1/2} \|\pi_0^H \lambda - \lambda\|_{0,\Gamma_C} \|\gamma^{1/2}(\lambda^H - \lambda)\|_{0,\Gamma_C} \\ &\quad + \gamma_0^{1/2} h^{1/2} \|\pi_0^H \lambda - \lambda\|_{0,\Gamma_C} \|\gamma^{1/2}(\sigma_n(\mathbf{u}) - R_h(\Pi^h \mathbf{u}))\|_{0,\Gamma_C} \\ &\quad + \gamma_0^{1/2} h^{1/2} \|\pi_0^H \lambda - \lambda\|_{0,\Gamma_C} \|\gamma^{1/2} R_h(\Pi^h \mathbf{u} - \mathbf{u}^h)\|_{0,\Gamma_C} \\ &\lesssim \gamma_0^{1/2} h^{1/2} H^{1/2} \|\lambda\|_{1/2,\Gamma_C} \|\gamma^{1/2}(\lambda^H - \lambda)\|_{0,\Gamma_C} \\ &\quad + \gamma_0^{1/2} h^{1/2} H^{1/2} \|\lambda\|_{1/2,\Gamma_C} h \|\mathbf{u} - \chi \mathbf{u}_s\|_{2,\Omega} \\ &\quad + \gamma_0 h^{1/2} H^{1/2} \|\lambda\|_{1/2,\Gamma_C} \|\mathbf{u}^h - \Pi^h \mathbf{u}\|.\end{aligned}$$

Since $\|\mathbf{u}^h - \Pi^h \mathbf{u}\| \lesssim \|\mathbf{u} - \mathbf{u}^h\| + h\|\mathbf{u} - \chi \mathbf{u}_s\|_{2,\Omega}$, for any $\alpha > 0$ sufficiently small, we deduce

$$\begin{aligned}&\int_{\Gamma_C} \gamma(\pi_0^H \lambda - \lambda)(\lambda^H - R_h(\mathbf{u}^h)) d\Gamma \\ &\lesssim \alpha \|\mathbf{u} - \mathbf{u}^h\|^2 + \alpha \|\gamma^{1/2}(\lambda^H - \lambda)\|_{0,\Gamma_C}^2 + \alpha h^2 \|\mathbf{u} - \chi \mathbf{u}_s\|_{2,\Omega}^2 + \alpha^{-1} h H \|\lambda\|_{1/2,\Gamma_C}^2. \end{aligned} \tag{3.28}$$

Then, by using the inequalities (3.22), (3.26), (3.27), (3.28) and Proposition 3.3.3 the proof of the theorem follows. □

Remark: Note that if we take $h = H$ the rate of convergence proved in Theorem 3.3.5 is $h^{3/4-\eta/2}$

3.3.2.2 Second contact condition: $M^{H-} = M_1^{H-}$

Now, we focus on the case of nonpositive continuous piecewise affine multipliers where M^{H-} is given by (3.10).

Theorem 3.3.6. *Let $(\mathbf{u}, \lambda)$ be the solution to Problem (3.6). Assume that $\mathbf{u}_r \in (H^2(\Omega))^2$. Let γ_0 be small enough and let $(\mathbf{u}^h, \lambda^H)$ be the solution to the discrete problem (3.12) where $M^{H-} = M_1^{H-}$. Then, we have for any $\eta > 0$*

$$\left|\!\left|\!\left| \left(\mathbf{u} - \mathbf{u}^h, \lambda - \lambda^H\right) \right|\!\right|\!\right| \lesssim h\|\mathbf{u} - \chi \mathbf{u}_s\|_{2,\Omega} + (H^{1-\frac{\eta}{2}} + h^{1/2})\|\lambda\|_{1/2,\Gamma_C} + H^{1-\frac{\eta}{2}} \|\mathbf{u}\|_{3/2-\eta,\Omega}.$$

Proof. We choose $\mu = 0$ in (3.24) which implies

$$\inf_{\mu \in M^-} \int_{\Gamma_C} (\mu - \lambda^H)[\![u_n]\!] d\Gamma \leq -\int_{\Gamma_C} \lambda^H [\![u_n]\!] d\Gamma \leq 0.$$

In the infimum (3.23) we choose $\mu^H = 0$. So

$$\begin{aligned}
&\inf_{\mu^H \in M_1^{H-}} \int_{\Gamma_C} (\mu^H - \lambda)([\![u_n^h]\!] + \gamma(\lambda^H - R_h(\mathbf{u}^h)))d\Gamma \\
\leq\ & -\int_{\Gamma_C} \lambda([\![u_n^h]\!] + \gamma(\lambda^H - R_h(\mathbf{u}^h)))d\Gamma \\
=\ & -\int_{\Gamma_C} \lambda\, r^H([\![u_n^h]\!] + \gamma(\lambda^H - R_h(\mathbf{u}^h)))d\Gamma \\
& -\int_{\Gamma_C} \lambda([\![u_n^h]\!] + \gamma(\lambda^H - R_h(\mathbf{u}^h)) - r^H([\![u_n^h]\!] + \gamma(\lambda^H - R_h(\mathbf{u}^h))))d\Gamma \\
\leq\ & -\int_{\Gamma_C} \lambda([\![u_n^h]\!] + \gamma(\lambda^H - R_h(\mathbf{u}^h)) - r^H([\![u_n^h]\!] + \gamma(\lambda^H - R_h(\mathbf{u}^h))))d\Gamma \\
=\ & \int_{\Gamma_C} \lambda(r^H[\![u_n^h]\!] - [\![u_n^h]\!])d\Gamma + \int_{\Gamma_C} \lambda(r^H(\gamma(\lambda^H - R_h(\mathbf{u}^h))) - \gamma(\lambda^H - R_h(\mathbf{u}^h)))d\Gamma, \qquad (3.29)
\end{aligned}$$

where $r^H : L^1(\Gamma_C) \mapsto W_1^H$ is a quasi-interpolation operator which preserves the nonpositivity defined for any function v in $L^1(\Gamma_C)$ by

$$r^H v = \sum_{\mathbf{x} \in N^H} \alpha_{\mathbf{x}}(v)\psi_{\mathbf{x}},$$

where N^H represents the set of nodes $\mathbf{x}_0, ..., \mathbf{x}_N$ in $\overline{\Gamma_C}$, $\psi_{\mathbf{x}}$ is the scalar basis function of W_1^H (defined on $\overline{\Gamma_C}$) at node $\mathbf{x}$ satisfying $\psi_{\mathbf{x}}(\mathbf{x}') = \delta_{\mathbf{x},\mathbf{x}'}$ for all $\mathbf{x}' \in N^H$ and

$$\alpha_{\mathbf{x}}(v) = \left(\int_{\Gamma_C} v\psi_{\mathbf{x}}\, d\Gamma \right) \left(\int_{\Gamma_C} \psi_{\mathbf{x}}\, d\Gamma \right)^{-1}.$$

The approximation properties of r^H are proved in [51]. We simply recall hereafter the two main results. The first result is concerned with L^2-stability property of r^H.

Lemma 3.3.7. *For any $v \in L^2(\Gamma_C)$ and any $E \in T^H$ we have*

$$\|r^H v\|_{0,E} \lesssim \|v\|_{0,\gamma_E},$$

where $\gamma_E = \cup_{\{F \in T^H :\, \bar{F} \cap \bar{E} \neq \emptyset\}} \bar{F}$.

Proof. Let $E \in T^H$ and ψ_1, ψ_1 the clasical scalar basic functions related to E. Using the definition of $\alpha_{\mathbf{x}}(\mathbf{v})$ and the Cauchy-Schwarz inequality we get:

$$\begin{aligned}
\|r^H v\|_{0,E} &\leq \alpha_1 \|\psi_1\|_{0,\Gamma_C} + \alpha_2 \|\psi_2\|_{0,\Gamma_C} \\
&\leq \|\mathbf{v}\|_{0,\gamma_E} \frac{\|\psi_1\|_{0,\Gamma_C}^2}{\int_{\Gamma_C} \psi_1\, d\Gamma} + \|\mathbf{v}\|_{0,\gamma_E} \frac{\|\psi_2\|_{0,\Gamma_C}^2}{\int_{\Gamma_C} \psi_2\, d\Gamma} \\
&\lesssim \|v\|_{0,\gamma_E},
\end{aligned}$$

□

Note that the proof of this lemma is also given in [51] using the additional assumption that the mesh T^H is quasi-uniform. The second result is concerned with the L^2-approximation properties of r^H.

Lemma 3.3.8. *For any $v \in H^\eta(\Gamma_C)$, $0 \leq \eta \leq 1$, and any $E \in T^H$ we have*

$$\|v - r^H v\|_{0,E} \lesssim H^\eta \|v\|_{\eta,\gamma_E}, \tag{3.30}$$

where $\gamma_E = \cup_{\{F \in E_C^H:\, \bar{F}\cap\bar{E}\neq\emptyset\}} \bar{F}$.

Consequently, the first integral term in (3.29) is estimated using (3.30) as follows

$$\begin{aligned}
\int_{\Gamma_C} \lambda(r^H[\![u_n^h]\!] - [\![u_n^h]\!])d\Gamma &\leq \int_{\Gamma_C} \lambda(r^H([\![u_n^h]\!] - [\![u_n]\!]) - ([\![u_n^h]\!] - [\![u_n]\!]))d\Gamma + \int_{\Gamma_C} \lambda(r^H[\![u_n]\!] - [\![u_n]\!])d\Gamma,\\
&\lesssim \|\lambda\|_{0,\Gamma_C} H^{1/2}\|\mathbf{u} - \mathbf{u}^h\| + \|\lambda\|_{0,\Gamma_C} H^{1-\eta}\|[\![u_n]\!]\|_{1-\eta,\Gamma_C},\\
&\lesssim \|\lambda\|_{1/2,\Gamma_C} H^{1/2}\|\mathbf{u} - \mathbf{u}^h\| + \|\lambda\|_{1/2,\Gamma_C} H^{1-\eta}\|[\![u_n]\!]\|_{1-\eta,\Gamma_C},\\
&\lesssim H^{1/2}\|\lambda\|_{1/2,\Gamma_C}\|\mathbf{u} - \mathbf{u}^h\| + H^{1-\frac{\eta}{2}}\|\lambda\|_{1/2,\Gamma_C} H^{1-\frac{\eta}{2}}\|[\![u_n]\!]\|_{1-\eta,\Gamma_C}.
\end{aligned}$$

Therefore, for any $\alpha > 0$ we write

$$\begin{aligned}
&\int_{\Gamma_C} \lambda(r^H[\![u_n^h]\!] - [\![u_n^h]\!])d\Gamma\\
&\lesssim \alpha\|\mathbf{u} - \mathbf{u}^h\|^2 + \alpha H^{1-\eta}\|\mathbf{u}\|^2_{3/2-\eta,\Omega} + \alpha^{-1}(H^{1-\eta} + H)\|\lambda\|^2_{1/2,\Gamma_C}.
\end{aligned} \tag{3.31}$$

Now, we consider the second integral term in (3.29):

$$\begin{aligned}
&\int_{\Gamma_C} \lambda(r^H(\gamma(\lambda^H - R_h(\mathbf{u}^h))) - \gamma(\lambda^H - R_h(\mathbf{u}^h)))d\Gamma\\
&\leq \|\lambda\|_{0,\Gamma_C}\|r^H(\gamma(\lambda^H - R_h(\mathbf{u}^h))) - \gamma(\lambda^H - R_h(\mathbf{u}^h))\|_{0,\Gamma_C}\\
&\lesssim \|\lambda\|_{0,\Gamma_C}\|\gamma(\lambda^H - R_h(\mathbf{u}^h))\|_{0,\Gamma_C}\\
&\lesssim \gamma_0^{1/2}h^{1/2}\|\lambda\|_{0,\Gamma_C}\left\|\gamma^{1/2}\left((\lambda^H - \lambda) + \sigma_n(\mathbf{u}) - R_h(\Pi^h\mathbf{u}) + R_h(\Pi^h\mathbf{u} - \mathbf{u}^h)\right)\right\|_{0,\Gamma_C}\\
&\lesssim \gamma_0^{1/2}h^{1/2}\|\lambda\|_{1/2,\Gamma_C}\left(\|\gamma^{1/2}(\lambda^H - \lambda)\|_{0,\Gamma_C} + h\|\mathbf{u} - \chi\mathbf{u}_s\|_{2,\Omega} + \gamma_0^{1/2}\|\mathbf{u} - \mathbf{u}^h\|\right).
\end{aligned}$$

As a consequence, for any $\alpha > 0$ we have

$$\begin{aligned}
&\int_{\Gamma_C} \lambda(r^H(\gamma(\lambda^H - R_h(\mathbf{u}^h))) - \gamma(\lambda^H - R_h(\mathbf{u}^h)))d\Gamma\\
&\lesssim \alpha(\|\mathbf{u} - \mathbf{u}^h\|^2 + \|\gamma^{1/2}(\lambda^H - \lambda)\|^2_{0,\Gamma_C}) + \alpha h^2\|\mathbf{u} - \chi\mathbf{u}_s\|^2_{2,\Omega} + \alpha^{-1}h\|\lambda\|^2_{1/2,\Gamma_C}.
\end{aligned} \tag{3.32}$$

The proof of the theorem then follows by using the inequalities (3.22), (3.29), (3.31), (3.32) and Proposition 3.3.3. □

Remark: Note that if we take $h = H$ the rate of convergence proved in Theorem 3.3.6 is $h^{1-\frac{\eta}{2}}$

3.3.2.3 Third contact condition: $M^{H-} = M^{H-}_{1,*}$

This choice corresponds to "weakly nonpositive" continuous piecewise affine multipliers where M^{H-} is given by (3.11).

Theorem 3.3.9. *Let $(\mathbf{u},\lambda)$ be the solution to Problem (3.6). Assume that $\mathbf{u}_r \in (H^2(\Omega))^2$. Let γ_0 be small enough and let $(\mathbf{u}^h,\lambda^H)$ be the solution to the discrete problem (3.12) where $M^{H-}=M_{1,*}^{H-}$. Then, for any $\eta>0$ we have*

$$\left|\!\left|\!\left|\left(\mathbf{u}-\mathbf{u}^h,\lambda-\lambda^H\right)\right|\!\right|\!\right| \lesssim h\|\mathbf{u}-\chi\mathbf{u}_s\|_{2,\Omega}+(h^{1/2}+H^{3/2-\eta})\|\lambda\|_{1/2,\Gamma_C}+h^{-1/2}H^{1-\eta}\|\mathbf{u}\|_{3/2-\eta,\Omega}.$$

Proof. By setting $\mu=0$ in (3.24) we obtain

$$\begin{aligned}
\inf_{\mu\in M^-}\int_{\Gamma_C}(\mu-\lambda^H)[\![u_n]\!]d\Gamma &\leq -\int_{\Gamma_C}\lambda^H[\![u_n]\!]d\Gamma,\\
&= \int_{\Gamma_C}\lambda^H(I^H[\![u_n]\!]-[\![u_n]\!])d\Gamma-\int_{\Gamma_C}\lambda^H I^H[\![u_n]\!]d\Gamma,\\
&\leq \int_{\Gamma_C}\lambda^H(I^H[\![u_n]\!]-[\![u_n]\!])d\Gamma,\\
&= \int_{\Gamma_C}(\lambda^H-\lambda)(I^H[\![u_n]\!]-[\![u_n]\!])d\Gamma+\int_{\Gamma_C}\lambda(I^H[\![u_n]\!]-[\![u_n]\!])d\Gamma,\\
&\leq \|\gamma^{1/2}(\lambda^H-\lambda)\|_{0,\Gamma_C}\|\gamma^{-1/2}(I^H[\![u_n]\!]-[\![u_n]\!])\|_{0,\Gamma_C},\\
&\quad +\|\lambda\|_{0,\Gamma_C}\|I^H[\![u_n]\!]-[\![u_n]\!]\|_{0,\Gamma_C},\\
&\lesssim H^{1-\eta}h^{-1/2}\|\mathbf{u}\|_{3/2-\eta,\Omega}\|\gamma^{1/2}(\lambda^H-\lambda)\|_{0,\Gamma_C}+\|\lambda\|_{1/2,\Gamma_C}H^{1-\eta}\|\mathbf{u}\|_{3/2-\eta,\Omega},
\end{aligned}$$

where I^H is the Lagrange interpolation operator onto W_1^H. The operator I^H is defined for any $v\in\mathscr{C}(\Gamma_C)$ and satisfies the following error estimates for any $1/2<r\leq 2$:

$$\|v-I^Hv\|_{0,\Gamma_C}\lesssim H^r\|v\|_{r,\Gamma_C}.$$

Therefore, for any $\alpha>0$ we have

$$\begin{aligned}
&\inf_{\mu\in M^-}\int_{\Gamma_C}(\mu-\lambda^H)[\![u_n]\!]d\Gamma\\
&\lesssim \alpha h^{-1}H^{2(1-\eta)}\|\mathbf{u}\|^2_{3/2-\eta,\Omega}+\alpha^{-1}\left(\|\gamma^{1/2}(\lambda^H-\lambda)\|^2_{0,\Gamma_C}+h\|\lambda\|^2_{1/2,\Gamma_C}\right)
\end{aligned}\tag{3.33}$$

In the infimum (3.23) we choose $\mu^H=\pi_1^H\lambda$ where π_1^H denotes the $L^2(\Gamma_C)$-projection onto W_1^H. The operator π_1^H is defined for any $v\in L^2(\Gamma_C)$ by

$$\pi_1^Hv\in W_1^H,\quad \int_{\Gamma_C}(v-\pi_1^Hv)\mu\,d\Gamma=0,\quad \forall\mu\in W_1^H,$$

and satisfies, for any $0\leq r\leq 2$, the following error estimates

$$H^{-1/2}\|v-\pi_1^Hv\|_{-1/2,\Gamma_C}+\|v-\pi_1^Hv\|_{0,\Gamma_C}\leq CH^r\|v\|_{r,\Gamma_C}.\tag{3.34}$$

Clearly $\pi_1^H\lambda\in M_{1,*}^{H-}$, so that

$$\begin{aligned}
&\inf_{\mu^H\in M_{1,*}^{H-}}\int_{\Gamma_C}(\mu^H-\lambda)([\![u_n^h]\!]+\gamma(\lambda^H-R_h(\mathbf{u}^h)))d\Gamma\\
&\leq \int_{\Gamma_C}(\pi_1^H\lambda-\lambda)[\![u_n^h]\!]d\Gamma+\int_{\Gamma_C}\gamma(\pi_1^H\lambda-\lambda)(\lambda^H-R_h(\mathbf{u}^h))d\Gamma.
\end{aligned}\tag{3.35}$$

The first integral term in (3.35) is estimated using (3.34) as follows

$$\begin{aligned}\int_{\Gamma_C}(\pi_1^H\lambda-\lambda)[\![u_n^h]\!]d\Gamma &= \int_{\Gamma_C}(\pi_1^H\lambda-\lambda)([\![u_n^h]\!]-[\![u_n]\!])d\Gamma+\int_{\Gamma_C}(\pi_1^H\lambda-\lambda)[\![u_n]\!]d\Gamma,\\ &= \int_{\Gamma_C}(\pi_1^H\lambda-\lambda)([\![u_n^h]\!]-[\![u_n]\!])d\Gamma+\int_{\Gamma_C}(\pi_1^H\lambda-\lambda)([\![u_n]\!]-\pi_1^H[\![u_n]\!])d\Gamma,\\ &\leq \|\pi_1^H\lambda-\lambda\|_{-1/2,\Gamma_C}\|[\![u_n^h]\!]-[\![u_n]\!]\|_{1/2,\Gamma_C}+\|\pi_1^H\lambda-\lambda\|_{0,\Gamma_C}\|[\![u_n]\!]-\pi_1^H[\![u_n]\!]\|_{0,\Gamma_C},\\ &\lesssim H\|\lambda\|_{1/2,\Gamma_C}\|\mathbf{u}-\mathbf{u}^h\|+H^{1/2}\|\lambda\|_{1/2,\Gamma_C}H^{1-\eta}\|\mathbf{u}\|_{3/2-\eta,\Omega}.\end{aligned}$$

Therefore, for any $\alpha>0$, we have

$$\begin{aligned}&\int_{\Gamma_C}(\pi_1^H\lambda-\lambda)[\![u_n^h]\!]d\Gamma\\ &\lesssim \alpha\left(\|\mathbf{u}-\mathbf{u}^h\|^2+H^{3/2-\eta}\|\mathbf{u}\|^2_{3/2-\eta,\Omega}\right)+\alpha^{-1}(H^2+H^{3/2-\eta})\|\lambda\|^2_{1/2,\Gamma_C}.\end{aligned}\tag{3.36}$$

For the second integral term in (3.35) by using the bounds given in (3.34), (3.13), (3.21) we get

$$\begin{aligned}\int_{\Gamma_C}\gamma(\pi_1^H\lambda-\lambda)(\lambda^H-R_h(\mathbf{u}^h))d\Gamma &= \int_{\Gamma_C}\gamma(\pi_1^H\lambda-\lambda)(\lambda^H-\lambda)d\Gamma\\ &\quad+\int_{\Gamma_C}\gamma(\pi_1^H\lambda-\lambda)(\sigma_n(\mathbf{u})-R_h(\Pi^h\mathbf{u}))d\Gamma\\ &\quad+\int_{\Gamma_C}\gamma(\pi_1^H\lambda-\lambda)(R_h(\Pi^h\mathbf{u})-R_h(\mathbf{u}^h))d\Gamma\\ &\lesssim \gamma_0^{1/2}h^{1/2}\|\pi_1^H\lambda-\lambda\|_{0,\Gamma_C}\|\gamma^{1/2}(\lambda^H-\lambda)\|_{0,\Gamma_C}\\ &\quad+\gamma_0^{1/2}h^{1/2}\|\pi_1^H\lambda-\lambda\|_{0,\Gamma_C}\|\gamma^{1/2}(\sigma_n(\mathbf{u})-R_h(\Pi^h\mathbf{u}))\|_{0,\Gamma_C}\\ &\quad+\gamma_0^{1/2}h^{1/2}\|\pi_1^H\lambda-\lambda\|_{0,\Gamma_C}\|\gamma^{1/2}R_h(\Pi^h\mathbf{u}-\mathbf{u}^h)\|_{0,\Gamma_c}\\ &\lesssim \gamma_0^{1/2}h^{1/2}H^{1/2}\|\lambda\|_{1/2,\Gamma_C}\|\gamma^{1/2}(\lambda^H-\lambda)\|_{0,\Gamma_C}\\ &\quad+\gamma_0^{1/2}h^{1/2}H^{1/2}\|\lambda\|_{1/2,\Gamma_C}h\|\mathbf{u}-\chi\mathbf{u}_s\|_{2,\Omega}\\ &\quad+\gamma_0h^{1/2}H^{1/2}\|\lambda\|_{1/2,\Gamma_C}\|\mathbf{u}^h-\Pi^h\mathbf{u}\|.\end{aligned}$$

Since $\|\mathbf{u}^h-\Pi^h\mathbf{u}\|\leq\|\mathbf{u}-\mathbf{u}^h\|+Ch\|\mathbf{u}-\chi\mathbf{u}_s\|_{2,\Omega}$, for any small $\alpha>0$ we get

$$\begin{aligned}&\int_{\Gamma_C}\gamma(\pi_1^H\lambda-\lambda)(\lambda^H-R_h(\mathbf{u}^h))d\Gamma\\ &\lesssim \alpha\|\mathbf{u}-\mathbf{u}^h\|^2+\alpha\|\gamma^{1/2}(\lambda^H-\lambda)\|^2_{0,\Gamma_C}+\alpha h^2\|\mathbf{u}-\chi\mathbf{u}_s\|^2_{2,\Omega}+\alpha^{-1}hH\|\lambda\|^2_{1/2,\Gamma_C}.\end{aligned}\tag{3.37}$$

Finally, the theorem is established by combining Proposition 3.3.3 and the inequalities (3.33), (3.35), (3.36), (3.37) and (3.22). □

Remark: Note that if we take $h=H$ the rate of convergence proved in Theorem 3.3.9 is $h^{1/2-\eta}$

3.4 Numerical experiments

The numerical tests are performed on a non-cracked square defined by

$$\bar{\Omega} = [0,1] \times [-0.5, 0.5],$$

and the considered crack is the line segment $\Gamma_C =]0, 0.5[\times \{0\}$ (see Fig. 3.5). Three degrees

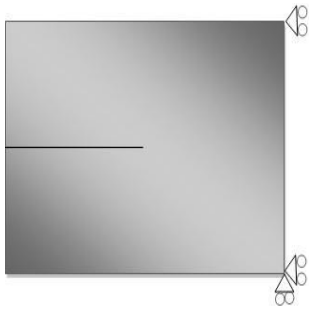

Figure 3.5: Cracked specimen.

of freedom are blocked in order to eliminate the rigid body motions (Fig. 3.5). In order to have both a contact zone and a non contact zone between the crack lips, we impose the following body force vector field

$$\mathbf{f}(x,y) = \begin{pmatrix} 0 \\ 3.5x(1-x)y\cos(2\pi x) \end{pmatrix}.$$

Neumann boundary conditions are prescribed as follows:

$$\begin{aligned} \mathbf{g}(0,y) = \mathbf{g}(1,y) &= \begin{pmatrix} 0 \\ 4\cdot 10^{-2}\sin(2\pi y) \end{pmatrix} && -0.5 \le y \le 0.5, \\ \mathbf{g}(x,-0.5) = \mathbf{g}(x,0.5) &= \begin{pmatrix} 0 \\ 0 \end{pmatrix} && 0 \le x \le 1. \end{aligned}$$

An example of a non structured mesh used is presented in Fig. 3.6. The numerical tests are performed with GETFEM++, the C++ finite-element library developed by our team (see [52]).

3.4.1 Numerical solving

The algebraic formulation of Problem (3.12) is given as follows

$$\text{(3.38)} \qquad \begin{cases} \text{Find } U \in \mathbb{R}^N \text{ and } L \in \overline{M}^{H-} \text{ such that} \\ (K - K_\gamma)U - (B - C_\gamma)^T L = F, \\ (\overline{L} - L)^T((B - C_\gamma)U + D_\gamma L) \ge 0, \quad \forall \overline{L} \in \overline{M}^{H-}, \end{cases}$$

where U is the vector of degrees of freedom (d.o.f.) for $\mathbf{u}^h$, L is the vector of d.o.f. for the multiplier λ^H, $\overline{M}^{H-}$ is the set of vectors L such that the corresponding multiplier lies in M^{H-}, K is the classical stiffness matrix coming from the term $a(\mathbf{u}^h, \mathbf{v}^h)$, F is the right-hand side corresponding to the Neumann boundary condition and the volume forces, and B, K_γ, C_γ, D_γ are

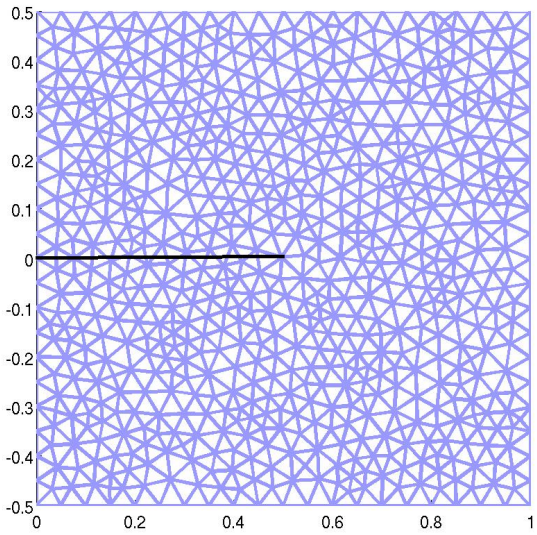

Figure 3.6: Non-structured mesh.

the matrices corresponding to the terms $b(\lambda^H, \mathbf{v}^h)$, $\int_{\Gamma_C} \gamma R_h(\mathbf{u}^h) R_h(\mathbf{v}^h)\, d\Gamma$, $\int_{\Gamma_C} \gamma \lambda^H R_h(\mathbf{v}^h)\, d\Gamma$, $\int_{\Gamma_C} \gamma \lambda^H \mu^H\, d\Gamma$, respectively.

The inequality in (3.38) can be expressed as an equivalent projection

$$L = P_{\overline{M}^{H-}}(L - r((B - C_\gamma)U + D_\gamma L)), \tag{3.39}$$

where r is a positive augmentation parameter. This last step transforms the contact condition into a nonlinear equation and we have to solve the following system:

$$\left\{ \begin{array}{l} \text{Find } U \in \mathbb{R}^N \text{ and } L \in \overline{M}^{H-} \text{ such that} \\ (K - K_\gamma)U - (B - C_\gamma)^T L - F = 0, \\ -\dfrac{1}{r}\left[L - P_{\overline{M}^{H-}}(L - r((B - C_\gamma)U + D_\gamma L))\right] = 0. \end{array} \right. \tag{3.40}$$

This allows us to use the semi-smooth Newton method (introduced for contact and friction problems in [53]) to solve Problem (3.40). The term 'semi-smooth' comes from the fact that projections are only piecewise differentiable. Practically, it is one of the most robust algorithms to solve contact problems with or without friction. In order to write a Newton step, one has to compute the derivative of the projection (3.39). An analytical expression can only be obtained when the projection itself is simple to express. This is the case for instance when the set M^{H-} is chosen to be the set of multipliers having non-positive values on each finite-element node of the contact boundary (such as M_0^{H-} or M_1^{H-}). In this case, the projection can be expressed component-wise (see [54]).

In order to keep the independence between the mesh and the crack, the approximation space W^H for the multiplier is chosen to be the trace on Γ_C of a Lagrange finite-element method defined on the same mesh as $\mathbf{V}^h$ (in that sense $H = h$) and its degree will be specified in the following.

Let us denote X^h the space corresponding to the Lagrange finite-element method. The choice of a basis of the trace space $W^H = X^h{}_{|\Gamma_C}$ is not completely straightforward. Indeed, the traces on Γ_C of the shape functions of X^h may be linearly dependent. A way to overcome this difficulty is to eliminate the redundant functions. Our approach in the presented numerical experiments is as follows. In a first time, we eliminate locally dependent columns of the mass matrix $\int_{\Gamma_C} \psi_i \psi_j d\Gamma$, where ψ_i is the finite-element shape functions of X^h, with a block-wise Gram-Schmidt algorithm. In a second time, we detect the potential remaining kernel of the mass matrix with a Lanczos algorithm.

3.4.2 Numerical tests

In this section, we present numerical tests of the stabilized and non stabilized unilateral contact problem for the following, differently enriched, finite-element methods: P_2/P_1, P_2/P_0, P_1+/P_1, P_1/P_1, P_1/P_0. The notation P_i/P_j (resp. P_1+/P_1) means that the displacement is approximated with a P_i extended finite-element method (resp. a P_1 extended finite-element method with an additional cubic bubble function) and the multiplier with a continuous P_j finite-element method for $j > 0$ (resp. continuous P_1 finite-element method).

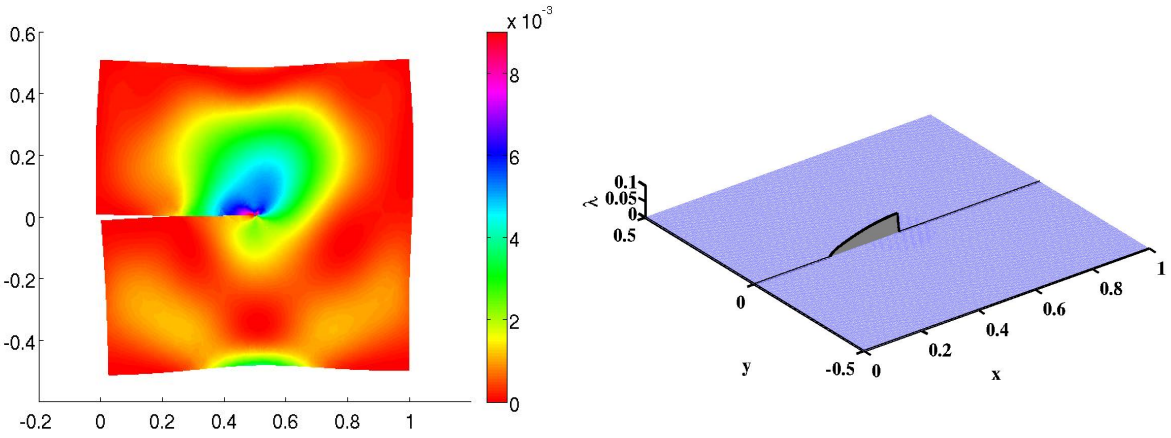

(a) Von Mises stress for the reference solution

(b) Normal contact stress for the reference solution

Figure 3.7: Von Mises stress and normal contact stress for the reference solution

The numerical tests are performed on non-structured meshes with $h = 0.088,\ 0.057,\ 0.03,\ 0.016,\ 0.008$ respectively. The reference solution is obtained with a structured P_2/P_1 method and $h = 0.0027$. The Von Mises stress of the reference solution is presented in Fig. 3.7(a). Its distribution shows that the Von Mises stress is not singular at the crack lips. The normal contact stress of the reference solution is presented in Fig. 3.7(b). The normal contact stress is not singular at the crack lips which confirms the theoretical result presented in Lemma A.1.

Without stabilization: The curves in the non stabilized case are given in Fig. 3.8(a) for the error in the $L^2(\Omega)$-norm on the displacement, in Fig. 3.8(b) for the error in the $H^1(\Omega)$-norm on the displacement and in Fig. 3.8(c) for the error in the $L^2(\Gamma_C)$-norm on the contact

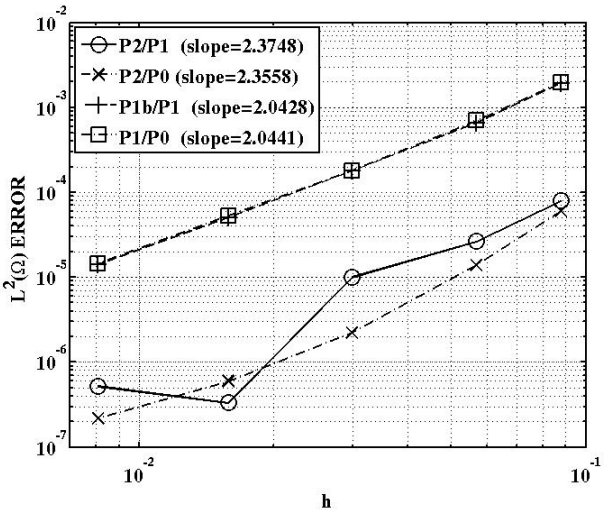

(a) Error in $L^2(\Omega)$-norm of the displacement

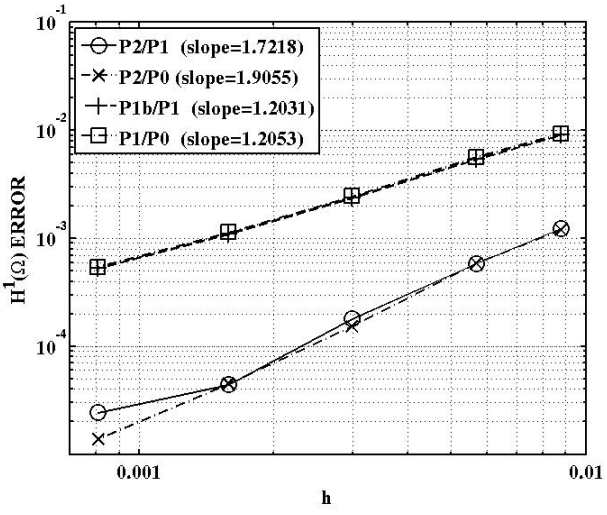

(b) Error in $H^1(\Omega)$-norm of the displacement

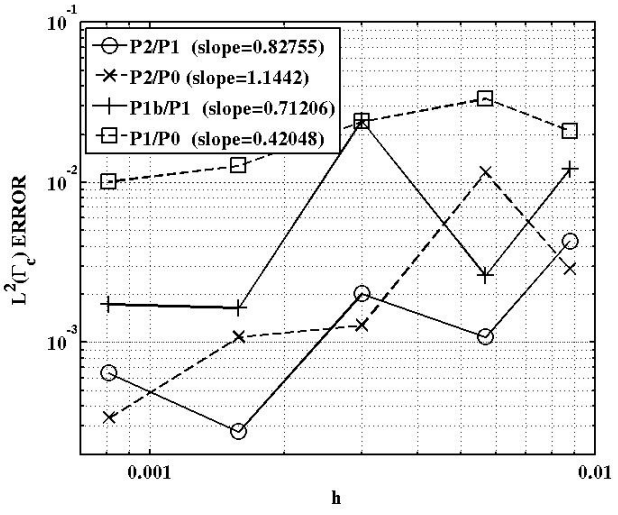

(c) Error in $L^2(\Gamma_C)$-norm of the contact stress

Figure 3.8: Convergence curves in the non stabilized case

stress. The P_1/P_1 method is not plotted because it does not work without stabilization. The P_2/P_1 and P_1/P_0 versions generally work without stabilization even though a uniform inf-sup condition cannot be proven. Fig. 3.8(a) shows that the rate of convergence in the error $L^2(\Omega)$-norm is of order 2.4 for the P_2/P_j methods and of order 2 for the P_1/P_j methods. This rate of convergence is close to optimality because the singularity due to the transition between contact and non contact is expected to be in $H^{5/2-\eta}(\Omega)$ for any $\eta > 0$ (under the assumptions of lemma A.1). Theoretically, this limits the convergence rate to $3/2 - \eta$ in the $H^1(\Omega)$-norm. Fig. 3.8(b) shows that the rate of convergence in energy norm is optimal for all pairs of elements considered. Fig. 3.8(c) shows that, except the P_1/P_0 method, the rate of convergence in the $L^2(\Gamma_C)$-norm is optimal but there are very large oscillations. For the P_1/P_0 method the rate of convergence in the $L^2(\Gamma_C)$-norm is not optimal (of order 0.42). It seems that the presence of some spurious modes affects this rate of convergence.

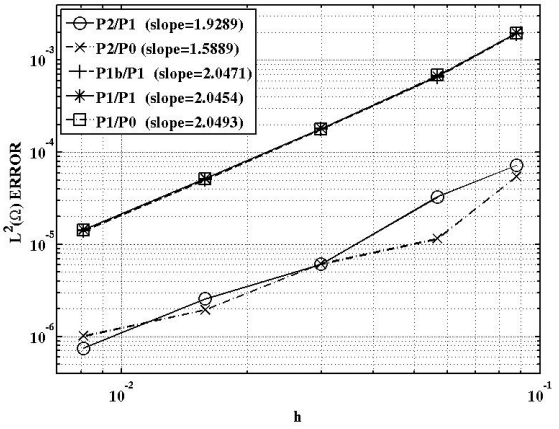

(a) Error in $L^2(\Omega)$-norm of the displacement

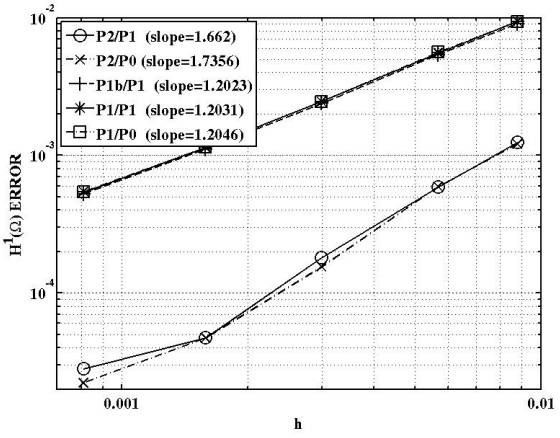

(b) Error in $H^1(\Omega)$-norm of the displacement

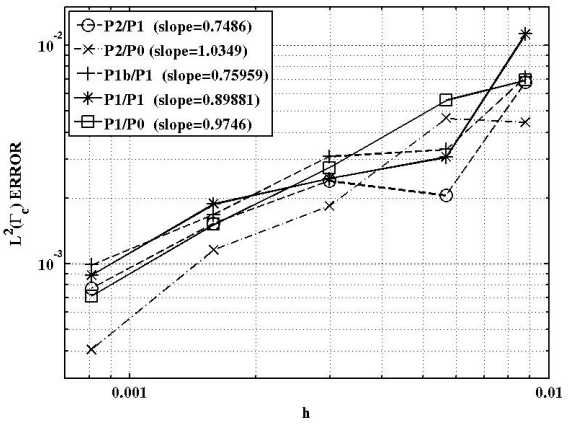

(c) Error in $L^2(\Gamma_C)$-norm of the contact stress

Figure 3.9: Convergence curves in the stabilized case

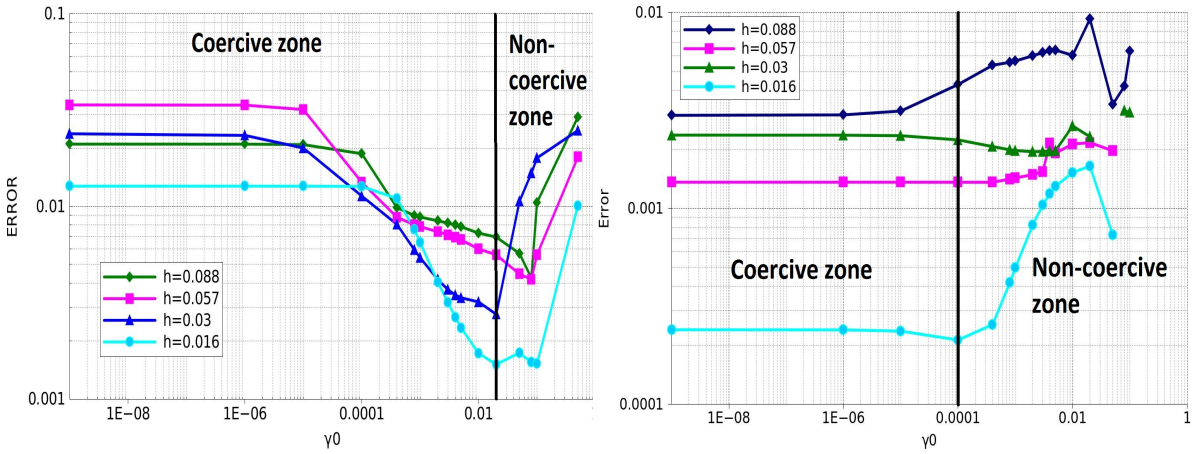

(a) P_1/P_0-elements (b) P_2/P_1-elements

Figure 3.10: Influence of the stabilization parameter in $L^2(\Gamma_C)$-norm of the contact stress

Stabilized method: The curves in the stabilized case are given in Fig. 3.9(a) for the error in the $L^2(\Omega)$-norm on the displacement, in Fig. 3.9(b) for the error in the $H^1(\Omega)$-norm on the displacement and in Fig. 3.9(c) for the error in the $L^2(\Gamma_C)$-norm of the contact stress. Similarly to the non stabilized method, Fig. 3.9(b) shows that we have an optimal rate of convergence, with a slight difference, for the error in the $H^1(\Omega)$-norm on the displacement. Concerning the error in the $L^2(\Omega)$-norm the rate of convergence is affected by the stabilization for the quadratic elements P_2/P_1 and P_2/P_0. For the error in the $L^2(\Gamma_C)$-norm of the contact stress, Fig. 3.9(c) shows that the Barbosa-Hughes stabilization eliminates the spurious modes for the P_1/P_1 and P_1/P_0 methods. For the remaining pairs of elements, the stabilization also allows to reduce the oscillations in the convergence of the contact stress.

The stabilization parameter is chosen in such a way that it is as large as possible but keeps the coercivity of the stiffness matrix. To check the coercivity, we calculate the smallest eigenvalue of the stiffness matrix. For the $L^2(\Gamma_C)$-norm on the contact stress, the value of the stabilization parameter can be divided into two zones. A coercive area where the error decreases when increasing the stabilization parameter γ_0 and a non-coercive zone where the error evolves randomly according to the stabilization parameter (see Fig. 3.10(a) and 3.10(b)). Fig. 3.11 shows that the stabilization parameter has no influence on the error in $L^2(\Omega)$ and $H^1(\Omega)$-norms of the displacement.

3.5 Conclusion

Concerning the three contact conditions we considered theoretically, the given a priori error estimates are obviously sub-optimal. This limitation of the mathematical analysis is not specific to the approximation of contact problems in the framework of XFEM. It is in fact particularly true for the approximation of the contact condition with Lagrange multiplier. This is probably

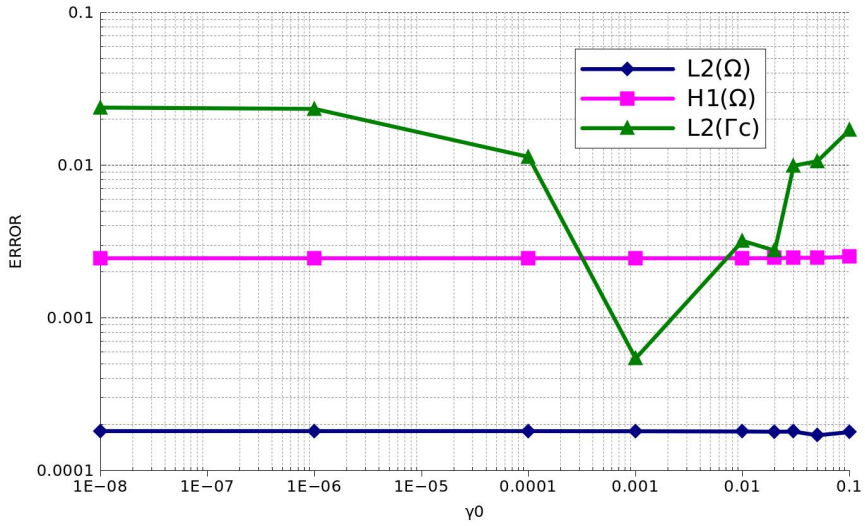

Figure 3.11: Influence of the stabilization parameter for P_1/P_0 method

due to technical reasons. The approximation with Lagrange multiplier is made necessary here to apply the Barbosa-Hughes stabilization technique (see [30]).

In the numerical tests we considered, the stabilized methods have indeed an optimal rate of convergence. More surprisingly, the unstabilized methods have also an optimal rate of convergence concerning the displacement (except the P_1/P_1 method whose linear system was not invertible). This may lead to the conclusion that no locking phenomenon were present in the numerical situation we studied despite the non-satisfaction of the discrete inf-sup condition. The fact that such a locking situation may exist or not in the studied framework (contact problem on crack lips for a linear elastic body) is an open question.

Chapter 4

A local projection stabilization of fictitious domain method for elliptic boundary value problems

This chapter is submitted for publication [55]

Contents

Introduction

The fictitious domain method is a technique allowing the use of regular structured meshes on a simple shaped fictitious domain containing the real domain. Generally, this technique is used for solving elliptic problems in domains with unknown or moving boundary without having to build a body fitted mesh. There exist two main approaches of fictitious domain method. The "thin" interface approach where the approached interface has the same dimension as the original interface. This approach was initiated by V.K. Saul'ev in [56]. In this context, there exist different techniques to take account of the boundary condition: the technique where the fictitious domain mesh is modified locally to take account of the boundary condition (see for instance reference [56, 57]); The technique of penalization which allows to conserve the Cartesian mesh of the fictitious domain (see for instance reference [58, 59]) and the technique of Lagrange multiplier introduced by R. Glowinski et al. [59, 60, 61, 62] where a second mesh is considered to conserve the Cartesian mesh of the fictitious domain and to take account of the boundary condition.

The second approach of fictitious domain method is the "Spread" interface approach where the approximate interface is larger than the physical interface. The approximate interface has one dimension more than the original one. It was introduced by Rukhovets [63]. For example, the following methods can be found in this group: Immersed boundary method [64, 65] and Fat boundary method [66, 67].

Recently, fictitious domain methods with a thin interface have been proposed in the context of the extended finite element method (X-FEM) introduced by Moes, Dolbow and Belytscko [7]. Different approaches are proposed in [68, 69, 70] to directly enforce an inf-sup condition on a multiplier to prescribe a Dirichlet boundary condition. Another possibility is the use of the stabilized Nitsche's method [71] which is close to a penalization technique but preserving the consisting and avoiding large penalty terms that would otherwise deteriorate the conditioning of the matrix system [72]. We can cite also the method introduced in [73] which uses a stabilized Lagrange multipliers method using piecewise constant multipliers and an additional stabilization term employing the inter-element jumps of the multipliers. Finally, let us mention [74] where an a priori error estimate for non-stabilized Dirichlet problem is given and an optimal method is developed using a Barbosa-Hughes stabilization (see [39, 40]).

In this paper, we perform a study similar to [74] for a local projection stabilization applied to the fictitious domain method inspired by the X-FEM. To our knowledge, this technique was used for the first time by Dohrmann et al. [75]. Recently, this new technique was proposed and analyzed by Burman [76] in the context of the Lagrange finite element method and by Barrenechea et al. [77] in the context of a more classical fictitious domain approch (uncut mesh). The principle of the used local projection stabilization is to penalize the difference of the multiplier with its projection on some pre-defined patches. The advantage of this technique is of at least threefold: the method is asymptotic consistent, there is no use of mesh other than the (possibly Cartesian) one of the fictitious domain and the additional term concerns only the multiplier and is not model dependent such as the Barbosa-Hughes stabilization technique.

The paper is organized as follows. In Section 1 we introduce the Poisson model problem and in Section 2, the non-stabilized fictitious domain method. We present our new stabilization technique in Section 3 together with the theoretical convergence analysis. Finally, Section 4 is devoted to two and three-dimensional numerical experiments and the comparison with the use of Barbosa-Hughes stabilization technique.

4.1 The model problem

For the sake of simplicity, the presentation and the theoretical analysis is made for a two-dimensional regular domain Ω, although the method extends naturally to higher dimensions. Let $\widetilde{\Omega} \subset \mathbb{R}^2$ be a fictitious domain containing Ω in its interior (and generally assumed to have a simple shape). We consider that the boundary Γ of Ω is split into two parts Γ_N and Γ_D (see Fig. 4.1). It is assumed that Γ_D has a nonzero one-dimensional Lebesgue measure. Let us consider

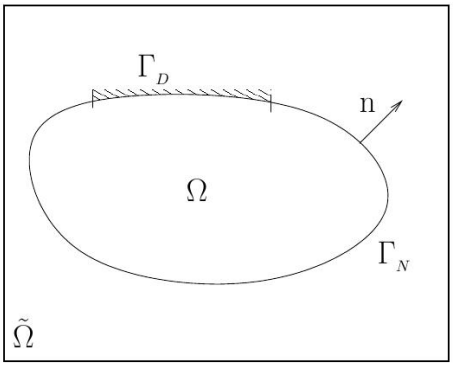

Figure 4.1: *Fictitious $\tilde{\Omega}$ and real Ω domains.*

the following elliptic problem in Ω:

$$\begin{cases} \text{Find } u : \Omega \mapsto \mathbb{R} \text{ such that:} \\ -\Delta u = f \qquad \text{in } \Omega, \\ u = 0 \qquad \text{on } \Gamma_D, \\ \partial_n u = g \qquad \text{on } \Gamma_N, \end{cases} \tag{4.1}$$

where $f \in L^2(\Omega)$ and $g \in L^2(\Gamma_N)$ are given data. Concidering a Lagrange multiplier multiplier to prescribe the Dirichlet boundary condition, a classical weak formulation of this problem reads as follows:

$$\begin{cases} \text{Find } u \in V \text{ and } \lambda \in W \text{ such that} \\ a(u,v) + \langle \lambda, v \rangle_{W,X} = l(v) \quad \forall v \in V, \\ \langle \mu, u \rangle_{W,X} = 0 \quad \forall \mu \in W, \end{cases} \tag{4.2}$$

where

$$V = H^1(\Omega),\ X = \left\{ w \in L^2(\Gamma_D) : \exists v \in V, w = v_{|\Gamma_D} \right\}, \quad W = X',$$

$$a(u,v) = \int_\Omega \nabla u . \nabla v d\Omega, \quad l(v) = \int_\Omega f\, v\, d\Omega + \int_{\Gamma_N} g\, v\, d\Gamma,$$

and $\langle \mu, v \rangle_{W,X}$ denotes the duality pairing between W and X. Let $V_0 = \left\{ v \in V : \int_{\Gamma_D} v\, d\Gamma = 0 \right\}$. Then, a direct consequence of Peetre-Tartar lemma (see [78]) is that $a(.,.)$ is coercive on V_0 *i.e.* there exists $\alpha > 0$ such that

$$a(v,v) \geq \alpha \|v\|_V^2 \quad \forall v \in V_0. \tag{4.3}$$

From this, the existence and uniqueness of a solution to Problem (4.2) follows. Classically, Problem (4.2) is also equivalent to the problem of finding the saddle point of the Lagrangian

$$\mathcal{L}(v,\mu) = \frac{1}{2} a(v,v) + \langle \mu, v \rangle_{W,X} - l(v), \tag{4.4}$$

defined on $V \times X$. The existence and uniqueness of a solution to Problem (4.2) is obtained by standard techniques.

4.2 The fictitious domain method

The fictitious domain approach requires the introduction of two finite-element spaces on the fictitious domain $\widetilde{\Omega}$. Namely $\widetilde{V}^h \subset H^1(\widetilde{\Omega})$ and $\widetilde{W}^h \subset L^2(\widetilde{\Omega})$. Note that $\widetilde{\Omega}$ may always be chosen as a sufficiently large rectangle $(a,b)\times(c,d)$ such that $\Omega \subset (a,b)\times(c,d)$ which allows $\widetilde{V}^h$ and $\widetilde{W}^h$ to be defined on the same structured mesh $\mathcal{T}^h$ (see Fig. 4.2). In what follows, we shall assume that

$$\widetilde{V}^h = \{v^h \in \mathcal{C}(\overline{\widetilde{\Omega}}) : v^h{}_{|T} \in P(T)\ \forall T \in \mathcal{T}^h\}, \tag{4.5}$$

where $P(T)$ is a finite-dimensional space of regular functions satisfying $P(T) \supseteq P_k(T)$ for some integer $k \geq 1$.

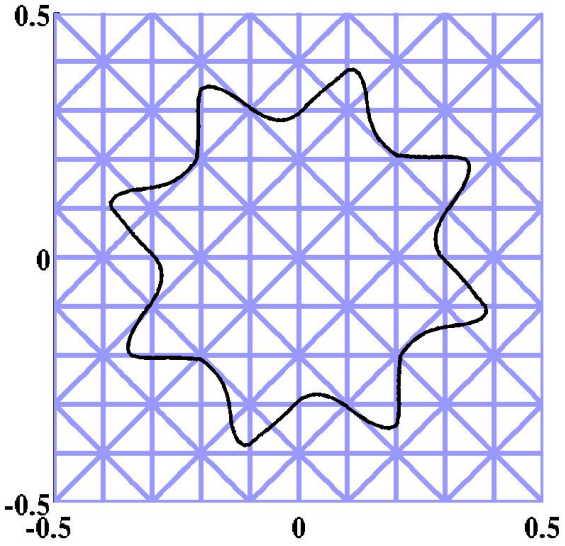

Figure 4.2: *Example of a real domain and a structured mesh of the fictitious domain.*

For the approximation on the real domain Ω, we consider the following restriction of $\widetilde{V}^h$ and $\widetilde{W}^h$ on Ω and Γ_D, respectively:

$$V^h = \widetilde{V}^h{}_{|\Omega}, \quad \text{and} \quad W^h = \widetilde{W}^h{}_{|\Gamma_D},$$

which are natural discretization of V and W. An approximation of Problem (4.2) is then defined as follows:

$$\begin{cases} \text{Find } u^h \in V^h \text{ and } \lambda^h \in W^h \text{ such that} \\ a(u^h, v^h) + \displaystyle\int_{\Gamma_D} \lambda^h v^h d\Gamma = l(v^h) \quad \forall v^h \in V^h, \\ \displaystyle\int_{\Gamma_D} \mu^h u^h d\Gamma = 0 \quad \forall \mu^h \in W^h. \end{cases} \tag{4.6}$$

We choose $\widetilde{W}^h$ and $\widetilde{V}^h$ in such a way that the following condition is satisfied:

$$1_{|\Gamma_D} \in W^h. \tag{4.7}$$

Let us define the following space:

$$V_0^h = \{v^h \in V^h : \int_{\Gamma_D} \mu^h v^h d\Gamma = 0 \ \ \forall \mu^h \in W^h\}. \tag{4.8}$$

Then $a(.,.)$ is V_0^h-elliptic since $V_0^h \subset V_0$. Without any additional treatment, the following result is proved in [74]:

Proposition 6. *Let $\widetilde{V}^h$ defined by (4.5), assume (4.7) is satisfied and, in addition*

$$\inf_{\mu^h \in W^h} \|\lambda - \mu^h\|_W \leq h^\beta, \quad \beta \geq 1/2. \tag{4.9}$$

$$\overline{\mu}^h \in W^h : \int_{\Gamma_D} \overline{\mu}^h v^h d\Gamma = 0 \ \ \forall v^h \in V^h \Longrightarrow \overline{\mu}^h = 0. \tag{4.10}$$

Then, one has the following error estimate:

$$\|u^h - u\|_V \leq C\sqrt{h}, \quad h \to 0+.$$

This means that, without any treatment, the guaranteed rate of convergence is limited to $O(\sqrt{h})$ which is confirmed is some numerical situations. This reflects a certain kind of numerical locking phenomenon.

4.3 A local projection stabilized formulation

In this section, we present a stabilization technique consisting in the addition of a supplementary term involving the local orthogonal projection of the multiplier on a patch decomposition of the mesh.

Let S^h be the one-dimensional mesh resulting in the intersection of $\mathcal{T}^h$ and Γ_D. The idea is to aggregate the possibly very small elements of S^h in order to obtain a set of patches having a minimal and a maximal size (for instance between $3h$ and $6h$). In practice, this operation can be done rather easily (even for three-dimensional problems). A practical way to obtain such a patch decomposition will be described in the next section. An example of patch aggregation is presented in Fig. 4.3.

Let H be the minimum length of these patches and denote by S^H the corresponding subdivision of Γ_D. Let

$$W^H = \left\{\mu^H \in L^2(\Gamma_D) : \mu^H{}_{|S} \in P_0(S), \ \forall S \in S_H\right\},$$

be the space of piecewise constants on this mesh. A classical result, presented in [61], states that under a reasonable regularity assumption on Γ_D, an inf-sup condition is satisfied between W^H and V^h for minimal size of $3h$ for the patches. This implies in particular that an optimal convergence can be reached if the multiplier is taken in W^H. However, this assumes a relatively coarse approximation of the multiplier. Our approach is to use this result in order to stabilize the approximation obtained with the multiplier defined on the finer discretization W^h.

Let us first recall the result of Girault and Glowinski in [61]. Under the assumption that Γ_D is of class $\mathscr{C}^{1,1}$ and a condition for the patches $S \in S^H$ to be approximated by a fixed set of line segments having approximatively the same length (see [61], condition (4.17)) with a length greater or equal to $3h$ then the following inf-sup (or LBB) condition holds for a constant $\beta^* > 0$, independent of h and H:

$$\forall \mu^H \in W^H, \qquad \sup_{v^h \in V^h} \frac{\int_{\Gamma_D} v^h \, \mu^H \, d\Gamma}{\|v^h\|_V} \geq \beta^* \|\mu^H\|_{-1/2,\Gamma_D}. \tag{4.11}$$

In the following, we will assume that the conditions to obtain this inf-sup condition are satisfied.

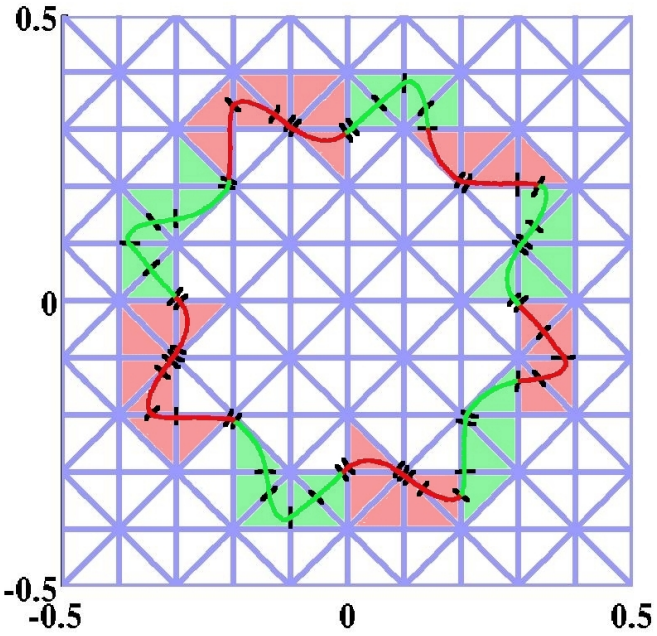

Figure 4.3: *Example of a patch aggregation (in red and green) of size approximatively* $2h$ *of the intersection of the boundary of the real domain and the mesh. Note the practically inevitable presence of very small intersections.*

Let P_{W^H} be the local orthogonal projection operator from $L^2(\Gamma_D)$ onto W^H which is defined by

$$\forall \mu \in L^2(\Gamma_D), \ \forall S \in S^H \qquad P_{W^H}(\mu)\,|_S = \frac{1}{mes(S)} \int_S \mu d\Gamma.$$

The stabilized formulation consists in approximate the Lagrangian (4.4) by:

$$\mathcal{L}_h(v^h, \mu^h) = \mathcal{L}(v^h, \mu^h) - \frac{\gamma}{2} \int_{\Gamma_D} (\mu_h - P_{W^H}(\mu^h))^2 d\Gamma,$$

where, for the sake of simplicity, γ is a chosen constant. The corresponding optimality system reads as follows:

$$\begin{cases} \text{Find } u^h \in V^h \text{ and } \lambda^h \in W^h \text{ such that} \\ a(u^h, v^h) + \displaystyle\int_{\Gamma_D} \lambda^h v^h d\Gamma = l(v^h) \quad \forall v^h \in V^h, \\ \displaystyle\int_{\Gamma_D} \mu^h u^h d\Gamma - \gamma \int_{\Gamma_D} (\lambda^h - P_{W^H}(\lambda^h))(\mu^h - P_{W^H}(\mu^h)) d\Gamma = 0 \quad \forall \mu^h \in W^h. \end{cases} \tag{4.12}$$

Lemma 4.3.1. *Assume that (4.7) and (4.11) hold, then for any $\gamma > 0$ there exists a unique solution of the stabilized problem (4.12).*

Proof. Suppose (u_1^h, λ_1^h) and (u_2^h, λ_2^h) are two solutions to Problem (4.12). Let us denote $\bar{u}^h = u_1^h - u_2^h$, $\bar{\lambda}^h = \lambda_1^h - \lambda_2^h$ and $\bar{\lambda}^H = P_{W^H}(\lambda_1^h) - P_{W^H}(\lambda_2^h)$. Then, from Problem (4.12) we obtain

$$\begin{cases} a(\bar{u}^h, \bar{u}^h) + \displaystyle\int_{\Gamma_D} \bar{\lambda}^h \bar{u}^h d\Gamma = 0, \\ \displaystyle\int_{\Gamma_D} \bar{\lambda}^h \bar{u}^h d\Gamma - \gamma \int_{\Gamma_D} (\bar{\lambda}^h - \bar{\lambda}^H)^2 d\Gamma = 0 \quad \forall \mu^h \in W^h. \end{cases} \tag{4.13}$$

Consequently,

$$a(\bar{u}^h, \bar{u}^h) + \gamma \int_{\Gamma_D} (\bar{\lambda}^h - \bar{\lambda}^H)^2 d\Gamma = 0, \tag{4.14}$$

which implies that $\bar{u}^h = 0$ and $\bar{\lambda}^h = \bar{\lambda}^H$ (i.e. $\bar{\lambda}^h \in W^H$). Moreover, it follows from (4.11) that there exists $v^h \in V^h$ such that

$$\int_{\Gamma_D} \bar{\lambda}^H v^h \geq \beta^* \|\bar{\lambda}^H\|_{-1/2,\Gamma_D} \|v^h\|_V, \tag{4.15}$$

and thus

$$\beta^* \|\bar{\lambda}^H\|_{-1/2,\Gamma_D} \leq \frac{1}{\|v^h\|_V} \int_{\Gamma_D} \bar{\lambda}^H v^h d\Gamma = \frac{1}{\|v^h\|_V} \int_{\Gamma_D} \bar{\lambda}^h v^h d\Gamma = \frac{1}{\|v^h\|_V} a(\bar{u}^h, v^h) = 0.$$

This implies the uniqueness of the solution and, since the dimension of the linear system (4.12) is finite, the existence as well. □

4.3.1 Convergence analysis

In this section, we establish an optimal *a priori* error estimate for the following standard finite element spaces:

$$\widetilde{V}^h = \{v^h \in \mathcal{C}(\overline{\widetilde{\Omega}}) : v^h{}_{|T} \in P(T) \ \forall T \in \mathcal{T}^h\}, \tag{4.16}$$

$$\widetilde{W}^h = \{\mu^h \in L^2(\widetilde{\Omega}) : \mu^h{}_{|T} \in P'(T) \ \forall T \in \mathcal{T}^h\}, \tag{4.17}$$

where $P(T)$ (resp. $P'(T)$) is a finite-dimensional space of regular functions satisfying $P(T) \supseteq P_k(T)$ (resp. $P(T) \supseteq P_{k'}(T)$) for an integer $k \geq 1$ (resp. $k' \geq 0$).

Theorem 4.3.2. *Let $\widetilde{V}^h$ and $\widetilde{W}^h$ be defined by (4.16) and (4.17), respectively such that (4.7) is satisfied. Let (u,λ) be the solution of the continuous problem (4.2) such that $u \in H^2(\Omega)$ and $\lambda \in H^{1/2}(\Gamma_{_D})$. Assume that (4.11) is satisfied and assume also the existence of a constant $\eta > 1$ with $H \leq \eta h$. Then, the following estimate holds for $C > 0$ a constant independent of h:*

$$\left|\!\left|\!\left| \Big(u - u^h, \lambda - \lambda^h\Big) \right|\!\right|\!\right| \leq Ch\Big(\|u\|_{2,\Omega} + \|\lambda\|_{1/2,\Gamma_{_D}} \Big), \tag{4.18}$$

where $|||(u,\lambda)|||^2 = \|u\|_V^2 + \|\lambda\|^2_{-1/2,\Gamma_{_D}}$ and (u^h,λ^h) is the solution to Problem (4.12).

Proof. Let $\lambda^H = P_{W^H}(\lambda^h)$. As u and u^h are both in V^0 then for all $v^h \in V^h$ and $\mu^H \in W^H$ we have:

$$\begin{aligned}
\alpha\|u^h - u\|_V^2 &\leq a(u^h - u, u^h - u) = a(u^h - u, v^h - u) + a(u^h - u, u^h - v^h),\\
&\leq M\|u^h - u\|_V\|v^h - u\|_V - \int_{\Gamma_{_D}} (\lambda^h - \lambda)(u^h - v^h)d\Gamma,\\
&= M\|u^h - u\|_V\|v^h - u\|_V - \int_{\Gamma_{_D}} \lambda^h u^h d\Gamma + \int_{\Gamma_{_D}} \lambda u^h d\Gamma + \int_{\Gamma_{_D}} (\lambda^h - \lambda)(v^h - u)d\Gamma,\\
&= M\|u^h - u\|_V\|v^h - u\|_V - \gamma\|\lambda^h - \lambda^H\|^2_{0,\Gamma_{_D}} + \int_{\Gamma_{_D}} (\lambda - \mu^H)(u^h - u)d\Gamma\\
&\quad + \int_{\Gamma_{_D}} (\lambda^h - \lambda)(v^h - u)d\Gamma,
\end{aligned}$$

because in particular $\displaystyle\int_{\Gamma_{_D}} (\lambda^h - \lambda)u\, d\Gamma = 0$. Then, still for all $v^h \in V^h$ and $\mu^H \in W^H$, we deduce that

$$\begin{aligned}
\alpha\|u^h - u\|_V^2 \;+\; &\gamma\|\lambda^h - \lambda^H\|^2_{-1/2,\Gamma_{_D}} \leq M\|u^h - u\|_V\|v^h - u\|_V\\
&+\|\lambda - \mu^H\|_{-1/2,\Gamma_{_D}}\|u^h - u\|_V + \|\lambda^h - \lambda\|_{-1/2,\Gamma_{_D}}\|u - v^h\|_V.
\end{aligned} \tag{4.19}$$

Besides,

$$\int_{\Gamma_{_D}} (\lambda - \lambda^h)v^h d\Gamma = a(u^h - u, v^h) \qquad \forall v^h \in V^h,$$

and therefore one obtains

$$\int_{\Gamma_{_D}} (\bar{\mu}^h - \lambda^h)v^h d\Gamma = a(u^h - u, v^h) + \int_{\Gamma_{_D}} (\bar{\mu}^h - \lambda)v^h d\Gamma \qquad \forall v^h \in V^h;\ \forall \bar{\mu}^h \in W^h. \tag{4.20}$$

Now, for $\mu^H = \lambda^H - \bar{\mu}^H \in W^H$ with $\bar{\mu}^H = P_{W^H}(\bar{\mu}^h)$, the inf-sup condition (4.11) ensures the existence of $v^h \in V^h$ such that together with (4.20) we get

$$\begin{aligned}
\beta^*\|\lambda^H - \bar{\mu}^H\|_{-1/2,\Gamma_{_D}} &\leq \frac{1}{\|v^h\|_V}\int_{\Gamma_{_D}} (\bar{\mu}^H - \lambda^H)v^h d\Gamma,\\
&\leq \frac{1}{\|v^h\|_V}\int_{\Gamma_{_D}} (\bar{\mu}^h - \lambda^h)v^h d\Gamma + \frac{1}{\|v^h\|_V}\int_{\Gamma_{_D}} (\bar{\mu}^H - \lambda^H - (\bar{\mu}^h - \lambda^h))v^h d\Gamma,\\
&\leq M\|u^h - u\|_V + \|\bar{\mu}^h - \lambda\|_{-1/2,\Gamma_{_D}} + \|\bar{\mu}^H - \lambda^H - (\bar{\mu}^h - \lambda^h)\|_{-1/2,\Gamma_{_D}}.
\end{aligned}$$

As a consequence, one has

$$\begin{aligned}\beta^*\|\lambda^H-\lambda\|_{-1/2,\Gamma_D} &\leq \beta^*\|\lambda-\bar\mu^H\|_{-1/2,\Gamma_D}+M\|u^h-u\|_V+\|\bar\mu^h-\lambda\|_{-1/2,\Gamma_D}\\ &\quad+\|\bar\mu^H-\bar\mu^h\|_{-1/2,\Gamma_D}+\|\lambda^H-\lambda^h\|_{-1/2,\Gamma_D},\end{aligned}$$

and

$$\begin{aligned}\beta^{*2}\|\lambda^H-\lambda\|^2_{-1/2,\Gamma_D} &\leq 5M^2\|u-u^h\|_V^2+5\beta^{*2}\|\lambda-\bar\mu^H\|^2_{-1/2,\Gamma_D}+5\|\lambda-\bar\mu^h\|^2_{-1/2,\Gamma_D}\\ &\quad+5\|\bar\mu^H-\bar\mu^h\|^2_{-1/2,\Gamma_D}+5\|\lambda^H-\lambda^h\|^2_{-1/2,\Gamma_D}\quad\forall\bar\mu^h\in W^h.\end{aligned}\tag{4.21}$$

By combining inequalities (4.19) and (4.21) one obtains for all $\bar\mu^h\in W^h$, $\mu^H\in W^H$ and $v^h\in V^h$

$$\begin{aligned}&(\alpha-5M^2\delta)\|u-u^h\|_V^2+\delta\beta^{*2}\|\lambda-\lambda^H\|^2_{-1/2,\Gamma_D}+(\gamma-5\delta)\|\lambda^h-\lambda^H\|^2_{-1/2,\Gamma_D}\\ \leq\;& M\|u^h-u\|_V\|v^h-u\|_V+\|\lambda-\mu^H\|_{-1/2,\Gamma_D}\|u^h-u\|_V+\|\lambda-\lambda^h\|_{-1/2,\Gamma_D}\|u-v^h\|_V\\ &+5\delta\beta^{*2}\|\lambda-\bar\mu^H\|^2_{-1/2,\Gamma_D}+5\delta\|\lambda-\bar\mu^h\|^2_{-1/2,\Gamma_D}+5\delta\|\bar\mu^h-\bar\mu^H\|^2_{-1/2,\Gamma_D},\\ \leq\;&\frac{\delta}{2}M^2\|u-u^h\|_V^2+\frac{1}{2\delta}\|u-v^h\|_V^2+\frac{\delta}{2}\|u-u^h\|_V^2+\frac{1}{2\delta}\|\lambda-\mu^H\|^2_{-1/2,\Gamma_D}+\frac{\xi}{2}\|\lambda-\lambda^h\|^2_{-1/2,\Gamma_D}\\ &+\frac{1}{2\xi}\|u-v^h\|_V^2+5\delta\beta^{*2}\|\lambda-\bar\mu^H\|^2_{-1/2,\Gamma_D}+5\delta\|\lambda-\bar\mu^h\|^2_{-1/2,\Gamma_D}+5\delta\|\bar\mu^h-\bar\mu^H\|^2_{-1/2,\Gamma_D}.\end{aligned}$$

Let δ and ξ be such that $\delta<\min\big(\frac{2\alpha}{11M^2+1};\frac{\gamma}{5}\big)$ and $\xi<\min\big(2\delta\beta^{*2};2(\gamma-5\delta)\big)$, then, still for all $\bar\mu^h\in W^h$, $\mu^H\in W^H$ and $v^h\in V^h$, one deduces that

$$\begin{aligned}&(\alpha-\delta\frac{11M^2+1}{2})\|u-u^h\|_V^2+(\gamma-5\delta-\frac{\xi}{2})\|\lambda^h-\lambda^H\|^2_{-1/2,\Gamma_D}+(\delta\beta^{*2}-\frac{\xi}{2})\|\lambda-\lambda^H\|^2_{-1/2,\Gamma_D}\\ \leq\;&(\frac{1}{2\delta}+\frac{1}{2\xi})\|u-v^h\|_V^2+\frac{1}{2\delta}\|\lambda-\mu^H\|^2_{-1/2,\Gamma_D}+8\delta\beta^{*2}\|\lambda-\bar\mu^H\|^2_{-1/2,\Gamma_D}+8\delta\|\lambda-\bar\mu^h\|^2_{-1/2,\Gamma_D}\\ &+8\delta\|\bar\mu^h-\bar\mu^H\|^2_{-1/2,\Gamma_D},\quad\forall\,\bar\mu^h\in W^h.\end{aligned}$$

Denoting by Π^h (resp. P_{W^h}) the Lagrange interpolation operator (resp. the $L^2(\Gamma_D)$-projection) in V^h (resp. in W^h), we have the following standard finite-element estimates:

$$\begin{aligned}\|u-\Pi^h u\|_V &\leq Ch\|u\|_{2,\Omega},\\ \|\lambda-P_{W^h}(\lambda)\|_{-1/2,\Gamma_D} &\leq Ch\|\lambda\|_{1/2,\Gamma_D},\\ \|\lambda-P_{W^H}(\lambda)\|_{-1/2,\Gamma_D} &\leq CH\|\lambda\|_{1/2,\Gamma_D}.\end{aligned}$$

Finally, the theorem is established by taking $v^h=\Pi^h u$, $\bar\mu^h=P_{W^h}(\lambda)$ and $\mu^H=P_{W^H}(\lambda)$. □

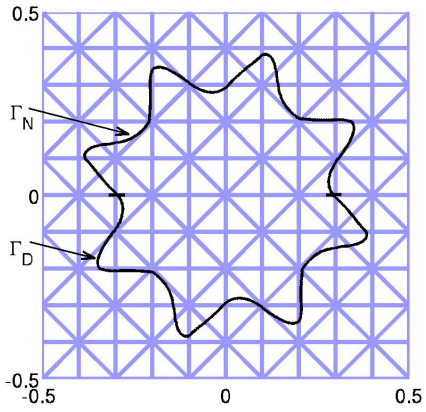

Figure 4.4: Example of a two-dimensional triangular structured mesh used for the numerical test and partition of the boundary for Neumann and Dirichlet conditions.

4.4 Numerical tests

In this section, we present 2D and 3D-numerical tests for a fictitious domain being $\widetilde{\Omega} =]-1/2, 1/2[^d$ for $d = 2$ and $d = 3$, respectively. The two-dimensional exact solution is chosen to be $u(x) = -5(R^4 - r^4(2.5 + 1.5\sin(8\theta + \frac{2\pi}{9})))$ where $r = \sqrt{x_1^2 + x_2^2}$, $R = 0.47$ and the three-dimensional one is $u(x) = 5(\rho^3 - R^3)$ with $\rho = \sqrt{x_1^2 + x_2^2 + x_3^3}$. In both cases, the real domain is $\Omega = \{x \in \mathbb{R}^d : u(x) < 0\}$ and the Dirichlet and Neumann boundary conditions are defined on $\Gamma_{_D} = \Gamma \cap \{x \in \mathbb{R}^d : x_d < 0\}$ and $\Gamma_{_N} = \Gamma \cap \{x \in \mathbb{R}^d : x_d > 0\}$, respectively. The two-dimensional domain is represented in Fig. 4.4 with an example of a triangular structured mesh. The exact solutions are shown in Fig. 4.5.

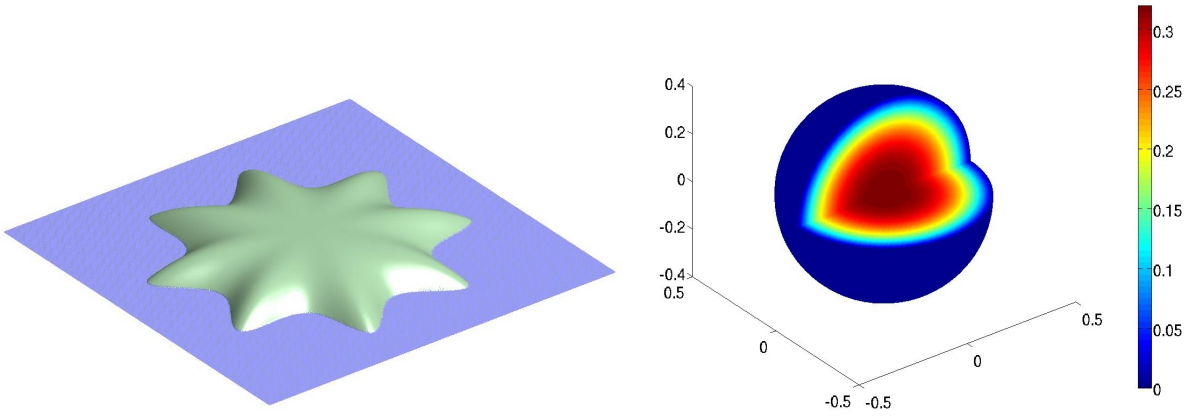

(a) Two-dimensional exact solution

(b) Three-dimensional exact solution

Figure 4.5: Exact solutions

The numerical tests are performed with GETFEM++, the C++ finite-element library developed by our team (see [52]).

4.4.1 Numerical solving

The algebraic formulation of Problem (4.12) reads

$$\begin{cases} \text{Find } U \in \mathbb{R}^{N_u} \text{ and } L \in \mathbb{R}^{N_\lambda} \text{ such that} \\ KU + B^T L = F, \\ BU - M_\gamma L = 0, \end{cases} \tag{4.22}$$

where U is the vector of degrees of freedom for u^h, L the one for the multiplier λ^h, N_u and N_λ the dimensions of V^h and W^h, respectively, K is the stiffness matrix coming from the term $a(u^h, v^h)$, F is the right-hand side corresponding to the term $\ell(v^h)$, and B and M_γ are the matrices corresponding to the terms $\int_{\Gamma_D} \lambda^h v^h d\Gamma$ and $\gamma \int_{\Gamma_D} (\lambda^h - P_{W^H}(\lambda^h))(\mu^h - P_{W^H}(\mu^h))d\Gamma$, respectively.

Before presenting the numerical experiments, we shall describe in details two important aspects of the implementation of the method. Namely, the extraction of a basis for W^h and the repartition of the elements having an intersection with Γ_D into patches.

The extraction of a basis of W^h could be non-trivial in some cases, except when a piecewise constants (P_0) finite-element method is used to approximate the multiplier or in some other cases when Γ_D is curved. Indeed, if one selects all the shape functions of $\widetilde{W}^h$ whose supports intersect Γ_D, some of them can be linearly dependent, especially when Γ_D is a straight line. In order to eliminate linearly dependent shape functions, the choice here is to consider the mass matrix $\int_{\Gamma_D} \psi_i \psi_j d\Gamma$ where the ψ_i are the finite-element shape functions of $\widetilde{W}^h$. A block-wise Gram-Schmidt algorithm is used to eliminate local dependencies and then the potential remaining kernel of the mass matrix is detected by a Lanczos algorithm. In the presented numerical tests, since curved boundaries are considered the kernel of the mass matrix is either reduced to 0 or is very small. In [18] some numerical experiments are presented for a straight line in 2D using the same technique. The selection of a basis of W^h using this technique took far less computational time than the assembly of the stiffness matrix.

The decomposition into patches is made using a graph partitioner algorithm. In the presented numerical tests we use the free software METIS [79]. The nodes of the graph consist in the elements having an intersection with Γ_D and the edges connect adjacent elements. Additionally, a load corresponding to the size of the intersection is considered on each elements. The partition is a very fast operation.

4.4.2 Comparison with the Barbosa-Hughes stabilization technique

In our numerical test, we compare the new stabilization technique to the one studied in [74] in the same framework which use the technique introduced by Barbosa and Hughes in [39, 40]. For the self consistency of the paper, we briefly recall the principle of the symmetric version of the Barbosa-Hughes stabilization technique applied to Problem (4.6) as it is presented in [74].

This technique is based on the addition of a supplementary term involving an approximation of the normal derivative on $\Gamma_{_D}$. Let us assume that we have at our disposal an operator

$$R^h : V^h \longrightarrow L^2(\Gamma_{_D}),$$

which approximates the normal derivative on $\Gamma_{_D}$ (*i.e.* for $v^h \in V^h$ converging to a sufficiently smooth function v, $R^h(v^h)$ tends to $\partial_n v$ in an appropriate sense). Several choices of R^h are proposed in [74]. To obtain the stabilized problem, the Lagrangian (4.4) is approximated by the following one

$$\mathcal{L}_h(v^h, \mu^h) = \mathcal{L}(v^h, \mu^h) - \frac{\gamma}{2}\int_{\Gamma_{_D}} (\mu^h + R^h(v^h))^2 d\Gamma, \quad v^h \in V^h, \mu^h \in W^h,$$

where the stabilization parameter γ depend on the mesh parameter $\gamma := h\gamma_0$, with γ_0 a positive constant over Ω. The corresponding discrete problem reads as follows:

$$\left\{\begin{array}{l} \text{Find } u^h \in V^h \text{ and } \lambda^h \in W^h \text{ such that} \\ a(u^h, v^h) + \displaystyle\int_{\Gamma_{_D}} \lambda^h v^h d\Gamma - \gamma \int_{\Gamma_{_D}} (\lambda^h + R^h(u^h))R^h(v^h) d\Gamma = l(v^h) \quad \forall v^h \in V^h, \\ \displaystyle\int_{\Gamma_{_D}} \mu^h u^h d\Gamma - \gamma \int_{\Gamma_{_D}} (\lambda^h + R^h(u^h))\mu^h d\Gamma = 0 \quad \forall \mu^h \in W^h. \end{array}\right. \tag{4.23}$$

More details and a convergence analysis can be found in [74]. Note that this is also a consistent modification of the Lagrangian and that a close relationship between Barbosa-Hughes stabilization technique and Nitsche's one [71] has been explained in [41].

4.4.3 Two-dimensional numerical tests

A comparison is done between the non-stabilized problem (4.6), the local projection stabilized problem (4.12) and the Barbosa-Hughes stabilized one (4.23) in the two-dimensional case. Additionally, we test different pairs of elements for the main unknown u and the multiplier. Namely, we test the following methods: P_2/P_1, P_1/P_1, P_1/P_0, P_1/P_2, Q_1/Q_0 and Q_1/Q_0. The notation P_i/P_j (resp. Q_i/Q_j) means that solution u is approximated with a P_i finite-element method (resp. a Q_i finite-element method) and the multiplier with a continuous P_j finite-element method (resp. continuous Q_j finite-element method).

Without stabilization. A solution is plotted in Fig. 4.6 for a P_1/P_2 method. Of course, for this pair of elements, a uniform discrete inf-sup cannot be satisfied since the multiplier is discretized with a reacher element than the main unknown. As a consequence, a local locking phenomenon (Fig. 4.6(a)) on the Dirichlet boundary (flat part of the solution) holds together with a very noisy multiplier (Fig. 4.6(b)). This indicates the presence of spurious modes. Some similar results can be observed with the P_1/P_1 and P_1/P_0 methods.

The convergence curves in the non-stabilized case are given in Fig. 4.7(a) for the error in the $L^2(\Omega)$-norm on u, in Fig. 4.7(b) for the error in the $H^1(\Omega)$-norm on u and in Fig. 4.7(c) for the error in the $L^2(\Gamma_{_D})$-norm on the multiplier. One notes that the convergence rate for the P_1/P_2, P_1/P_1 and P_1/P_0 methods in $H^1(\Omega)$-norm are close to 0.5 which is in good agreement with the general result of Proposition 6. In this cases, there is no convergence of the multiplier

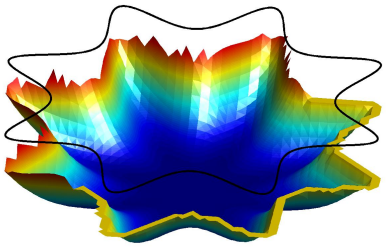

(a) Solution on Ω with no stabilization for the P_1/P_2 method.

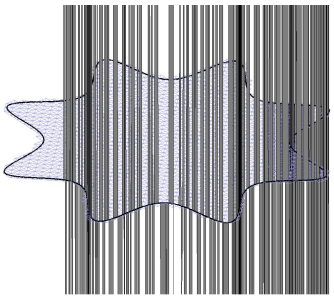

(b) Multiplier on Γ_D with no stabilization for the P_1/P_2 method.

Figure 4.6: Non-stabilized case with the P_1/P_2 method.

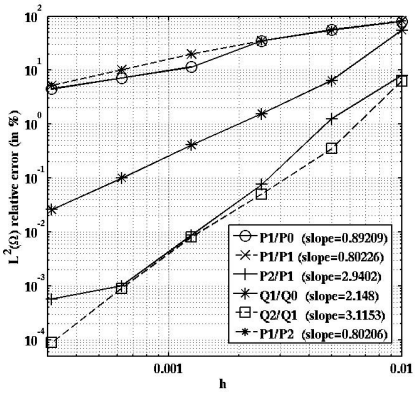

(a) Convergence of $\|u - u^h\|_{0,\Omega}$

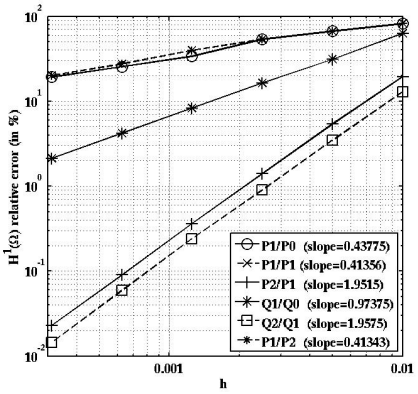

(b) Convergence of $\|u - u^h\|_{1,\Omega}$

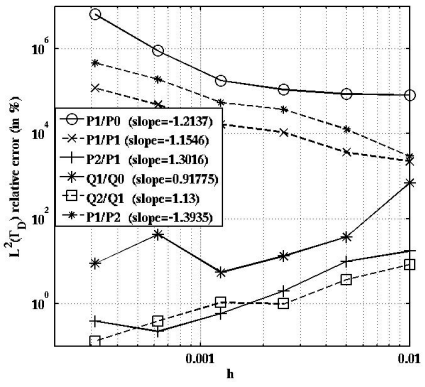

(c) Convergence of $\|\lambda^h - \lambda\|_{0,\Gamma_D}$

Figure 4.7: Convergence curves in the non-stabilized case.

(still due to the presence of some spurious modes). Conversely, for the P_2/P_1, Q_2/Q_1 and Q_1/Q_0 methods, one observes a nearly optimal convergence rate. This do not imply that a mesh independent inf-sup condition is systematically satisfied in these cases. In [74], some numerical experiments show that the solution can be deteriorated in the vicinity of very small intersections between the mesh and $\Gamma_{_D}$ (especially for the multiplier).

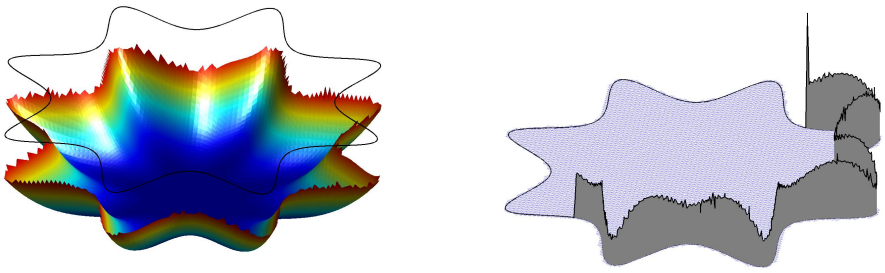

(a) Solution on Ω with Barbosa-Hughes stabilization for the P_1/P_1 method.

(b) Multiplier on $\Gamma_{_D}$ with Barbosa-Hughes stabilization for the P_1/P_1 method.

Figure 4.8: Barbosa-Hughes stabilized case with the P_1/P_1 method.

Barbosa-Hughes stabilization. Fig. 4.8 shows that the Barbosa-Hughes stabilization technique eliminates the locking phenomenon (Fig. 4.8(a)) and the spurious modes on the multiplier (Fig. 4.8(b)). The convergence curves in the Barbosa-Hughes stabilized case are given in Fig. 4.9(a) for the error in the $L^2(\Omega)$-norm on u, in Fig. 4.9(b) for the error in the $H^1(\Omega)$-norm on u and in Fig. 4.9(c) for the error in the $L^2(\Gamma_{_D})$-norm on the multiplier. The rate of convergence for the error in $L^2(\Omega)$-norm (resp. $H^1(\Omega)$-norm) on u with Barbosa-Hughes stabilization are optimal: of order 3 (resp. of order close to 2) for both P_2/P_1 and Q_2/Q_1 and of order 2 (resp. order 1) for the remaining pairs of elements. Fig. 4.9(c) shows that the approximation of the multiplier is considerably improved. Concerning the error in $L^2(\Gamma_{_D})$-norm for the multiplier the rate of convergence is also close to optimality for all pairs of elements.
We refer to [18] for the study of the influence of the stabilization parameter. A rather small influence is noted on the error in $L^2(\Omega)$ and $H^1(\Omega)$-norms on u. Concerning the error in $L^2(\Gamma_D)$-norm of the multiplier, the value of the stabilization parameter can be divided into two zones. A coercive zone where the error decreases when the stabilization parameter γ_0 increases and a non-coercive zone for large values of the stabilization parameter where the error evolves randomly according to the stabilization parameter.

Local projection stabilization. Similarly to the Barbosa-Hughes stabilization, the local projection stabilization gives some optimal rates of convergence for all pairs of elements and eliminates the locking phenomena (Fig. 4.10(a)) and the spurious modes on the multiplier (Fig. 4.8(b)). The convergence curves are shown in Fig. 4.11(a) for the error in the $L^2(\Omega)$-norm on u, in Fig. 4.11(b) for the error in the $H^1(\Omega)$-norm on u and in Fig. 4.11(c) for the error in the $L^2(\Gamma_{_D})$-norm on the multiplier. The rate of convergence for the P_1/P_2, P_1/P_1, P_1/P_0 and Q_1/Q_0 methods are in good agreement with the theoretical result of Theorem 4.3.2. For the

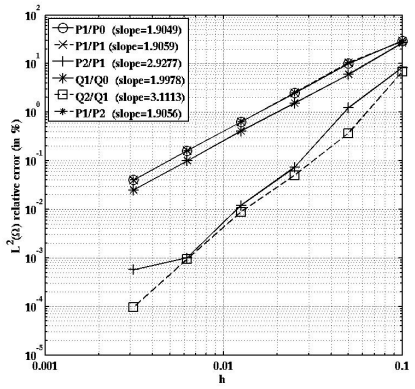

(a) Convergence of $\|u - u^h\|_{0,\Omega}$

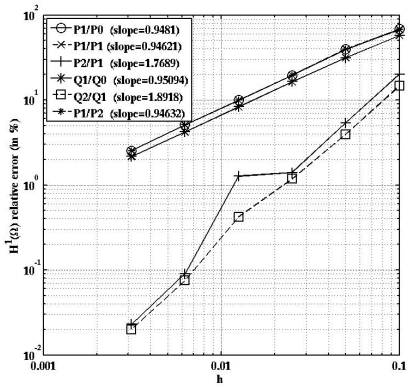

(b) Convergence of $\|u - u^h\|_{1,\Omega}$

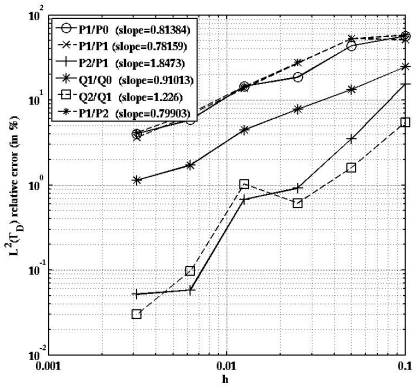

(c) Convergence of $\|\lambda^h - \lambda\|_{0,\Gamma_D}$

Figure 4.9: Convergence curves in the Barbosa-Hughes stabilized case.

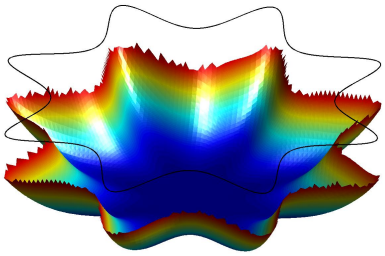

(a) Solution on Ω with local projection stabilization for the P_1/P_1 method.

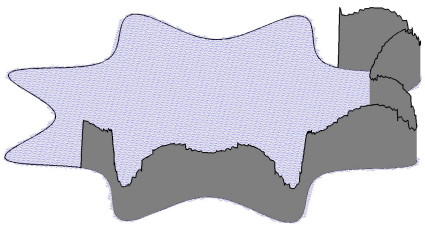

(b) Multiplier on Γ_D with local projection stabilization for the P_1/P_1 method.

Figure 4.10: Local projection stabilized case with the P_1/P_1 method.

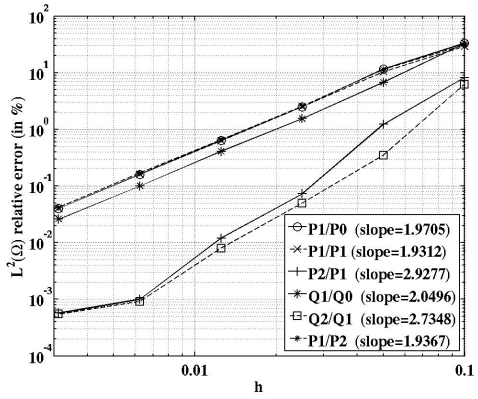

(a) Convergence of $\|u - u^h\|_{0,\Omega}$

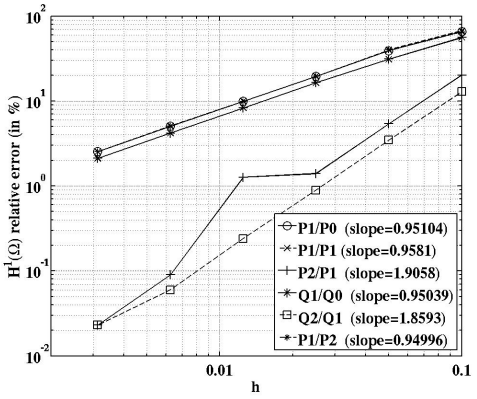

(b) Convergence of $\|u - u^h\|_{1,\Omega}$

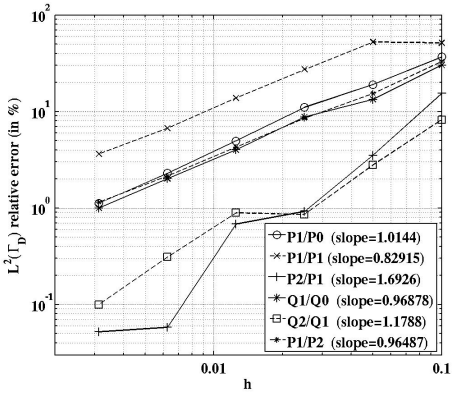

(c) Convergence of $\|\lambda^h - \lambda\|_{0,\Gamma_D}$

Figure 4.11: Convergence curves in the local projection stabilized case.

P_2/P_1 and Q_2/Q_1 methods, the rates are close to optimality. For these methods, if one tries to extend the result of Theorem 4.3.2 to a $H^3(\Omega)$ regular exact solution, one find that the rate of convergence of the error estimate depends on the interpolation error of the local orthogonal projection which limits the rate of convergence to 3/2 for the $H^1(\Omega)$-norm and 1 for the $L^2(\Gamma_D)$-norm on the multiplier (The same observation was shown in the case of Stokes and Darcy's equations by Burman [80]). This limitation is observed on Fig. 4.11(c) on the multiplier of the Q_2/Q_1 method, but not for the P_2/P_1 method (for an unknown reason).
Concerning the error in $L^2(\Gamma_D)$-norm the value of the stabilization parameter can also be divided into two zones (see Figs. 4.12, 4.13 and 4.14). The first zone where the error decreases when the stabilization parameter γ increases. The second zone, for large values of the parameter, where the error increases (Figs. 4.13, 4.14) or remain almost constant (Fig. 4.12). Figure 4.12 for the P_1/P_0 elements indicates that a large value of the stabilization parameter does not affect too much the quality of the solution. This behavior has been noted whenever a piecewise constant multiplier is considered. Conversely, for all remaining couples of elements, an excessive value of the stabilization parameter leads to a bad quality solution (see Figs. 4.13, 4.14).
Now, concerning the minimal patch size, the inf-sup condition is proven to be satisfied in [61] for a size equal or greater to $3h$. Numerically, the inf-sup condition seems to be satisfied for smaller values of the minimal patch size. In our numerical experiments we found an optimal value between h and $2h$. For the P_1/P_0 method, a minimal patch size equal to h seems to be inadequate (Fig. 4.12(a)). A value of $2h$ is found to be more optimal (Fig. 4.12(b)). Conversely, a value of h is slightly more optimal for the $P1/P1$ pair of elements (Fig. 4.13).

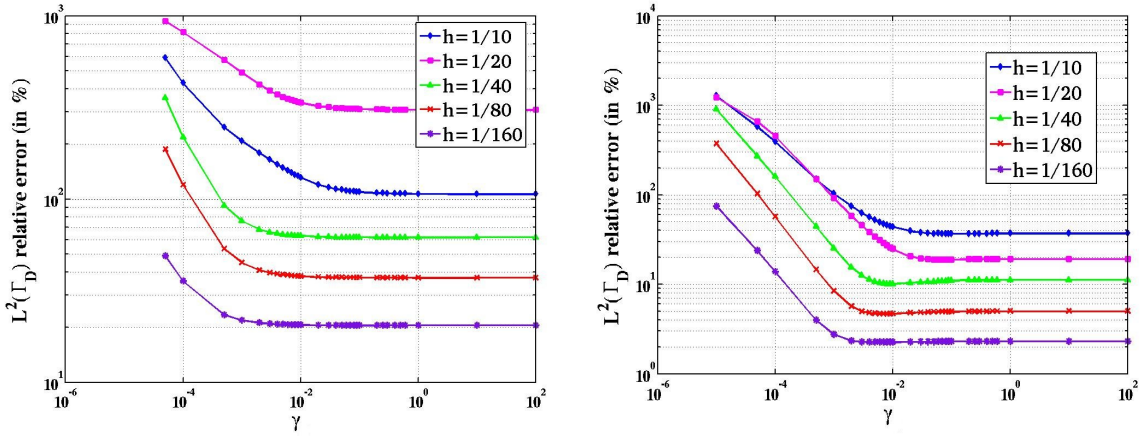

(a) With a minimal patch size equal to h

(b) With a minimal patch size equal to 2h

Figure 4.12: Influence of the stabilization parameter for the error in the $L^2(\Gamma_D)$-norm of the multiplier for the P_1/P_0-element.

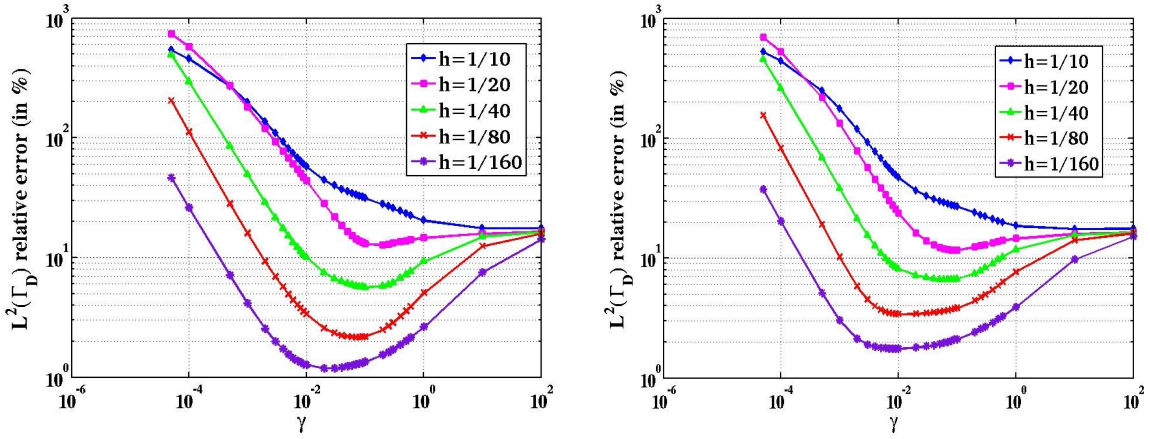

(a) With a minimal patch size equal to h

(b) With a minimal patch size equal to 2h

Figure 4.13: Influence of the stabilization parameter for the error in the $L^2(\Gamma_D)$-norm of the multiplier for the P_1/P_1-element.

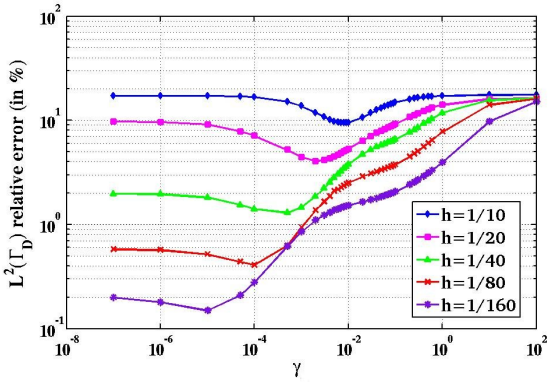

Figure 4.14: Influence of the stabilization parameter for the error in the $L^2(\Gamma_D)$-norm of the multiplier for the P_2/P_1-element (with a minimal patch size equal to h).

4.4.4 Three-dimensional numerical tests

In this section, we compare the non-stabilized three-dimensional case to the local projection stabilized three-dimensional case with the following pairs of finite-element methods: P_2/P_1, P_1/P_1, P_1/P_0, P_1/P_2, Q_2/Q_1 and Q_1/Q_0.

Without stabilization. Convergence curves in the non-stabilized case are shown in Fig. 4.15. Perhaps due to the simple chosen geometry and exact solution, no locking phenomenon is observed for the P_1/P_2, P_1/P_1 and P_1/P_0 methods. However, in these cases, the multiplier does not converge probably due to the presence of spurious modes. The rate of convergence in the $H^1(\Omega)-$ norm on u is optimal for the P_1/P_1, P_1/P_0, P_1/P_2 and Q_1/Q_0 methods (see Fig. 4.15(b)). For the remaining elements (Q_2/Q_1 and P_2/P_1) the rate of convergence is limited to 3/2.

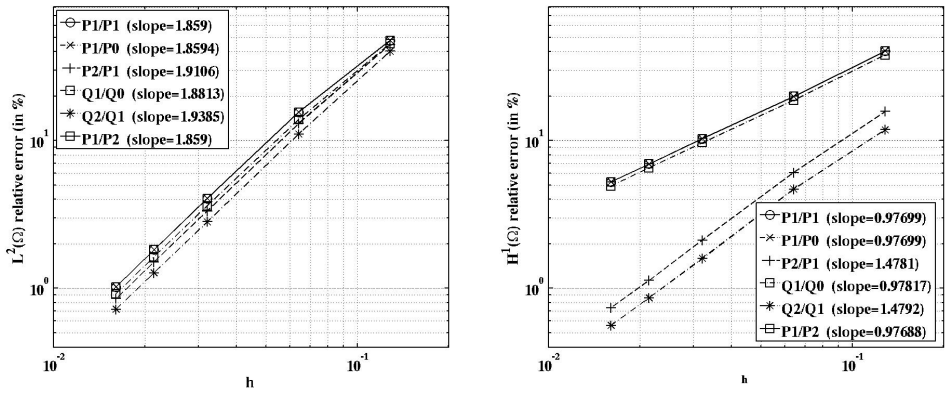

(a) Convergence of $\|u - u^h\|_{0,\Omega}$ (b) Convergence of $\|u - u^h\|_{1,\Omega}$

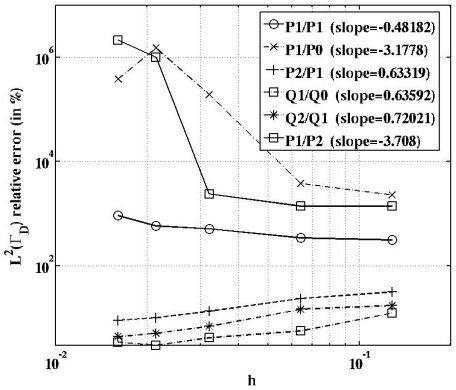

(c) Convergence of $\|\lambda^h - \lambda\|_{0,\Gamma_D}$

Figure 4.15: Convergence curves in the three-dimensional non-stabilized case.

Local projection stabilization. The local projection stabilization gives an optimal rate of convergence for all pairs of elements and eliminates the spurious modes for the P_1/P_1, P_1/P_0 and P_1/P_2 methods. Especially, the rate of convergence in the $H^1(\Omega)$-norm for the Q_2/Q_1 and P_2/P_1 are improved compared to the non-stabilized case.

Except for the Q_2/Q_1 pair of elements, the convergence rate for the $L^2(\Gamma_{_D})$-norm for the multiplier are optimal (more than 1.5). For the Q_2/Q_1 pair of elements, the convergence rate for the $L^2(\Gamma_{_D})$-norm is optimal but limited to 1.1 (we did not find any interpretation for that). The rate of convergence in the $L^2(\Omega)$-norm is limited to 2 for all methods. For quadratic methods, the that we used level set function of order 1 to approximate the curved domain limits theoretically the rate of convergence to 3/2.

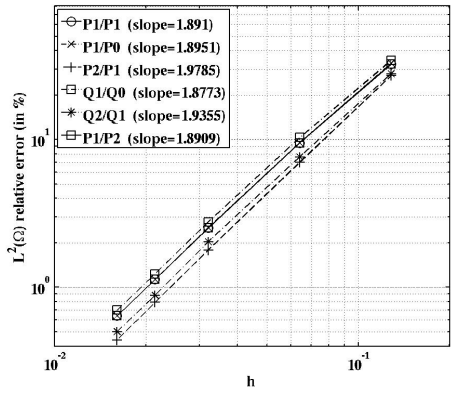

(a) Convergence of $\|u - u^h\|_{0,\Omega}$

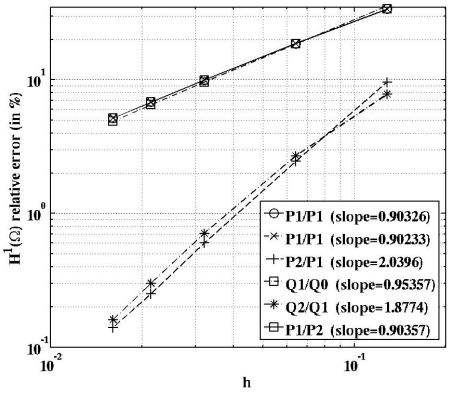

(b) Convergence of $\|u - u^h\|_{1,\Omega}$

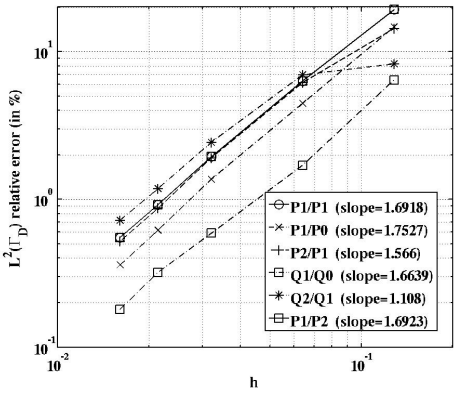

(c) Convergence of $\|\lambda^h - \lambda\|_{0,\Gamma_{_D}}$

Figure 4.16: Convergence curves in the three-dimensional local projection stabilized case.

4.5 Concluding remarks

In this paper, we presented a stabilization technique based on local projections for the fictitious domain method inspired by the X-FEM introduced in [72, 74].

A main advantage compared to some other stabilization techniques like the Barbosa-Hughes one, is that it only affects the multiplier equation in a manner that is independent of the problem to be solved. This makes the extension to other linear or nonlinear problems very easy.

The two-dimensional theoretical result does not ensure an optimal rate of convergence when a quadratic finite element is used for the main unknown due to the fact that the local projection is made on piecewise constants. The method could be generalized to the projection on (discontinuous) piecewise affine or piecewise quadratic functions for high-order approximations.

The extension to the three-dimensional case of the theoretical result is of course subject to obtaining an inf-sup condition of the same kind of the one obtained in [61].

Chapter 5

A local projection stabilized extended finite element approximation of cracked bodies subject to contact with Tresca friction

Contents

5.1 Introduction

The modeling of contact phenomena presents a great challenge for industrial applications. This phenomenon played an important role in the behavior of structures: deformations, movements and distribution of efforts. Taking into account this contact condition presents serious difficulties: conceptual, mathematical and computational. These difficulties come from the non-linearity of the contact conditions. The accuracy of the approximated method depends essentially on the manner in which it applies the contact condition. Indeed, this condition may be prescribed strongly or relaxed and expressed in the weaker sense. In the context of isotropic linear elasticity, small deformations and contact with rigid foundations (Signorini problem) different studies were made. Under H^2-regularity on the displacement, we summarize these results as follows:
In the case of the frictionless contact problem, when primal formulation (displacement is the only unknown) and conforming or non conforming discretization are considered, an order of $h^{3/4}$

was obtained in the works of Haslinger et al. [81, 82, 46]. This result is ameliorated recently, an order of $h\sqrt{|\log(h)|}$ was obtained in the paper of Renard [83] without any assumption. Using the supplementary assumption that we have a finite number of transitions between contact and non-contact zones, an order of $h\sqrt{|\log(h)|}$ (resp. $h\sqrt[4]{|\log(h)|}$ for only conforming discretization) was proved in the paper of Ben Belgacem [29] (resp. Ben belgacem et al. [25]). An order of h was obtained in the work of Hüeber [84] using the same supplementary assumption and an additional modified Lagrange interpolation operator. For the mixed formulation of the frictionless contact problem Lhalouani et al. [85] proved that the rate of convergence is of order $h^{3/4}$ if we use piecewise constant multiplier. Coorevits et al.[86] show that the rate of convergence is of order $h^{3/4}$ if we use weakly linear multiplier (see also [25]), of oder $h^{1/4}$ for piecewise linear multiplier with the additional assumption that there exists $\varepsilon > 0$ sufficiently small such that the multiplier is contained in the Sobolev space $H^{\varepsilon+1/2}$, of order $h\sqrt{|\log(h)|}$ if we use weakly piecewise linear multiplier with the additional assumption that we have a finite number of transitions between contact and non-contact zones, and of order h if we use weakly piecewise linear multiplier with some additional assumptions. In 2003 Ben begacem et al. [25], show an order of $h^{1/2}$ with weakly piecewise linear multiplier. Also, in the same reference, an order of $h\sqrt[4]{|\log(h)|}$ is proved for the same formulation with the additional assumption that we have a finite number of transitions between contact and non-contact zones. An optimal rate of convergence of order h is proved in [87] for the piecewise linear multiplier with specific finite element approximation method and the additional assumptions that a finite number of transitions between contact and non-contact zones.
In the case of Tresca contact problem with a given slip stress $s \in L^2(\Gamma_C)$, an order of $h^{3/4}$ is proved using continuous piecewise linear normal multiplier and weakly continuous piecewise linear tangent multiplier [88] and an order of $h\sqrt[4]{|\log(h)|}$ is proved with the additional assumptions that we have a finite number of transitions between contact and non-contact zones, the jump of the displacement on Γ_C is in $W^{1,\infty}$, the tangent stress $\lambda_t \in L^\infty(\Gamma_C)$ and the given slip $s \in L^\infty(\Gamma_C)$. In the same context of [88] an order of $h^{1/2}$ is proved using piecewise constant shape function (see [89] and [90]). This estimate can be improved (a convergence rate of order $h^{3/4}$) under the additional assumption that the slip bound s is a positive constant on Γ_C (see [89] and [90]).

In all the works cited above, a discrete compatibility condition between the finite-element space for the displacement and the one for the multiplier is required in order to obtain a good approximation of the solution. To overcome these difficulties many method are used. We can cite the Barbosa-Hughes stabilization where the stability is assured by adding a supplementary term involving an approximation of the normal derivative of the primal variable on Γ_C (see [50] and [18]). The local projection stabilization technique introduced in [55] where the difference of the multiplier with its projection on some pre-defined patches is penalized to ensure the stability of the problem. This stabilized technique is asymptotic consistent and affects only the multiplier equations in a manner that is independent of the problem to be solved. Note that in our case the presence of the crack presents a supplementary difficulty.
The purpose of this contribution is to apply the local projection stabilization technique to the enriched finite-element approximation of contact problems with Tresca friction of cracked elastic bodies. In Section 5.2, we introduce the formulation of the unilateral contact problem with

Tresca friction on a crack of an elastic structure. In Section 5.3, we present the elasticity problem approximated by both the enrichment strategy introduced in [12] and the local projection stabilized Lagrange multiplier method [55]. We show the existence and uniqueness of the solution of the stabilized formulation. Also we prove a priori error estimates following three different discrete contact conditions (the study is restricted to piecewise affine and constant finite element methods). Finally, in Section 5.4, we present some numerical experiments on a very simple situation. We compare the stabilized and the non-stabilized cases for different finite-element approximations. The influence of the stabilization parameters is also investigated.

5.2 Formulation of the continuous problem

We introduce some useful notations and several functional spaces. In what follows, bold letters like $\mathbf{u}, \mathbf{v}$, indicate vector-valued quantities, while the capital ones (e.g., $\mathbf{V}, \mathbf{K}, \ldots$) represent functional sets involving vector fields. As usual, we denote by $(L^2(.))^d$ and by $(H^s(.))^d$, $s \geq 0, d = 1, 2$ the Lebesgue and Sobolev spaces in d-dimensional space (see [15]). The usual norm of $(H^s(D))^d$ is denoted by $\|\cdot\|_{s,D}$ and we keep the same notation when $d = 1$ or $d = 2$. For shortness, the $(L^2(D))^d$-norm will be denoted by $\|\cdot\|_D$ when $d = 1$ or $d = 2$. In the sequel the symbol $|\cdot|$ will denote either the Euclidean norm in $\mathbb{R}^2$, the length of a line segment, or the area of a planar domain.

Let us consider the deformation of a cracked elastic body occupying, in the initial configuration, a domain Ω in $\mathbb{R}^2$ where plane small strain are assumed. The boundary $\partial\Omega$ of the domain Ω is assumed to be polygonal (for simplicity) and consists of three non-overlapping parts Γ_D, Γ_N and Γ_C with $\text{meas}(\Gamma_D) > 0$ and $\text{meas}(\Gamma_C) > 0$. The body is clamped on Γ_D. It is subjected to volume forces $\mathbf{f} = (f_1, f_2) \in (L^2(\Omega))^2$ and to surface loads $\mathbf{g} = (g_1, g_2) \in (L^2(\Gamma_N))^2$. The boundary part Γ_C (or the crack location) is supposed to be a straight line segment. We denote by Γ_{C+} and Γ_{C-} each of the two sides of the crack (see Fig. 5.1). We suppose that we have a frictional contact between Γ_{C+} and Γ_{C-} as a contact between two elastic bodies. Of course, in the initial configuration, both Γ_{C+} and Γ_{C-} coincide. Let $\mathbf{n} = \mathbf{n}^+ = -\mathbf{n}^- = (n_1, n_2)$ denote the outward normal unit vector on Γ_{C+} and $\mathbf{t} = (-n_2, n_1)$ an associated unit tangent vector.

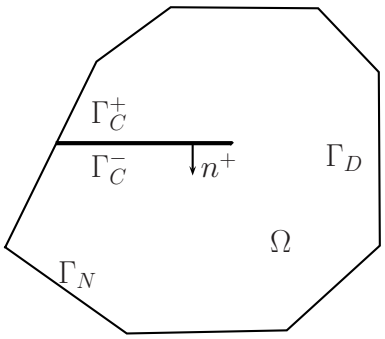

Figure 5.1: *A cracked domain.*

Under plane small strain assumptions, the problem of homogeneous isotropic linear elasticity consists in finding the displacement field $\mathbf{u} : \Omega \to \mathbb{R}^2$ satisfying

$$\begin{aligned}
\text{(5.1)} \qquad \operatorname{div} \boldsymbol{\sigma}(\mathbf{u}) + \mathbf{f} &= \mathbf{0} && \text{in } \Omega,\\
\text{(5.2)} \qquad \boldsymbol{\sigma}(\mathbf{u}) &= \lambda_{_L}\, \operatorname{tr} \boldsymbol{\varepsilon}(\mathbf{u})\, I + 2\mu_{_L}\, \boldsymbol{\varepsilon}(\mathbf{u}), && \text{in } \Omega,\\
\text{(5.3)} \qquad \mathbf{u} &= \mathbf{0} && \text{on } \Gamma_D,\\
\text{(5.4)} \qquad \boldsymbol{\sigma}(\mathbf{u})\mathbf{n} &= \mathbf{g} && \text{on } \Gamma_N,
\end{aligned}$$

where $\boldsymbol{\sigma} = (\sigma_{ij})$, $1 \le i, j \le 2$, stands for the stress tensor field, $\boldsymbol{\varepsilon}(\mathbf{v}) = (\boldsymbol{\nabla}\mathbf{v} + \boldsymbol{\nabla}\mathbf{v}^{^T})/2$ represents the linearized strain tensor field, $\lambda_{_L} \ge 0$, $\mu_{_L} > 0$ are the Lamé coefficients, and I denotes the identity tensor. For a displacement field $\mathbf{v}$ and a density of surface forces $\boldsymbol{\sigma}(\mathbf{v})\mathbf{n}$ defined on $\partial\Omega$, we adopt the following notations:

$$\mathbf{v}^+ = v_n^+\mathbf{n}^+ + v_t^+\mathbf{t}, \quad \mathbf{v}^- = v_n^-\mathbf{n}^- + v_t^-\mathbf{t} \quad \text{and} \quad \boldsymbol{\sigma}(\mathbf{v})\mathbf{n} = \sigma_n(\mathbf{v})\mathbf{n} + \sigma_t(\mathbf{v})\mathbf{t},$$

where $\mathbf{v}^+$ (resp. $\mathbf{v}^-$) is the trace of displacement on Γ_C on the Γ_C^+ side (resp. on the Γ_C^- side). The conditions describing the normal contact on Γ_C are:

$$\text{(5.5)} \qquad [\![u_n]\!] = u_n^+ + u_n^- \le 0, \qquad \sigma_n(\mathbf{u}) \le 0, \qquad \sigma_n(\mathbf{u}) \cdot [\![u_n]\!] = 0,$$

where $[\![u_n]\!]$ is the jump of the normal displacement across the crack Γ_C. Denoting by $s \ge 0$ the given slip stress coefficient on Γ_C (which is assumed to be constant for the sake simplicity). The static Tresca friction condition reads as follows:

$$\text{(5.6)} \qquad \begin{cases} |\sigma_t(\mathbf{u})| \le s, & \text{a.e. on } \Gamma_C,\\ \text{if} \quad |\sigma_t(\mathbf{u})| < s, & \text{then } [\![\mathbf{u}_t]\!] = 0,\\ \text{if} \quad |\sigma_t(\mathbf{u})| = s, & \text{then there exist } \nu \ge 0 \text{ such that } [\![\mathbf{u}_t]\!] = -\nu\sigma_t(\mathbf{u}), \end{cases}$$

To give some classical weak formulation of Problem (5.1)−(5.6), we first introduce the following Hilbert spaces:

$$\mathbf{V} = \Big\{\mathbf{v} \in \big(H^1(\Omega)\big)^2 : \quad \mathbf{v} = \mathbf{0} \text{ on } \Gamma_D\Big\}, \qquad W_N = \Big\{[\![v_n]\!]_{|\Gamma_C} : \mathbf{v} \in \mathbf{V}\Big\}, \qquad W_T = \Big\{[\![v_t]\!]_{|\Gamma_C} : \mathbf{v} \in \mathbf{V}\Big\}$$

and their topological dual spaces $\mathbf{V}'$, W_N', W_T', endowed with their usual norms. Next we define the convex set of Lagrange multipliers denoted:

$$\mathbf{M}(s) = M_N \times M_T(s),$$

$$M_N = \Big\{\mu_n \in W_N' : \ \big\langle \mu_n, v_n\big\rangle_{W_N', W_N} \ge 0 \quad \text{for all } v_n \in W_N, v_n \le 0 \ \text{ a.e. on } \Gamma_C\Big\},$$

$$M_T(s) = \Big\{\mu_t \in W_T' : \ \big\langle \mu_t, v_t\big\rangle_{W_T', W_T} + \big\langle s, |v_t|\big\rangle_{W_T', W_T} \ge 0 \quad \text{for all } v_t \in W_T, \ \text{ a.e. on } \Gamma_C\Big\},$$

where the notation $\langle\cdot,\cdot\rangle_{W_N', W_N}$ stands for the duality pairing between W_N' and W_N. The mixed formulation of the Tresca contact problem (5.1)−(5.6) consists then in finding $\mathbf{u} \in \mathbf{V}$ and $\boldsymbol{\lambda} \in \mathbf{M}(s)$ such that

$$\text{(5.7)} \qquad \begin{cases} a(\mathbf{u}, \mathbf{v}) - b(\boldsymbol{\lambda}, \mathbf{v}) = L(\mathbf{v}), & \forall\, \mathbf{v} \in \mathbf{V},\\ b(\boldsymbol{\mu} - \boldsymbol{\lambda}, \mathbf{u}) \ge 0, & \forall\, \boldsymbol{\mu} \in \mathbf{M}(s), \end{cases}$$

where

$$a(\mathbf{u},\mathbf{v}) = \int_\Omega \boldsymbol{\sigma}(\mathbf{u}) : \boldsymbol{\varepsilon}(\mathbf{v})\, d\Omega, \qquad b(\mu,\mathbf{v}) = \langle \mu_n, [\![v_n]\!] \rangle_{W_N', W_N} + \langle \mu_t, [\![v_t]\!] \rangle_{W_T', W_T}$$
$$L(\mathbf{v}) = \int_\Omega \mathbf{f}\cdot\mathbf{v}\, d\Omega + \int_{\Gamma_N} \mathbf{g}\cdot\mathbf{v}\, d\Gamma.$$

An equivalent formulation of (5.7) consists in finding $(\mathbf{u},\boldsymbol{\lambda}) \in \mathbf{V}\times\mathbf{M}(s)$ satisfying

$$\mathscr{L}(\mathbf{u},\boldsymbol{\mu}) \le \mathscr{L}(\mathbf{u},\boldsymbol{\lambda}) \le \mathscr{L}(\mathbf{v},\boldsymbol{\lambda}), \qquad \forall \mathbf{v}\in\mathbf{V},\ \forall \boldsymbol{\mu}\in\mathbf{M}(s),$$

where $\mathscr{L}(\cdot,\cdot)$ is the classical Lagrangian of the system defined as

$$\mathscr{L}(\mathbf{v},\boldsymbol{\mu}) = \frac{1}{2}a(\mathbf{v},\mathbf{v}) - L(\mathbf{v}) - b(\boldsymbol{\mu},\mathbf{v}). \tag{5.8}$$

Another classical weak formulation of problem (5.1)−(5.6) is given by the following variational inequality: find $\mathbf{u}\in\mathbf{K}$ such that

$$a(\mathbf{u},\mathbf{v}-\mathbf{u}) + j(s,\mathbf{v}) - j(s,\mathbf{u}) \ge L(\mathbf{v}-\mathbf{u}), \qquad \forall \mathbf{v}\in\mathbf{K}, \tag{5.9}$$

where $j(s,\mathbf{v}) = \langle s, |[\![v_t]\!]| \rangle_{W_T', W_T}$ and $\mathbf{K}$ denotes the closed convex cone of admissible displacement fields satisfying the non-interpenetration condition

$$\mathbf{K} = \{\mathbf{v}\in\mathbf{V} : \quad [\![v_n]\!] \le 0 \text{ on } \Gamma_C\}.$$

Moreover, the first argument $\mathbf{u}$ solution to (5.7) is also the unique solution of problem (5.9) and one has $\lambda_n = \sigma_n(\mathbf{u})$ in W_N' and $\lambda_t = \sigma_t(\mathbf{u})$ in W_T' .

5.3 Discretization with the stabilized Lagrange multiplier method

5.3.1 The discrete problem

We shall now describe the enriched finite elements used in the approximation of the mixed problem (5.7). For any given discretization parameter $h>0$, let $\mathcal{T}^h$, be a partition of the untracked domain $\overline{\Omega}$ with a maximal size h, $\overline{\Omega} = \bigcup_{T\in\mathcal{T}^h}\overline{T}$. Moreover, $\mathcal{T}^h$ is assumed to be regular, i.e., there exists $\beta>0$ such that $\forall T\in\mathcal{T}^h$, $h_T/\rho_T \le \beta$ where ρ_T denotes the radius of the inscribed circle in T (see [47]). We consider the variant, called the cut-off XFEM, introduced in [12] in which the whole area around the crack tip is enriched by using a cut-off function denoted by $\chi(\cdot)$. In this variant, the enriched finite-element space $\mathbf{V}^h$ is defined as

$$\mathbf{V}^h = \left\{\mathbf{v}^h \in (\mathscr{C}(\bar\Omega))^2 \ : \ \mathbf{v}^h = \sum_{i\in\mathcal{N}_h} \mathbf{a}_i\varphi_i + \sum_{i\in\mathcal{N}_h^H} \mathbf{b}_i H\varphi_i + \chi\sum_{j=1}^{4}\mathbf{c}_j F_j, \quad \mathbf{a}_i,\mathbf{b}_i,\mathbf{c}_j\in\mathbb{R}^2\right\} \subset \mathbf{V}.$$

Here $(\mathscr{C}(\bar\Omega))^2$ is the space of continuous vector fields over $\bar\Omega$, $H(\cdot)$ is the Heaviside-like function used to represent the discontinuity across the straight crack and defined by

$$H(\mathbf{x}) = \begin{cases} +1 & \text{if } (\mathbf{x}-\mathbf{x}^*)\cdot\mathbf{n}^+ \ge 0, \\ -1 & \text{otherwise,} \end{cases}$$

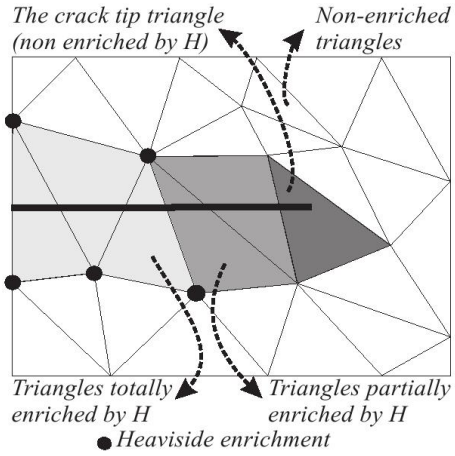

Figure 5.2: *A cracked domain.*

where $\mathbf{x}^*$ denotes the position of the crack tip. The notation φ_i represents the scalar-valued shape function associated with the classical degree one finite-element method at the node of index i, $\mathcal{N}_h$ denotes the set of all node indices, and $\mathcal{N}_h^H$ denotes the set of nodes indices enriched by the function $H(\cdot)$, i.e., nodes indices for which the support of the corresponding shape function is completely cut by the crack (see Fig. 5.2). The cut-off function is a $\mathscr{C}^1$ piecewise third order polynomial on $[r_0, r_1]$ such that:

$$\begin{cases} \chi(r) = 1 & \text{if } r < r_0, \\ \chi(r) \in (0,1) & \text{if } r_0 < r < r_1, \\ \chi(r) = 0 & \text{if } r > r_1. \end{cases}$$

The functions $\{F_j(\mathbf{x})\}_{1\leq j\leq 4}$ are defined in polar coordinates located at the crack tip by

$$\{F_j(\mathbf{x}),\ 1 \leq j \leq 4\} = \left\{ \sqrt{r}\sin\frac{\theta}{2}, \sqrt{r}\cos\frac{\theta}{2}, \sqrt{r}\sin\frac{\theta}{2}\sin\theta, \sqrt{r}\cos\frac{\theta}{2}\sin\theta \right\}. \tag{5.10}$$

These functions allows to generate the asymptotic non-smooth displacement at the crack tip (see [48]).

An important point of the approximation is whether the normal and tangent contact pressure (σ_n and σ_t) are regular or not at the crack tip. If it were singular, it should be taken into account by the discretization of the multiplier. Nevertheless, it seems that this is not the case in homogeneous isotropic linear elasticity. This results has not been proved yet, and seems to be a difficult issue. However, if we consider the formulation (5.7) and if we assume that there is a finite number of transition points between contact and non contact zones near the crack tip, we can easily extend the proved result in the case of frictionless contact [18], to show that the normal and tangent contact stress σ_n and σ_t are in $H^{1/2}(\Gamma_C)$.
Now, concerning the discretization of the multiplier, let $\mathbf{x}_0, ..., \mathbf{x}_N$ be given distinct points lying in $\overline{\Gamma_C}$ and comming from the intersection between $\mathcal{T}^h$ and $\overline{\Gamma_C}$. These nodes form a one-dimensional family of meshes of Γ_C denoted by S^h. The mesh S^h allows us to define a finite-dimensional space

W^h approximating W_N or W_T and a nonempty closed convex set $M_N^h \subset W^h$ (resp. $M_T^h(s) \subset W^h$) approximating M_N (resp $M_T(s)$). We consider two possible elementary choices of W^h:

$$W_0^h = \left\{ \mu^h \in L^2(\Gamma_C) : \mu^h{}_{|(\mathbf{x}_i,\mathbf{x}_{i+1})} \in P_0(\mathbf{x}_i,\mathbf{x}_{i+1}), \forall\, 0 \leq i \leq N-1 \right\},$$

$$W_1^h = \left\{ \mu^h \in \mathscr{C}(\Gamma_C) : \mu^h{}_{|(\mathbf{x}_i,\mathbf{x}_{i+1})} \in P_1(\mathbf{x}_i,\mathbf{x}_{i+1}), \forall\, 0 \leq i \leq N-1 \right\},$$

where $P_k(E)$ denotes the space of polynomials of degree less or equal to k on E. This allows to provide the following three elementary definitions of M_N^h and $M_T^h(s)$:

$$M_{N0}^h = \left\{ \mu^h \in W_0^h : \mu^h \leq 0 \text{ on } \Gamma_C \right\}, \tag{5.11}$$

$$M_{T0}^h(s) = \left\{ \mu^h \in W_0^h : |\mu^h| \leq s \text{ on } \Gamma_C \right\}, \tag{5.12}$$

$$M_{N1}^h = \left\{ \mu^h \in W_1^h : \mu^h \leq 0 \text{ on } \Gamma_C \right\}, \tag{5.13}$$

$$M_{T1}^h(s) = \left\{ \mu^h \in W_1^h : |\mu^h| \leq s \text{ on } \Gamma_C \right\}, \tag{5.14}$$

$$M_{N1,*}^h = \left\{ \mu^h \in W_1^h : \int_{\Gamma_C} \mu^h \psi^h d\Gamma \geq 0, \forall\, \psi^h \in M_{N1}^h \right\}. \tag{5.15}$$

$$M_{T1,*}^H(s) = \left\{ \mu^h \in W_1^h : \int_{\Gamma_C} \mu^h \psi^h d\Gamma + s \int_{\Gamma_C} |\psi^h| \geq 0, \forall\, \psi^H \in W_1^h \right\}. \tag{5.16}$$

Let $\mathbf{W}^h = W^h \times W^h$ and $\mathbf{W} = W_N \times W_T$. In the forthcoming convergence analysis, we will need more information on the compatibillity between the spaces $\mathbf{V}^h$ and $\mathbf{W}^h$. To overcom this dificulty, we use the local projection stabilization technique introduced in [55]. This technique consists in adding a supplementary term, involving the local orthogonal projection of the multiplier on a patch decomposition of the mesh, to the discrete mixed formulation. The set of patches is build from S^h. Indeed we aggregate the possibly very small elements of S^h in order to obtain a set of patches having a minimal and a maximal size (for instance between $3h$ and $6h$). In practice, this operation can be done rather easily (even for three-dimensional problems). A practical way to obtain such a patch decomposition will be described in the next section. An example of patch aggregation is presented in Fig. 5.3. Let H be the maximum length of these patches and denote by S^H the corresponding subdivision of Γ_C. Let

$$W^H = \left\{ \mu^H \in L^2(\Gamma_C) : \mu^H{}_{|S} \in P_0(S),\ \forall S \in S^H \right\},$$

be the space of piecewise constants on this mesh and let $\mathbf{W}^H = W^H \times W^H$. Similarly to the classical result presented in [61], we prove that an inf-sup condition is satisfied between $\mathbf{V}^h$ and $\mathbf{W}^H$ for minimal size of $3h$ for the patches (see Appendix C: This proof, done with scalar field,

can be straightforwardly generalized to vector field). This implies in particular that an optimal convergence can be reached if the multiplier is taken in $\mathbf{W}^H$. However, this suppose a relatively coarse approximation of the multiplier. Our approach is to use this result in order to stabilize the approximation obtained with the multiplier defined on the finer discretization $\mathbf{W}^h$.

Let us first recall the result in Appendix C. Under a condition for the patches $S \in S^H$ to be approximated by a fixed set of line segments having approximatively the same length with a length greater or equal to $3h$, the following inf-sup (or LBB) condition holds for a constant $\beta^* > 0$, independent of h and H:

$$\forall \boldsymbol{\mu}^H \in \mathbf{W}^H, \qquad \sup_{\mathbf{v}^h \in \mathbf{V}^h} \frac{b(\boldsymbol{\mu}^H, \mathbf{v}^h)}{\|\mathbf{v}^h\|_{\mathbf{V}}} \geq \beta^* \|\boldsymbol{\mu}^H\|_{\mathbf{W}'}. \tag{5.17}$$

We will assume in the following that the conditions to obtain this inf-sup condition are satisfied.

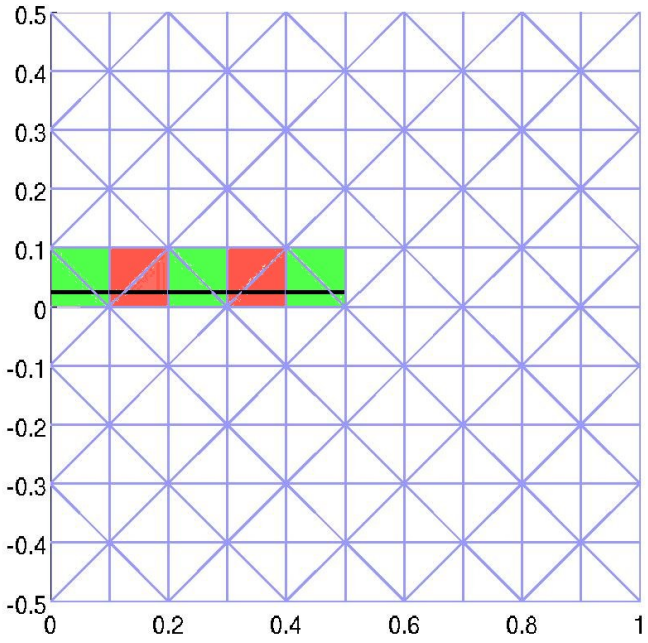

Figure 5.3: *Example of a patch aggregation (in red and green) of size approximatively h of the intersection between crack and the mesh.*

Let P_{W^H} be the local orthogonal projection operator from $L^2(\Gamma_C)$ onto W^H which is defined by

$$\forall \mu \in L^2(\Gamma_C),\ \forall S \in S^H \qquad P_{W^H}(\mu)\,|_S = \frac{1}{\text{mes}(S)} \int_S \mu d\Gamma$$

and $P_{\mathbf{W}^H}$ be the vector local orthogonal projection operator from $L^2(\Gamma_C) \times L^2(\Gamma_C)$ onto $\mathbf{W}^H$ which is defined by $P_{\mathbf{W}^H}(\boldsymbol{\mu}) = (P_{W^H}(\mu_n), P_{W^H}(\mu_t)),\ \forall \boldsymbol{\mu} = (\mu_n, \mu_t) \in L^2(\Gamma_C) \times L^2(\Gamma_C)$. The

stabilized formulation consists in replacing the Lagrangian (5.8) by the following one:

$$\mathcal{L}_h(v^h,\mu^h)=\frac{1}{2}a(\mathbf{v}^h,\mathbf{v}^h)-L(\mathbf{v}^h)-b(\boldsymbol{\mu}^h,\mathbf{v}^h)-\frac{\gamma}{2}\int_{\Gamma_c}(\mu_n^h-P_{W^H}(\mu_n^h))^2d\Gamma-\frac{\gamma}{2}\int_{\Gamma_c}(\mu_t^h-P_{W^H}(\mu_t^h))^2d\Gamma,$$

where, γ is a constant. Let $\mathbf{M}^h(s)=M_N^h\times M_T^h(s)$ then the corresponding optimality system reads as follows:

(5.18)

$$\begin{cases}\text{Find } u^h\in V^h \text{ and } \boldsymbol{\lambda}^h=(\lambda_n^h,\lambda_t^h)\in M^h(s) \text{ such that:}\\ a(\mathbf{u}^h,\mathbf{v}^h)-b(\lambda^h,\mathbf{v}^h)=L(\mathbf{v}^h),\quad \forall\,\mathbf{v}^h\in\mathbf{V}^h,\\ \\ b(\boldsymbol{\mu}^h-\boldsymbol{\lambda}^h,\mathbf{u}^h)+\gamma\displaystyle\int_{\Gamma_c}(\lambda_n^h-P_{W^H}(\lambda_n^h))((\mu_n^h-\lambda_n^h)-(P_{W^H}(\mu_n^h)-P_{W^H}(\lambda_n^h)))d\Gamma\\ \qquad+\gamma\displaystyle\int_{\Gamma_c}(\lambda_t^h-P_{W^H}(\lambda_t^h))((\mu_t^h-\lambda_t^h)-(P_{W^H}(\mu_t^h)-P_{W^H}(\lambda_t^h)))d\Gamma\geq 0,\ \forall\,\boldsymbol{\mu}^h=(\mu_n^h,\mu_t^h)\in\mathbf{M}^h(s),\end{cases}$$

5.3.2 Existence and uniqueness of the solution of the stabilized problem

Lemma 5.3.1. *For any $\gamma>0$ there exists a unique solution of the stabilized problem (5.18).*

Proof. Let $\boldsymbol{\mu}^h=(\mu_n^h,\mu_t^h)\in\mathbf{M}^h(s)$ and $\mathbf{u}^h$ be the solution of the following problem:

$$a(\mathbf{u}^h,\mathbf{v}^h)-L(\mathbf{v}^h)=b(\boldsymbol{\mu}^h,\mathbf{v}^h)=\left\langle\mu_n^h,[\![v_n^h]\!]\right\rangle_{W^{h\prime},W^h}+\left\langle\mu_t^h,[\![v_t^h]\!]\right\rangle_{W^{h\prime},W^h}\quad\forall\,\mathbf{v}^h\in\mathbf{V}^h$$

then using the fact that the inf-sup condition is satisfied in the ortogonal of the kernel of $b(.,.)$ (which contains $\mathbf{W}^h$) we prove that there exists a constant C such that:

$$C\|\mathbf{u}^h\|_{\mathbf{V}}+\|L\|_{V'}\geq\|P_{\mathbf{W}^H}(\boldsymbol{\mu}^h)\|_{\mathbf{W}'}\tag{5.19}$$

We have

$$\begin{aligned}\mathcal{L}_h(\mathbf{u}^h,\boldsymbol{\mu}^h)&=\frac{1}{2}a(\mathbf{u}^h,\mathbf{u}^h)-L(\mathbf{u}^h)-b(\boldsymbol{\mu}^h,\mathbf{u}^h)-\frac{\gamma}{2}\int_{\Gamma_C}(\mu_n^h-P_{W^H}(\mu_n^h))^2d\Gamma\\&\quad-\frac{\gamma}{2}\int_{\Gamma_C}(\mu_t^h-P_{W^H}(\mu_t^h))^2d\Gamma,\\&=-\frac{1}{2}a(\mathbf{u}^h,\mathbf{u}^h)-\frac{\gamma}{2}\int_{\Gamma_C}(\mu_n^h-P_{W^H}(\mu_n^h))^2d\Gamma-\frac{\gamma}{2}\int_{\Gamma_C}(\mu_t^h-P_{W^H}(\mu_t^h))^2d\Gamma,\\&=-\frac{1}{2}\|\mathbf{u}^h\|_{\mathbf{V}}^2-\frac{\gamma}{2}\|\mu_n^h-P_{W^H}(\mu_n^h)\|_{0,\Gamma_C}^2-\frac{\gamma}{2}\|\mu_t^h-P_{W^H}(\mu_t^h)\|_{0,\Gamma_C}^2\end{aligned}$$

When $\|\boldsymbol{\mu}^h\|_{\mathbf{W}'}\to\infty$ we have $\|P_{\mathbf{W}^H}(\boldsymbol{\mu}^h)\|_{\mathbf{W}'}\to\infty$ (using inequality (5.19) we have $\|\mathbf{u}^h\|_{\mathbf{V}}\to\infty$) or/and $\|\boldsymbol{\mu}^h-P_{\mathbf{W}^H}(\boldsymbol{\mu}^h)\|_{\mathbf{W}'}\to\infty$, which implies that

$$\lim_{\boldsymbol{\mu}^h\in\mathbf{M}^h(s),\|\boldsymbol{\mu}^h\|_{\mathbf{W}'}\to\infty}\mathcal{L}_\gamma(\mathbf{u}^h,\boldsymbol{\mu}^h)=-\infty$$

Now the existence of a solution to Problem (5.18) follows from the fact that $\mathbf{V}^h$ and $\mathbf{M}^h(s)$ are two nonempty closed convex sets, $\mathcal{L}_\gamma(\cdot,\cdot)$ is continuous on $\mathbf{V}^h\times\mathbf{W}^h$, $\mathcal{L}_\gamma(\mathbf{v}^h,.)$

(resp. $\mathcal{L}_\gamma(\cdot,\boldsymbol{\mu}^h)$) is concave (resp. strictly convex) for any $\mathbf{v}^h \in \mathbf{V}^h$ (resp. for any $\mu^h \in \mathbf{M}^h$) and $\lim_{\mathbf{v}^h\in\mathbf{V}^h,\|\mathbf{v}^h\|_{\mathbf{V}^h}\to\infty} \mathcal{L}_\gamma(\mathbf{v}^h,0) = +\infty$ for any $\boldsymbol{\mu}^h \in \mathbf{M}^h(s)$ (resp. $\lim_{\boldsymbol{\mu}^h\in\mathbf{M}^h(s),\|\boldsymbol{\mu}^h\|_{\mathbf{W}^h}\to\infty} \mathcal{L}_\gamma(\mathbf{u}^h,\boldsymbol{\mu}^h) = -\infty$), see [46, pp. 338–339]. The strict convexity of $a(.,.)$ imply the uniqueness of the first argument $\mathbf{u}^h$. Now let $\boldsymbol{\lambda}_1^h$ and $\boldsymbol{\lambda}_2^h$ two solution of (5.18) then we have:

$$\begin{aligned} b(\boldsymbol{\lambda}_2^h-\boldsymbol{\lambda}_1^h,\mathbf{u}^h) \quad + \quad & \gamma\int_{\Gamma_c}(\lambda_{1n}^h - P_{W^H}(\lambda_{1n}^h))((\lambda_{2n}^h-\lambda_{1n}^h)-(P_{W^H}(\lambda_{1n}^h)-P_{W^H}(\lambda_{2n}^h)))d\Gamma \\ & +\gamma\int_{\Gamma_c}(\lambda_{1t}^h - P_{W^H}(\lambda_{1t}^h))((\lambda_{2t}^h-\lambda_{1t}^h)-(P_{W^H}(\lambda_{1t}^h)-P_{W^H}(\lambda_{2t}^h)))d\Gamma \geq 0 \\ b(\boldsymbol{\lambda}_1^h-\boldsymbol{\lambda}_2^h,\mathbf{u}^h) \quad + \quad & \gamma\int_{\Gamma_c}(\lambda_{2n}^h - P_{W^H}(\lambda_{2n}^h))((\lambda_{1n}^h-\lambda_{2n}^h)-(P_{W^H}(\lambda_{2n}^h)-P_{W^H}(\lambda_{1n}^h))) \\ & +\gamma\int_{\Gamma_c}(\lambda_{2t}^h - P_{W^H}(\lambda_{2t}^h))((\lambda_{1t}^h-\lambda_{2t}^h)-(P_{W^H}(\lambda_{2t}^h)-P_{W^H}(\lambda_{1t}^h)))d\Gamma \geq 0 \end{aligned}$$

and by summation of the last two inequalities we have:

$$\|(\lambda_{1n}^h-\lambda_{2n}^h)-(P_{W^H}(\lambda_{1n}^h)-P_{W^H}(\lambda_{2n}^h))\|_{0,\Gamma_C}^2 + \|(\lambda_{1t}^h-\lambda_{2t}^h)-(P_{W^H}(\lambda_{1t}^h)-P_{W^H}(\lambda_{2t}^h))\|_{0,\Gamma_C}^2 \leq 0$$

therefore $\lambda_{1n}^h-\lambda_{2n}^h = P_{W^H}(\lambda_{2n}^h)-P_{W^H}(\lambda_{1n}^h)$ and $\lambda_{1t}^h-\lambda_{2t}^h = P_{W^H}(\lambda_{2t}^h)-P_{W^H}(\lambda_{1t}^h)$ (i.e. $\lambda_{1n}^h-\lambda_{2n}^h \in W^H$ and $\lambda_{1t}^h-\lambda_{2t}^h \in W^H$). Let $\bar{\boldsymbol{\lambda}}^h = (\lambda_{1n}^h-\lambda_{2n}^h,\lambda_{1t}^h-\lambda_{2t}^h)$ and $\bar{\boldsymbol{\lambda}}^H = (P_{W^H}(\lambda_{1n}^h)-P_{W^H}(\lambda_{2n}^h),P_{W^H}(\lambda_{1t}^h)-P_{W^H}(\lambda_{2t}^h))$. From inequality (5.17) there exists $\mathbf{v}^h \in \mathbf{V}^h$ such that

$$b(\bar{\boldsymbol{\lambda}}^H,\mathbf{v}^h) \geq \beta^*\|\bar{\boldsymbol{\lambda}}^H\|_{\mathbf{W}'}\|\mathbf{v}^h\|_{\mathbf{V}}, \tag{5.20}$$

and thus

$$\beta^*\|\bar{\boldsymbol{\lambda}}^H\|_{\mathbf{W}'} \leq \frac{1}{\|\mathbf{v}^h\|_{\mathbf{V}}}b(\bar{\boldsymbol{\lambda}}^H,\mathbf{v}^h) = \frac{1}{\|\mathbf{v}^h\|_{\mathbf{V}}}b(\bar{\boldsymbol{\lambda}}^h,\mathbf{v}^h) = \frac{1}{\|\mathbf{v}^h\|_{\mathbf{V}}}a(\bar{\mathbf{u}}^h,\mathbf{v}^h) = 0.$$

This implies the uniqueness of the second argument $\boldsymbol{\lambda}^h$, therefore (5.18) has a unique solution.

5.3.3 Convergence analysis

In order to study the convergence error, we recall the definition of the XFEM interpolation operator Π^h introduced in [17].

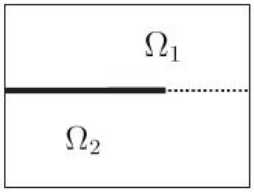

Figure 5.4: *Decomposition of* Ω *into* Ω_1 *and* Ω_2.

We assume that the displacement has the regularity $(H^2(\Omega))^2$ except in the vicinity of the crack-tip where the singular part of the displacement is a linear combination of the functions $\{F_j(\mathbf{x})\}_{1\leq j\leq 4}$ given by (5.10) (see [49] for a justification). Let us denote by $\mathbf{u}_s$ the singular part of $\mathbf{u}$, $\mathbf{u}_r = \mathbf{u} - \chi\mathbf{u}_s$ the regular part of $\mathbf{u}$, and $\mathbf{u}_r^k$ the restriction of $\mathbf{u}_r$ to Ω_k, $k \in \{1,2\}$. Then, for $k \in \{1,2\}$, there exists an extension $\widetilde{\mathbf{u}}_r^k \in (H^2(\overline{\Omega}))^2$ of $\mathbf{u}_r^k$ to $\overline{\Omega}$ such that (see [15])

$$\|\widetilde{\mathbf{u}}_r^1\|_{2,\overline{\Omega}} \lesssim \|\mathbf{u}_r^1\|_{2,\Omega_1},$$
$$\|\widetilde{\mathbf{u}}_r^2\|_{2,\overline{\Omega}} \lesssim \|\mathbf{u}_r^2\|_{2,\Omega_2}.$$

Here and throughout the paper, we use the notation $a \lesssim b$ to signify that there exists a constant $C > 0$, independent of the mesh parameter h, the solution and the position of the crack-tip, such that $a \leq Cb$.

Definition 2 ([17]). *Given a displacement field* $\mathbf{u}$ *satisfying* $\mathbf{u}-\mathbf{u}_s \in H^2(\Omega)$, *and two extensions* $\widetilde{\mathbf{u}}_r^1$ *and* $\widetilde{\mathbf{u}}_r^2$ *in* $H^2(\overline{\Omega})$ *of* $\mathbf{u}_r^1$ *and* $\mathbf{u}_r^2$, *respectively, we define* $\Pi^h\mathbf{u}$ *as the element of* $\mathbf{V}^h$ *such that*

$$\Pi^h\mathbf{u} \;=\; \sum_{i\in\mathcal{N}_h} \mathbf{a}_i\varphi_i \;+\; \sum_{i\in\mathcal{N}_h^H} \mathbf{b}_i H\varphi_i \;+\; \chi\mathbf{u}_s,$$

where $\mathbf{a}_i$, $\mathbf{b}_i$ *are given as follows for* $\mathbf{y}_i$ *the finite-element node associated to* φ_i:

if $i \in \{\mathcal{N}_h \setminus \mathcal{N}_h^H\}$ *then* $\mathbf{a}_i = \mathbf{u}_r(\mathbf{y}_i)$,
if $i \in \mathcal{N}_h^H$ *and* $\mathbf{y}_i \in \overline{\Omega}_k$ *for* $k \in \{1,2\}$ *then for* $l = 3-k$:

$$\begin{cases} \mathbf{a}_i = \dfrac{1}{2}\left(\mathbf{u}_r^k(\mathbf{y}_i) + \widetilde{\mathbf{u}}_r^l(\mathbf{y}_i)\right), \\ \mathbf{b}_i = \dfrac{(-1)^k}{2}\left(\mathbf{u}_r^k(\mathbf{y}_i) - \widetilde{\mathbf{u}}_r^l(\mathbf{y}_i)\right). \end{cases}$$

This XFEM interpolation operator satisfies the following interpolation error estimate [17]:

$$\|\mathbf{u} - \Pi^h\mathbf{u}\| \lesssim h\|\mathbf{u} - \chi\mathbf{u}_s\|_{2,\Omega}. \tag{5.21}$$

Lemma 5.3.2. *Let* $(\mathbf{u},\boldsymbol{\lambda}) \in V \times \mathbf{M}(s)$ *be the solution of (5.7) and* $(\mathbf{u}^h,\boldsymbol{\lambda}^h) \in \mathbf{V}^h \times \mathbf{M}^h(s)$ *be the solution of (5.18). Then we have:*

$$\begin{aligned} \alpha\|\mathbf{u}^h-\mathbf{u}\|^2 \;\leq\; & M\|\mathbf{u}^h-\mathbf{u}\|\|\mathbf{v}^h-\mathbf{u}\| + \|\boldsymbol{\lambda}^h-\boldsymbol{\lambda}\|_{-1/2,\Gamma_C}\|\mathbf{u}-\mathbf{v}^h\| + b(\boldsymbol{\mu}^h-\boldsymbol{\lambda},\mathbf{u}^h-\mathbf{u}) \\ & + b(\boldsymbol{\lambda}^h-\boldsymbol{\mu}^h,\mathbf{u}^h) + b(\boldsymbol{\mu}^h-\boldsymbol{\lambda},\mathbf{u}) + b(\boldsymbol{\lambda}-\boldsymbol{\lambda}^h,\mathbf{u}), \quad \forall\mathbf{v}^h \in \mathbf{V}^h, \boldsymbol{\mu}^h \in \mathbf{W}^h, \end{aligned} \tag{5.22}$$

$$\begin{aligned} \beta^{*2}\|\boldsymbol{\lambda}^H-\boldsymbol{\lambda}\|_{\mathbf{W}'}^2 \;\leq\; & 8M^2\|\mathbf{u}-\mathbf{u}^h\|^2 + 8\beta^{*2}\|\boldsymbol{\lambda}-\bar{\boldsymbol{\mu}}^H\|_{\mathbf{W}'}^2 + 8\|\boldsymbol{\lambda}-\bar{\boldsymbol{\mu}}^h\|_{\mathbf{W}'}^2 \\ & + 8\|\bar{\boldsymbol{\mu}}^H-\bar{\boldsymbol{\mu}}^h\|_{\mathbf{W}'}^2 + 8\|\boldsymbol{\lambda}^H-\boldsymbol{\lambda}^h\|_{\mathbf{W}'}^2 \quad \forall\bar{\boldsymbol{\mu}}^h = (\bar{\mu}_n^h,\bar{\mu}_t^h) \in \mathbf{W}^h, \end{aligned} \tag{5.23}$$

with $\boldsymbol{\lambda}^H = P_{\mathbf{W}^H}(\boldsymbol{\lambda}^h)$, $\bar{\boldsymbol{\mu}}^H = P_{\mathbf{W}^H}(\bar{\boldsymbol{\mu}}^h)$.

Proof. For all $\mathbf{v}^h \in \mathbf{V}^h$, $\boldsymbol{\mu}^h \in \mathbf{W}^h$ one has

$$\begin{aligned} a(\mathbf{u}^h-\mathbf{u},\mathbf{u}^h-\mathbf{u}) &= a(\mathbf{u}^h-\mathbf{u},\mathbf{v}^h-\mathbf{u}) + a(\mathbf{u}^h-\mathbf{u},\mathbf{u}^h-\mathbf{v}^h) \\ &= a(\mathbf{u}^h-\mathbf{u},\mathbf{v}^h-\mathbf{u}) + b(\boldsymbol{\lambda}^h-\boldsymbol{\lambda},\mathbf{u}^h-\mathbf{v}^h) \\ &= a(\mathbf{u}^h-\mathbf{u},\mathbf{v}^h-\mathbf{u}) + b(\boldsymbol{\lambda}^h-\boldsymbol{\lambda},\mathbf{u}-\mathbf{v}^h) + b(\boldsymbol{\lambda}^h-\boldsymbol{\lambda},\mathbf{u}^h-\mathbf{u}) \\ &= a(\mathbf{u}^h-\mathbf{u},\mathbf{v}^h-\mathbf{u}) + b(\boldsymbol{\lambda}^h-\boldsymbol{\lambda},\mathbf{u}-\mathbf{v}^h) + b(\boldsymbol{\mu}^h-\boldsymbol{\lambda},\mathbf{u}^h-\mathbf{u}) \\ &\quad + b(\boldsymbol{\lambda}^h-\boldsymbol{\mu}^h,\mathbf{u}^h) + b(\boldsymbol{\mu}^h-\boldsymbol{\lambda},\mathbf{u}) + b(\boldsymbol{\lambda}-\boldsymbol{\lambda}^h,\mathbf{u}) \end{aligned}$$

From the $\mathbf{V}$-ellipticity and the continuity of the bilinear form $a(.,.)$ we prove the first inequality of Lemma 5.3.2. Now we shall give an estimate of the second inequality of Lemma 5.3.2. Noticing that

$$\int_{\Gamma_C} (\boldsymbol{\lambda} - \boldsymbol{\lambda}^h) \cdot [\![\mathbf{v}^h]\!] d\Gamma = a(\mathbf{u}^h - \mathbf{u}, \mathbf{v}^h) \qquad \forall \mathbf{v}^h \in \mathbf{V}^h,$$

one obtains

$$\begin{aligned} \int_{\Gamma_C} (\bar{\boldsymbol{\mu}}^h - \boldsymbol{\lambda}^h) \cdot [\![\mathbf{v}^h]\!] d\Gamma &= a(\mathbf{u}^h - \mathbf{u}, \mathbf{v}^h) \\ &\quad + \int_{\Gamma_C} (\bar{\boldsymbol{\mu}}^h - \boldsymbol{\lambda}) \cdot [\![\mathbf{v}^h]\!] d\Gamma, \ \forall (\mathbf{v}^h, \bar{\boldsymbol{\mu}}^h) \in \mathbf{V}^h \times \mathbf{W}^h. \end{aligned} \tag{5.24}$$

Now, for $\boldsymbol{\mu}^H = \boldsymbol{\lambda}^H - \bar{\boldsymbol{\mu}}^H \in \mathbf{W}^H$ with $\bar{\boldsymbol{\mu}}^H = P_{\mathbf{W}^H}(\bar{\boldsymbol{\mu}}^h)$ the inf-sup condition (5.17) ensure the existence of $\mathbf{v}^h \in \mathbf{V}^h$ such that together with (5.24) we get

$$\begin{aligned} \beta^* \|\boldsymbol{\lambda}^H - \bar{\boldsymbol{\mu}}^H\|_{\mathbf{W}'} &\leq \frac{1}{\|\mathbf{v}^h\|} \int_{\Gamma_C} (\bar{\boldsymbol{\mu}}^H - \boldsymbol{\lambda}^H) \cdot [\![\mathbf{v}^h]\!] \, d\Gamma, \\ &\leq \frac{1}{\|\mathbf{v}^h\|} \int_{\Gamma_C} (\bar{\boldsymbol{\mu}}^h - \boldsymbol{\lambda}^h) \cdot [\![\mathbf{v}^h]\!] \, d\Gamma + \frac{1}{\|\mathbf{v}^h\|} \int_{\Gamma_C} (\bar{\boldsymbol{\mu}}^H - \boldsymbol{\lambda}^H - (\bar{\boldsymbol{\mu}}^h - \boldsymbol{\lambda}^h)) \cdot [\![\mathbf{v}^h]\!] \, d\Gamma, \\ &\leq M\|\mathbf{u}^h - \mathbf{u}\| + \|\bar{\boldsymbol{\mu}}^h - \boldsymbol{\lambda}\|_{\mathbf{W}'} + \|\bar{\boldsymbol{\mu}}^H - \boldsymbol{\lambda}^H - (\bar{\boldsymbol{\mu}}^h - \boldsymbol{\lambda}^h)\|_{\mathbf{W}'}. \end{aligned}$$

As a consequence, one has

$$\begin{aligned} \beta^* \|\boldsymbol{\lambda}^H - \boldsymbol{\lambda}\|_{\mathbf{W}'} &\leq \beta^* \|\boldsymbol{\lambda} - \bar{\boldsymbol{\mu}}^H\|_{\mathbf{W}'} + M\|\mathbf{u}^h - \mathbf{u}\| + \|\bar{\boldsymbol{\mu}}^h - \boldsymbol{\lambda}\|_{\mathbf{W}'} \\ &\quad + \|\bar{\boldsymbol{\mu}}^H - \bar{\boldsymbol{\mu}}^h\|_{\mathbf{W}'} + \|\boldsymbol{\lambda}^H - \boldsymbol{\lambda}^h\|_{\mathbf{W}'}, \end{aligned}$$

and

$$\begin{aligned} \beta^{*2} \|\boldsymbol{\lambda}^H - \boldsymbol{\lambda}\|^2_{\mathbf{W}'} &\leq 8M^2\|\mathbf{u} - \mathbf{u}^h\|^2 + 8\beta^{*2}\|\boldsymbol{\lambda} - \bar{\boldsymbol{\mu}}^H\|^2_{\mathbf{W}'} + 8\|\boldsymbol{\lambda} - \bar{\boldsymbol{\mu}}^h\|^2_{\mathbf{W}'} \\ &\quad + 8\|\bar{\boldsymbol{\mu}}^H - \bar{\boldsymbol{\mu}}^h\|^2_{\mathbf{W}'} + 8\|\boldsymbol{\lambda}^H - \boldsymbol{\lambda}^h\|^2_{\mathbf{W}'} \quad \forall \bar{\boldsymbol{\mu}}^h \in \mathbf{W}^h. \end{aligned} \tag{5.25}$$

□

In order to estimate these terms, we need to distinguish the different contact conditions (i.e., we must specify the definition of $\mathbf{M}^h(s)$). We consider hereafter three different standard discrete contact conditions.

5.3.3.1 Conforming piecewise discontinuous discretization for multiplier $M_N^h = M_{N0}^h$ and $M_T^h(s) = M_{T0}^h(s)$

We first consider the case of nonpositive discontinuous piecewise constant multipliers where M_N^h is defined by (5.11) and $M_T^h(s)$ is defined by (5.12). It is a conforming discretistion on multiplier as $M_{N0}^h \subset M_N$ and $M_{T0}^h(s) \subset M_T(s)$.

Theorem 5.3.3. *Let $(\mathbf{u}, \boldsymbol{\lambda})$ be the solution to Problem (5.7). Assume that $\mathbf{u}_r \in (H^2(\Omega))^2$ and $\boldsymbol{\lambda} \in (H^{1/2}(\Gamma_C))^2$. Let $(\mathbf{u}^h, \boldsymbol{\lambda}^H)$ be the solution to the discrete problem (5.18) where $M_N^h = M_{N0}^h$ and $M_T^h(s) = M_{T0}^h(s)$. Then, for any $\eta > 0$ we have*

$$\|\mathbf{u} - \mathbf{u}^h\| + \|\boldsymbol{\lambda} - \boldsymbol{\lambda}^h\|_{\mathbf{W}'} \lesssim h\|\mathbf{u} - \chi\mathbf{u}_s\|_{2,\Omega} + H^{\frac{3}{4}-\frac{\eta}{2}} \big(\|\mathbf{u}\|_{3/2-\eta,\Omega} + \|\boldsymbol{\lambda}\|_{1/2,\Gamma_C}\big).$$

Proof. In (5.22) we choose $\boldsymbol{\mu}^h = P_{\mathbf{W}^H}(\boldsymbol{\lambda}) = (P_{W^H}(\lambda_n), P_{W^H}(\lambda_t))$. We recall that the operator P_{W^H} is defined for any $v \in L^2(\Gamma_C)$ by

$$P_{W^H}(v) \in W^H, \quad \int_{\Gamma_C} (v - P_{W^H}(v))\mu^H \, d\Gamma = 0, \quad \forall \mu^H \in W^H,$$

and satisfies the following error estimates for any $0 \leq r \leq 1$ (see [25])

$$H^{-1/2}\|v - P_{W^H}(v)\|_{-1/2,\Gamma_C} + \|v - P_{W^H}(v)\|_{0,\Gamma_C} \lesssim H^r \|v\|_{r,\Gamma_C}. \tag{5.26}$$

Clearly, $\boldsymbol{\mu}^h \in M^h(s)$ and using the inequality comming from (5.18) we have

$$b(\boldsymbol{\lambda}^h - \boldsymbol{\mu}^h, \mathbf{u}^h) \leq -\gamma \|\boldsymbol{\lambda}^h - \boldsymbol{\lambda}^H\|^2_{0,\Gamma_C}, \tag{5.27}$$

with $\boldsymbol{\lambda}^H = P_{\mathbf{W}^H}(\boldsymbol{\lambda}^h) = (P_{W^H}(\lambda_n^h), P_{W^H}(\lambda_t^h))$. Moreover

$$b(\boldsymbol{\mu}^h - \boldsymbol{\lambda}, \mathbf{u}^h - \mathbf{u}) = b(P_{\mathbf{W}^H}(\boldsymbol{\lambda}) - \boldsymbol{\lambda}, \mathbf{u}^h - \mathbf{u}) \leq \|P_{\mathbf{W}^H}(\boldsymbol{\lambda}) - \boldsymbol{\lambda}\|_{\mathbf{W}'} \|\mathbf{u}^h - \mathbf{u}\| \tag{5.28}$$

and

$$\begin{aligned}
b(\boldsymbol{\mu}^h - \boldsymbol{\lambda}, \mathbf{u}) &= \int_{\Gamma_C} (P_{W^H}(\lambda_n) - \lambda_n)[\![u_n]\!] d\Gamma + \int_{\Gamma_C} (P_{W^H}(\lambda_t) - \lambda_t)[\![u_t]\!] d\Gamma \\
&= \int_{\Gamma_C} (P_{W^H}(\lambda_n) - \lambda_n)([\![u_n]\!] - P_{W^H}([\![u_n]\!])) d\Gamma \\
&\quad + \int_{\Gamma_C} (P_{W^H}(\lambda_t) - \lambda_t)([\![u_t]\!] - P_{W^H}([\![u_t]\!])) d\Gamma \\
&\leq \|P_{W^H}(\lambda_n) - \lambda_n\|_{W'} \|[\![u_n]\!] - P_{W^H}([\![u_n]\!])\|_W \\
&\quad + \|P_{W^H}(\lambda_t) - \lambda_t\|_{\mathbf{W}'} \|[\![u_t]\!] - P_{W^H}([\![u_t]\!])\|_W \\
&\leq \|P_{\mathbf{W}^H}(\boldsymbol{\lambda}) - \boldsymbol{\lambda}\|_{\mathbf{W}'} \|[\![\mathbf{u}]\!] - P_{\mathbf{W}^H}([\![\mathbf{u}]\!])\|_{\mathbf{W}}
\end{aligned} \tag{5.29}$$

Noting that $M^h_{N0} \subset M_N$ and $M^h_{T0} \subset M_T$ wich implies

$$b(\boldsymbol{\lambda} - \boldsymbol{\lambda}^h, \mathbf{u}) \leq 0. \tag{5.30}$$

Using inequalities (5.22), (5.27), (5.28), (5.29) and (5.30) we have

$$\begin{aligned}
\alpha\|\mathbf{u}^h - \mathbf{u}\|^2 + \gamma\|\boldsymbol{\lambda}^h - \boldsymbol{\lambda}^H\|^2_{0,\Gamma_C} \leq\ & M\|\mathbf{u}^h - \mathbf{u}\|\|\mathbf{v}^h - \mathbf{u}\| + \|\boldsymbol{\lambda}^h - \boldsymbol{\lambda}\|_{\mathbf{W}'}\|\mathbf{u} - \mathbf{v}^h\| \\
&+ \|P_{\mathbf{W}^H}(\boldsymbol{\lambda}) - \boldsymbol{\lambda}\|_{\mathbf{W}'}\|\mathbf{u}^h - \mathbf{u}\| \\
&+ \|P_{\mathbf{W}^H}(\boldsymbol{\lambda}) - \boldsymbol{\lambda}\|_{\mathbf{W}'}\|[\![\mathbf{u}]\!] - P_{\mathbf{W}^H}([\![\mathbf{u}]\!])\|_{\mathbf{W}}
\end{aligned} \tag{5.31}$$

By combining inequalities (5.23) and (5.31) one obtains for all $\bar{\boldsymbol{\mu}}^h \in \mathbf{W}^h$ and $\mathbf{v}^h \in \mathbf{V}^h$

$$\begin{aligned}
&(\alpha - 8M^2\delta)\|\mathbf{u} - \mathbf{u}^h\|^2 + \delta\beta^{*2}\|\boldsymbol{\lambda} - \boldsymbol{\lambda}^H\|^2_{\mathbf{W}'} + (\gamma - 8\delta)\|\boldsymbol{\lambda}^h - \boldsymbol{\lambda}^H\|^2_{\mathbf{W}'} \\
\leq\ & M\|\mathbf{u}^h - \mathbf{u}\|\|\mathbf{v}^h - \mathbf{u}\| + \|P_{\mathbf{W}^H}\boldsymbol{\lambda} - \boldsymbol{\lambda}\|_{\mathbf{W}'}\|\mathbf{u}^h - \mathbf{u}\| + \|\boldsymbol{\lambda}^h - \boldsymbol{\lambda}\|_{\mathbf{W}'}\|\mathbf{u} - \mathbf{v}^h\| \\
&+ \|P_{\mathbf{W}^H}(\boldsymbol{\lambda}) - \boldsymbol{\lambda}\|_{\mathbf{W}'}\|[\![\mathbf{u}]\!] - P_{\mathbf{W}^H}([\![\mathbf{u}]\!])\|_{\mathbf{W}} + 8\delta\beta^{*2}\|\boldsymbol{\lambda} - \bar{\boldsymbol{\mu}}^H\|^2_{\mathbf{W}'} \\
&+ 8\delta\|\boldsymbol{\lambda} - \bar{\boldsymbol{\mu}}^h\|^2_{\mathbf{W}'} + 8\delta\|\bar{\boldsymbol{\mu}}^h - \bar{\boldsymbol{\mu}}^H\|^2_{\mathbf{W}'}, \\
\leq\ & \frac{\delta}{2}M^2\|\mathbf{u} - \mathbf{u}^h\|^2 + \frac{1}{2\delta}\|\mathbf{u} - \mathbf{v}^h\|^2 + \frac{\delta}{2}\|\mathbf{u} - \mathbf{u}^h\|^2 + \frac{1}{2\delta}\|\boldsymbol{\lambda} - P_{\mathbf{W}^H}(\boldsymbol{\lambda})\|^2_{\mathbf{W}'} \\
&+ \frac{\xi}{2}\|\boldsymbol{\lambda} - \boldsymbol{\lambda}^h\|^2_{\mathbf{W}'} + \frac{1}{2\xi}\|\mathbf{u} - \mathbf{v}^h\|^2 + \|P_{\mathbf{W}^H}(\boldsymbol{\lambda}) - \boldsymbol{\lambda}\|_{\mathbf{W}'}\|[\![\mathbf{u}]\!] - P_{\mathbf{W}^H}[\![\mathbf{u}]\!]\|_{\mathbf{W}} \\
&+ 8\delta\beta^{*2}\|\boldsymbol{\lambda} - \bar{\boldsymbol{\mu}}^H\|^2_{\mathbf{W}'} + 8\delta\|\boldsymbol{\lambda} - \bar{\boldsymbol{\mu}}^h\|^2_{\mathbf{W}'} + 8\delta\|\bar{\boldsymbol{\mu}}^h - \bar{\boldsymbol{\mu}}^H\|^2_{\mathbf{W}'}.
\end{aligned}$$

Then, for all $\bar{\boldsymbol{\mu}}^h \in \mathbf{W}^h$ and $\mathbf{v}^h \in \mathbf{V}^h$, we deduce

$$\begin{aligned}
&(\alpha - \delta\frac{17M^2+1}{2})\|\mathbf{u}-\mathbf{u}^h\|^2 + (\gamma - 8\delta - \frac{\xi}{2})\|\boldsymbol{\lambda}^h - \boldsymbol{\lambda}^H\|^2_{\mathbf{W}'} + (\delta\beta^{*2} - \frac{\xi}{2})\|\boldsymbol{\lambda}-\boldsymbol{\lambda}^H\|^2_{\mathbf{W}'} \\
\leq\ & (\frac{1}{2\delta}+\frac{1}{2\xi})\|\mathbf{u}-\mathbf{v}^h\|^2 + \frac{1}{2\delta}\|P_{\mathbf{W}^H}(\boldsymbol{\lambda})-\boldsymbol{\lambda}\|^2_{\mathbf{W}'} + 8\delta\beta^{*2}\|\boldsymbol{\lambda}-\bar{\boldsymbol{\mu}}^H\|^2_{\mathbf{W}'} \\
&+\|P_{\mathbf{W}^H}(\boldsymbol{\lambda})-\boldsymbol{\lambda}\|_{\mathbf{W}'}\|[\![\mathbf{u}]\!] - P_{\mathbf{W}^H}([\![\mathbf{u}]\!])\|_{\mathbf{W}} + 8\delta\|\boldsymbol{\lambda}-\bar{\boldsymbol{\mu}}^h\|^2_{\mathbf{W}'} + 8\delta\|\bar{\boldsymbol{\mu}}^h - \bar{\boldsymbol{\mu}}^H\|^2_{\mathbf{W}'}.
\end{aligned}$$

we recall the following standard finite-element estimates:

$$\|\mathbf{u} - \Pi^h\mathbf{u}\| \leq Ch\|\mathbf{u}_r\|_{2,\Omega},$$

$$\|\mathbf{u} - P_{\mathbf{W}^H}(\mathbf{u})\|_{1/2} \leq CH^{\frac{1}{2}-\eta}\|\mathbf{u}\|_{1-\eta,\Gamma_C}.$$

$$\|\boldsymbol{\lambda} - P_{\mathbf{W}^h}(\boldsymbol{\lambda})\|_{-1/2} \leq Ch\|\boldsymbol{\lambda}\|_{1/2,\Gamma_C},$$

$$\|\boldsymbol{\lambda} - P_{\mathbf{W}^H}(\boldsymbol{\lambda})\|_{-1/2} \leq CH\|\boldsymbol{\lambda}\|_{1/2,\Gamma_C}.$$

Finally, the theorem is established by taking $\delta < \min\big(\frac{2\alpha}{17M^2+1}; \frac{\gamma}{8}\big)$, $\xi < \min\big(2\delta\beta^{*2}; 2(\gamma-8\delta)\big)$, $\mathbf{v}^h = \Pi^h\mathbf{u}$ and $\bar{\boldsymbol{\mu}}^h = P_{\mathbf{W}^h}(\boldsymbol{\lambda})$. □

5.3.3.2 Conforming piecewise continuous discretization for multiplier $M_N^h = M_{N1}^h$ and $M_T^h(s) = M_{T1}^h(s)$

Now, we focus on the case of nonpositive continuous piecewise affine multipliers where M_N^h is given by (5.13) and $M_T^h(s)$ is given by (5.14)

Theorem 5.3.4. *Let $(\mathbf{u}, \boldsymbol{\lambda})$ be the solution to Problem (5.7). Assume that $\mathbf{u}_r \in (H^2(\Omega))^2$ and $\boldsymbol{\lambda} \in (H^{1/2}(\Gamma_C))^2$. Let $(\mathbf{u}^h, \boldsymbol{\lambda}^h)$ be the solution to the discrete problem (5.18) where $M_N^h = M_{N1}^h$ and $M_T^h = M_{T1}^h$. Then, for any $\eta > 0$ we have*

$$\|\mathbf{u}-\mathbf{u}^h\| + \|\boldsymbol{\lambda}-\boldsymbol{\lambda}^h\|_{\mathbf{W}'} \lesssim h\|\mathbf{u}-\chi\mathbf{u}_s\|_{2,\Omega} + H^{\frac{1}{4}}\big(\|\mathbf{u}\|_{3/2-\eta,\Omega} + \|\boldsymbol{\lambda}\|_{1/2,\Gamma_C}\big).$$

Proof. We choose $\boldsymbol{\mu}^h = \mathbf{r}^h(\boldsymbol{\lambda}) = (r^h\lambda_n, r^h\lambda_t)$ in (5.22) where $r^h : L^1(\Gamma_C) \mapsto W_1^h$ is a quasi-interpolation operator which preserves the nonpositivity defined for any function v in $L^1(\Gamma_C)$ by

$$r^h v = \sum_{\mathbf{x}\in N^H} \alpha_{\mathbf{x}}(v)\psi_{\mathbf{x}},$$

where N^h represents the set of nodes $\mathbf{x}_0, ..., \mathbf{x}_N$ in $\overline{\Gamma_C}$, $\psi_{\mathbf{x}}$ is the scalar basis function of W_1^h (defined on $\overline{\Gamma_C}$) at node $\mathbf{x}$ satisfying $\psi_{\mathbf{x}}(\mathbf{x}') = \delta_{\mathbf{x},\mathbf{x}'}$ for all $\mathbf{x}' \in N^h$ and

$$\alpha_{\mathbf{x}}(v) = \Big(\int_{\Gamma_C} v\psi_{\mathbf{x}}\, d\Gamma\Big)\Big(\int_{\Gamma_C}\psi_{\mathbf{x}}\, d\Gamma\Big)^{-1}.$$

The approximation properties of r^h are proved in [51]. We simply recall hereafter the two main results. The first result is concerned with L^2-stability property of r^h.

Lemma 5.3.5. *For any $v \in L^2(\Gamma_C)$ and any $E \in T^h$ we have*

$$\|r^h v\|_{0,E} \lesssim \|v\|_{0,\gamma_E},$$
$$\text{if } |v| \leq s \text{ then } |r^h v| \leq s \text{ on } \Gamma_C,$$

where $\gamma_E = \cup_{\{F \in T^H:\, \bar{F} \cap \bar{E} \neq \emptyset\}} \bar{F}$.

Proof. Let $E \in T^H$ and ψ_1, ψ_2 be the clasical scalar basic functions related to E. Using the definition of $\alpha_{\mathbf{x}}(v)$ and the Cauchy-Schwarz inequality we get:

$$\begin{aligned} \|r^h v\|_{0,E} &\leq \alpha_1 \|\psi_1\|_{0,\Gamma_C} + \alpha_2 \|\psi_2\|_{0,\Gamma_C} \\ &\leq \|v\|_{0,\gamma_E} \frac{\|\psi_1\|^2_{0,\Gamma_C}}{\int_{\Gamma_C} \psi_1 \, d\Gamma} + \|v\|_{0,\gamma_E} \frac{\|\psi_2\|^2_{0,\Gamma_C}}{\int_{\Gamma_C} \psi_2 \, d\Gamma} \\ &\lesssim \|v\|_{0,\gamma_E}. \end{aligned}$$

Using the definition of $\alpha_{\mathbf{x}}(\mathbf{v})$ and the partition of unity we have the second inequality:

$$\begin{aligned} |r^h v| &= |\sum_{\mathbf{x} \in N^H} \alpha_{\mathbf{x}}(v) \psi_{\mathbf{x}}|, \\ &\leq \sum_{\mathbf{x} \in N^H} |\alpha_{\mathbf{x}}(v)| \psi_{\mathbf{x}}, \\ &\leq s. \end{aligned}$$

□

Note that the proof of the first inequality of this lemma is also given in [51] using the additional assumption that the mesh T^h is quasi-uniform. The second result is concerned with the L^2-approximation properties of r^h.

Lemma 5.3.6. *For any $v \in H^\eta(\Gamma_C)$, $0 \leq \eta \leq 1$, and any $E \in T^h$ we have*

$$\|v - r^h v\|_{0,E} \lesssim h^\eta \|v\|_{\eta,\gamma_E}, \tag{5.32}$$

where $\gamma_E = \cup_{\{F \in E_C^H:\, \bar{F} \cap \bar{E} \neq \emptyset\}} \bar{F}$.

Noting that $\lambda_n \leq 0$ on Γ_C (resp. $|\lambda_t| \leq s$ on Γ_C) then $r^h \lambda_n \leq 0$ on Γ_C (resp. $|r^h \lambda_t| \leq s$ on Γ_C) which implies $r^h \lambda_n \in M^h_{N1}$ (resp. $r^h \lambda_t \in M^h_{T1}(s)$). Using the inequality coming from (5.18) we have

$$\begin{aligned} b(\boldsymbol{\lambda}^h - \boldsymbol{\mu}^h, \mathbf{u}^h) &\leq \gamma \int_{\Gamma_c} (\boldsymbol{\lambda}^h - \boldsymbol{\lambda}^H)((\boldsymbol{\mu}^h - \boldsymbol{\lambda}^h) - (\boldsymbol{\mu}^H - \boldsymbol{\lambda}^H)) d\Gamma, \\ &= -\gamma \|\boldsymbol{\lambda}^h - \boldsymbol{\lambda}^H\|^2_{0,\Gamma_C} + \gamma \int_{\Gamma_c} (\boldsymbol{\lambda}^h - \boldsymbol{\lambda}^H)(\boldsymbol{\mu}^h - \boldsymbol{\mu}^H) d\Gamma, \\ &\leq -\frac{\gamma}{2} \|\boldsymbol{\lambda}^h - \boldsymbol{\lambda}^H\|^2_{0,\Gamma_C} + \frac{\gamma}{2} \|\boldsymbol{\mu}^h - \boldsymbol{\mu}^H\|^2_{0,\Gamma_C}. \end{aligned} \tag{5.33}$$

Moreover

$$b(\boldsymbol{\mu}^h - \boldsymbol{\lambda}, \mathbf{u}^h - \mathbf{u}) = b(\mathbf{r}^h(\boldsymbol{\lambda}) - \boldsymbol{\lambda}, \mathbf{u}^h - \mathbf{u}) \leq \|\mathbf{r}^h(\boldsymbol{\lambda}) - \boldsymbol{\lambda}\|_{0,\Gamma_C} \|\mathbf{u}^h - \mathbf{u}\|. \tag{5.34}$$

Then we have

$$\begin{aligned} b(\boldsymbol{\mu}^h-\boldsymbol{\lambda},\mathbf{u}) &= \int_{\Gamma_C}(r^h\lambda_n-\lambda_n)[\![u_n]\!]d\Gamma+\int_{\Gamma_C}(r^h\lambda_t-\lambda_t)[\![u_t]\!]d\Gamma,\\ &\leq \|r^h\lambda_n-\lambda_n\|_{0,\Gamma_C}\|[\![u_n]\!]\|_{0,\Gamma_C}+\|r^h\lambda_t-\lambda_t\|_{0,\Gamma_C}\|[\![u_t]\!]\|_{0,\Gamma_C}d\Gamma,\\ &\leq \|\mathbf{r}^h(\boldsymbol{\lambda})-\boldsymbol{\lambda}\|_{0,\Gamma_C}\|[\![\mathbf{u}]\!]\|_{0,\Gamma_C}. \end{aligned} \tag{5.35}$$

We have $M_{N1}^h\subset M_N$ and $M_{T1}^h\subset M_T$ then

$$b(\boldsymbol{\lambda}-\boldsymbol{\lambda}^h,\mathbf{u})\leq 0. \tag{5.36}$$

Using inequalities (5.33), (5.34), (5.35) and (5.36) we have

$$\begin{aligned} \alpha\|\mathbf{u}^h-\mathbf{u}\|^2+\frac{\gamma}{2}\|\boldsymbol{\lambda}^h-\boldsymbol{\lambda}^H\|_{0,\Gamma_C}^2 \leq\ & M\|\mathbf{u}^h-\mathbf{u}\|\|\mathbf{v}^h-\mathbf{u}\|+\|\boldsymbol{\lambda}^h-\boldsymbol{\lambda}\|_{\mathbf{W}'}\|\mathbf{u}-\mathbf{v}^h\|\\ &+\|\mathbf{r}^h(\boldsymbol{\lambda})-\boldsymbol{\lambda}\|_{0,\Gamma_C}\|\mathbf{u}^h-\mathbf{u}\|+\|\mathbf{r}^h(\boldsymbol{\lambda})-\boldsymbol{\lambda}\|_{0,\Gamma_C}\|[\![\mathbf{u}]\!]\|_{0,\Gamma_C}\\ &+\frac{\gamma}{2}\|\boldsymbol{\mu}^h-\boldsymbol{\mu}^H\|_{0,\Gamma_C}^2. \end{aligned} \tag{5.37}$$

By combining inequalities (5.23) and (5.37) one obtains for all $\bar{\boldsymbol{\mu}}^h\in\mathbf{W}^h$ and $\mathbf{v}^h\in\mathbf{V}^h$

$$\begin{aligned} &(\alpha-8M^2\delta)\|\mathbf{u}-\mathbf{u}^h\|^2+\delta\beta^{*2}\|\boldsymbol{\lambda}-\boldsymbol{\lambda}^H\|_{\mathbf{W}'}^2+(\frac{\gamma}{2}-8\delta)\|\boldsymbol{\lambda}^h-\boldsymbol{\lambda}^H\|_{\mathbf{W}'}^2\\ \leq\ & M\|\mathbf{u}^h-\mathbf{u}\|\|\mathbf{v}^h-\mathbf{u}\|+\|\boldsymbol{\lambda}^h-\boldsymbol{\lambda}\|_{\mathbf{W}'}\|\mathbf{u}-\mathbf{v}^h\|+\|\mathbf{r}^h(\boldsymbol{\lambda})-\boldsymbol{\lambda}\|_{0,\Gamma_C}\|\mathbf{u}^h-\mathbf{u}\|\\ &+\|\mathbf{r}^h(\boldsymbol{\lambda})-\boldsymbol{\lambda}\|_{0,\Gamma_C}\|[\![\mathbf{u}]\!]\|_{0,\Gamma_C}+8\delta\beta^{*2}\|\boldsymbol{\lambda}-\bar{\boldsymbol{\mu}}^H\|_{\mathbf{W}'}^2+8\delta\|\boldsymbol{\lambda}-\bar{\boldsymbol{\mu}}^h\|_{\mathbf{W}'}^2\\ &+8\delta\|\bar{\boldsymbol{\mu}}^h-\bar{\boldsymbol{\mu}}^H\|_{\mathbf{W}'}^2+\frac{\gamma}{2}\|\boldsymbol{\mu}^h-\boldsymbol{\mu}^H\|_{0,\Gamma_C}^2,\\ \leq\ & \frac{\delta}{2}M^2\|\mathbf{u}-\mathbf{u}^h\|^2+\frac{1}{2\delta}\|\mathbf{u}-\mathbf{v}^h\|^2+\frac{\delta}{2}\|\mathbf{u}-\mathbf{u}^h\|^2+\frac{1}{2\delta}\|\mathbf{r}^h(\boldsymbol{\lambda})-\boldsymbol{\lambda}\|_{0,\Gamma_C}^2+\frac{\xi}{2}\|\boldsymbol{\lambda}-\boldsymbol{\lambda}^h\|_{\mathbf{W}'}^2\\ &+\frac{1}{2\xi}\|\mathbf{u}-\mathbf{v}^h\|^2+\|\mathbf{r}^h(\boldsymbol{\lambda})-\boldsymbol{\lambda}\|_{0,\Gamma_C}\|[\![\mathbf{u}]\!]\|_{0,\Gamma_C}+\frac{\gamma}{2}\|\boldsymbol{\mu}^h-\boldsymbol{\mu}^H\|_{0,\Gamma_C}^2\\ &+8\delta\beta^{*2}\|\boldsymbol{\lambda}-\bar{\boldsymbol{\mu}}^H\|_{\mathbf{W}'}^2+8\delta\|\boldsymbol{\lambda}-\bar{\boldsymbol{\mu}}^h\|_{\mathbf{W}'}^2+8\delta\|\bar{\boldsymbol{\mu}}^h-\bar{\boldsymbol{\mu}}^H\|_{\mathbf{W}'}^2. \end{aligned}$$

Then, for all $\bar{\boldsymbol{\mu}}^h\in\mathbf{W}^h$ and $\mathbf{v}^h\in\mathbf{V}^h$, we deduce

$$\begin{aligned} &(\alpha-\delta\frac{17M^2+1}{2})\|\mathbf{u}-\mathbf{u}^h\|^2+(\frac{\gamma}{2}-8\delta-\frac{\xi}{2})\|\boldsymbol{\lambda}^h-\boldsymbol{\lambda}^H\|_{\mathbf{W}'}^2+(\delta\beta^{*2}-\frac{\xi}{2})\|\boldsymbol{\lambda}-\boldsymbol{\lambda}^H\|_{\mathbf{W}'}^2\\ \leq\ & (\frac{1}{2\delta}+\frac{1}{2\xi})\|\mathbf{u}-\mathbf{v}^h\|^2+\frac{1}{2\delta}\|\mathbf{r}^h(\boldsymbol{\lambda})-\boldsymbol{\lambda}\|_{0,\Gamma_C}+\|\mathbf{r}^h(\boldsymbol{\lambda})-\boldsymbol{\lambda}\|_{0,\Gamma_C}\|[\![\mathbf{u}]\!]\|_{0,\Gamma_C}+\frac{\gamma}{2}\|\boldsymbol{\mu}^h-\boldsymbol{\mu}^H\|_{0,\Gamma_C}^2\\ &+8\delta\beta^{*2}\|\boldsymbol{\lambda}-\bar{\boldsymbol{\mu}}^H\|_{\mathbf{W}'}^2+8\delta\|\boldsymbol{\lambda}-\bar{\boldsymbol{\mu}}^h\|_{\mathbf{W}'}^2+8\delta\|\bar{\boldsymbol{\mu}}^h-\bar{\boldsymbol{\mu}}^H\|_{\mathbf{W}'}^2. \end{aligned}$$

Finally, the theorem is established by taking $\delta<\min\big(\frac{2\alpha}{17M^2+1};\frac{\gamma}{16}\big)$, $\xi<\min\big(2\delta\beta^{*2};\gamma-16\delta\big)$, $\mathbf{v}^h=\Pi^h\mathbf{u}$ and $\bar{\boldsymbol{\mu}}^h=P_{\mathbf{W}^h}(\boldsymbol{\lambda})$. □

5.3.3.3 Nonconforming piecewise continuous discretization for multiplier $M_N^h=M_{N1,*}^h$ and $M_T^h=M_{T1,*}^h(s)$

This choice corresponds to "weakly nonpositive" continuous piecewise affine multipliers where $M_N^h=M_{N1,*}^h$ is given by (5.15) and $M_T^h=M_{T1,*}^h(s)$ is given by (5.16).

Theorem 5.3.7. *Let $(\mathbf{u},\boldsymbol{\lambda})$ be the solution to Problem (5.7). Assume that $\mathbf{u}_r \in (H^2(\Omega))^2$ and $\boldsymbol{\lambda} \in (H^{1/2}(\Gamma_C))^2$. Let $(\mathbf{u}^h,\boldsymbol{\lambda}^H)$ be the solution to the discrete problem (5.18) where $M_N^h = M_{N1,*}^h$ and $M_T^h = M_{T1,*}^h(s)$. Then, for any $\eta > 0$ we have*

$$\|\mathbf{u}-\mathbf{u}^h\| + \|\boldsymbol{\lambda}-\boldsymbol{\lambda}^h\|_{\mathbf{W}'} \lesssim h\|\mathbf{u}-\chi\mathbf{u}_s\|_{2,\Omega} + H^{\frac{1}{2}-\frac{\eta}{2}}\big(\|\mathbf{u}\|_{3/2-\eta,\Omega} + \|\boldsymbol{\lambda}\|_{1/2,\Gamma_C}\big).$$

Proof. In (5.22) we choose $\mu^h = P_{\mathbf{W}^h}(\boldsymbol{\lambda}) = (P_{W^h}(\boldsymbol{\lambda}_n), P_{W^h}(\boldsymbol{\lambda}_t))$ where P_{W^h} denotes the $L^2(\Gamma_C)$-projection onto W_1^H. We recall that the operator P_{W^h} is defined for any $v \in L^2(\Gamma_C)$ by

$$P_{W^h}(v) \in W_1^h, \quad \int_{\Gamma_C}(v - P_{W^h}(v))\mu\, d\Gamma = 0, \quad \forall \mu \in W_1^h,$$

and satisfies the following error estimates for any $0 \le r \le 2$ (see [25])

$$H^{-1/2}\|v - P_{W^h}(v)\|_{-1/2,\Gamma_C} + \|v - P_{W^h}(v)\|_{0,\Gamma_C} \le Ch^r\|v\|_{r,\Gamma_C}. \tag{5.38}$$

Clearly, $P_{\mathbf{W}^h}(\boldsymbol{\lambda}) \in \mathbf{M}^h(s)$ and using the inequality comming from (5.18) we have

$$\begin{aligned} b(\boldsymbol{\lambda}^h - \boldsymbol{\mu}^h, \mathbf{u}^h) &\le \gamma\int_{\Gamma_c}(\boldsymbol{\lambda}^h - \boldsymbol{\lambda}^H)((\boldsymbol{\mu}^h - \boldsymbol{\lambda}^h) - (\boldsymbol{\mu}^H - \boldsymbol{\lambda}^H))d\Gamma, \\ &= -\gamma\|\boldsymbol{\lambda}^h - \boldsymbol{\lambda}^H\|^2_{0,\Gamma_C} + \gamma\int_{\Gamma_c}(\boldsymbol{\lambda}^h - \boldsymbol{\lambda}^H)(\boldsymbol{\mu}^h - \boldsymbol{\mu}^H)d\Gamma, \\ &\le -\frac{\gamma}{2}\|\boldsymbol{\lambda}^h - \boldsymbol{\lambda}^H\|^2_{0,\Gamma_C} + \frac{\gamma}{2}\|\boldsymbol{\mu}^h - \boldsymbol{\mu}^H\|^2_{0,\Gamma_C}. \end{aligned} \tag{5.39}$$

Moreover

$$b(\boldsymbol{\mu}^h - \boldsymbol{\lambda}, \mathbf{u}^h - \mathbf{u}) = b(P_{\mathbf{W}^h}(\boldsymbol{\lambda}) - \boldsymbol{\lambda}, \mathbf{u}^h - \mathbf{u}) \le \|P_{\mathbf{W}^h}(\boldsymbol{\lambda}) - \boldsymbol{\lambda}\|_{\mathbf{W}'}\|\mathbf{u}^h - \mathbf{u}\|. \tag{5.40}$$

and

$$\begin{aligned} b(\boldsymbol{\mu}^h - \boldsymbol{\lambda}, \mathbf{u}) &= \int_{\Gamma_C}(P_{W^h}\lambda_n - \lambda_n)[\![u_n]\!]d\Gamma + \int_{\Gamma_C}(P_{W^h}\lambda_t - \lambda_t)[\![u_t]\!]d\Gamma, \\ &= \int_{\Gamma_C}(P_{W^h}\lambda_n - \lambda_n)([\![u_n]\!] - P_{W^h}[\![u_n]\!])d\Gamma \\ &\quad + \int_{\Gamma_C}(P_{W^h}\lambda_t - \lambda_t)([\![u_t]\!] - P_{W^h}[\![u_t]\!])d\Gamma, \\ &\le \|P_{W^h}\lambda_n - \lambda_n\|_{W_N'}\|[\![u_n]\!] - P_{W^h}[\![u_n]\!]\|_{W_N} \\ &\quad + \|P_{W^h}\lambda_t - \lambda_t\|_{W_T'}\|[\![u_t]\!] - P_{W^h}[\![u_t]\!]\|_{W_T}, \\ &\le \|P_{\mathbf{W}^h}(\boldsymbol{\lambda}) - \boldsymbol{\lambda}\|_{\mathbf{W}'}\|[\![\mathbf{u}]\!] - P_{\mathbf{W}^h}([\![\mathbf{u}]\!])\|_{\mathbf{W}}. \end{aligned} \tag{5.41}$$

We have

$$b(\boldsymbol{\lambda} - \boldsymbol{\lambda}^h, \mathbf{u}) = \int_{\Gamma_C}(\lambda_n - \lambda_n^h)[\![u_n]\!]d\Gamma + \int_{\Gamma_C}(\lambda_t - \lambda_t^h)[\![u_t]\!]d\Gamma. \tag{5.42}$$

$$
\begin{aligned}
\int_{\Gamma_C}(\lambda_n-\lambda_n^h)[\![u_n]\!]d\Gamma &= -\int_{\Gamma_C}\lambda_n^h[\![u_n]\!]d\Gamma,\\
&\leq \int_{\Gamma_C}\lambda_n^h(I^h([\![u_n]\!])-[\![u_n]\!])d\Gamma,\\
&\leq \int_{\Gamma_C}(\lambda_n^h-\lambda)(I^h([\![u_n]\!])-[\![u_n]\!])d\Gamma+\int_{\Gamma_C}\lambda(I^h([\![u_n]\!])-[\![u_n]\!])d\Gamma,\\
&\leq \|\lambda_n^h-\lambda_n\|_{W_N'}\|I^h([\![u_n]\!])-[\![u_n]\!]\|_{W_n}\\
&\quad +\|\lambda_n\|_{0,\Gamma_C}\|I^h([\![u_n]\!])-[\![u_n]\!]\|_{0,\Gamma_C}. \qquad (5.43)
\end{aligned}
$$

$$
\begin{aligned}
\int_{\Gamma_C}(\lambda_t-\lambda_t^h)[\![u_t]\!]d\Gamma &= \int_{\Gamma_C}(\lambda_t-\lambda_t^h)([\![u_t]\!]-I^h[\![u_t]\!])d\Gamma+\int_{\Gamma_C}(\lambda_t-\lambda_t^h)I^h[\![u_t]\!]d\Gamma\\
&\quad -\int_{\Gamma_C}\lambda_t[\![u_t]\!]d\Gamma-s\int_{\Gamma_C}|[\![u_t]\!]|d\Gamma,\\
&\leq \int_{\Gamma_C}(\lambda_t-\lambda_t^h)([\![u_t]\!]-I^h([\![u_t]\!]))d\Gamma+\int_{\Gamma_C}\lambda_t(I^h([\![u_t]\!])-[\![u_t]\!])d\Gamma\\
&\quad +s\int_{\Gamma_C}(|I^h([\![u_t]\!])|-|[\![u_t]\!]|)d\Gamma,\\
&\leq \int_{\Gamma_C}(\lambda_t-\lambda_t^h)([\![u_t]\!]-I^h([\![u_t]\!]))d\Gamma+\int_{\Gamma_C}\lambda_t(I^h([\![u_t]\!])-[\![u_t]\!])d\Gamma\\
&\quad +s\int_{\Gamma_C}|I^h([\![u_t]\!])-[\![u_t]\!]|d\Gamma,\\
&\leq \|\lambda_t-\lambda_t^h\|_{W_T'}\|[\![u_t]\!]-I^h([\![u_t]\!])\|_{W_T}\\
&\quad +\|\lambda_t\|_{0,\Gamma_C}\|[\![u_t]\!]-I^h([\![u_t]\!])\|_{0,\Gamma_C}+s\|[\![u_t]\!]-I^h([\![u_t]\!])\|_{0,\Gamma_C}. \qquad (5.44)
\end{aligned}
$$

Using 5.43 and 5.44 we have

$$
\begin{aligned}
b(\boldsymbol{\lambda}-\boldsymbol{\lambda}^h,\mathbf{u}) &\leq \|\boldsymbol{\lambda}-\boldsymbol{\lambda}^h\|_{\mathbf{W}'}\|[\![\mathbf{u}]\!]-I^h[\![\mathbf{u}]\!]\|_{\mathbf{W}}+\|\boldsymbol{\lambda}\|_{0,\Gamma_C}\|[\![\mathbf{u}]\!]-I^h([\![\mathbf{u}]\!])\|_{0,\Gamma_C}\\
&\quad +s\|[\![u_t]\!]-I^h([\![u_t]\!])\|_{0,\Gamma_C}. \qquad (5.45)
\end{aligned}
$$

Using inequalities (5.39), (5.40), (5.41) and (5.45) we have

$$
\begin{aligned}
\alpha\|\mathbf{u}^h-\mathbf{u}\|^2+\gamma\|\boldsymbol{\lambda}^h-\boldsymbol{\lambda}^H\|_{0,\Gamma_C}^2 &\leq M\|\mathbf{u}^h-\mathbf{u}\|\|\mathbf{v}^h-\mathbf{u}\|+\|\boldsymbol{\lambda}^h-\boldsymbol{\lambda}\|_{\mathbf{W}'}\|\mathbf{u}-\mathbf{v}^h\|\\
&\quad +\|P_{\mathbf{W}^h}(\boldsymbol{\lambda})-\boldsymbol{\lambda}\|_{\mathbf{W}'}\|\mathbf{u}^h-\mathbf{u}\|\\
&\quad +\|P_{\mathbf{W}^h}(\boldsymbol{\lambda})-\boldsymbol{\lambda}\|_{\mathbf{W}'}\|[\![\mathbf{u}]\!]-P_{\mathbf{W}^h}([\![\mathbf{u}]\!])\|_{\mathbf{W}}\\
&\quad +\|\boldsymbol{\lambda}-\boldsymbol{\lambda}^h\|_{\mathbf{W}'}\|[\![\mathbf{u}]\!]-I^h[\![\mathbf{u}]\!]\|_{\mathbf{W}}\\
&\quad +\|\boldsymbol{\lambda}\|_{0,\Gamma_C}\|[\![\mathbf{u}]\!]-I^h([\![\mathbf{u}]\!])\|_{0,\Gamma_C}\\
&\quad +s\|[\![u_t]\!]-I^h([\![u_t]\!])\|_{0,\Gamma_C}+\frac{\gamma}{2}\|\boldsymbol{\mu}^h-\boldsymbol{\mu}^H\|_{0,\Gamma_C}^2. \qquad (5.46)
\end{aligned}
$$

By combining inequalities (5.23) and (5.46) one obtain for all $\bar{\boldsymbol{\mu}}^h \in \mathbf{W}^h$ and $\mathbf{v}^h \in \mathbf{V}^h$

$$
\begin{aligned}
& (\alpha - 8M^2\delta)\|\mathbf{u}-\mathbf{u}^h\|^2 + \delta\beta^{*2}\|\boldsymbol{\lambda}-\boldsymbol{\lambda}^H\|^2_{\mathbf{W}'} + (\gamma - 8\delta)\|\boldsymbol{\lambda}^h-\boldsymbol{\lambda}^H\|^2_{\mathbf{W}'} \\
\leq\ & M\|\mathbf{u}^h-\mathbf{u}\|\|\mathbf{v}^h-\mathbf{u}\| + \|\boldsymbol{\lambda}^h-\boldsymbol{\lambda}\|_{\mathbf{W}'}\|\mathbf{u}-\mathbf{v}^h\| + \|P_{\mathbf{W}^h}(\boldsymbol{\lambda})-\boldsymbol{\lambda}\|_{\mathbf{W}'}\|\mathbf{u}^h-\mathbf{u}\| \\
& + \|P_{\mathbf{W}^h}(\boldsymbol{\lambda})-\boldsymbol{\lambda}\|_{\mathbf{W}'}\|[\![\mathbf{u}]\!] - P_{\mathbf{W}^h}([\![\mathbf{u}]\!])\|_{\mathbf{W}} + 8\delta\beta^{*2}\|\boldsymbol{\lambda}-\bar{\boldsymbol{\mu}}^H\|^2_{\mathbf{W}'} \\
& + \|\boldsymbol{\lambda}-\boldsymbol{\lambda}^h\|_{\mathbf{W}'}\|[\![\mathbf{u}]\!] - I^h[\![\mathbf{u}]\!]\|_{\mathbf{W}} + \|\boldsymbol{\lambda}\|_{0,\Gamma_C}\|[\![\mathbf{u}]\!] - I^h([\![\mathbf{u}]\!])\|_{0,\Gamma_C} \\
& + s\|[\![u_t]\!] - I^h([\![u_t]\!])\|_{0,\Gamma_C} + \frac{\gamma}{2}\|\boldsymbol{\mu}^h-\boldsymbol{\mu}^H\|^2_{0,\Gamma_C} + 8\delta\|\boldsymbol{\lambda}-\bar{\boldsymbol{\mu}}^h\|^2_{\mathbf{W}'} + 8\delta\|\bar{\boldsymbol{\mu}}^h-\bar{\boldsymbol{\mu}}^H\|^2_{\mathbf{W}'}, \\
\leq\ & \frac{\delta}{2}M^2\|\mathbf{u}-\mathbf{u}^h\|^2 + \frac{1}{2\delta}\|\mathbf{u}-\mathbf{v}^h\|^2 + \frac{\delta}{2}\|\mathbf{u}-\mathbf{u}^h\|^2 + \frac{1}{2\delta}\|\boldsymbol{\lambda}-P_{\mathbf{W}^h}(\boldsymbol{\lambda})\|^2_{\mathbf{W}'} \\
& + \frac{1}{2\xi}\|\mathbf{u}-\mathbf{v}^h\|^2 + \|P_{\mathbf{W}^h}(\boldsymbol{\lambda})-\boldsymbol{\lambda}\|_{\mathbf{W}'}\|[\![\mathbf{u}]\!] - P_{\mathbf{W}^H}[\![\mathbf{u}]\!]\|_{\mathbf{W}} + \frac{\xi}{2}\|\boldsymbol{\lambda}-\boldsymbol{\lambda}^h\|^2_{\mathbf{W}'} \\
& + 8\delta\beta^{*2}\|\boldsymbol{\lambda}-\bar{\boldsymbol{\mu}}^H\|^2_{\mathbf{W}'} + 8\delta\|\boldsymbol{\lambda}-\bar{\boldsymbol{\mu}}^h\|^2_{\mathbf{W}'} + 8\delta\|\bar{\boldsymbol{\mu}}^h-\bar{\boldsymbol{\mu}}^H\|^2_{\mathbf{W}'}. \\
& + \frac{\xi}{2}\|\boldsymbol{\lambda}-\boldsymbol{\lambda}^h\|^2_{\mathbf{W}'} + \frac{1}{2\xi}\|[\![\mathbf{u}]\!] - I^h[\![\mathbf{u}]\!]\|^2_{\mathbf{W}} + \|\boldsymbol{\lambda}\|_{0,\Gamma_C}\|[\![\mathbf{u}]\!] - I^h([\![\mathbf{u}]\!])\|_{0,\Gamma_C} \\
& + s\|[\![u_t]\!] - I^h([\![u_t]\!])\|_{0,\Gamma_C} + \frac{\gamma}{2}\|\boldsymbol{\mu}^h-\boldsymbol{\mu}^H\|^2_{0,\Gamma_C}.
\end{aligned}
$$

Then, for all $\bar{\boldsymbol{\mu}}^h \in \mathbf{W}^h$ and $\mathbf{v}^h \in \mathbf{V}^h$, we deduces

$$
\begin{aligned}
& (\alpha - \delta\frac{17M^2+1}{2})\|\mathbf{u}-\mathbf{u}^h\|^2 + (\frac{\gamma}{2} - 8\delta - \xi)\|\boldsymbol{\lambda}^h-\boldsymbol{\lambda}^H\|^2_{\mathbf{W}'} + (\delta\beta^{*2} - \xi)\|\boldsymbol{\lambda}-\boldsymbol{\lambda}^H\|^2_{\mathbf{W}'} \\
\leq\ & (\frac{1}{2\delta} + \frac{1}{2\xi})\|\mathbf{u}-\mathbf{v}^h\|^2 + \frac{1}{2\delta}\|P_{\mathbf{W}^h}(\boldsymbol{\lambda})-\boldsymbol{\lambda}\|_{0,\Gamma_C} + \|P_{\mathbf{W}^h}(\boldsymbol{\lambda})-\boldsymbol{\lambda}\|_{\mathbf{W}'}\|[\![\mathbf{u}]\!] - P_{\mathbf{W}^H}[\![\mathbf{u}]\!]\|_{\mathbf{W}} \\
& + \frac{\gamma}{2}\|\boldsymbol{\mu}^h-\boldsymbol{\mu}^H\|^2_{0,\Gamma_C} + 8\delta\beta^{*2}\|\boldsymbol{\lambda}-\bar{\boldsymbol{\mu}}^H\|^2_{\mathbf{W}'} + 8\delta\|\boldsymbol{\lambda}-\bar{\boldsymbol{\mu}}^h\|^2_{\mathbf{W}'} + 8\delta\|\bar{\boldsymbol{\mu}}^h-\bar{\boldsymbol{\mu}}^H\|^2_{\mathbf{W}'} \\
& + \frac{1}{2\xi}\|[\![\mathbf{u}]\!] - I^h[\![\mathbf{u}]\!]\|^2_{\mathbf{W}} + \|\boldsymbol{\lambda}\|_{0,\Gamma_C}\|[\![\mathbf{u}]\!] - I^h([\![\mathbf{u}]\!])\|_{0,\Gamma_C} + s\|[\![u_t]\!] - I^h([\![u_t]\!])\|_{0,\Gamma_C}.
\end{aligned}
$$

Finally, the theorem is established by taking $\delta < \min\big(\frac{2\alpha}{17M^2+1}; \frac{\gamma}{16}\big)$, $\xi < \min\big(\delta\beta^{*2}; \frac{\gamma}{2} - 8\delta\big)$, $\mathbf{v}^h = \mathit{\Pi}^h\mathbf{u}$ and $\bar{\boldsymbol{\mu}}^h = P_{\mathbf{W}^h}(\boldsymbol{\lambda})$. □

Remark: Let us remark that if we suppose that $\mathbf{u} \in (H^2(\Omega))^2$ in Theorem 5.3.7 the proved rate of convergence becomes $h^{3/4}$.

5.4 Numerical experiments

The numerical tests were performed on a uncracked square defined by

$$\bar{\Omega} = [0,1] \times [-0.5, 0.5],$$

and the considered crack is the line segment $\Gamma_C =]0, 0.5[\times \{0\}$ (see Fig. 5.5). Three degrees of freedom are blocked in order to eliminate rigid body motions (Fig. 5.5). In order to have both a contact and non contact, slip and non slip zones between the crack lips, we impose the following body force vector field

$$\mathbf{f}(x,y) = \begin{pmatrix} 0 \\ 3.5x(1-x)y\cos(2\pi x) \end{pmatrix}.$$

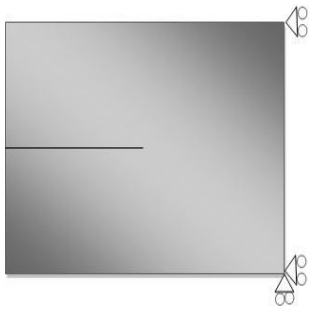

Figure 5.5: Cracked specimen.

Neumann boundary conditions are prescribed as follows:

$$\mathbf{g}(0,y) = \mathbf{g}(1,y) = \begin{pmatrix} 0 \\ 0.4\sin(2\pi y) \end{pmatrix} \qquad -0.5 \leq y \leq 0.5,$$
$$\mathbf{g}(x,-0.5) = \mathbf{g}(x,0.5) = \begin{pmatrix} 0 \\ 0 \end{pmatrix} \qquad 0 \leq x \leq 1.$$

We assume that the slip bound is constant ($s = 0.09$). An example of a non structured mesh used is presented in Fig. 5.6. The numerical tests are performed with GETFEM++, the C++ finite-element library developed by Y. Renard's team (see [52]).

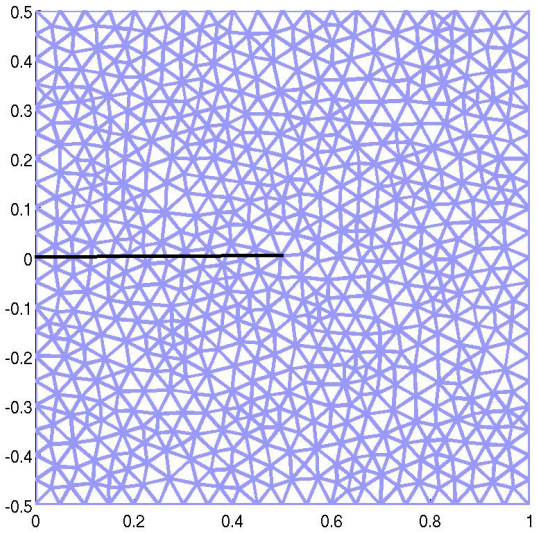

Figure 5.6: Non-structured mesh.

5.4.1 Numerical solution

The algebraic formulation of Problem (5.18) is given as follows

$$\begin{cases} \text{Find } U \in \mathbb{R}^N,\ L_N \in \overline{M}_N^h \text{ and } L_T \in \overline{M}_T^h(s) \text{ such that} \\ KU - B_N^T L_N - B_T^T L_T = F, \\ (\overline{L}_N - L_N)^T (B_N U + D_{N\gamma} L_N) \geq 0, \quad \forall \overline{L_N} \in \overline{M}_N^h, \\ (\overline{L}_T - L_T)^T (B_T U + D_{T\gamma} L_T) \geq 0, \quad \forall \overline{L_T} \in \overline{M}_T^h(s), \end{cases} \tag{5.47}$$

where U is the vector of degrees of freedom (d.o.f.) for $\mathbf{u}^h$, L_N (resp. L_T) is the vector of d.o.f. for the normal multiplier λ_n^h (resp. for the tangant multiplier λ_t^h), $\overline{M}_N^h$ (resp. $\overline{M}_T^h(s)$) is the set of vectors L_N (resp. L_T) such that the corresponding multiplier lies in M_N^h (resp. in $M_T^h(s)$), K is the classical stiffness matrix coming from the term $a(\mathbf{u}^h, \mathbf{v}^h)$, F is the right-hand side corresponding to the Neumann boundary condition and the volume forces, and B_N, B_T, $D_{N\gamma}$, $D_{T\gamma}$ are the matrices corresponding to the terms $b(\lambda_n^h, \mathbf{v}^h)$, $b(\lambda_t^h, \mathbf{v}^h)$, $\gamma \int_{\Gamma_c} (\lambda_n^h - P_{W^H}(\lambda_n^h))(\mu_n^h - \lambda_n^h) d\Gamma$ and $\gamma \int_{\Gamma_c} (\lambda_t^h - P_{W^H}(\lambda_t^h))(\mu_t^h - \lambda_t^h) d\Gamma$, respectively.
The inequalities in (5.47) can be expressed as an equivalent projection

$$L_N = P_{\overline{M}_N^h}(L_N - r(B_N U + D_{N\gamma} L_N)), \tag{5.48}$$

$$L_T = P_{\overline{M}_T^h(s)}(L_T - r(B_T U + D_{T\gamma} L_T)), \tag{5.49}$$

where r is a positive augmentation parameter. This last step transforms the contact conditions into nonlinear equations and we have to solve the following system:

$$\begin{cases} \text{Find } U \in \mathbb{R}^N, L_N \in \overline{M}_N^h \text{ and } L_T \in \overline{M}_T^h \text{ such that} \\ KU - B_N^T L_N - B_T^T L_T - F = 0, \\ -\frac{1}{r}\left[L_N - P_{\overline{M}_N^h}(L_N - r(B_N U + D_{N\gamma} L_N))\right] = 0, \\ -\frac{1}{r}\left[L_T - P_{\overline{M}_T^h(s)}(L_T - r(B_T U + D_{T\gamma} L_T))\right] = 0. \end{cases} \tag{5.50}$$

This allows us to use the semi-smooth Newton method (introduced for contact and friction problems in [53]) to solve Problem (5.50). The term 'semi-smooth' comes from the fact that projections are only piecewise differentiable. Practically, it is one of the most robust algorithms to solve contact problems with or without friction. In order to write a Newton step, one has to compute the derivative of the projection (5.48) and (5.49). An analytical expression can only be obtained when the projection itself is simple to express. This is the case for instance when the set $\mathbf{M}^h(s)$ is chosen such that the contact condition is satisfied on each finite-element node of the contact boundary (such as $\mathbf{M}_0^h(s)$ or $\mathbf{M}_1^h(s)$). In this case, the projection can be expressed component-wise (see [54]).

In order to keep the independence between the mesh and the crack, the approximation space W^h for the multiplier is chosen to be the trace on Γ_C of a Lagrange finite-element method defined on the same mesh as $\mathbf{V}^h$ and its degree will be specified in the following. Let us denote X^h the

space corresponding to the Lagrange finite-element method. The choice of a basis of the trace space $W^h = X^h|_{\Gamma_C}$ is not completely straightforward. Indeed, the traces on Γ_C of the shape functions of X^h may be linearly dependent. A way to overcome this difficulty is to eliminate the redundant functions. Our approach in the presented numerical experiments is as follows. In a first time, we eliminate locally dependent columns of the mass matrix $\int_{\Gamma_C} \psi_i \psi_j d\Gamma$, where ψ_i is the finite-element shape function of X^h, with a block-wise Gram-Schmidt algorithm. In a second time, we detect the potential remaining kernel of the mass matrix with a Lanczos algorithm.

The decomposition into patches is made using a graph partitioner algorithm. In the presented numerical tests we use the free software METIS [79]. The nodes of the graph consist in the elements having an intersection with Γ_C and the edges connect adjacent elements. Additionally, a load corresponding to the size of the intersection is considered on each elements. The partition is a very fast operation.

5.4.2 Numerical tests

In this section, we present numerical tests of the stabilized and non stabilized unilateral contact problems for the following, differently enriched, finite-element methods: P_2/P_1, P_2/P_0, P_1+/P_1, P_1/P_1, P_1/P_0. The notation P_i/P_j (resp. P_1+/P_1) means that the displacement is approximated with a P_i extended finite-element method (resp. a P_1 extended finite-element method with an additional cubic bubble function) and the multiplier with a continuous P_j finite-element method for $j > 0$ (resp. continuous P_1 finite-element method).

The numerical tests were performed on non-structured meshes with $h = 0.108,\ 0.057,\ 0.03,\ 0.016,\ 0.008$ respectively. The reference solution is obtained with a structured P_2/P_1 method and $h = 0.0021$. The Von Mises stress of the reference solution is presented in Fig. 5.7(c). Its distribution shows that the von Mises stress is not singular at the crack lips. The normal and tangent contact stress of the reference solution are presented in Fig. 5.7(a) and Fig. 5.7(b) respectively. The normal and tangent contact stresses are not singular at the crack lips which confirms the theoretical result.

Without stabilization: The curves in the non-stabilized case are given in Fig. 5.8(a) for the error in the $L^2(\Omega)$-norm on the displacement, in Fig. 5.8(b) for the error in the $H^1(\Omega)$-norm on the displacement and in Fig. 5.8(c) for the error in the $L^2(\Gamma_C)$-norm on the contact stress. The P_1/P_1 and P_1/P_0 versions generally work without stabilization even though a uniform inf-sup condition cannot be proven. Fig. 5.8(a) shows that the rate of convergence in the error $L^2(\Omega)$-norm is approximatively of order 2.2 for the P_2/P_j methods and of order 1.6 for the P_1/P_j methods. Note that the singularity due to the transition between contact and non contact is expected to be in $H^{5/2-\eta}(\Omega)$ for any $\eta > 0$. Theoretically, this limits the convergence rate to $3/2 - \eta$ in the $H^1(\Omega)$-norm.

Fig. 5.8(b) shows that the rate of convergence in energy norm is approximatively of order 2 for the P_2/P_j methods and of order 1.2 for the P_1/P_j methods. Fig. 5.8(c) shows that, the rate of convergence in the error $L^2(\Gamma_C)$-norm is optimal for the P_2/P_j methods (of order 1) and not optimal for the remaining couple of elements (approximatively of order 0.3 for the P_1/P_1 and P_1/P_0 methods and approximatively of order 0.7 for the $P_1 + /P_1$ method). It seems that the presence of some spurious modes affects these rates of convergence.

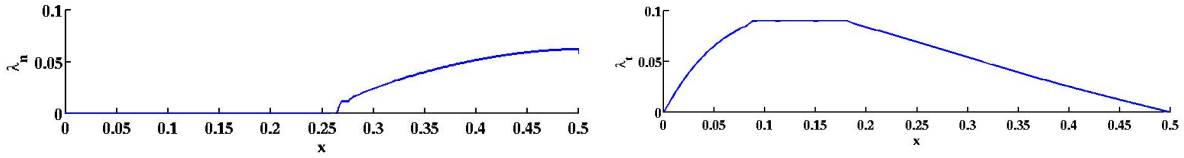

(a) Normal contact stress for the reference solution (b) Tangent contact stress for the reference solution

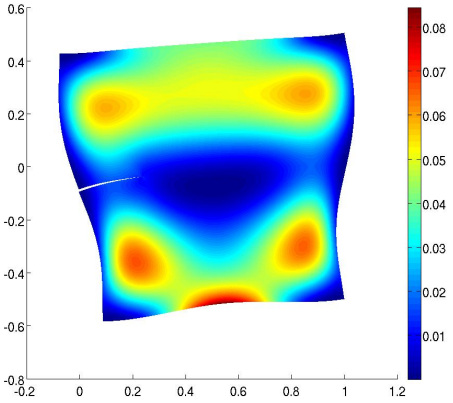

(c) Von Mises stress for the reference solution

Figure 5.7: Von Mises stress and contact stress for the reference solution (Note that the presence of friction in the non-contact zone (i.e. $\lambda_n \neq 0$) is du to the use of Tresca model).

Stabilized method: The curves in the stabilized case are given in Fig. 5.9(a) for the error in the $L^2(\Omega)$-norm on the displacement, in Fig. 5.9(b) for the error in the $H^1(\Omega)$-norm on the displacement and in Fig. 5.9(c) for the error in the $L^2(\Gamma_C)$-norm of the contact stress. Similarly to the non stabilized method, Fig. 5.9(b) shows that we have an optimal rate of convergence, with a slight difference, for the error in the $L^2(\Omega)$-norm and the $H^1(\Omega)$-norm on the displacement. For the error in the $L^2(\Gamma_C)$-norm of the contact stress, Fig. 5.9(c) shows that the local projection stabilization eliminates the spurious modes for the P_1/P_1, P_1/P_0 and $P_1 + /P_1$ methods.
Concerning the error in $L^2(\Gamma_C)$-norm the value of the stabilization parameter can also be divided into two zones (see Fig. 5.10(a), and Fig. 5.10(b)). The first zone is where the error remains almost constant when the stabilization parameter γ increases. The second zone is where the error increases when the stabilization parameter γ increases. Note that for a relatively large mesh size, the local projection stabilization has no influence. Now, concerning the minimal patch size, the

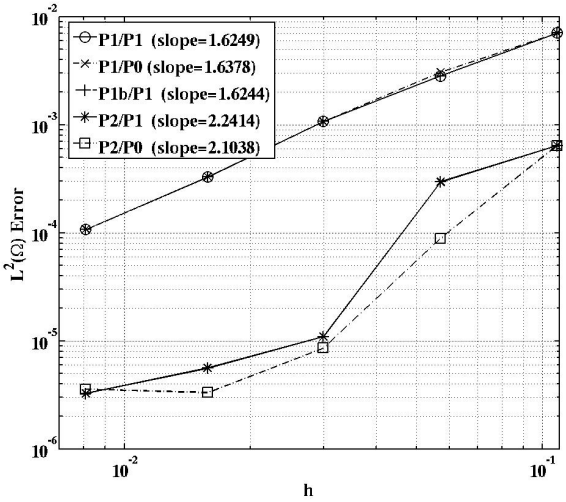

(a) Error in $L^2(\Omega)$-norm of the displacement

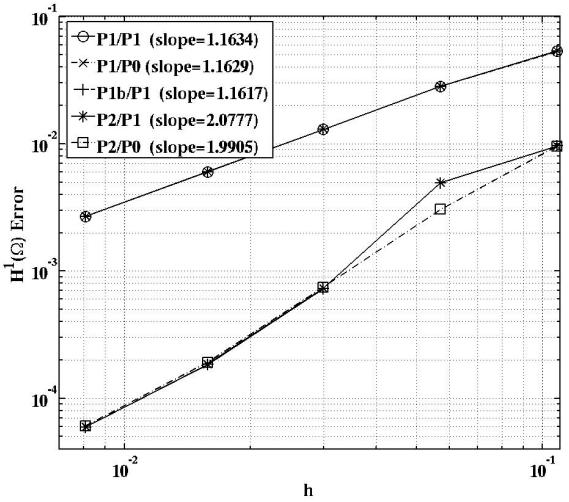

(b) Error in $H^1(\Omega)$-norm of the displacement

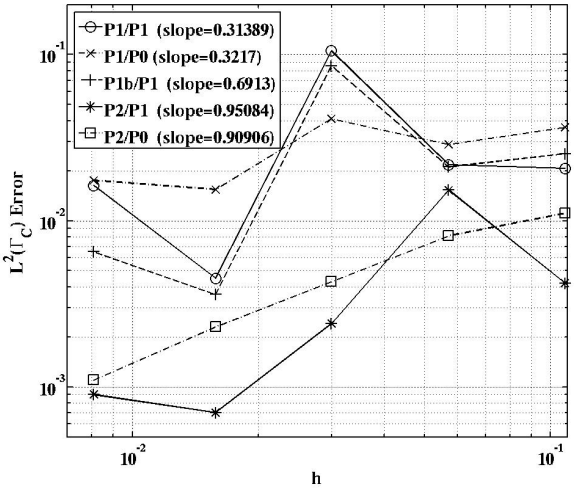

(c) Error in $L^2(\Gamma_C)$-norm of the contact stress

Figure 5.8: Convergence curves in the non stabilized case

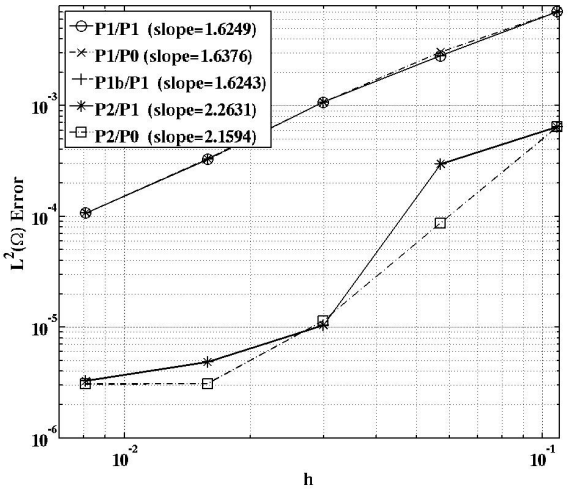

(a) Error in $L^2(\Omega)$-norm of the displacement

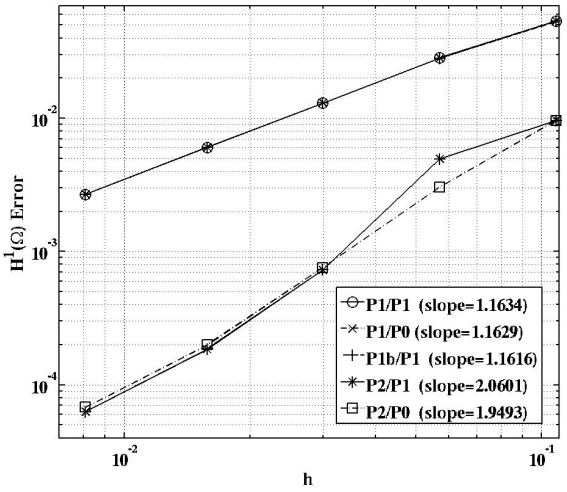

(b) Error in $H^1(\Omega)$-norm of the displacement

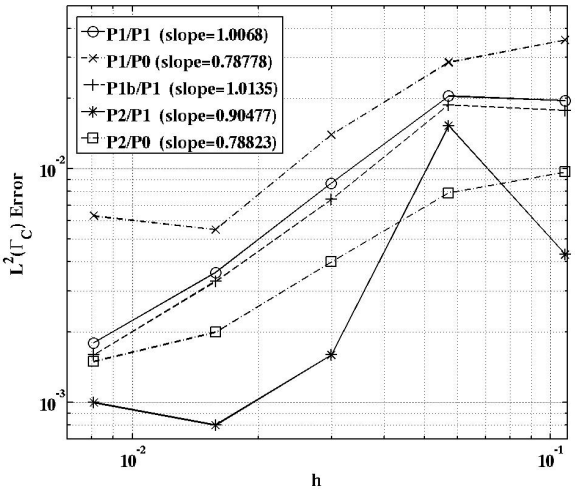

(c) Error in $L^2(\Gamma_C)$-norm of the contact stress

Figure 5.9: Convergence curves in the stabilized case

inf-sup condition is proven to be satisfied in [61] for a size greater or equal to $3h$. Numerically, the inf-sup condition seems to be satisfied for smaller values of the minimal patch size. In our numerical experiments, we found an optimal value between h and $2h$. For this interval of values we have the same result, with a slight difference, as presented in Fig. 5.10(a) and Fig. 5.10(b).

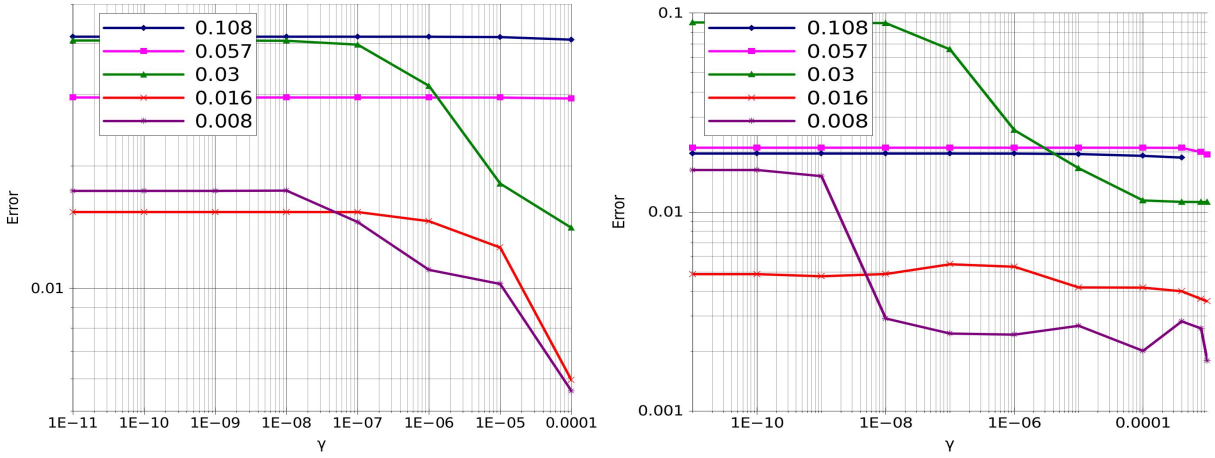

(a) P_1/P_0-elements (b) P_1/P_1-elements

Figure 5.10: Influence of the stabilization parameter in $L^2(\Gamma_C)$-norm of the contact stress

5.5 Conclusion

We adapt the local projection stabilization technique to the nonlinear small strain elastostatics problem with Tresca frictional contact. A main advantage compared to some other stabilization techniques like the Barbosa-Hughes one is that is only affects the multiplier equation in a manner that is independent of the problem to be solved.
We have obtained an existance and uniqueness results for the approximated Tresca frictional contact problem in elasticity. Concerning the three contact conditions we considered theoretically, the given a priori error estimates are obviously sub-optimal. This is probably due to technical reasons.
In the numerical tests we considered, the stabilized methods have indeed an optimal rate of convergence. Similarly to [18], the unstabilized methods have also an optimal rate of convergence concerning the displacement. This may lead to the conclusion that no locking phenomenon was present in the numerical situation we studied despite the non-satisfaction of the discrete inf-sup condition. The fact that such a locking situation may exist or not in the studied framework (contact problem on crack lips for a linear elastic body) is an open question.

General conclusions

In this Ph.D. we gave a mathematical and numerical analysis of convergence and stability of some mixed or hybrid formulations resulting from the numerical solution of some constrained optimization problem with Lagrange multiplier method in the framework of the eXtended Finite Element Method (XFEM). Except the first chapter, each chapter of this thesis is the subject of a published or submitted paper. In Chapter 2 we saw, by using a general technique introduced by Brezzi and Fortin, that the mixed formulation with P_2/P_0 is stable whent the crack cuts the mesh far enough from the vertices. We have given a mathematical result of quasi-optimal error estimate. We have shown numerically that the X-FEM cut-off formulation is stable, regardless of the position of the crack. Similar to the X-FEM with fixed enrichment area, the X-FEM cut-off gives an optimal convergence rate but without a significant additional costs.
The second axis, which present the main content of the thesis, is dedicated to the use of some stabilized Lagrange multiplier methods. The particularity of these stabilized methods is that the stability of the multiplier is provided by adding supplementary terms in the weak formulation. In chapter 3 we studied the Barbosa-Hughes stabilization of the hybrid formulation of frictionless contact problems for cracked elastic bodies in the framework of X-FEM. Theoretically, the given a priori error estimates of the three contact conditions are obviously suboptimal. This limitation of the mathematical analysis is not specific to the approximation of contact problems in the framework of XFEM. It is in fact particularly true for the approximation of the contact condition with Lagrange multiplier. This is probably due to technical reasons. In the numerical tests we considered, the stabilized methods have indeed an optimal rate of convergence and no locking phenomenon was present in the numerical situation we studied despite the non-satisfaction of the discrete inf-sup condition.
In chapter 4, we presented a new consistent method based on local projections for the stabilization of elliptic boundary value problems in the framework of extended finite element method with a fictitious domain approach. A main advantage compared to some other stabilization techniques like the Barbosa-Hughes one is that it only affects the multiplier equation in a manner that is independent of the problem to be solved. This makes the extension to other linear or nonlinear problems very easy. In the contex of this new stabilized method we proved the existence and uniqueness of the stabilised approximated problem. A priori estimates are given. This result does not ensure an optimal rate of convergence when a quadratic finite element is used for the main unknown due to the fact that the local projection is made on piecewise constants. The method could be generalized to the projection on (discontinuous) piecewise affine or piecewise quadratic functions for high order approximations. In chapter 5 we adapt the local projection stabilization technique to the nonlinear small strain elastostatics problem with Tresca frictional contact. We have obtained a result of existence and uniqueness for the approximated Tresca frictional contact problem in elasticity. Concerning the three contact conditions we considered theoretically, the given a priori error estimates are obviously sub-optimal. This is also probably due to technical reasons. In the numerical tests we considered, the stabilized methods have indeed an optimal rate of convergence. The unstabilized methods have also an optimal rate of convergence concerning the displacement. This may lead to the conclusion that no locking

phenomenon was present in the numerical situation we studied despite the non-satisfaction of the discrete inf-sup condition. The fact that such a locking situation may exist or not in the studied framework (contact problem on crack lips for a linear elastic body) is an open question.

Appendix A

Appendix

Appendix A : Singularity of the contact stress

Lemma A.1. *Assume that we have a finite number of transition points between the contact and the non contact zones on the crack lips, then the contact stress σ_n is in $H^{1/2}(\Gamma_C)$.*

Proof. Let $\mathbf{m}$ be a transition point which delimits two zones of nonzero length, a non contact zone ($u_n < 0$) and a zone where the contact is effective ($u_n = 0$). Moussaoui et al. [48] show that the asymptotic displacement near this transition point is no more singular than $r^{3/2}\sin\left(\frac{3}{2}\theta\right)$ where (r, θ) are the polar coordinate relative to $\mathbf{m}$ and the transition point. Consequently, the normal contact stress is not singular near the transition points between the contact and the non contact zones. This analysis, done for the scalar Signorini problem, can be straightforwardly generalized to the Signorini problem for two dimensional elasticity. In order to shorten the proof we present only the analysis for the vicinity of the crack-tip.
We can restrict the study to the case of a contact occurring on a neighborhood of the crack-tip, since $\sigma_n = 0$ if there is no contact at the crack-tip.
Using the div-rot lemma, we rewrite the stress components in terms of an Airy function ϕ as follows:

$$\sigma_{xx} = \frac{\partial^2\phi}{\partial y^2}, \quad \sigma_{yy} = \frac{\partial^2\phi}{\partial x^2}, \quad \sigma_{xy} = \sigma_{yx} = -\frac{\partial^2\phi}{\partial x \partial y}.$$

In two-dimensional isotropic elasticity, the Hooke's law is given by:

$$\begin{aligned} \sigma_{xx} &= (\lambda_{_L} + 2\mu_{_L})\varepsilon_{xx} + \lambda_{_L}\varepsilon_{yy}, \\ \sigma_{yy} &= (\lambda_{_L} + 2\mu_{_L})\varepsilon_{yy} + \lambda_{_L}\varepsilon_{xx}, \\ \sigma_{xy} &= \mu_{_L}(\varepsilon_{xy} + \varepsilon_{yx}) = 2\mu_{_L}\varepsilon_{xy}. \end{aligned}$$

So

$$\begin{aligned} \varepsilon_{xy} &= \varepsilon_{yx} = -\frac{1}{2\mu_{_L}}\frac{\partial^2\phi}{\partial x \partial y}, \\ \varepsilon_{xx} &= \frac{1}{4\mu_{_L}(\lambda_{_L} + \mu_{_L})}\left((\lambda_{_L} + 2\mu_{_L})\frac{\partial^2\phi}{\partial y^2} - \lambda\frac{\partial^2\phi}{\partial x^2}\right), \\ \varepsilon_{yy} &= -\frac{1}{4\mu(\lambda_{_L} + \mu_{_L})}\left(\lambda_{_L}\frac{\partial^2\phi}{\partial y^2} - (\lambda_{_L} + 2\mu_{_L})\frac{\partial^2\phi}{\partial x^2}\right). \end{aligned}$$

The compatibility relations

$$\frac{\partial^2\varepsilon_{xx}}{\partial y^2} + \frac{\partial^2\varepsilon_{yy}}{\partial x^2} - 2\frac{\partial^2\varepsilon_{xy}}{\partial x \partial y} = 0,$$

lead to the bi-harmonic equation:

$$\frac{\lambda_L + 2\mu_L}{4\mu_L(\lambda_L + \mu_L)}\left[\frac{\partial^4\phi}{\partial x^4} + \frac{\partial^4\phi}{\partial y^4} + 2\frac{\partial^4\phi}{\partial x^2\partial y^2}\right] = 0 \quad \Longleftrightarrow \quad \Delta^2\phi = 0,$$

whose general solution in polar coordinates is a linear combination of the following elementary functions:

$$r^{s+1}\cos(s-1)\theta, \quad r^{s+1}\cos(s+1)\theta, \quad r^{s+1}\sin(s-1)\theta, \quad r^{s+1}\sin(s+1)\theta.$$

Let σ_{rr}, $\sigma_{\theta\theta}$ and $\sigma_{r\theta}$ be the polar stress components. By using $\mathbf{e}_r = (\cos\theta, \sin\theta)$, $\mathbf{e}_\theta = (-\sin\theta, \cos\theta)$ and the fact that $(\mathbf{e}_r, \mathbf{e}_\theta, \mathbf{k})$ is direct and $\nabla\phi \wedge \mathbf{k}$ is independent of x, y, we obtain

$$\sigma_{rr} = \frac{1}{r^2}\frac{\partial^2\phi}{\partial\theta^2} + \frac{1}{r}\frac{\partial\phi}{\partial r}, \quad \sigma_{\theta\theta} = \frac{\partial^2\phi}{\partial r^2}, \quad \sigma_{r\theta} = \frac{1}{r^2}\frac{\partial\phi}{\partial\theta} - \frac{1}{r}\frac{\partial^2\phi}{\partial\theta\partial r}.$$

Besides, we have

$$\begin{aligned}
\sigma_{xx} &= (\lambda_L + 2\mu_L)\frac{\partial u_x}{\partial x} + \lambda_L\frac{\partial u_y}{\partial y}, \\
\sigma_{yy} &= (\lambda_L + 2\mu_L)\frac{\partial u_y}{\partial y} + \lambda_L\frac{\partial u_x}{\partial x}, \\
\sigma_{xy} &= \mu_L(\varepsilon_{xy} + \varepsilon_{yx}) = \mu_L\left(\frac{\partial u_x}{\partial y} + \frac{\partial u_y}{\partial x}\right),
\end{aligned}$$

and $\nabla\mathbf{u} = \left(\frac{\partial u_r}{\partial r}\mathbf{e}_r + \frac{\partial u_\theta}{\partial r}\mathbf{e}_\theta\right) \otimes \mathbf{e}_r + \left(\frac{1}{r}\frac{\partial u_r}{\partial\theta}\mathbf{e}_r + \frac{1}{r}u_r\mathbf{e}_\theta - \frac{1}{r}u_\theta\mathbf{e}_r + \frac{1}{r}\frac{\partial u_\theta}{\partial\theta}\mathbf{e}_\theta\right) \otimes \mathbf{e}_\theta$ where u_r and u_θ are the radial and angular components of the displacement. So in polar coordinates, it becomes

$$\begin{aligned}
\sigma_{rr} &= (\lambda_L + 2\mu_L)\frac{\partial u_r}{\partial r} + \frac{\lambda_L}{r}\left(u_r + \frac{\partial u_\theta}{\partial\theta}\right), \\
\sigma_{\theta\theta} &= \frac{(\lambda_L + 2\mu_L)}{r}\left(u_r + \frac{\partial u_\theta}{\partial\theta}\right) + \lambda_L\frac{\partial u_r}{\partial r}, \\
\sigma_{r\theta} &= \mu_L\left(\frac{\partial u_\theta}{\partial r} + \frac{1}{r}\frac{\partial u_r}{\partial\theta} - \frac{1}{r}u_\theta\right).
\end{aligned}$$

Consequently,

$$\begin{aligned}
\frac{1}{r^2}\frac{\partial^2\phi}{\partial\theta^2} + \frac{1}{r}\frac{\partial\phi}{\partial r} &= (\lambda_L + 2\mu_L)\frac{\partial u_r}{\partial r} + \frac{\lambda_L}{r}\left(u_r + \frac{\partial u_\theta}{\partial\theta}\right), \\
\frac{\partial^2\phi}{\partial r^2} &= \frac{(\lambda_L + 2\mu_L)}{r}\left(u_r + \frac{\partial u_\theta}{\partial\theta}\right) + \lambda_L\frac{\partial u_r}{\partial r}, \\
\frac{1}{r^2}\frac{\partial\phi}{\partial\theta} - \frac{1}{r}\frac{\partial^2\phi}{\partial\theta\partial r} &= \mu_L\left(\frac{\partial u_\theta}{\partial r} + \frac{1}{r}\frac{\partial u_r}{\partial\theta} - \frac{1}{r}u_\theta\right).
\end{aligned}$$

In [49], Grisvard gives the corresponding displacement in polar coordinates with $\rho = 1 + \frac{2\mu_L}{\lambda_L + \mu_L}$:

$$\begin{aligned}
u_r &= r^s(a\sin(s+1)\theta + b\cos(s+1)\theta + c(\rho - s)\sin(s-1)\theta - d(\rho - s)\cos(s-1)\theta), \\
u_\theta &= r^s(a\cos(s+1)\theta - b\sin(s+1)\theta - c(\rho + s)\cos(s-1)\theta - d(\rho + s)\sin(s-1)\theta),
\end{aligned} \tag{A.1}$$

where a, b, c, d are generic constants. The P_1 finite-element method will not optimally approximate the terms of this form which are not in $H^2(\Omega)$. So we have to determine the terms for which the real part of s is such that $0 < Re(s) < 1$.
The boundary conditions for the effective contact without friction on the crack with $\theta = \pi$ can be expressed as:

$$\begin{aligned} u_\theta(r,\pi) - u_\theta(r,-\pi) &= 0, \\ \sigma_{\theta\theta}(r,\pi) - \sigma_{\theta\theta}(r,-\pi) &= 0, \\ \sigma_{r\theta}(r,\pi) = \sigma_{r\theta}(r,-\pi) &= 0. \end{aligned}$$

The first equality expresses the contact condition: the jump of the normal displacement is equal to zero because we are not in the opening mode, the second equation represents the action-reaction law and the last equality expresses the absence of friction.
By using (A.1), these conditions read as:

$$\begin{aligned} u_\theta(r,\pi) - u_\theta(r,-\pi) &= 2r^s(-b\sin(s+1)\pi - d(\rho+s)\sin(s-1)\pi) \\ &= 2r^s(b\sin(s\pi) + d(\rho+s)\sin(s\pi)), \\ \sigma_{r\theta}(r,\pi) &= \mu_{_L} r^{s-1}(2as\cos(s+1)\pi - 2bs\sin(s+1)\pi - 2cs^2\cos(s-1)\pi \\ &\quad -2ds^2\sin(s-1)\pi) \\ &= 2\mu_{_L} r^{s-1}(-as\cos(s\pi) + bs\sin(s\pi) + cs^2\cos(s\pi) + ds^2\sin(s\pi)), \\ \sigma_{r\theta}(r,-\pi) &= 2\mu_{_L} r^{s-1}(-as\cos(s\pi) - bs\sin(s\pi) + cs^2\cos(s\pi) - ds^2\sin(s\pi)), \\ \sigma_{\theta\theta}(r,\pi) - \sigma_{\theta\theta}(r,-\pi) &= r^{s-1}(\lambda_{_L}(2as\sin(s+1)\pi + 2c(\rho-s)s\sin(s-1)\pi) \\ &\quad +(\lambda_{_L}+2\mu_{_L})(-2as\sin(s+1)\pi + 2cs(\rho+s-2)\sin(s-1)\pi)) \\ &= r^{s-1}(4\mu_{_L} as\sin(s\pi) - 4cs\mu_{_L}(s+1)\sin(s\pi)). \end{aligned}$$

The determinant of the corresponding linear system can be written as:

$$\begin{aligned} D &= 32\mu_{_L}^3 s^3 r^{4s-3}\sin^2(s\pi)\begin{vmatrix} 0 & 1 & -\cos(s\pi) & -\cos(s\pi) \\ 1 & 0 & \sin(s\pi) & -\sin(s\pi) \\ 0 & -s-1 & (s-1)\cos(s\pi) & (s-1)\cos(s\pi) \\ \rho+s & 0 & (s-1)\sin(s\pi) & -(s-1)\sin(s\pi) \end{vmatrix} \\ &= 128\mu_{_L}^3 s^3 r^{4s-3}(\rho+1)\sin^3(\pi s)\cos(s\pi). \end{aligned}$$

So $D = 0$ reduces to $\sin^3(\pi s)\cos(s\pi) = 0$ and the only solution satisfying $0 < Re(s) < 1$ is $s = \dfrac{1}{2}$.
For $s = \dfrac{1}{2}$, we obtain:

$$a = \frac{3c}{2}, b = 0, d = 0$$

which means that only one singular mode is present. For this singular mode we have also: $\sigma_{\theta\theta}(r,\pi) = \sigma_{\theta\theta}(r,-\pi) = 0$. This property corresponds to the classical Neumann boundary condition on the crack lips. The consequence is there is no supplementary singular mode to the classical shear mode and the normal stress component is not singular on the crack lips.

Appendix B

Appendix

Appendix B : Proof of Lemma 3.3.2

In order to prove Lemma 3.3.2, we distinguish three cases: totally enriched triangles, partial enriched triangles and the triangle containing the crack tip.

First, for a totally enriched triangle (Fig. 3.4(a)) we have $\Pi^h \mathbf{u}_r|_{T\cap\Omega_i} = I^h \widetilde{\mathbf{u}}_r^i|_{T\cap\Omega_i}$ (see Lemma 3.3.1). Then, $E_T^i \mathbf{u}_r = I^h \widetilde{\mathbf{u}}_r^i$ and we have

$$\begin{aligned} \|\widetilde{\mathbf{u}}_r^i - E_T^i \mathbf{u}_r\|_{0,T} &= \|\widetilde{\mathbf{u}}_r^i - I^h \widetilde{\mathbf{u}}_r^i\|_{0,T}, \\ &\lesssim h^2 \|\widetilde{\mathbf{u}}_r^i\|_{2,T}, \\ \|\widetilde{\mathbf{u}}_r^i - E_T^i \mathbf{u}_r\|_{1,T} &\lesssim h \|\widetilde{\mathbf{u}}_r^i\|_{2,T}. \end{aligned}$$

Second, for a partially enriched triangle and considering the particular case shown in Fig. 3.4(b) we have:

$$\begin{aligned} \Pi^h \mathbf{u}_r|_{T\cap\Omega_1} &= \mathbf{u}_r^1(\mathbf{x}_1)\varphi_1 + \mathbf{u}_r^2(\mathbf{x}_2)\varphi_2 + \mathbf{u}_r^1(\mathbf{x}_3)\varphi_3, \\ &= \Pi^h \widetilde{\mathbf{u}}_r^1 + (\widetilde{\mathbf{u}}_r^1(\mathbf{x}_2) - \mathbf{u}_r^2(\mathbf{x}_2))\varphi_2, \\ \Pi^h \mathbf{u}_r|_{T\cap\Omega_2} &= \mathbf{u}_r^1(\mathbf{x}_1)\varphi_1 + \mathbf{u}_r^2(\mathbf{x}_2)\varphi_2 + \widetilde{\mathbf{u}}_r^2(\mathbf{x}_3)\varphi_3, \\ &= \Pi^h \widetilde{\mathbf{u}}_r^2 + (\widetilde{\mathbf{u}}_r^2(\mathbf{x}_1) - \mathbf{u}_r^1(\mathbf{x}_1))\varphi_1. \end{aligned}$$

In this case $E_T^1 \mathbf{u}_r = \Pi^h \widetilde{\mathbf{u}}_r^1 + (\widetilde{\mathbf{u}}_r^1(\mathbf{x}_2) - \mathbf{u}_r^2(\mathbf{x}_2))\varphi_2$ and $E_T^2 \mathbf{u}_r = \Pi^h \widetilde{\mathbf{u}}_r^2 + (\widetilde{\mathbf{u}}_r^2(\mathbf{x}_1) - \mathbf{u}_r^1(\mathbf{x}_1))\varphi_1$. Then we have:

$$\begin{aligned} \|\widetilde{\mathbf{u}}_r^1 - E_T^1 \mathbf{u}_r\|_{0,T} &= \|\widetilde{\mathbf{u}}_r^i - \Pi^h \widetilde{\mathbf{u}}_r^1 - (\widetilde{\mathbf{u}}_r^1(\mathbf{x}_2) - \mathbf{u}_r^2(\mathbf{x}_2))\varphi_2\|_{0,T}, \\ &\lesssim \|\widetilde{\mathbf{u}}_r^1 - \Pi^h \widetilde{\mathbf{u}}_r^1\|_{0,T} + \mid \widetilde{\mathbf{u}}_r^1(\mathbf{x}_2) - \mathbf{u}_r^2(\mathbf{x}_2) \mid \|\varphi_2\|_{0,T}, \\ \|\widetilde{\mathbf{u}}_r^1 - E_T^1 \mathbf{u}_r\|_{1,T} &\lesssim \|\widetilde{\mathbf{u}}_r^1 - \Pi^h \widetilde{\mathbf{u}}_r^1\|_{1,T} + \mid \widetilde{\mathbf{u}}_r^1(\mathbf{x}_2) - \mathbf{u}_r^2(\mathbf{x}_2) \mid . \end{aligned}$$

Furthermore, we have from [17]:

$$\mid \widetilde{\mathbf{u}}_r^1(\mathbf{x}_2) - \mathbf{u}_r^2(\mathbf{x}_2) \mid \lesssim h_T \mid \widetilde{\mathbf{u}}_r^1 - \widetilde{\mathbf{u}}_r^2 \mid_{2,B(\mathbf{x}^*,h_T)},$$

and since $\|\varphi_2\|_{0,T} \lesssim h$ we can conclude that:

$$\begin{aligned} \|\widetilde{\mathbf{u}}_r^1 - E_T^1 \mathbf{u}_r\|_{0,T} &\lesssim h_T^2 \Big(\|\widetilde{\mathbf{u}}_r^1\|_{2,T} + \mid \widetilde{\mathbf{u}}_r^1 - \widetilde{\mathbf{u}}_r^2 \mid_{2,B(\mathbf{x}^*,h_T)} \Big), \\ \|\widetilde{\mathbf{u}}_r^1 - E_T^1 \mathbf{u}_r\|_{1,T} &\lesssim h_T \Big(\|\widetilde{\mathbf{u}}_r^1\|_{2,T} + \mid \widetilde{\mathbf{u}}_r^1 - \widetilde{\mathbf{u}}_r^2 \mid_{2,B(\mathbf{x}^*,h_T)} \Big). \end{aligned}$$

In the same way we have:

$$\begin{aligned}\|\widetilde{\mathbf{u}}_r^2 - E_T^2\mathbf{u}_r\|_{0,T} &\lesssim h_T^2\Big(\|\widetilde{\mathbf{u}}_r^2\|_{2,T} + \mid \widetilde{\mathbf{u}}_r^1 - \widetilde{\mathbf{u}}_r^2 \mid_{2,B(\mathbf{x}^*,h_T)}\Big),\\ \|\widetilde{\mathbf{u}}_r^2 - E_T^2\mathbf{u}_r\|_{1,T} &\lesssim h_T\Big(\|\widetilde{\mathbf{u}}_r^2\|_{2,T} + \mid \widetilde{\mathbf{u}}_r^1 - \widetilde{\mathbf{u}}_r^2 \mid_{2,B(\mathbf{x}^*,h_T)}\Big).\end{aligned}$$

A similar reasoning can be applied to the other situations of partially enriched triangles to obtain the same result.
Finally, for the triangle containing the crack tip, and in the particular case described in Fig. 3.4(c) we have:

$$\begin{aligned}\Pi^h\mathbf{u}_r|_{T\cap\Omega_1} &= \mathbf{u}_r^1(\mathbf{x}_1)\varphi_1 + \mathbf{u}_r^2(\mathbf{x}_2)\varphi_2 + \mathbf{u}_r^2(\mathbf{x}_3)\varphi_3,\\ &= \Pi^h\widetilde{\mathbf{u}}_r^1 + (\mathbf{u}_r^2(\mathbf{x}_2) - \widetilde{\mathbf{u}}_r^1(\mathbf{x}_2))\varphi_2 + (\mathbf{u}_r^2(\mathbf{x}_3) - \widetilde{\mathbf{u}}_r^1(\mathbf{x}_3))\varphi_3,\\ \Pi^h\mathbf{u}_r|_{T\cap\Omega_2} &= \mathbf{u}_r^1(\mathbf{x}_1)\varphi_1 + \mathbf{u}_r^2(\mathbf{x}_2)\varphi_2 + \mathbf{u}_r^2(\mathbf{x}_3)\varphi_3,\\ &= \Pi^h\widetilde{\mathbf{u}}_r^2 + (\mathbf{u}_r^1(\mathbf{x}_1) - \widetilde{\mathbf{u}}_r^2(\mathbf{x}_1))\varphi_1.\end{aligned}$$

Thus, we have $E_T^1\mathbf{u}_r = \Pi^h\widetilde{\mathbf{u}}_r^1 + (\mathbf{u}_r^2(\mathbf{x}_2) - \widetilde{\mathbf{u}}_r^1(\mathbf{x}_2))\varphi_2 + (\mathbf{u}_r^2(\mathbf{x}_3) - \widetilde{\mathbf{u}}_r^1(\mathbf{x}_3))\varphi_3$ and $E_T^2\mathbf{u}_r = \Pi^h\widetilde{\mathbf{u}}_r^2 + (\mathbf{u}_r^1(\mathbf{x}_1) - \widetilde{\mathbf{u}}_r^2(\mathbf{x}_1))\varphi_1$. Note that we have (see [17]):

$$\mid \mathbf{u}_r^i(\mathbf{x}_j) - \widetilde{\mathbf{u}}_r^l(\mathbf{x}_j) \mid \lesssim h_T \mid \widetilde{\mathbf{u}}_r^1 - \widetilde{\mathbf{u}}_r^2 \mid_{2,B(\mathbf{x}^*,h_T)},$$

with $j \in \{1,2,3\}$, $i \in \{1,2\}$, $l = 3-i$ and $\mathbf{x}_j$ a node belonging to a partially enriched triangle or triangle containing the crack tip. Then, by the same way in the case of partially enriched triangle we have the following result for $i \in \{1,2\}$:

$$\begin{aligned}\|\widetilde{\mathbf{u}}_r^1 - E_T^i\mathbf{u}_r\|_{0,T} &\lesssim h_T^2\Big(\|\widetilde{\mathbf{u}}_r^i\|_{2,T} + \mid \widetilde{\mathbf{u}}_r^1 - \widetilde{\mathbf{u}}_r^2 \mid_{2,B(\mathbf{x}^*,h_T)}\Big),\\ \|\widetilde{\mathbf{u}}_r^2 - E_T^i\mathbf{u}_r\|_{1,T} &\lesssim h_T\Big(\|\widetilde{\mathbf{u}}_r^i\|_{2,T} + \mid \widetilde{\mathbf{u}}_r^1 - \widetilde{\mathbf{u}}_r^2 \mid_{2,B(\mathbf{x}^*,h_T)}\Big).\end{aligned}$$

This concludes the proof, since a similar reasoning can be applied to the other situations of a triangle containing the crack tip. □

Appendix C

Appendix

Appendix C : Proof of the Inf-sup condition

Lemma A.2. *Assume that the length of segment of S^H is not less than $3h$. Then, there exists a constant $\beta^* > 0$, independent of h and H, such that*

$$\forall \mu^H \in (W^H)', \qquad \sup_{v^h \in V^h} \frac{b(v^h, \mu^h)}{\|v^h\|_V} \geq \beta^* \|\mu^H\|_{W'}. \tag{C.1}$$

with $b(v^h, \mu^h) = \langle \mu^h, [\![v^h]\!] \rangle_{W',W}$

Proof. In order to proof this condition we use a general technique introduced by Brezzi and Fortin in their book [1]. This technique can be summarized in the following proposition:

Proposition 7 ([1]). *Suppose that*

$$\forall\, \mu \in W', \qquad \sup_{v \in V} \frac{b(v, \mu)}{\| v \|_V} \geq \beta \, \|\mu\|_{W'}, \tag{C.2}$$

and assume that there exists a family of uniformly continuous operators Π_h from V into V^h satisfying:

$$b(\Pi_h w - w, \mu^h) = 0, \qquad \forall \mu^h \in (W^h)', \tag{C.3a}$$

$$\| \Pi_h v \|_V \leqslant c \, \| v \|_v, \tag{C.3b}$$

with c independent of h. Then we have

$$\forall\, \mu^h \in (W^h)', \qquad \sup_{v^h \in V^h} \frac{b(v^h, \mu^h)}{\| v^h \|_{V^h}} \geq k_0 \, \|\mu^h\|_{W'}, \tag{C.4}$$

with $k_0 = \dfrac{\beta}{c}$.

In our case the inf-sup condition (C.2) is true. Indeed, in the rest of this chapter, we proof the LBB condition relying on Proposition 7.

We have the length of each segment of S^H is not less than $4h$, then similarly to [61] we can find a node a_S such that the macro-element Δ_S consisting of the six triangles of $\mathcal{T}^h$ with common vertex a_S satisfies the following properties:

- S intersects at least one interior segment of Δ_S at a distance from a_S that is no larger then half the length of this segment.

- The end point of S do not belong to the interior of Δ_S.
- If S and $S^{'}$ are any two segments of S^H, $\Delta_S \bigcap \Delta_{S'}$ is either empty or reduced to a node or a segment of $\mathcal{T}^h$, in the other worlds, the macro-elements related to S^H do not overlap.

Let Π_1 the H_1-stable interpolation operator of V_h defined in Chapter 2. Then for any $v \in H^1(\Omega)$, we propose the following restriction $\Pi_h v$:

$$\Pi_h v = \Pi_1 v + \sum_{S \in S^H} C_S \mathcal{H} \varphi_{a_S}, \tag{C.5}$$

where φ_{a_S} denotes the basis function of V^h, with support Δ_S, that take the value 1 at the node a_S and 0 at all other nodes of $\mathcal{T}^h$, $\mathcal{H}$ is the Heaviside function and each constant C_S is chosen such that

$$\int_S [\![\Pi_h v]\!] d\Gamma = \int_S [\![hv]\!] d\Gamma. \tag{C.6}$$

It remains to show that such constant C_S exist and to establish the stability inequality C.3a. Using the definition of $\Pi_h v$ we have

$$\int_S [\![\Pi_1 v]\!] - [\![v]\!] d\Gamma + \sum_{k \in S^H} C_k \int_S \varphi_{a_k} d\Gamma = 0.$$

Using the properties of Δ_S we have

$$C_S = -\frac{1}{\int_S \varphi_{a_S} d\Gamma} \int_S [\![\Pi_1 v]\!] - [\![v]\!] d\Gamma. \tag{C.7}$$

To derive an upper bound for the numerator of C.7, we require the next two lemmas.

Lemma A.3. *[61] Let $\widehat{T}$ denote the reference unit triangle and let $\widehat{l}$ be any straight line segment that intersects $\widehat{T}$. Then, there exist a constant $\widehat{C}$, independent of $\widehat{l}$ such that*

$$\forall \widehat{w} \in H^1(\widehat{T}), \qquad \|\widehat{w}\|_{0,\widehat{l}} \leq \widehat{C} \|\widehat{w}\|_{1,\widehat{l}} \tag{C.8}$$

Lemma A.4. *[61] Let l be a straight line segment that intersects a non degenerate triangle T and let $\widehat{l}$ be its image on the reference unit triangle $\widehat{T}$ by the affine transformation that maps $\widehat{T}$ onto T. Let J_T denote the Jacobian matrix of this transformation and let $\|\det(J_T)\|$ be its Euclidean norm. Then,*

$$\frac{|l|}{|\widehat{l}|} \leq \|J_T\| \tag{C.9}$$

Using this two last lemma we can prove

Lemma A.5. *[61] We always have:*

$$\int_S \varphi_{a_S} d\Gamma \geq \frac{1}{4\sqrt{2}} h. \tag{C.10}$$

Now let us show that the operator $\Pi_h v$ defined by C.5 satisfies the stability estimate C.3b with a constant C independent of h and H. For any $v \in H^1(\Omega)$, we have

$$\|\Pi_h v\|_{1,\Omega} \leq \|\Pi_1 v\|_{1,\Omega} + \|\sum_{S\in S^H} C_S \mathcal{H}\varphi_{a_S}\|_{1,\Omega},$$

As each φ_{a_S} has support Δ_S and these supports are all disjoint, we have

$$\|\sum_{S\in S^H} C_S \mathcal{H}\varphi_{a_S}\|_{1,\Omega} \leq \Big(\sum_{S\in S^H} |C_S|^2 \|\varphi_{a_S}\|^2_{1,\Delta_S}\Big)^{1/2}$$

we can see easy as in [61] that there exist a constant $\widehat{C}_3$ independent of h and H such that

$$\|\varphi_{a_S}\|_{1,\Delta_S} \leq \widehat{C}_3. \tag{C.11}$$

Next let us find a bound for C_S. Let l_i denote the straight line segments of S and T_i the element of $\mathcal{T}^h$ intersected by l_i. We denote by E^1 (resp. E^2) the continuous extension of $\Pi_1 v_{|\Omega_1}$ (resp. $\Pi_1 v_{|\Omega_2}$) defined by:

$$\begin{cases} E^1 v = \sum_{j\in I\setminus I_H} \boldsymbol{\alpha}_j \varphi_j + \sum_{j\in I_H} \boldsymbol{\beta}_j \varphi_j & \text{in } \Omega_1, \\ E^2 v = \sum_{j\in I\setminus I_H} \boldsymbol{\alpha}_j \varphi_j + \sum_{j\in I_H} \boldsymbol{\gamma}_i \varphi_j H_2 & \text{in } \Omega_2, \end{cases}$$

with

$$\begin{aligned} \boldsymbol{\alpha}_i \quad &= \tfrac{1}{|\Delta_i|}\int_{\Delta_i} \tilde{\mathbf{u}}^k \mathrm{d}x \ \text{ if } \mathbf{x}_\mathrm{i} \in \Omega_\mathrm{k}, \quad \boldsymbol{\beta}_\mathrm{i} = \tfrac{1}{|\Delta_\mathrm{i}|}\int_{\Delta_\mathrm{i}} \tilde{\mathbf{u}}^1 \mathrm{dx}, \\ \boldsymbol{\gamma}_i \quad &= \tfrac{1}{|\Delta_i|}\int_{\Delta_i} \tilde{\mathbf{u}}^2 \mathrm{d}x, \ S_j := \bigcup\{S \in \tau_h : \mathrm{supp}(\varphi_j) \cap S \neq \emptyset\}, \end{aligned}$$

where Δ_j is the maximal ball centered at x_j such that $\Delta_j \subset S_j$ and $\{\mathbf{x}_j\}_{j=1}^J$ are the interior nodes of mesh τ_h.
From C.7 and C.10, we have for all $S \in S^H$

$$\begin{aligned} |C_S| &\leq \frac{4\sqrt{2}}{h}\Big|\int_S [\![\Pi_1 v]\!] - [\![v]\!] d\Gamma\Big|, \\ &\leq \frac{4\sqrt{2}}{h}\Big(\Big|\int_S \Pi_1 v_{|\Omega_1} - v_1 d\Gamma\Big| + \Big|\int_S \Pi_1 v_{|\Omega_2} - v_2 d\Gamma\Big|\Big), \\ &\leq \frac{4\sqrt{2}}{h}\Big(\sum_i |l_i|^{1/2}\|\Pi_1 v_{|\Omega_1} - v_1\|_{0,l_i} + \sum_j |l_j|^{1/2}\|\Pi_1 v_{|\Omega_2} - v_2\|_{0,l_j}\Big), \\ &\leq \frac{4\sqrt{2}}{h}\Big(\sum_i |l_i|^{1/2}\|\Pi_1 v_{|\Omega_1} - \widetilde{v}_1\|_{0,l_i} + \sum_j |l_j|^{1/2}\|\Pi_1 v_{|\Omega_2} - \widetilde{v}_2\|_{0,l_j}\Big), \end{aligned}$$

Then switching to the reference element and applying Lemmas A.3 and A.4, we obtain

$$|C_S| \leq \frac{4\sqrt{2}}{h}\widehat{C}\Big(\sum_i |l_i|^{1/2}\|J_{T_i}\|^{1/2}\|\widehat{E^1}v - \widehat{\widetilde{v}}_1\|_{1,\widehat{T}} + \sum_j |l_j|^{1/2}\|J_{T_j}\|^{1/2}\|\widehat{E^2}v - \widehat{\widetilde{v}}_2\|_{1,\widehat{T}}\Big),$$

where $\widehat{C}$ is the constant of Lemma A.3. Now, switching back to T_i and T_j, we have

$$|C_S| \leq \frac{4\sqrt{2}}{h}\widehat{C} \quad \Bigg(\sum_i |l_i|^{1/2}\|J_{T_i}\|^{1/2}|\det J_{T_i}|^{-1/2}\big(\|E^1 v - \widetilde{v}_1\|^2_{0,T_i} + \|J_{T_i}\|^2\|E^1 v - \widetilde{v}_1\|^2_{1,T_i}\big)^{1/2}$$

$$+ \sum_j |l_j|^{1/2}\|J_{T_j}\|^{1/2}|\det J_{T_j}|^{-1/2}\big(\|E^2_{T_j} v - \widetilde{v}_2\|_{0,T_j} + \|J_{T_j}\|^2\|E^2_{T_j} v - \widetilde{v}_2\|_{1,T_j}\big)^{1/2}\Bigg), \tag{C.12}$$

As the triangulation $\mathcal{T}^h$ is trivial regular, C.11 and C.12 yield

$$\Big(\sum_{S\in S^H} |C_S|^2\|\varphi_{a_S}\|^2_{1,\Delta_S}\Big)^{1/2} \leq \frac{1}{h}\widehat{C}_4\sqrt{L} \quad \Bigg(\sum_{j=1}^{2}\Big(\sum_{T\bigcap\Gamma_c\neq 0} \|E^j_T v - \widetilde{v}_j\|^2_{0,T} + h^2\|E^j_T v - \widetilde{v}_j\|^2_{1,T}\Big)^{1/2}\Bigg)$$

Using the same argument of the proof of Lemma 1 of chapter 2 we show easy that

$$\Big(\sum_{S\in S^H} |C_S|^2\|\varphi_{a_S}\|^2_{1,\Delta_S}\Big)^{1/2} \leq \widehat{C}_5\|v\|_{1,\Omega}$$

Using this last result with Lemma 1 of chapter 2 we have inequality C.3b wich finishes the proof of Lemma A.2.

Bibliography

[1] F. Brezzi and M. Fortin. *Mixed and Hybrid Finite Element Methods*, volume 15. Springer Series in Computational Mathematics, New York, 1991. (Cited on pages 3, 5, 6, 18, 19, 20, 25 and 113.)

[2] O. C. Zienkiewicz and R. L. Taylor. *The Finite Element Method*, volume 2. Butterworth-Heinemann, Solid Mechnics, fifth edition, 2000. (Cited on page 3.)

[3] D. Chapelle and K. J. Bathe. The inf-sup test. *Computers and Structures*, 47(4/5):537–545, 1993. (Cited on pages 7 and 19.)

[4] H. Hertz. Über die berührung fester elastischer korper. *J.f. Math. (Crelle)*, 92, 1882. (Cited on page 7.)

[5] A. Signorini. Questioni de elasticita non linearizzata e semi linearizzata. *Rend. de Matematica*, 18:95–139, 1959. (Cited on page 7.)

[6] G. Fichera. Existence theorems in elasticity-boundary value problem of elasticity with unilateral constraints. *Encyclopedia of Physics*, 2:347–427, 1972. (Cited on page 7.)

[7] N. Moës, J. Dolbow, and T. Belytschko. A finite element method for cracked growth without remeshing. *Int. J. Numer. Meth. Engng.*, 46:131–150, 1999. (Cited on pages 8, 10, 17, 31 and 58.)

[8] N. Moës and T. Belytschko. Nouvelle frontiére pour les eléments finis. *Revue Europénne des Éléments Finis*, 11:131–150, 1999. (Cited on page 10.)

[9] E. Béchet, H. Minnebo, N. Moës, and B. Burgardt. Improved implementation and robustness study of the X-FEM for stress analysis around cracks. *Int. J. Numer. Meth. Engng.*, 64:1033–1056, 2005. (Cited on pages 11 and 12.)

[10] F. Stazi, É. Budyn, J. Chessa, and T. Belytschko. An extended finite element method with high-order elements for curved cracks. *Computational Mechanics*, 31:38–48, 2003. (Cited on page 12.)

[11] P. Laborde, Y. Renard, J. Pommier, and M. Salaun. High order extended finite element method for cracked domains. *Int. J. Numer. Meth. Engng.*, 2005. (Cited on pages 12 and 19.)

[12] E. Chahine, P. Laborde, and Y. Renard. Crack-tip enrichment in the Xfem method using a cut-off function. *Int. J. Numer. Meth. Engng.*, 75(6):629–646, 2008. (Cited on pages 13, 14, 17, 31, 32, 33, 36, 81 and 83.)

[13] S. Amdouni, K. Mansouri, Y. Renard, M. Arfaoui, and M. Moakher. Numerical convergence and stability of mixed formulation with x-fem cut-off. *European Journal of Computational Mechanics/Revue Européenne de Mécanique Numérique*, 0(0):1–14, 2012. (Cited on page 17.)

[14] G. Legrain, N. Moes, and A. Huerta. Stability of incompressible formulations enriched with X-FEM. *Comput. Meth. Appl. Mech. Engrg.*, 197:1835–1849, 2008. (Cited on page 19.)

[15] R.A. Adams. *Sobolev spaces*. Academic Press, New York, 1975. (Cited on pages 21, 33, 39, 81 and 89.)

[16] Z. Chen and R. H. Nochetto. Residual-type a posteriori error estimates for elliptic obstacle problems. *Numerische Mathematik*, 84:527–548, 2000. (Cited on pages 21 and 22.)

[17] S. Nicaise, Y. Renard, and E. Chahine. Optimal convergence analysis for the extended finite element method. *Internat. J. Numer. Methods Engrg.*, 86(4-5):528–548, 2011. (Cited on pages 25, 32, 39, 40, 88, 89, 111 and 112.)

[18] S. Amdouni, P. Hild, V. Lleras, M. Moakher, and Y. Renard. A stabilized Lagrange multiplier method for the enriched finite-element approximation of contact problems of cracked elastic bodies. *ESAIM Math. Model. Numer. Anal.*, 46(4):813–839, 2012. (Cited on pages 31, 67, 70, 80, 84 and 104.)

[19] G. Strang and G. Fix. *An analysis of the finite element method*. Prentice-Hall Englewood Cliffs, 1973. (Cited on page 31.)

[20] S. Bordas and M. Duflot. Derivative recovery and a posteriori error estimate for extended finite elements. *Comput. Methods Appl. Mech. Engrg.*, 196(35-36):3381–3399, 2007. (Cited on page 32.)

[21] M. Duflot and S. Bordas. A posteriori error estimation for extended finite elements by an extended global recovery. *Internat. J. Numer. Methods Engrg.*, 76(8):1123–1138, 2008. (Cited on page 32.)

[22] S. Bordas, M. Duflot, and P. Le. A simple error estimator for extended finite elements. *Comm. Numer. Methods Engrg.*, 24(11):961–971, 2008. (Cited on page 32.)

[23] J. J. Ródenas, O. A. González-Estrada, J. E. Tarancón, and F. J. Fuenmayor. A recovery-type error estimator for the extended finite element method based on singular+smooth stress field splitting. *Internat. J. Numer. Methods Engrg.*, 76(4):545–571, 2008. (Cited on page 32.)

[24] V. Lleras P. Hild and Y. Renard. A residual error estimator for the XFEM approximation of the elasticity problem. *in revision*. (Cited on page 32.)

[25] F. Ben Belgacem and Y. Renard. Hybrid finite element methods for the Signorini problem. *Math. Comp.*, 72:1117–1145, 2003. (Cited on pages 32, 44, 80, 91 and 95.)

[26] P. Hild. Numerical implementation of two nonconforming finite element methods for unilateral contact. *Appl. Mech. Engng.*, 184:1:99–123, 2000. (Cited on page 32.)

[27] P. Laborde and Y. Renard. Fixed point strategies for elastostatic frictional contact problems. *Math. Meth. Appl. Sci.*, 31:415–441, 2008. (Cited on page 32.)

[28] S. Hüeber and B. Wohlmuth. An optimal error estimate for nonlinear contact problems. *SIAM J. Numer. Anal.*, 43:156–173, 2005. (Cited on page 32.)

[29] F. Ben Belgacem. Numerical simulation of some variational inequalities arisen from unilateral contact problems by the finite element method. *SIAM J. Numer. Anal.*, 37:1198–1216, 2000. (Cited on pages 32 and 80.)

[30] P. Hild and Y. Renard. A stabilized Lagrange multiplier method for the finite element approximation of contact problems in elastostatics. *Numer. Math.*, 115(1):101–129, 2010. (Cited on pages 32, 33, 37, 41 and 56.)

[31] N. Kikuchi and J.T. Oden. *Contact problems in elasticity*. SIAM, 1988. (Cited on page 32.)

[32] A. Khoei and M. Nikbakht. Contact friction modeling with the extended finite element method (XFEM). *Journal of Materials Processing Technology*, 177:58–62, 2006. (Cited on page 32.)

[33] A. Khoei and M. Nikbakht. An enriched finite element algorithm for numerical computation of contact friction problems. *Int. J. Mech. Sci.*, 49:183–199, 2007. (Cited on page 32.)

[34] J. Dolbow, N. Moës, and T. Belytschko. An extended finite element method for modeling crack growth with frictional contact. *Comput. Methods Appl. Mech. Engrg.*, 190(51-52):6825–6846, 2001. (Cited on page 32.)

[35] S. Geniaut. *Approche XFEM pour la fissuration sous contact des structures industrielles*. ProQuest LLC, Ann Arbor, MI, 2006. Thesis (Ph.D.)– Ecole Centrale Nantes. (Cited on page 32.)

[36] P. Massin S. Geniaut and N. Moës. A stable 3d contact formulation for cracks using XFEM. *Revue Européenne de Mécanique Numerique: Calculs avec méthodes sans maillage*, 16:259–275, 2007. (Cited on page 32.)

[37] H. Ben Dhia and M. Zarroug. Hybrid frictional contact particles in elements. *Revue Européenne des éléments Finis*, 9:417–430, 2002. (Cited on page 32.)

[38] M.-C. Baietto E. Pierres and A. Gravouil. A two-scale extended finite element method for modeling 3d crack growth with interfacial contact. *Comput. Methods Appl. Mech. Engrg.*, 199:1165–1177, 2010. (Cited on page 32.)

[39] H. J.C. Barbosa and T.J.R. Hughes. The finite element method with Lagrange multipliers on the boundary: circumventing the Babuvska-Brezzi condition. *Comput. Methods Appl. Mech. Engrg.*, 85:109–128, 1991. (Cited on pages 33, 58 and 67.)

[40] H. J.C. Barbosa and T.J.R. Hughes. Boundary Lagrange multipliers in finite element methods: error analysis in natural norms. *Numer. Math.*, 62:1–15, 1992. (Cited on pages 33, 58 and 67.)

[41] Rolf Stenberg. On some techniques for approximating boundary conditions in the finite element method. *J. Comput. Appl. Math.*, 63(1-3):139–148, 1995. International Symposium on Mathematical Modelling and Computational Methods Modelling 94 (Prague, 1994). (Cited on pages 33 and 68.)

[42] H. J.C. Barbosa and T.J.R. Hughes. Circumventing the Babuvska-Brezzi condition in mixed finite element approximations of elliptic variational inequalities. *Comput. Methods Appl. Mech. Engrg.*, 97:193–210, 1992. (Cited on page 33.)

[43] R. Becker, P. Hansbo, and R. Stenberg. A finite element method for domain decomposition with non-matching grids. *Math. Model. Numer. Anal.*, 37:209–225, 2003. (Cited on page 33.)

[44] P. Hansbo, C. Lovadina, I. Perugia, and G. Sangalli. A Lagrange multiplier method for the finite element solution of elliptic interface problems using nonmatching meshes. *Numer. Math.*, 100:91–115, 2005. (Cited on page 33.)

[45] P. Heintz and P. Hansbo. Stabilized Lagrange multiplier methods for bilateral elastic contact with friction. *Comput. Methods Appl. Mech. Engrg.*, 195:4323–4333, 2006. (Cited on page 33.)

[46] J. Haslinger, I. Hlavávcek, and J. Nevcas. Numerical methods for unilateral problems in solid mechanics. In P.G. Ciarlet and J.-L. Lions, editors, *Handbook of Numerical Analysis, Volume IV, Part 2*, pages 313–485. North Holland, 1996. (Cited on pages 35, 38, 80 and 88.)

[47] P.G. Ciarlet. The finite element method for elliptic problems. In P.G. Ciarlet and J.L. Lions, editors, *Handbook of Numerical Analysis, Volume II, Part 1*, pages 17–352. North Holland, 1991. (Cited on pages 36 and 83.)

[48] M. Moussaoui and K. Khodja. Regularité des solutions d'un problème mêlé Dirichlet-Signorini dans un domaine polygonal plan. *Commun. Partial Differential Equations*, 17:805–826, 1992. (Cited on pages 36, 84 and 107.)

[49] P. Grisvard. *Elliptic problems in nonsmooth domains*. Pitman, 1985. (Cited on pages 39, 89 and 108.)

[50] J. Haslinger and Y. Renard. A new fictitious domain approach inspired by the extended finite element method. *to appear in SIAM J. Numer. Anal.* (Cited on pages 42 and 80.)

[51] P. Hild and Y. Renard. An error estimate for the Signorini problem with Coulomb friction approximated by finite elements. *SIAM J. Numer. Anal.*, 45(5):2012–2031 (electronic), 2007. (Cited on pages 46, 92 and 93.)

[52] J. Pommier and Y. Renard. Getfem++, an open source generic C++ library for finite element methods. `http://www-gmm.insa-toulouse.fr/getfem`. (Cited on pages 50, 67 and 98.)

[53] P. Alart and A. Curnier. A mixed formulation for frictional contact problems prone to Newton like solution methods. *Comput. Methods Appl. Mech. Engrg.*, 92(3):353–375, 1991. (Cited on pages 51 and 99.)

[54] H. B. Khenous, J. Pommier, and Y. Renard. Hybrid discretization of the Signorini problem with Coulomb friction. Theoretical aspects and comparison of some numerical solvers. *Appl. Numer. Math.*, 56(2):163–192, 2006. (Cited on pages 51 and 99.)

[55] S. Amdouni, M. Moakher, and Y. Renard. A local projection stabilization of fictitious domain method for elliptic boundary value problems. *submitted*. (Cited on pages 57, 80, 81 and 85.)

[56] V.K. Saul'ev. On the solution of some boundary value problems on high performance computers by fictitious domain method. *Siberian Math. Journal*, 4:4:912–925, 1963 (in Russian). (Cited on page 57.)

[57] G. I. Marchuk. *Methods of numerical mathematics*, volume 2 of *Applications of Mathematics*. Springer-Verlag, New York, second edition, 1982. Translated from the Russian by Arthur A. Brown. (Cited on page 57.)

[58] P. Angot, C.-H. Bruneau, and P. Fabrie. A penalization method to take into account obstacles in incompressible viscous flows. *Numerische Mathematik*, 81:497–520, 1999. (Cited on page 57.)

[59] R. Glowinski, T. W. Pan, Raymond O. Wells, Jr., and X. Zhou. Wavelet and finite element solutions for the Neumann problem using fictitious domains. *J. Comput. Phys.*, 126(1):40–51, 1996. (Cited on page 57.)

[60] E. J. Dean, Q. V. Dinh, R. Glowinski, J. He, T.-W. Pan, and J. Périaux. Least squares/domain imbedding methods for Neumann problems: applications to fluid dynamics. In *Fifth International Symposium on Domain Decomposition Methods for Partial Differential Equations (Norfolk, VA, 1991)*, pages 451–475. SIAM, Philadelphia, PA, 1992. (Cited on page 57.)

[61] V. Girault and R. Glowinski. Error analysis of a fictitious domain method applied to a Dirichlet problem. *Japan J. Indust. Appl. Math.*, 12(3):487–514, 1995. (Cited on pages 57, 61, 62, 73, 77, 85, 103, 113, 114 and 115.)

[62] R. Glowinski and Y. Kuznetsov. On the solution of the Dirichlet problem for linear elliptic operators by a distributed Lagrange multiplier method. *C. R. Acad. Sci. Paris Sér. I Math.*, 327(7):693–698, 1998. (Cited on page 57.)

[63] L.A. Rukhovets. *A remark on the method of fictive domains*, volume 3,4. Russian, 1967. (Cited on page 58.)

[64] C.S. Peskin. Flow patterns around heart valves: A numerical method. *J. Comput. Phys*, 10(2):252–271, 1972. (Cited on page 58.)

[65] C. S. Peskin. The immersed boundary method. *Acta Numer.*, 11:479–517, 2002. (Cited on page 58.)

[66] B. Maury. A fat boundary method for the Poisson problem in a domain with holes. *J. Sci. Comput.*, 16(3):319–339, 2001. (Cited on page 58.)

[67] S. Bertoluzza, M. Ismail, and B. Maury. The fat boundary method: Semi-discrete scheme and some numerical experiments. In *Domain Decomposition Methods in Science and Engineering*, volume 40 of *Lecture Notes in Computational Science and Engineering*, pages 513–520. Springer Berlin Heidelberg, 2005. (Cited on page 58.)

[68] N. Moës, É. Béchet, and M. Tourbier. Imposing Dirichlet boundary conditions in the extended finite element method. *Internat. J. Numer. Methods Engrg.*, 67(12):1641–1669, 2006. (Cited on page 58.)

[69] N. Sukumar, D. L. Chopp, N. Moës, and T. Belytschko. Modeling holes and inclusions by level sets in the extended finite-element method. *Comput. Methods Appl. Mech. Engrg.*, 190(46-47):6183–6200, 2001. (Cited on page 58.)

[70] É. Béchet, N. Moës, and B. Wohlmuth. A stable Lagrange multiplier space for stiff interface conditions within the extended finite element method. *Internat. J. Numer. Methods Engrg.*, 78(8):931–954, 2009. (Cited on page 58.)

[71] J. Nitsche. über ein Variationsprinzip zur Lösung von Dirichlet-Problemen bei Verwendung von Teilräumen, die keinen Randbedingungen unterworfen sind. *Abh. Math. Univ. Hamburg*, 36:9–15, 1971. (Cited on pages 58 and 68.)

[72] E. Burman and P. Hansbo. Fictitious domain finite element methods using cut elements: II. A stabilized Nitsche method. *Appl. Numer. Math.*, 62(4):328–341, 2012. (Cited on pages 58 and 76.)

[73] E. Burman and P. Hansbo. Fictitious domain finite element methods using cut elements: I. A stabilized Lagrange multiplier method. *Comput. Methods Appl. Mech. Engrg.*, 199(41-44):2680–2686, 2010. (Cited on page 58.)

[74] J. Haslinger and Y. Renard. A new fictitious domain approach inspired by the extended finite element method. *SIAM J. Numer. Anal.*, 47(2):1474–1499, 2009. (Cited on pages 58, 61, 67, 68, 70 and 76.)

[75] C. R. Dohrmann and P. B. Bochev. A stabilized finite element method for the stokes problem based on polynomial pressure projections. *International Journal for Numerical Methods in Fluids*, 46(2):183–201, 2004. (Cited on page 58.)

[76] E. Burman. Projection stabilisation of lagrange multipliers for the imposition of constraints on interfaces and boundaries. *ArXiv e-prints*, March 2012. (Cited on page 58.)

[77] G. R. Barrenechea and F. Chouly. A local projection stabilized method for fictitious domains. *Applied Mathematics Letters*, 25(12):2071 – 2076, 2012. (Cited on page 58.)

[78] A. Ern and J.-L. Guermond. *Theory and Practice of Finite Elements*, volume 159. Springer-Verlag, Applied Mathematical Sciences, New York, 2004. (Cited on page 59.)

[79] G. Karypis and V. Kumar. Metis: Unstructured graph partitioning and sparse matrix ordering system. `http://www.cs.umn.edu/~metis`. (Cited on pages 67 and 100.)

[80] E. Burman. Pressure projection stabilizations for galerkin approximations of Stokes' and Darcy's problem. *Numerical Methods for Partial Differential Equations*, 24(1):127–143, 2008. (Cited on page 73.)

[81] J.Haslinger. Finite element analysis for unilateral problems with obstacles on the boundary. *Apl. Mat.*, 22(3):180–188, 1977. (Cited on page 80.)

[82] J. Haslinger and I. Hlavá**v**cek. Contact between elastic bodies -2. finite element analysis. *Aplikace Matematiky*, 26:263–290, 1981. (Cited on page 80.)

[83] Y. Renard. An improved a priori error analysis for finite element approximations of Signorini's problem. *Siam J. on Numer. Anal*, to appear. (Cited on page 80.)

[84] S. Hüeber and B. Wohlmuth. An optimal error estimate for nonlinear contact problems. *SIAM J. Numer. Anal.*, 43:156–173, 2005. (Cited on page 80.)

[85] K. Lhalouani and T. Sassi. Méthode d'éléments finis hybrides en décomposition de domaines pour des problèmes de contact unilatéral. *C. R. Acad. Sci. Paris Sér. I Math.*, 327(10):901–905, 1998. (Cited on page 80.)

[86] P. Coorevits, P. Hild, K. Lhalouani, and T. Sassi. Mixed finite element methods for unilateral problems: convergence analysis and numerical studies. *Math. Comp.*, 71:1–25, 2002. (Cited on page 80.)

[87] P Hild. Une méthode par éléments finis mixte préservant la positivité pour le problème de contact en élasticité. *C. R. Math. Acad. Sci. Paris*, 343(3):209–212, 2006. (Cited on page 80.)

[88] L. Baillet and T. Sassi. Mixed finite element methods for the Signorini problem with friction. *Numer. Methods Partial Differential Equations*, 22(6):1489–1508, 2006. (Cited on page 80.)

[89] T. Sassi. Conconforming mixed variational formulation for the signorini problem with a given friction. *Preprint of MAPLY Laboratoire de Mathématiques Appliquées de LYon*, 2003. (Cited on page 80.)

[90] J. Haslinger and T. Sassi. Mixed finite element approximation of 3D contact problems with given friction: error analysis and numerical realization. *M2AN Math. Model. Numer. Anal.*, 38(3):563–578, 2004. (Cited on page 80.)

Abstract: This Ph.D. thesis was done in collaboration with "**La Manufacture Française des Pneumatiques Michelin**". It concerns the mathematical and numerical analysis of convergence and stability of mixed or hybrid formulation of constrained optimization problem with Lagrange multiplier method in the framework of the eXtended Finite Element Method (XFEM). First we try to prove the stability of the X-FEM discretization for incompressible elastostatic problem by ensured a LBB condition. The second axis, which present the main content of the thesis, is dedicated to the use of some stabilized Lagrange multiplier methods. The particularity of these stabilized methods is that the stability of the multiplier is provided by adding supplementary terms in the weak formulation. In this context, we study the Barbosa-Hughes stabilization technique applied to the frictionless unilateral contact problem with XFEM-cut-off. Then we present a new consistent method based on local projections for the stabilization of a Dirichlet condition in the framework of extended finite element method with a fictitious domain approach. Moreover we make comparative study between the local projection stabilization and the Barbosa-Hughes stabilization. Finally we use the local projection stabilization to approximate the two-dimensional linear elastostatics unilateral contact problem with Tresca frictional in the framework of the eXtended Finite Element Method X-FEM.
Keywords: XFEM, Fictitious domain, Unilateral contact, mixed formulation, Stabilization.

Résumé: Ce mémoire de thèse à été réalisée dans le cadre d'une collaboration scientifique avec "**La Manufacture Française des Pneumatiques Michelin**". Il porte sur l'analyse mathématique et numérique de la convergence et de la stabilité de formulations mixtes ou hybrides de problèmes d'optimisation sous contrainte avec la méthode des multiplicateurs de Lagrange et dans le cadre de la méthode éléments finis étendus (XFEM). Tout d'abord, nous essayons de démontrer la stabilité de la discrétisation X-FEM pour le problème d'élasticité linéaire incompressible en statique. Le deuxième axe, qui représente le contenu principal de la thèse est dédié à l'étude de certaines méthodes de multiplicateur de Lagrange stabilisées. La particularité de ces méthodes est que la stabilité du multiplicateur est assurée par l'ajout de termes supplémentaires dans la formulation faible. Dans ce contexte, nous commençons par l'étude de la méthode de stabilisation de Barbosa-Hughes appliquée au problème de contact unilatéral sans frottement avec XFEM cut-off. Ensuite, nous construisons une nouvelle méthode basée sur des techniques de projections locales pour stabiliser un problème de Dirichlet dans le cadre de X-FEM et une approche de type domaine fictif. Nous faisons aussi une étude comparative entre la stabilisation avec la technique de projection locale et la stabilisation de Barbosa-Hughes. Enfin, nous appliquons cette nouvelle méthode de stabilisation aux problèmes de contact unilatéral en élastostatique avec frottement de Tresca dans le cadre de X-FEM.
Mots clés: XFEM, Domaine fictif, Contact unilatéral, Formulation mixte, Stabilisation.